

Università degli Studi di Genova -
Scuola Politecnica
Dipartimento di Ingegneria Meccanica, Energetica, Gestionale e
dei Trasporti (DIME)
Sez. TEC (Termoenergetica e Condizionamento ambientale)



Ph.D. Thesis in Technical Physics
XXXIII Cycle

**APPLICATION OF SOLAR ASSISTED HEAT PUMP
TECHNOLOGY TO THE PALACUS SPORT PALACE:
RENEWABLE SOURCES INTEGRATION FOR HIGHLY
EFFICIENT AND LOW ENERGY CONSUMPTION SYSTEMS**

Supervisors:

Prof. A. Marchitto

PhD candidate:

Chiara Marafioti

Acknowledgement

The Palacus pilot plant, installed at Sport Palace “Carminio Romanzi”, University of Genoa, has been developed with a co-funding of FSE Regione Liguria, Bando Azione 2.1 “Efficienza Energetica e Produzione di Energia da Fonti Rinnovabili – Enti Pubblici” – Posizione n.2, included in the PRIN 2015 MIUR grant 2015M8S2PA “Clean Heating and Cooling Technologies for energy efficient smart grid”. The control and monitoring systems have been completed with the co-funding of the University of Genoa in the context of the “Grandi Attrezzature” 2018, DR n. 3404, 19/07/2018 project and CARIGE 2018/0012 project.

SUMMARY

Nomenclature	4
List of Figures	6
List of Tables.....	10
A foreword	11
1. Solar assisted heat pump technology.....	15
State of art.....	15
1.1. Solar panels.....	15
1.2. Heat pump	25
1.3. Solar assisted heat pump.....	30
1.4. Palacus pilot plant.....	38
1.5. Palacus SAHP-PVT pilot plant – a description.....	42
1.6. SAHP – another example in Liguria and the untapped potential	61
References.....	63
2. The issue of acceptance	69
2.2 Introduction.....	69
2.3 The concept of acceptance	70
2.3.2. Socio-political acceptance.....	71
2.3.3. Community acceptance	72
2.3.4. Market acceptance	73
2.3.5. Technological acceptance	74
2.4 Means to overcome the issue of acceptance	76
2.5 Ways for acceptance measurement	79
2.5.1. Indicators	80
2.5.2. Indices	80
2.6 Methodology to collect experimental data on acceptance	81

2.7	“Carmin Romanzi” Sport Palace (Palacus)	83
2.7.1.	SAHP-PVT installation recall of the significative parameters	83
2.8	Innovative approach	85
2.9	Case study: the acceptance evaluation of the DHW subsystem	92
2.9.1.	Case 1 – sudden stops of the heat pump	93
2.9.2.	Case 2 – evaluation of the acceptance level for the DHW system	100
2.9.3.	Case 3 - evaluation of the level of acceptance over time	103
2.10	Conclusions	106
	References	107
3.	NUMERICAL MODELLING OF THE SAHP-PVT PLANT	112
3.1.	Numerical model of the DHW subsystem	113
3.2.	Model assembly	118
3.3.	Stratification	124
3.4.	Differences between the configuration with two distinct boiler and the one with only a storage with double volume and double height	137
3.5.	Conclusions and future developments	147
	References	147
4.	HYPOTHESIS OF REVAMPING FOR THE SAHP-PVT INSTALLATION AT PALACUS	151
4.1.	Leakages in the solar field – integration of the HP configuration	151
4.2.	Integration of the DAS	166
4.3.	Conclusions	169
	REFERENCES	170
	FINAL CONCLUSIONS	172
	Publications	175
	Annex A – part I	176
	Annex A – part II	183

NOMENCLATURE

Abbreviations

HP	Heat pump
PVT	Photovoltaic/thermal
SH	Space heating
DHW	Domestic hot water
GB	Gas burner
WST	Water storage tank
MES	Manager energy services
CS	Exchange contribution
COP	Coefficient of performance
SCOP	Seasonal coefficient of performance
EER	Energy efficiency ratio
SAHP	Solar assisted heat pump
VCC	Variable capacity compressor
EEV	Electronic expansion valve
ATU	Air treatment unit
DAS	Data acquisition and control system
PLC	Programmable logic controller
DD	Degrees days
PES	Primary energy saving
IT	Information technologies
IoT	Internet of Things
AAL	Ambient assisted living
TRL	Technological readiness level
AE	Acceptability engineering
IHTP	Inverse heat transfer problem
H	Height
D	Diameter
CFD	Computational fluid dynamics

Subscripts

nom	nominal
el	electrical
th	thermal
p	panel
tot	total
sol	solar
consump	consumption
work	working period
eff	effective

Symbol	Quantity	SI Unit
L	Mechanical work	J
Q	Heat pump heat	J
T	Temperature	K
S	Entropy	J/kgK
E	Energy	J
m'	Mass flow rate	kg/s
c	Specific heat	J/kg·K
T	Temperature	K
A	Area	m ²
G	Irradiance	W/m ²
COP	Coefficient of performance	-
SCOP	Seasonal coefficient of performance	-
E	Energy	kWh
g	Gravity acceleration	m/s ²
U	Trasmittance	W/m ² K
u	Characteristic inlet fluid velocity	m/s
V	Volume	m ³

Greek symbols	Quantity	SI Unit
τ	Time	s
η	Dimensionless efficiency	[-]
ρ	Density	kg/m ³
λ	Thermal conductivity	W/mK
β	Volumetric coefficient of thermal expansion	1/K

LIST OF FIGURES

Figure 1.1. Conceptual scheme of the PVT panel and typical stratigraphy.	15
Figure 1.2. Trend of the peak current intensity (y-axis) as a function of the peak voltage (x-axis) of a photovoltaic cell according to different temperatures, T_{cell} [°C], [4].	16
Figure 1.3. Average yearly value of the Single National Price for electricity [9]	19
Figure 1.4. Example of the detailed energy bill for civil electricity meters [12].	20
Figure 1.5. Electricity prices from 2017 to 2019 for households [14]	22
Figure 1.6. Inverse cycle scheme, with the main components of the heat pump.	26
Figure 1.7. T-S diagram with a classic vapor compression inverse cycle. T_1 and T_2 are respectively the temperatures at the condenser and at the evaporator.	27
Figure 1.8. Different expansion valves: capillary (a); thermostatic (b); automatic (c).	28
Figure 1.9. P-H diagram, representation of an inverse cycle with subcooling (area in pink).	29
Figure 1.10. Basic version of a direct expansion SAHP.	31
Figure 1.11. Plant scheme of the SAHP analyzed in [31].	32
Figure 1.12. Basic version of an indirect expansion SAHP.	33
Figure 1.13. Different SAHP dual source configurations. a) Serial direct expansion SAHP, b) parallel direct expansion SAHP, c) parallel indirect expansion SAHP, d) serial indirect expansion SAHP	36
Figure 1.14. Traditional thermal solar panel concept.	37
Figure 1.15. Qualitative trend of the efficiency for different kinds of solar thermal collectors as a function of the thermal gradient between the collector and the surrounding environment [42]. ..	37
Figure 1.16. Integrated solar assisted heat pump with gas burner back-up heater.	38
Figure 1.17. General overview of the SAHP prototype.	39
Figure 1.18. The SAHP-PVT prototype – main components.	40
Figure 1.19. Plant scheme of the prototype and name of the main components.	41
Figure 1.20. Block diagram of the pilot plant at Palacus Sport Palace, University of Genoa.	42
Figure 1.21. a) the position of the Palacus sport palace over the district of Albaro, Genoa and b) the multi-sportive complex with Palacus and the neighbouring sport courts [47].	43
Figure 1.22. Some gyms inside the Palacus building.	44
Figure 1.23. The solar hybrid subsystem. On the background, the Palacus sport palace and the heating plant.	45
Figure 1.24. Location of the solar field with respect to the heating plant [48].	46
Figure 1.25. Schematic representation of the PVT solar field.	46
Figure 1.26. Heat pump of the Palacus pilot heating plant.	49
Figure 1.27. Schematic representation of the HP and the hot/cold storages.	50
Figure 1.28. Three-dimensional graph showing the COP of the HP as a function of the outlet temperatures on the evaporator and condenser side.	52
Figure 1.29. Integration gas burners of the Palacus pilot plant for SH and DHW (a) and only DHW (b).	52
Figure 1.30. Detail of the Domestic Hot Water subsystem production at Palacus.	53
Figure 1.31. Schematic representation of the SH integration burners and the supplies.	55
Figure 1.32. Control panels.	58
Figure 1.33. Plant scheme of the SAHP at the public swimming pool, Sestri Levante, [50]. The red circuit represents the bypass which directly connects the thermal solar field to the storage tank.	

The HP cycle is represented by the blue line and the numbers shown correspond to the ones used in section 1.2	61
Figure 1.34. Values of the Primary Energy Saving (PES) index according to the different 110 Italian municipalities. The equation of the regression line and correlation index R are reported on the graph [50].....	63
Figure 2.1. Three-point division of acceptance [4]	71
Figure 2.2. Witty and thorny comic strip showing the NIMBY attitude in an ironic way [19].....	72
Figure 2.3. Minimum distance for accepting a technology, [2]	73
Figure 2.4. European energy sources trend during the last decades; the increase from early years 2000 is evident [26].....	76
Figure 2.5. Moore's chasm in the lifecycle of a technology [29]	79
Figure 2.6. Block diagram of the SAHP-PVT pilot plant installed at Palacus.....	84
Figure 2.7. Solar radiation of a generic day: total irradiance (area swept by the blue line) used for C_3 computation and the total irradiance with the active solar thermal subsystem (dashed green areas) used for the S_{np} evaluation. The reference (monitored) signal is P_1 activation.....	90
Figure 2.8. Trend of irradiance $G(\tau)$ and external temperature $T_{ext}(\tau)$ on May, 2nd. The grey and yellow vertical lines represent respectively the hour at which the HP arrested (about 10.00 a.m.) and the hour at which the plant might have worked (7.00 p.m.).	94
Figure 2.9. Detail of the functional scheme of the HP (shown in Figure 1.27 before a) and after b) the introduction of the three-way mixing valve.	96
Figure 2.10. Plot (on the left y-axis) of the temperature in the DHW2 water storage tank (blue line) against (on the right y-axis) irradiance G (orange line) associated to almost sunny days.	102
Figure 2.11. Plot (on the left y-axis) of the temperature in the DHW2 water storage tank (blue line) against (on the right y-axis) irradiance G (orange line) associated to cloudy days.	102
Figure 2.12. DHW usage based on DHW hot storage tank temperature profiles. Typical day trends for a) winter and b) summer.	105
Figure 3.1 Schematic representation of the DHW subsystem and its measured parameters	115
Figure 3.2. Water storage tanks DHW1 (on the left) and DHW2 (on the right). The twin pumps P_8 of the fossil burner circuit can be identified near DHW1	115
Figure 3.3. Temperatures trend of T_{14} , T_{19} and T_{20} during September, 28 th and 29 th , 2019	116
Figure 3.4. Temperatures trend of T_{14} , T_{19} and T_{20} during October, 1 st and 2 nd , 2019.....	117
Figure 3.5. Simplified scheme of the DHW subsystem for numerical overnight modelling.....	118
Figure 3.6. TRNSYS simplified model corresponding to the scheme in Figure 3. 5	119
Figure 3.7. Plot of the numerical and measured time-temperature profile of T_{20} (assumed minimum water flow rate $m = 7$ kg/h with variable temperatures in the range 57-53°C).	120
Figure 3.8. Plot of the numerical and measured overnight trends for T_{14} (DHW1) and T_{19} (DHW2) (in between the on-off status of the plant).	122
Figure 3.9. Comparison between measured data (dotted lines) and the temperatures obtained from the numerical model (continuous lines) (a). The correspondent water flow is shown in grey (ref. right axis)	122
Figure 3.10. Density of water as function of temperature	125
Figure 3.11 Fully stratified tank (on the left) vs fully mixed one (on the right). They both have the same average temperature	125

Figure 3.12. Division of the tank into layers (on the left), each one divided into crowns and sectors (on the right) according to the temperature zonal models.....	128
Figure 3.13. Initial values of temperature and correspondent scheme of T14/T19 used to estimate the initial conditions based on the measured values	129
Figure 3.14. Cooling trend of the tank with 1 node.....	130
Figure 3.15. Cooling trend of the tank with 4 nodes and their positioning inside the tank.....	131
Figure 3.16. Cooling trend of the tank with 6 nodes and their positioning inside the tank.....	132
Figure 3.17. Cooling trend of the tank with 6 nodes and their positioning inside the tank.....	133
Figure 3.18. Cooling trend of the tank with 10 nodes and their positioning inside the tank	134
Figure 3.19. Mixing inside a 12 nodes tank performed with different time steps (30 minutes and 1 minute).....	135
Figure 3.20. Cooling process of a 12 node tank with no water flow rate with 30 minutes time step (in red) and 1 minute time step (in blue).....	136
Figure 3.21. Basic TRNSYS models used to test if the simulation with the two distinct boilers (a) leads to the same results as in the case of the two tanks stacked (b)	137
Figure 3.22. Comparison between the case of distinct boilers (a) and stacked together (b). The first two hours of simulation have been considered. The red, dotted lines represent the TRNSYS simulated curves while the continuous ones are concerned with the measured trends for temperature.....	139
Figure 3.23. Mix number over different time steps for the case of no water flow inlet inside the storage	140
Figure 3.24. Temperature trend at the different nodes using the models reported in Figure 3. 20.	141
Figure 3.25. Mix number over different time steps for the case of small water flow inlet (7 kg/h at 14.7 °C) inside the storage	142
Figure 3.26. Trend in temperature for two boilers joined (a) and single boiler (b) with 100 kg/h of water flow rate at the constant temperature of 14.7 °C.....	143
Figure 3.27. Detail of Figure 3. 23a	143
Figure 3.28. Detail of Figure 3. 23b.....	144
Figure 3.29. Mix number over different time steps for the case of higher water flow inlet (100 kg/h at 14.7 °C) inside the storage.....	144
Figure 3.30. Trend in temperature for two boilers joined (a) and single boiler (b) with 1000 kg/h of water flow rate at the constant temperature of 14.7 °C.....	145
Figure 3.31. Detail of Figure 3. 26a	146
Figure 3.32. Detail of Figure 3. 26b.....	146
Figure 3.33. Mix number over different time steps for the case of significant water flow inlet (1000 kg/h at 14.7 °C) inside the storage.....	147
Figure 4.1 Cross section of the roll bonded thermal panel below the photovoltaic layers	151
Figure 4.2. Functional scheme of the thermal side of the solar field and part of the heat pump at the Palacus pilot plant.....	152
Figure 4.3. Monthly energy consumption for the HP, photovoltaic production and net monthly balance for the SAHP at Palacus	154
Figure 4.4. Old yearly feed in premium balance based on the values reported in Figure 4. 3 against the new monthly feed in premium strategy	154

Figure 4.5. Satellite vie of the site [3]	159
Figure 4.6. Tridimensional views of the site [4]	160
Figure 4.7. View of the solar field and of the hills towards East/South East.....	161
Figure 4.8. Actual configuration of the storage on the cold side of the HP and of the inlet/outlet with the solar field	164
Figure 4.9. Basic design configuration of the interface exchanger between the storage on the cold side of the HP and the inlet/outlet with the solar field	165

LIST OF TABLES

Table 1.1. Variable COP according to the water operative outlet condenser and evaporator temperatures [$^{\circ}\text{C}$] (water-water HP).	51
Table 1.2. Main annual operating data and costs of the Palacus Sport Palace.....	59
Table 2.1 Nominal and actual working hours of the solar field and computation of $C1, T_h, \text{solar}$ under nominal and actual conditions	97
Table 2.2. Maximum panel temperature (T_{panel} , [$^{\circ}\text{C}$]) according to external air temperature (T_{ext} , in green) and solar radiation (G , W/m^2 , in blue). Red values represent temperatures higher than 25°C	99
Table 2.3. Mean air temperature for each month [52].	99
Table 2.4. Indicators computed assuming nominal and effective usage of the solar thermal field for DHW production	100
Table 2.5. Parameters evaluation under nominal and effective usage for DHW application with the contribution of the solar field, updated over time (periods A and B).	104
Table 3.1. Additional information (a) and estimation of the global thermal loss coefficient for DHW tanks (b).	121
Table 3.2. Interspacing of the nodes (Δh), height referred to the bottom of the tank (h) initial values of temperature (T_{in})	131
Table 3.3. Interspacing of the nodes (Δh), height referred to the bottom of the tank (h) initial values of temperature (T_{in})	132
Table 3.4. Interspacing of the nodes (Δh), height referred to the bottom of the tank (h) initial values of temperature (T_{in})	133
Table 3.5. Interspacing of the nodes (Δh), height referred to the bottom of the tank (h) initial values of temperature (T_{in})	134
Table 4.1. Measured irradiance, monthly average temperature and photovoltaic energy collected by the hybrid field over a standard year ($A = 140 \text{ m}^2$).....	155
Table 4.2. Summary of the electricity consumed by the HP, the photovoltaic energy collected by the hybrid field over a standard year simulation and the difference between energy consumption and collection (negative values stand for net energy consumption from the grid).....	156
Table 4.3. Cost-benefit analysis for the replacement of 70 m^2 of hybrid damaged panels with thermal ones	162

A FOREWORD

The present work is concerned with the plant of the sport palace “Carmine Romanzi”, known also as “Palacus”, of University of Genoa (Italy), (Figure I). The facility consists of a heat pump coupled, on the cold side, with the thermal part of a solar hybrid field. The hot side of the heat pump has been designed to satisfy the space heating and domestic hot water needs of the structure. The photovoltaic production of the solar hybrid field grants the electricity need of the heat pump and any other electric auxiliary within the plant. Two traditional gas burners integrate the space heating or the domestic hot water production in case of severe boundary conditions (e.g. users’ needs and environmental conditions). Finally there is also a data acquisition and monitoring system in the installation to allow an almost continuous monitoring of the plant.

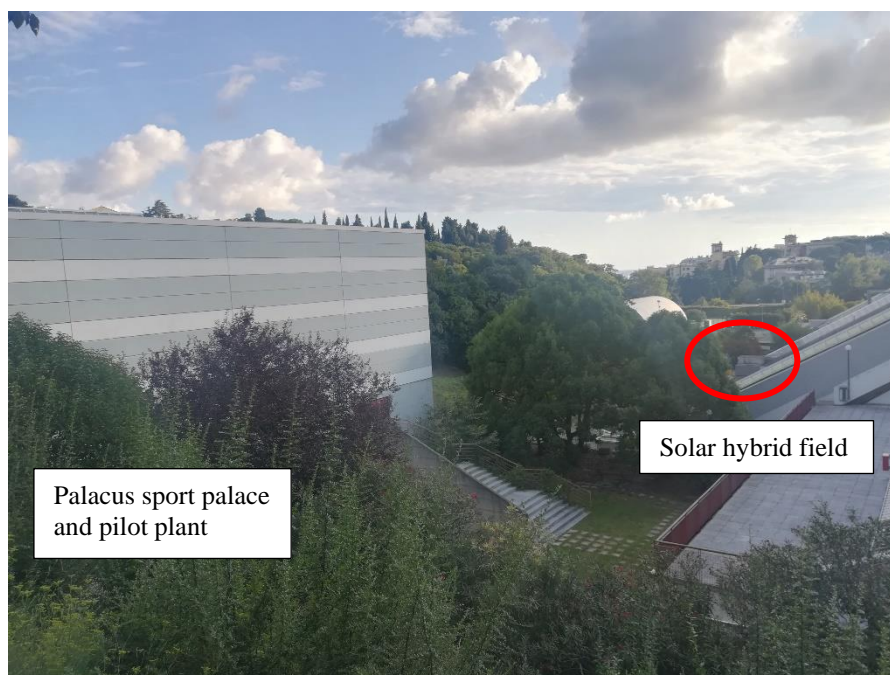


Figure I. Overall view of the sport palace Palacus (on the left) and of the solar hybrid field (on the right).

The research topic is about the plant monitoring with the aim of optimal strategies definition in order to maximize the exploitation of the renewable part of the plant. This objective has been achieved thanks to both the data acquired by means of the monitoring system and numerical dynamic simulations carried out with numerical codes (Matlab and TRNSYS).

The key role led by the data acquisition and monitoring system can be resumed through three main topics discussed in this work:

- Detection of design flaws or irregular working of one or more subsystems.
- Evaluation of how much the plant has been “accepted” by the users and it is employed within the facility management.
- Implementation of new regulation criteria to take the maximum advantage of the installation.

In my opinion, the technology of the solar assisted heat pump (SAHP) still hasn't been fully appreciated for technical and complexity reasons. Besides the academic and practical issues, the underlying goal of this work is to give a little contribution to reach more competitive and attractive asset. The expectation is to transmit the "hands-on" experience gained along the past three years of my PhD and make it available for others who might treasure it.

This study shows a very high level of multidisciplinary since the pilot plant provides the thermal needs of a real structure with real users. It no-longer belongs to a didactic workbench where the boundary conditions (e.g. external temperature, irradiance, thermal loads) were simulated "ad hoc". The plant faces every day the double challenge of the competition with the traditional heating installation trying to provide the users' needs (space heating, domestic hot water) with the maximum, optimal exploitation of the renewable sources.

This topic represents a challenge for my study program since I graduated as a structural engineer and then continued with a PhD in Technical Physics. During these three years I had the opportunity to gain a deeper insight in the single plant components (heat pump, gas burners, solar thermal/photovoltaic field). Their coupling and management was studied in a real heating plant application which provides the thermal needs of a working sport facility.

The approach to sustainable plant design requires the adoption of different renewable sources since the needs of a facility/building/flat cannot be entirely covered by a single renewable energy form. Therefore, the only valuable and competitive alternative to the traditional fossil burners consists in the synergy of different alternative green sources (e.g. solar thermal, photovoltaic, geothermal). This concept echoes in the Italian legislative requirements where, for instance, the thermal need of a new civil building must be provided with minimum percentages of different renewable sources. (e.g. DM 26/06/2015 and subsequent amendments). The synergy among different renewable sources, coupled with both high efficiency heat production systems (heat pump) and traditional gas burners represents another reason of keen interest in this issue. In fact the need of new solutions for the technical plants to minimize the consumption of fossil fuels is well known. However, the necessity of an interaction among different renewable sources still experiences a very low diffusion both at small scales (e.g. single houses) and at larger ones (e.g. apartment buildings or industrial).

The presence within a same installation of different sub-systems, with distinct optimal operating conditions and limits, which can work independently or not, leaves out the possibility of a "manual" management of the plant. This concept becomes particularly apparent for the civil sector. Indeed, it represents one of the major terms in the EU final energy consumption, as clearly outlined by many researches [1], [2] and therefore in this sector significative improvements can be made. Nevertheless, people belonging to the civil sector have different cultural backgrounds and this means in turn that they are not likely to manage innovative plants on their own. The correct and most efficient cooperation of different subsystems within the same plant can be achieved by means of a monitoring and control system. For instance, considering a traditional fossil burner, the necessary information to be acquired for its correct working is very few. Furthermore, the possible operating modes are usually restricted to the "on", "off" or "modulating" conditions. In addition,

there is a unique way that satisfies the users' needs (e.g. space heating, domestic hot water).

On the other side, the management of an innovative plant unavoidably requires the acquisition of a very large and time-updated database. Even if the users had the skills to manage the plant, they couldn't directly handle the extended amount of information associated to the installation. Moreover, the same demand (space heating, domestic hot water) can be fulfilled in different ways. Basically, even in a very simple plant which consists in a thermal solar field coupled with a fossil burner, the domestic hot water demand can be met by means either of only the solar field or of the burner. The question of which strategy would reveal more effective have multiple correct answers. During a day of Summer, for instance, the production of domestic hot water can be achieved through the solar field. On the other hand, during night or spring, the thermal circuit contribution might be significative but not enough to meet the users' needs or totally negligible. In this case the fossil burner should integrate or provide itself the hot water demanded. This brief instance shows how, even in a not so complex plant, many regulation criteria can be identified to meet the three main goals of an efficient plant:

- Satisfy the end users' needs.
- Maximize the exploitation of the renewable sources.
- Reduction of pollution and fossil fuels combustion.

In other words, the possibility to provide the thermal demands gain more degrees of freedom as the plant becomes more structured, according to the boundary conditions of the problem (e.g. environmental/external conditions and users' needs over time).

One last remark concerning this topic is represented by the crucial stage of the project. The pilot plant actually built is representative of a relatively high Technological Readiness Level (TRL 7 - System prototype demonstration in operational environment) since the previous stages were successfully achieved. The improvement of the monitoring and control system is the key step to gain a TRL 8 (System complete and qualified).

The main outlines and the basic structure of this thesis focus on the topics addressed during the three-years-period of my PhD activity and, in particular, on the papers written. They have been deepened and integrated preserving their conceptual structure, including specific introduction, conclusion and final bibliography.

The present work starts from a schematic overview of the state of art about solar assisted heat pump technologies interfaced with hybrid panels. Then the structure and working principles of the pilot plant at Palacus sport centre is presented step by step. Indeed the research activity carried out during the past three years revolves around the data monitoring and control of the SAHP plant. The possibility of an operating real size pilot plant is a powerful tool to study and perform analysis of such renewable plants. Indeed numerical/theoretical simulations cannot yet be separated from the experimental aspect (Chapter 1).

The structure of the following chapters is conceived as a report journal where each relevant issue has been illustrated in a specific section. The common goal is the achievement of a low consumption and energy efficient system that can be managed from two main approaches. Firstly, the topic of

acceptance namely how the end users' agreement influences the usage of the plant and therefore its performance (Chapter 2). Secondly, the field of numerical transient simulations for complex plants has been enquired by means of applications in Trnsys environment (Chapter 3). The two paths have led both to significative material improvements of the plant which have been realised during the past three years and they have provided the chance to deepen specific academic topics (e.g. stratification, validation of different numerical models to simulate specific subsystems of the plant, introduction of new methods to asses a level of acceptance of the facility).

In the end, the knowledge acquired by means of the almost continuous monitoring of the plant has been applied to support both the decision making and the design teams in the choice of the new configuration to give to the plant according to the revamping intervention which is taking place. In other words, the key concepts introduced in the last part of this work have been implemented in the revamping design to reach a better plant performance and they are the result of the experience, data acquisition and management, numerical analyses and simulations about the pilot plant performed during the past three years (Chapter 4).

1. SOLAR ASSISTED HEAT PUMP TECHNOLOGY

State of art

This chapter proposes a brief summary of the key concepts related to the components of a solar-assisted heat pump (basically solar panels and heat pump) and then a specific insight on the technology of solar assisted heat pumps is dealt.

1.1. Solar panels

Solar hybrid panels will be illustrated since they are coupled with the Heat Pump (HP) of the Palacus pilot plant. The term “hybrid” means a combination of photovoltaic (PV) and thermal (T) technologies within the same panel.

The basic structure of a hybrid panel (Figure 1.1) consists in the flow of a fluid (usually a mixture of water and glycol) located on the back of the panel, while the photovoltaic cells are on the front. One of the most diffused configurations is the so called “Sheet and tube” where a metal plate under the photovoltaic cells allows the anchorage of the pipes. This simple design allows an efficiency which is very close to the maximum attainable with other more complex configurations [3]. An inverter transforms the direct current generated by the cells into an alternating one that can be immitted into the national grid or directly employed for other devices.

Only hybrid panels cooled by means of forced water flow will be presented. The others where the fluid consists in either air or refrigerant will be neglected since not directly relevant to the topic of the thesis.

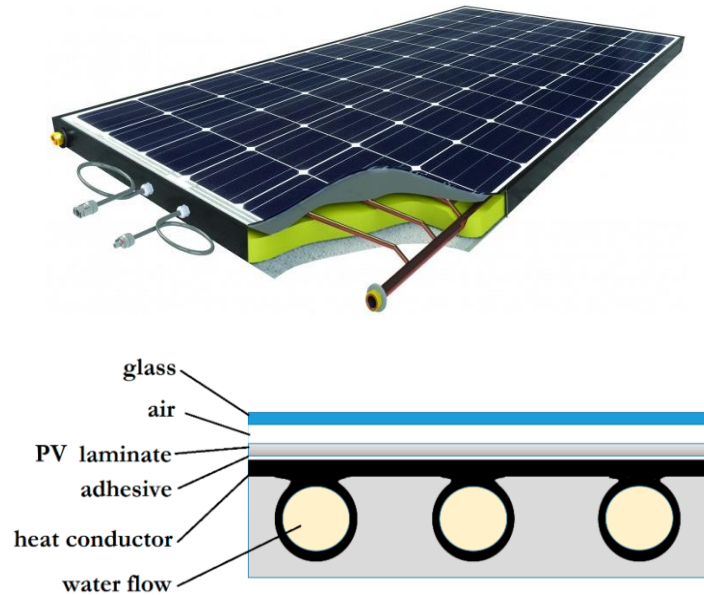


Figure 1.1. Conceptual scheme of the PVT panel and typical stratigraphy.

From a conceptual point of view, the idea of hybrid panels borrows from the trend of PV panels efficiency over temperature which increases as the panel mean working temperature decreases.

The electrical efficiency of the solar panel (η_{el}) can be expressed as the ratio between the peak power produced and the radiating incident power (Eq.(1.1))

$$\eta_{el} = \frac{V_{peak} I_{peak}}{G_{nom} A} \quad (1.1)$$

Where

V_{peak} , I_{peak} are respectively the peak voltage [V] and the peak current intensity [A].

G_{nom} is the nominal irradiance over the panel surface [W/m^2], equal to $1000 W/m^2$.

A is the panel area [m^2].

Considering Figure 1.2, the peak voltage and current intensity are reported for fixed temperatures at the cell. Their product equals the numerator of the electric efficiency (Eq.(1.1)). An immediate comparison shows that for a fixed voltage, the product $V_{peak} I_{peak}$ increases with the decrease of the cell temperature (T_{cell}). The same conclusion can be drawn if the current intensity is fixed and the voltage varies according to T_{cell} .

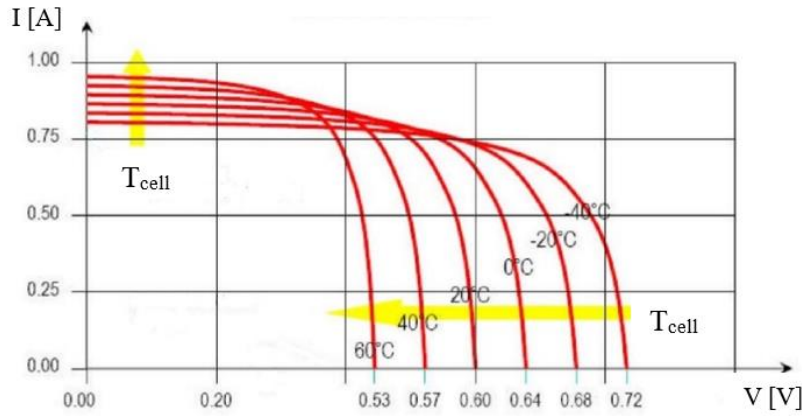


Figure 1.2. Trend of the peak current intensity (y-axis) as a function of the peak voltage (x-axis) of a photovoltaic cell according to different temperatures, T_{cell} [$^{\circ}C$], [4]

On the other hand, the thermal efficiency η_{th} of a solar panel can be computed by means of Eq.(1.2):

$$\eta_{th} = \frac{m' c_p (T_u - T_i)}{GA} \quad (1.2)$$

Where

m' is the water flow rate [kg/s].

c_p is the fluid specific heat [J/kg K].

T_u and T_i are respectively the outlet and inlet temperatures of the fluid [K].

G is the irradiance over the panel surface [W/m^2].

A is the panel area [m^2].

The overall efficiency of a hybrid panel (η_{tot}) can be determined by means of sum between the thermal (η_{th}) and electrical (η_{el}) ones. In symbols:

$$\eta_{tot} = \eta_{th} + \eta_{el} \quad (1.3)$$

This attempt to express the global performance with a unique parameter (Eq.(1.3) might result ambiguous in most cases even if it is commonly used when addressing to hybrid panels efficiency [5]. Indeed, the global efficiency of 70% can be determined by the sum of different electrical and thermal efficiencies. So, fixed a global efficiency of 70%, a panel with $\eta_{el} = 15\%$ and $\eta_{th} = 55\%$ is more attractive than one with $\eta_{el} = 10\%$ and $\eta_{th} = 60\%$ since the production of electricity is more valuable than the thermal aspect. Actually, the two magnitudes represented by electrical and thermal energy can be compared only once the national grid efficiency for the production of electricity (η_{grid}) is accounted (Eq.(1.4)):

$$\eta_{tot} = \eta_{th} + \frac{\eta_{el}}{\eta_{grid}} \quad (1.4)$$

The value of η_{grid} is periodically determined and updated by the Electricity and Gas Authority and it is equal to about 49% nowadays [6].

The main advantages associated to this technology consist in:

- Reduction of the overall dimensions and installation costs.
- Longer useful life of the panels thanks to the control of the panel temperature that extends the durability of the electrical connections among the cells.
- Conjoint production of thermal and electrical energy.

On the other side, two main negative aspects can be identified:

- Considering the solar thermal production over a standard year, the temperature levels reached can meet the thermal demand by themselves only in the summer months. During the remaining part of the year, an integration of the thermal production is required to provide Space Heating (SH) and Domestic Hot Water (DHW). For instance, this can be done with a traditional gas burner (GB) or with a heat pump.
- In statistical terms, the presence at the same time of electrical and thermal needs in time with solar irradiance availability is not very likely, especially with few and non-contemporaneous users. For instance, an apartment building, with respect to a single flat, is more likely to have thermal and electrical needs coincident in time when irradiance is available.

This means that solar panels always require storage systems for the energy produced (both photovoltaic and thermal). As far as the thermal field is concerned, the easiest solution is represented by insulated storage tanks (Water Storage Tanks, WSTs) where the thermal energy is collected and used when required by the users. On the contrary, the storage of electricity results to be a tougher task. In fact, the solution of accumulators or batteries doesn't lead to positive (or null) cost-benefit analysis with the actual state of art of this technology. In simpler words nowadays the cost of a photovoltaic (or hybrid) installation provided with batteries has a very high installation cost that cannot be amortised by means of the energy production during the entire useful life of the components. Apart from the economical aspect, in this way the electrical plant is radically modified and adjustments might result compulsory in many cases. In Italy a valuable alternative to the design of specific

batteries is provided by the “feed-in-premium” regulation introduced initially introduced with the law 133/1999 [7] and subsequent amendments as explained in the next paragraph.

1.1.1. Feed in premium strategy

This system is regulated by the Manager of Energy Services (MES) and it increases the value of the energy produced by renewable installations when the self-consumption of the instantly electricity produced is not possible. Following this strategy, the electrical energy produced and not immediately consumed is immitted into the national grid which acts as a virtual energy storage “collector”. Then, an economic compensation takes place between the energy delivered by national grid and the one produced and immitted by means of a bidirectional meter. This balance is obviously referred to a time range which has been widely modified by the body of laws come into force from 1999 up to now.

In other words, a fictitious partial contribution of the payed energy bills is acknowledged as a function of the electricity produced and not used sent into the national electrical grid. The self-consumed electricity does not take part to this balance. The refund (hereafter named as Exchange Contribution, CS) partially accounts for the electrical network services (e.g. dispatching and distribution costs) neglecting the taxes.

Any eventual unspent surplus in the electricity production within the reference time period is considered as an energy sale based on the average market price of the past year. This benefit cumulates with the refund coming from the CS. The difference between these two terms is that the CS is not taxed while the surplus energy sale is subjected to taxation as it is an “occasional income”.

1.1.2. Feed-in-premium: evaluation of the electricity produced

The current legislation ([8]) refers to the following relation (Eq. (1.5)), valid for systems with peak power production lower than 20 kW_E) to quantify the exchange contribution of the electricity sent into the national grid:

$$CS = \min[O_e; C_{ei}] + CU_{sf} \cdot E_s \quad (1.5)$$

Where

O_e [€] is the price of electricity paid by the users when it is delivered by the national grid. It can be expressed as the delivered kWh times the Single National Price (SNP), according to the simplifications introduced from the beginning of 2013. This quantity averages monthly the energy prices for every region and it has shown an almost constant trend during the past years equal to 0.05 €/kWh (50€/MWh) (Figure 1.3). The single national price (in Italian PUN) can be roughly conceived as the price paid by each energy supplier within the energy purchase.

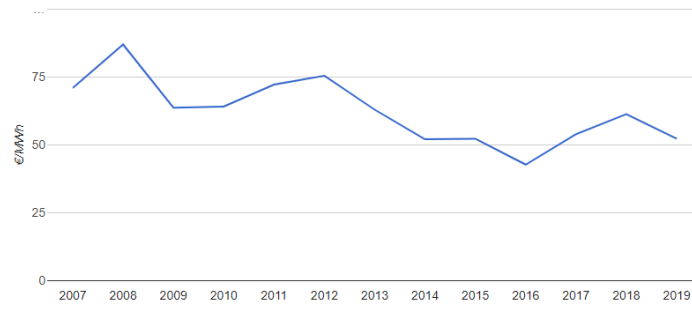


Figure 1.3. Average yearly value of the Single National Price for electricity [9]

C_{ei} [€] is the equivalent Cost of the immitted energy. It can be computed as the product between the immitted energy [kWh] and the average price for electricity in that specific location referred to the previous day [€/kWh]. It can show fluctuations depending for instance on the time over the day in which energy is sent into the national grid. A first estimation [10] can lead to a value of 0.06 €/kWh.

CU_{sf} [c€/kWh] is the unit price for standard exchange computed by the Manager of Energy Services adopting standard parameters (e.g. transmission, distribution and dispatching fees) in force during the current month. It represents the term that accounts for the fixed costs refunds to the users who adopt the feed-in-premium. An average value of 0.08 €/kWh can be considered with reference to the past years [11].

E_s [kWh] is the Exchanged energy, that means the electricity produced by the users, sent into the national grid and later used. Basically, it represents the minimum between the immitted kWh and the delivered ones over the year.

Whenever C_{ei} is greater than E_p , their difference is the surplus. As introduced above, this extra production of electricity can be sold (and taxed) or banked for the contributions of the following year.

1.1.3. Some qualitative remarks

Nowadays the feed in premium approach is not the main strategy to enhance the electricity produced with a PV field. The best and most valuable way is immediate self-consumption. The feed-in-premium is only an alternative to the non-used electricity which would be lost. The exchange contribution formulation is not so intuitive and depends on multiple parameters that vary with the market prices of electricity. So, a cost-benefit analysis about the feed-in-premium becomes tough to carry out, it shows a relevant dependence on the particular case under study and it depends on the effective quantities of electricity consumed and immitted into the electrical grid.

An ambiguous point of the feed-in-premium criterion is linked to the term “cost of energy”. Actually, the total cost of an energy bill is divided into three items (Figure 1.4):

- *Energy cost* (pink striped area): it covers the price for the electrical energy consumed, the grid losses and the dispatching cost.
- *Transport cost* (pink honeycomb area): it comprises the charge for energy transportation and distribution. The data management as well as the meter readings are included.

- *System cost* (pink area): it includes the expense for the activities of general interest on the system
- *Taxes* (grey area)

The last three quantities don't depend on the contract for electricity supply. The remaining quantities are equal for every energy provider since they are established by the ARERA (Autorità di Regolazione per Energia Reti e Ambiente, the authority for energy grid and environment regulation).

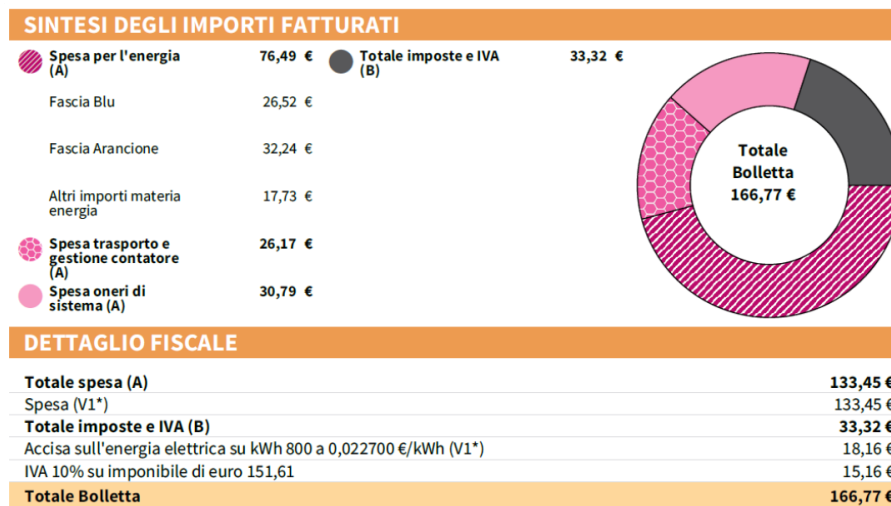


Figure 1.4. Example of the detailed energy bill for civil electricity meters [12].

With reference to Figure 1.4 it is very common for civil electricity meters that the energy expense is comprised between one third and half of the total import of the energy bill. As a consequence, the matter of fixed costs plays a fundamental role in the cost-effectiveness analysis since they are not negligible.

When the exchange contribution and the related refund are computed by means of Equation (1.5). The fixed costs are partially accounted, for instance by means of the coefficient CU_{se} . Indeed, the balance only in terms of fixed costs is negative. For the same given amount of energy imported and then consumed later, the users pay the fixed costs twice: once when the electricity is imported and once it is delivered again. The refund partially pays back only one of these two passages of electricity within the national grid. At first approximation, the fixed costs are always greater (between one and two times) than the ones paid in the context of a non-feed-in-premium contract for a given electricity consumption. Preliminarily, the increase of the fixed costs can be amortised in large installations where the economic amount of electricity exchanged is greater than the fixed costs.

Moreover, the feed-in-premium strategy allows the sale of any eventual surplus in the produced/consumed energy balance. According to the technical rules contained in the handbook issued by the GSE [13] the payable amount of the surplus energy of the i -th year is computed as

$$C_{surplus,i} = \max [0; C_{EI,i} - O_{E,i}] \quad (1.6)$$

At first glance with Equation (1.5), the term CU_{se} is missing. The concept behind the formulation is that whenever a sale of energy takes place in the feed-in-premium contract, no benefit on the paid fixed costs is accounted. This means that roughly 50-60% of the value coming from the sale of the energy is lost due to the fixed costs.

1.1.4. Some quantitative remarks

In this section a synthetic estimation of the order of magnitude for the energy cost under different conditions (standard energy supply, photovoltaic electricity self-consumption and feed-in-premium strategy) will be dealt.

- a) As far as standard energy bills for households in Europe are concerned, the average cost per kWh varies according to different parameters (e.g. consumption band, energy supply contracts). However, it generally fluctuates between about 0.20-0.30 €/kWh for households as shown in Figure 1.5.

Electricity prices, first semester of 2017-2019
(EUR per kWh)

	Households (*)		
	2017S1	2018S1	2019S1
EU-28	0.2043	0.2066	0.2159
Euro area	0.2210	0.2214	0.2294
Belgium	0.2857	0.2733	0.2839
Bulgaria	0.0955	0.0979	0.0997
Czechia	0.1438	0.1573	0.1748
Denmark	0.3049	0.3126	0.2984
Germany	0.3048	0.2987	0.3088
Estonia	0.1207	0.1348	0.1357
Ireland	0.2305	0.2369	0.2423
Greece	0.1711	0.1672	0.1650
Spain	0.2296	0.2383	0.2403
France	0.1704	0.1748	0.1765
Croatia	0.1196	0.1311	0.1321
Italy	0.2132	0.2067	0.2301
Cyprus	0.1863	0.1893	0.2203
Latvia	0.1586	0.1531	0.1629
Lithuania	0.1116	0.1097	0.1255
Luxembourg	0.1615	0.1671	0.1798
Hungary	0.1125	0.1123	0.1120
Malta	0.1328	0.1285	0.1305
Netherlands	0.1562	0.1706	0.2052
Austria	0.1950	0.1966	0.2034
Poland	0.1446	0.1410	0.1343
Portugal	0.2284	0.2246	0.2154
Romania	0.1198	0.1333	0.1358
Slovenia	0.1609	0.1613	0.1634
Slovakia	0.1435	0.1566	0.1577
Finland	0.1581	0.1612	0.1734
Sweden	0.1936	0.1891	0.2015
United Kingdom	0.1766	0.1887	0.2122
Iceland	0.1598	0.1545	0.1406
Liechtenstein	0.1724	:	:
Norway	0.1642	0.1751	0.1867
Montenegro	0.0983	0.1024	0.1032
North Macedonia	0.0820	0.0781	0.0783
Albania	0.0844	:	:
Serbia	0.0664	0.0705	0.0706
Turkey	0.1048	0.0904	0.0847
Bosnia and Herzegovina	0.0859	0.0864	0.0873
Kosovo (*)	0.0662	0.0633	0.0600
Moldova	0.0977	0.1020	0.0936
Georgia	:	0.0685	0.0809
Ukraine	0.0393	0.0410	0.0442

(:) not available

(p) Provisional

(*) Annual consumption: 2 500 kWh < consumption < 5 000 kWh.

(*) Annual consumption: 500 MWh < consumption < 2 000 MWh.

(*) This designation is without prejudice to positions on status, and is in line with UNSCR 1244 Independence.

Source: Eurostat (online data codes: nrg_pc_204 and nrg_pc_205)

Figure 1.5. Electricity prices from 2017 to 2019 for households [14]

- b) Photovoltaic electricity self-consumption: On the other hand, a photovoltaic plant in northern Italy can produce on average 1000 kWh per each kW_P installed, including the efficiency losses due to the ageing of materials [15]. Assuming a useful life 20 years long, the solar field is expected to produce about 20 MWh per each kW_P installed.

According to the current market standard, the total cost for PV panels installation is about 2500 €/kW_P while the maintenance costs can be quantified up to about 100 €/year [16], [17]. Indeed, the useful life of the inverter is shorter than the one of the PV plant (about 10 years vs 20 years). The distribution of the assumed average cost of 1000 € for the inverter over ten years of useful life leads to about 100 €/year. So, the total cost (installation + maintenance)

is about 4000-4500 €/kW_P. The cost of a kWh produced by means of PV field and self-consumed is about 0.20 €/kWh (= 4000/20000 €/MWh). This value benefits of a 50% reduction thank to the current tax incentives. In conclusion, the cost of the photovoltaic production for self-consumption is of about 0.09-0.10 €/kWh. In turn a saving of about 0.16 €/kWh can be reached with respect to case a).

- c) Feed in premium strategy: the following example can be considered. Over a fixed reference time (e.g. a year), a 3 kW_P PV plant produces 3500 kWh, sending to the grid 2500 kWh and taking 1700 kWh from it. The exchange contribution correspondent to the 1700 kWh produced and not-instantaneously consumed can be computed by means of Equation (1.5) assuming the average costs reported in the description of the equation:

$$CS = \min[O_e; C_{ei}] + CU_{sf} \cdot E_s \quad (1.7)$$

Where

$$O_e = 1700 \text{ kWh} \times 0.05 \text{ €/kWh} = 85 \text{ €}$$

$$C_{ei} = 2500 \text{ kWh} \times 0.06 \text{ €/kWh} = 150 \text{ €}$$

$$CS = \min[85; 150] + 0.08 \cdot 1700 = 221 \text{ €}$$

So, the feed-in-premium has led to a 221 € refund for 1700 kWh, namely 0.13 €/kWh back. The comparison with case a) depends on the ratio between the fixed costs with respect to the total cost. Assuming the fixed costs equal to one third of the total bill expense (Figure 1.4), the average price of 0.23 €/kWh normally paid in a standard energy bill (case a) is increased of:

- 0.07 €/kWh (one third of 0.23 €/kWh) to account for the further fixed costs due to the feed-in premium.
- 0.09 €/kWh to account for the costs of electricity production by means of the PV field (point b).

So, an average cost of 0.39 €/kWh is paid to consider the energy consumption, the cost electricity production by means of PV and twice the fixed costs. Including the refund of 0.13€/kWh the final expense is 0.26 €/kWh. This rough estimation has the only purpose to show that, up to now, the feed-in-premium strategy can lead, on average, to costs per kWh that are comparable with case a). Thus, they don't leave enough room for saving, as shown in the case of PV electricity self-consumption.

Actually, the real PV plants are associated to partial self-consumption and partial feed-in-premium strategy, so a preliminary estimation of a the cost can be obtained with the average of the costs reported in case b) (0.09 €/kWh) and c) (0.26 €/kWh) which leads to 0.16-0.18 €/kWh. The higher the self-consumption, the lower the cost and viceversa.

Always considering the example in case c), a surplus energy of 800 kWh has been produced over the reference time and it can be valued by means of Equation (1.6):

$$C_{surplus,i} = \max[0; C_{EI,i} - O_{E,i}] = (150 - 85)\text{€} = 65\text{€}$$

In this context, the gross price paid to the user is roughly of 0.08 €/kWh which cannot even cover the net cost for PV electricity production (about 0.09 €/kWh) without accounting for any other eventual fixed cost. A final remark is concerned with the location: as highlighted previously, the northern part of Italy has been considered. If the central/southern regions were considered, the electricity production per kW_p would increase up to 1500 kWh. In turn this would lead to a cost of about 0.06 €/kWh produced with the PV field (tax incentives already accounted). Even in this case the cost benefit analysis about the energy surplus sale might reveal negative or at most null (accounting for the fixed costs and the taxes associated to the energy sale).

Actually, the legislative change about the feed-in-premium strategy has implied as well an abrupt inversion in the trend in the PV diffusion, since the previous energy bill paid each kWh produced by means of PV about 0.40-0.45 €/kWh (the exact import depended on the size of the plant and on its architectural integration).

1.1.5. The main stages of the feed-in-premium laws over the past two decades

The legislative process that has led to the feed-in-premium approach is very complex and it consists in different laws followed by regulatory resolutions enacted by the Manager of Energy Services.

The original Law 133/1999 [18] allowed the feed-in-premium only for renewable plant with peak power production less than or equal to 20 kW_E. This law has been then confirmed by the Legislative Decree 387/2003 [19] and the relative resolution Legislative Decree n.28/2006 [20] of the MES. Here a net metering has been planned and it was represented by physical difference between immitted and delivered electricity.

Then the emanation of the “Integrated text of technical and economic terms and conditions for the feed in premium exchange” [21, 22] in 2009 and its related resolution for approval [23] introduced the following changes:

- Feed-in-premium extension to high efficiency cogeneration plants up to 200 kW. As far as the renewable ones are concerned, the Ministerial Decree 18/12/2008 [24], [25] included the installation with peak power production not greater than 20 kW_E.
- The management of the electricity exchange is carried out by the MES with a uniform approach all over the country.
- The old “net-metering” is substituted by the CS (energy contribution), the economic refund described in the previous section.

At the beginning of 2013 the Integrated text has been completely abrogated and replaced by the Ministerial Decree 06/07/2012 [22], [26]. The most significative change to the mechanism of the feed-in-premium consists in the adoption of a standard UP_{se} and the set of a maximum limit for the grid charges.

The most relevant variation in the laws concerning the feed-in-premium strategy was introduced by the Ministerial Decree 26/05/2015 (the so-called Minimum requirements decree). In particular, in annex 1, art.1, section iii, it stated that any eventual surplus in the electrical production by means

of renewable installations during some months couldn't be considered to cover the consumptions in other months with low electricity production.

The meaning of the rule is to encourage self-sufficient installations for electrical production where the electricity produced is almost directly self-consumed. In other words, the national grid can be considered as an accumulator to be used only in limit cases and always referring the energy balance to a monthly period. The aim of the legislator is to avoid the creation of installations with the specific purpose of energy production and sale to the national grid. Only the surplus electricity productions not entirely consumed by the installations shall be accepted within the feed-in-premium strategy.

As far as the civil and local applications are concerned, electricity can be produced only by means of photovoltaic applications. Indeed, hydroelectric or wind renewable energies best suit industrial/regional contexts in terms of both dimensions and installed power. So, the new legislative outline is a strong restriction to the design of photovoltaic plants since only two borderline cases are left:

- 1) Sizing of the plant in order to cover the electrical need in the month of maximum need. This implies a significative over-dimensioning of the plant with extremely high initial costs and surplus of unexploited energy.
- 2) Sizing of the plant in order to cover the electrical need in the month of minimum need. This strategy allows the consumption of the entire amount of electricity produced and it results in low installation costs. The electrical need of the facility surely requires an integration from the national grid and the contribution of the solar in the annual energy balance is minimal since the installation cannot fully take advantage of the irradiance available in summer.

Any other solution is included between these two extremes. Nevertheless, the full potential of photovoltaic applications is irremediably compromised due to the imposed monthly balance. In other words, this restriction cannot fit and exploit the ordinary variation of irradiance during a standard year in profitable way.

Actually the evolution of the incentives about solar fields and feed-in-premium strategies is still under development. The recent laws about Ecobonus 110% have introduced a radical change to the concept of feed-in-premium and the net-metering which will be briefly analysed in the last chapter about the revamping of the plant.

1.2. Heat pump

1.1.1 Key concepts

Heat pump (HP) is a very robust and versatile technology which works following the reverse cycle operating principle (Figure 1.6). Generally, in a reverse thermodynamic cycle, heat is transferred from a body with a lower temperature to a body with a higher temperature owing to the input of work inside the system.

1.2.1. Working and components of a heat pump

The following considerations are carried out under the simplified assumptions of steady state and no irreversibility (that means temperature gradient between the external ambient and the HP components, and internal reversible processes).

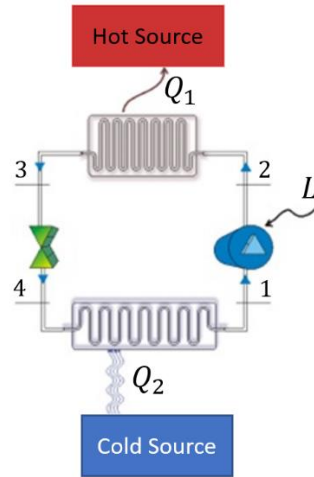


Figure 1.6. Inverse cycle scheme, with the main components of the heat pump.

Q_1 is the heat that the HP releases to the hot source, while Q_2 is the heat taken from the cold source. This heat transfer can be achieved by means of a mechanical work on the system, L . The performance of the HP can be quantified by the Coefficient Of Performance (COP) if considering Q_1 as the useful effect (in other words for heating applications). The COP structure is a ratio between useful effect and work spent to obtain it, Equation ((1.8):

$$COP = \frac{Q_1}{L} \quad (1.8)$$

As represented in Figure 1.6, the HP cycle belongs to inverse ones since a heat transfer from the cold source to the hot one is created in exchange for input work in the system.

The main typical components of the heat pump can be identified:

- **Compressor – section 1-2:** the refrigerant exiting the evaporator at low pressure and temperature is compressed up to a higher temperature and pressure level. The work input in the system reported in Figure 1 is associated to the electrical consumption of this component. The heat exchange determined by this component with the external environment can be neglected depending on whether the compression stage can be considered ideal or not.
- **Condenser – section 2-3:** within this exchanger, the refrigerating fluid exiting the compressor condensates, with a heat release to the hot source (the one to be heated, for instance a room).
- **Expansion valve – section 3-4:** it allows an expansion process to reduce the pressure of the refrigerating condensed fluid entering the evaporator. In standard vapor-compression

systems, this process is usually modelled as a throttling process during which enthalpy remains constant.

- *Evaporator – section 4-1*: within this exchanger, the refrigerating fluid exiting the expansion valve vaporizes subtracting heat from the cold source (for instance external air). In case of cooling, this heat flux is considered in Eq.(1) as the useful effect and the COP takes the name of EER (Energy Efficiency Ratio).

The main components identified above, with their respective sections, match with the temperature - entropy diagram (T-S plane) (Figure 1.7).

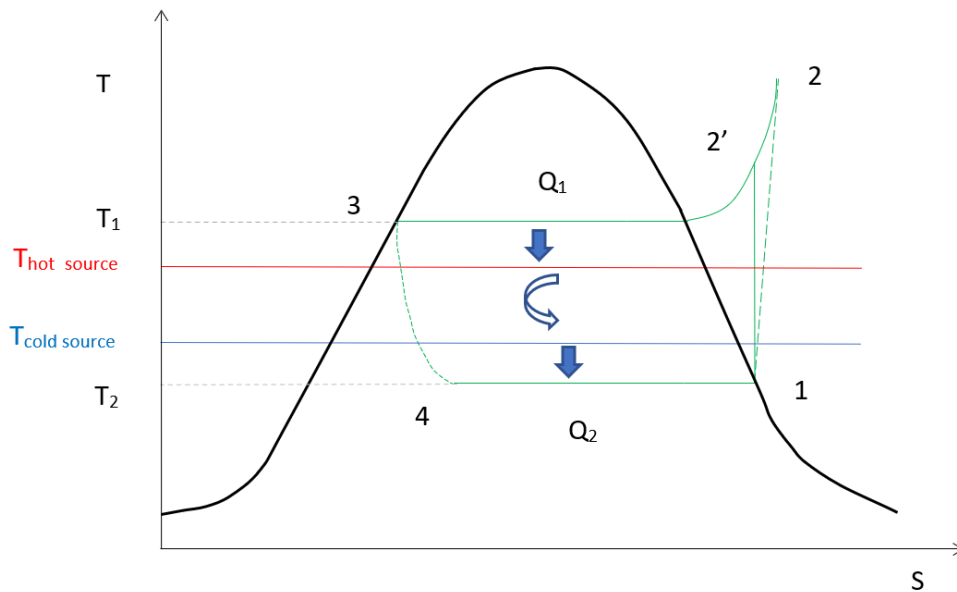


Figure 1.7. T-S diagram with a classic vapor compression inverse cycle. T_1 and T_2 are respectively the temperatures at the condenser and at the evaporator.

In particular:

- *Section 1-2 – compressor*: a compression takes place. The ideal process (isentropic) is represented by section 1-2'. In case the entropy production couldn't be considered negligible, the path 1-2 shall be considered. In an ideal process, point 1 should be on the saturated vapor curve. In a real inverse cycle, usually this point is "overheated" to grant a "dry" compression. In other words, to grant that only vapor enters the compressor to preserve it.
- *Section 2-3 – condenser*: isobar transformation – the refrigerant condensates. In an ideal inverse cycle, point 3 belongs to the saturated liquid curve. In real processes, this point is "subcooled" to ensure that only refrigerant in the liquid state enters the expansion valve.
- *Section 3-4 – expansion valve*: an isenthalpic process takes place and the fluid undergoes an expansion. Generally, two different kinds of valves can be employed:
 - *Capillary valve*: thanks to the friction inside the capillary holes, the refrigerant experiences a pressure drop (Figure 1.8(a)). Its use is mainly concerned with constant thermal loads application (e.g. domestic refrigerators or small-sized split), since this

valve can't modulate the refrigerant flow rate. In most cases, no fluid collector is employed because this would determine an excessive accumulation of refrigerant inside the evaporator with consequent problems on the start-up.

- *Thermostatic valve*: it controls the temperature of the refrigerant entering the evaporator and its level of overheating (Figure 1.8(b)). An almost constant liquid refrigerant flow rate at constant pressure is the target condition for an optimal working of the valve.
- *Automatic valve*: the expansion of the refrigerant occurs in order to maintain a constant level of pressure at the evaporator (Figure 1.8(c)). This means that this valve is not suitable for significant variation of thermal load. In fact, an increase in the suction pressure at the inlet of the compressor (e.g. due to the increase of thermal load) would determine a closure of the valve to keep the pressure at the evaporator constant. If then the suction pressure decreases significantly (thermal load reduction), a portion of refrigerant at the liquid state might enter the compressor.

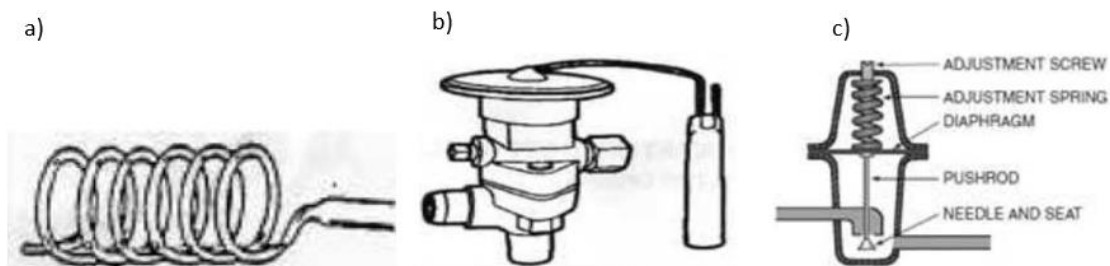


Figure 1.8. Different expansion valves: capillary (a); thermostatic (b); automatic (c).

- *Section 4-1 – evaporator*: transformation at constant pressure and temperature – the refrigerant evaporates.

As a change of state takes place both at the condenser and at the evaporator, temperature and pressure can be considered almost constant in the case of pure or azeotropic refrigerants.

1.2.2. Strategies to increase the HP COP

Focusing on Figure 2 and remembering Eq. (1.8) a higher COP can be reached in two ways:

- Increasing Q_1 – heat released to the environment to be heated (the hot source)

The quantity Q_1 is directly proportional the enthalpy gradient between points 2 and 3. This can be achieved by means of:

A) increase enthalpy at state 2. Actually, this increases Q_1 but at the same time it requires a higher electricity consumption at the compressor. As a consequence, the input work L increases and no significant benefit is obtained in terms of COP.

B) decrease enthalpy at state 3. This strategy is known as “subcooling” and it can be better understood referring to Figure 1.9. The points from 1 to 4 match with ones reported in Figure 1.7, while path 3-3’-4’-4 corresponds to the process of subcooling. An effective subcooling with relevant benefit in terms of COP can be obtained when the area in pink becomes

significant. This means that segment 3-3' has to be as large as possible, given a fixed expansion stage (segment 3-4 or 3'-4'). Actually, the length of this segment can even correspond to about 22 K of difference in temperature between points 3 and 3' that can be reached only with the addition of specific components (e.g. subcooler or condenser with subcooler integrated). In a standard inverse cycle with standard condenser, the length of segment 3-3' can reach about 4-5 K with no relevant improvement in the COP. In this case the subcooling takes place mainly to grant that only liquid refrigerant enters the expansion valve.

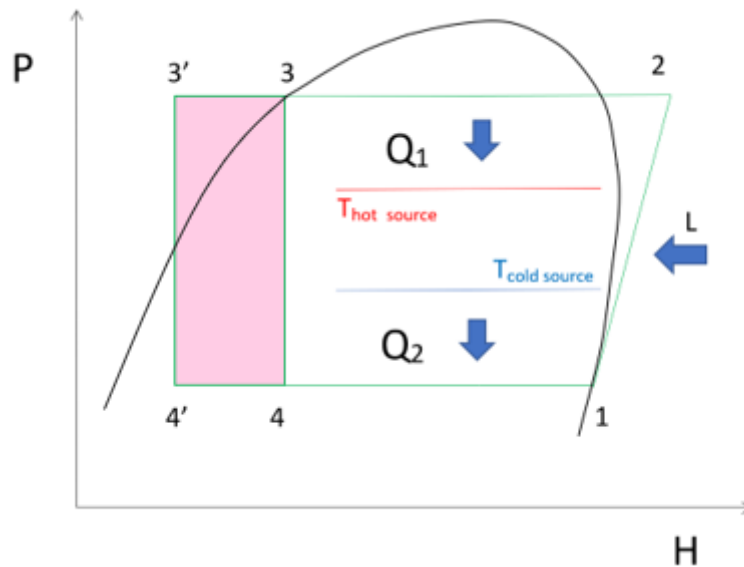


Figure 1.9. P-H diagram, representation of an inverse cycle with subcooling (area in pink).

- Decreasing L – mechanical work input, needed to pass from low to high pressure

The work, expressed by means of electricity consumed by the compressor, depends on the enthalpy leap between stages 1 and 2. In turn, these points depend on the temperature at the evaporator and the condenser. The smaller the enthalpy gradient between 1 and 2, the higher the COP. This target can be accomplished reducing the temperature gap between hot and cold side of the inverse cycle.

Considering an HP for heating purposes, the temperature at the condenser is fixed and related to the thermal demand of the building (e.g. the environment temperature) since it depends on the ambient temperature of the environment to be heated. Therefore, in this case the increase of the cold source temperature is the most remunerative way to increase COP. In other words, the main difficulty in the HP design for heating application is the choice of the proper thermal sources evaluated in terms of thermal inertia (stable thermal conditions and high thermal capacity). A brief summary of the main options is proposed below.

A) Exchange with external air: this is the most common and low-cost solution, especially for domestic HP applications. The main problem is connected to the extreme variability of the air temperature both in spatial and in temporal terms. For instance, during the cold season or when

considering the installation in cold places, the HP COP is strongly affected by the low temperatures. Furthermore, when approaching to the operation limit temperature (approximately 0°C) the HP stops and the evaporator is likely to freeze. Some advanced models have electrical boosters with defrosting function that active when the evaporator freezes. This affects negatively the COP since electricity is used to produce thermal energy basically by means of the Joule effect.

B) Exchange with ground: the ground temperature is more constant and experiences lower fluctuations with respect to the external air. In particular, a former thermally unstable layer where temperature varies according to the depth and the thermal season can be identified immediately below the ground level. Then moving deeper (between about 50 m up to 100 m) the temperature can be approximated as constant and equal to the yearly average temperature of the specific place considered. For depths greater than about 100m a geothermal gradient can be appreciated (approximately 3°C each 100m). These values are indicative and don't account for specific geothermal areas characterized by high enthalpy. The installation site has a strong influence on the performance of a geothermal heat pump system in terms of both morphology and enthalpy content. Furthermore, the initial installation costs are higher than the previous case.

C) Exchange with water: the evaporator exchanges with a water source that can be represented by the sea, a river, a lake or an underground aquifer. This solution is the least diffused due to the non-uniform availability of water and for environmental reasons. Indeed, sensible variations in temperature might have a negative impact on the fish fauna. Open circuit systems can be included in this context: water is directly withdrawn from the source (e.g. lake) and sent to an exchanger. In this case, the pollution of circulating water has to be considered as well as the previous environmental issues, leading to a very expensive design.

D) Exchange with the solar source: the evaporator exchanges with the water heated within a solar thermal circuit. This solution is affected by the time dependent environmental conditions. The initial installation cost results to be generally lower than for geothermal HP plants, especially when the solar collectors are employed only to heat the HP cold side and low efficiency ones can be installed.

1.3. Solar assisted heat pump

The Solar Assisted Heat Pump (SAHP) is conceived as an integrated system in which a heat pump is coupled with solar collectors. The technology itself is not so innovative because the concept was formerly proposed in 1955 [27] several solar-assisted-heat pump configurations have been investigated since the early years '80. Their diffusion on the market as profitable installations, alternative to the traditional renewable ones has always been limited. The main reasons can be identified in the technological complexity and the related highly developed control systems. These two aspects will be recalled along the following paragraph contained inside this SAHP – state of art

paragraph.

All the solar assisted heat pumps aim to increase the efficiency of the single components (HP COP and solar panel efficiency), as illustrated in paragraphs 1.1 and 1.2.2.

The SAHPs can be grouped in two main families:

- Direct expansion SAHP: it is the simplest version of this technology in which the solar panel works as the low temperature heat source (evaporator) as shown in Figure 1.10. The fluid flowing inside the panel is the HP refrigerant that evaporates subtracting heat from the energy collected by the panel. This condition is optimal to keep a stable level of the panel temperature since the fluid is subjected to a phase change. Nevertheless, this aspect doesn't prevent the risk of freezing inside the collector. Furthermore, no additional exchangers are required, and the related thermal losses are removed. In this configuration, the HP performance is strictly related to the features of the panel and the irradiance available. In particular, an increase in the volume of the panel capacity leads to a significative decrease in the condensing temperature with very small variation in the evaporation one. Consequently, the compression input work decreases with the rise of the COP [28]. At the same time, the uniformity in the distribution of the two-phase flow becomes more relevant as the size of the solar field increases [29]. One best way to cope with this problem is the separation of the solar thermal circuit from the HP one. In this way, refrigerant flows only within the HP while another fluid (e.g. water, air) can flow in the other circuit. Moreover, this reduces the global refrigerant charge in the plant with significant benefits in the pollution potential, eventual risk of flammability or poison (according to the refrigerant installed).

Experimental studies [28], [30] show that the COP varies between 4 and 6. [31] shows an average COP of 5.1 which is in good accordance with the previous range. Then, the COP drops to 3.5 during night when no solar irradiance is available and the ambient temperature is lower than the day.

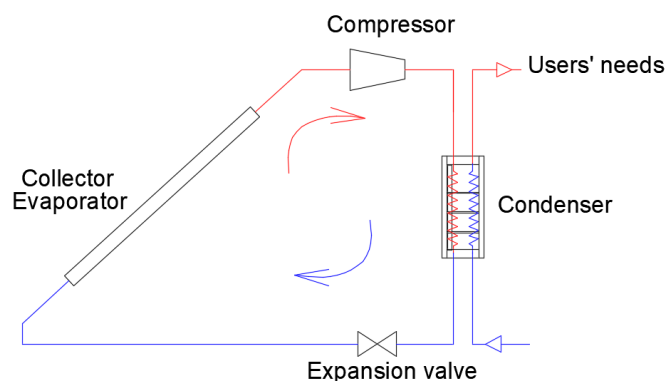


Figure 1.10. Basic version of a direct expansion SAHP.

In literature, many variants of this basic configuration can be found. For instance, the collector-evaporator of the SAHP studied in [31] benefits from both the incident irradiance and forced convection, thanks to a finned spiral collector provided with a fan. A schematic extract of the plant (Figure 1.11) is taken from the same paper.

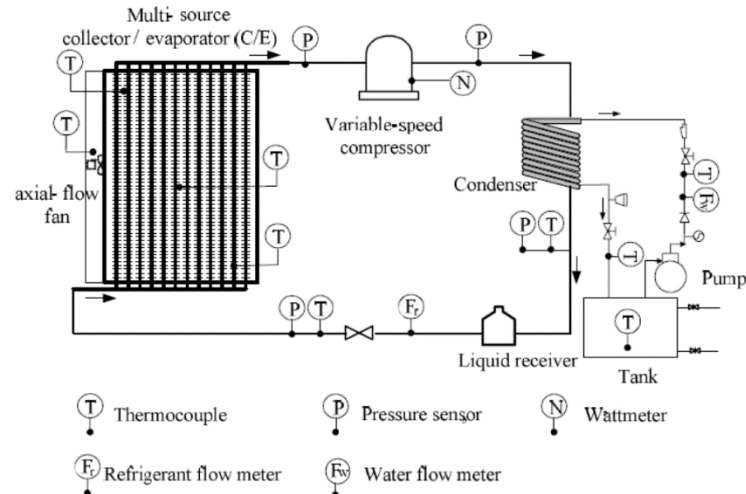


Figure 1.11. Plant scheme of the SAHP analyzed in [31].

Besides of the different setup of solar assisted heat pumps, a very important remark is concerned with the thick grid of measurement points (e.g. temperature, pressure, flow rates and electrical power) needed to correctly manage the plant. The simple addition of a fan creates three different regulation criteria of the collector:

- During sunny summer days there is wide availability of irradiance and the fan is off, since the evaporator temperature can be reached only with the contribution of solar radiation.
- When the solar irradiance isn't enough, the fan is activated as well.
- In case of absence of irradiance, only the fan is active.

The aim of this example consists in showing that even these simple installations require complex, time-varying plant management that can be hardly achieved by means of human intervention. A Data Acquisition and control System (DAS) becomes compulsory in the SAHP design since a more purposeful use of the auxiliaries would lead to a substantial increase in the COP.

Furthermore, the compressor has to allow variable speed in order to properly follow the variation in the thermal loads at the collector during different seasons [30].

- Indirect expansion SAHP: this plant results in a more complex scheme with respect to the direct expansion SAHP. The thermal solar circuit is interfaced with the exchanger on the HP evaporator. The solar thermal energy collected is used to increase the level of temperature on the HP cold side. Basically, three main subsystems can be identified (Figure 1.12):
 - Solar thermal field: the fluid flowing inside the panels can be a mix of water and glycol. It collects the solar energy by means of convection and radiation exchanges.
 - Heat pump: the refrigerant flows in the circuit and the evaporator benefits from the heat flux coming from the solar thermal field. The condenser interfaces with an exchanger to heat the water stored in the following subsystem.
 - Thermal storage system: it is connected to the distribution subsystem, to send SH and DHW to the users.

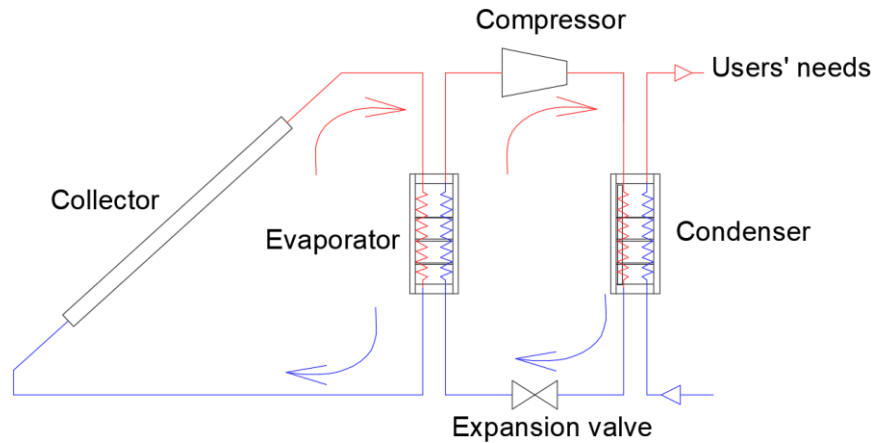


Figure 1.12. Basic version of an indirect expansion SAHP.

The presence of a heat exchanger that thermally connects the evaporator to the collector circuit allows a stable temperature at the HP cold side with consequent operative stability. Moreover, a hydraulic decoupling occurs and it grants the separation of the different circuits and it prevents mutual interference. On the other hand, the additional component causes supplementary heat losses and a decrease in the global efficiency. Different studies [32], [33] show that the benefit in the COP is really achieved if the electrical consumptions of the HP and its auxiliaries (e.g. circulation pumps) is kept low with respect to the size of the solar field. This means that the employment of indirect expansion SAHP is reasonable only in presence of medium/large size plants where the solar thermal power installed the plant justifies the complexity and consequent increase in electricity consumption. Many experimental simulations have been carried out [34], [35] obtaining a COP variable between 2.5-4.

1.3.1. Additional improvements for the SAHP

Besides of the primary distinction between direct and indirect expansion SAHP, there are multiple solutions that can be adopted separately or joined to reach an even more efficient configuration [36], [37], [38]. Some of the most common and interesting options are shortly illustrated below.

- Adoption of hybrid panels instead of the thermal ones. In this way, the addition of a properly sized photovoltaic field covers the electric consumption of the HP and of other auxiliary components. The COP benefits from the decrease of the input work L due to both the “free” photovoltaic electricity and the reduction of the thermal gap between cold and hot HP sides. In this case the SAHP is referred to SAHP-PVT which means Solar Assisted Heat Pump integrated with PVT (PhotoVoltaic-Thermal) panels. In this configuration the two components benefit one from the other. The HP increases its COP as illustrated before in paragraph 1.2.2 while the water flowing inside the panels maintains the operating temperatures low, with a significative increase of η_{th} and η_{el} (see Figure 1.2). The choice of hybrid panels optimises the space available since both thermal and photovoltaic energy is collected with the same panel. Secondly, the initial cost of a hybrid panel is smaller than the expensive for separate photovoltaic and thermal ones.

- Installation of other additional sources. The most common example consists in a dual asset SAHP where a solar source is arranged in serial (Figure 1.13a) and Figure 1.13c) or in parallel (Figure 1.13b) and Figure 1.13d) with an air source. The examples shown in Figure 1.13a) and Figure 1.13b) are the two possible combinations of the serial/parallel asset of the sources with direct expansion SAHP while Figure 1.13c) and Figure 1.13d) show the serial/parallel configuration for indirect expansion SAHP [39].

Some considerations on the two solutions:

- Serial asset: from the point of view of the plant scheme, no complication is introduced since the fluid flows within two successive exchangers. The crucial problem is represented by the priority given to the different sources. Indeed, “colder” source has to be put before the “hotter” one. Actually, this distinction is not fixed during a generic day: early in the morning, the air temperature contribution might result higher than the solar one. This trend might be reversed at about midday in summer sunny days where the maximum irradiance makes the air source contribution negligible. In other words, the order of the sources disposal binds the temperature of the fluid circulating inside the system. The relevance of the solar source with respect to the air one changes over the day and the in determined conditions the second exchanger might work inversely, losing the collected heat. This configuration can be profitable when each source involved has a stable or at least predictable variation and a fixed disposition can be identified. Otherwise this plant complication might reveal a worsening instead of an improvement. Considering a direct expansion SAHP (Figure 1.13a)), the serial asset makes optimisation strategies difficult: the variable solar contribution causes an overheating of the refrigerant fluctuating during the day. In turn the power consumed at the compressor is not stable and the COP varies as well.

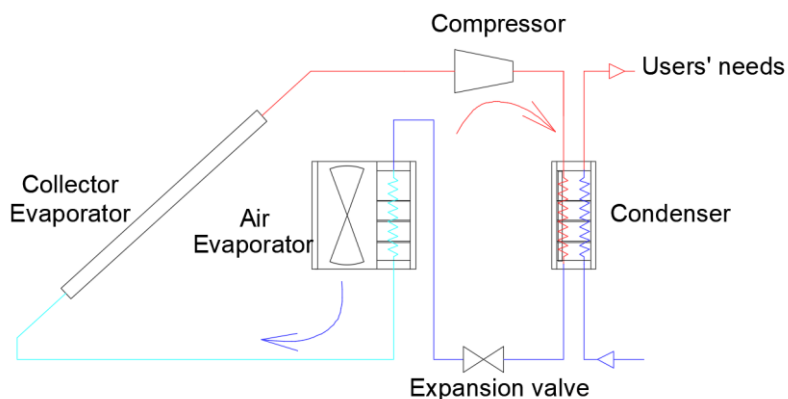
Figure 1.13c) represents the indirect expansion SAHP with serial connection between the solar and air sources. The heat absorption of the HP evaporator is supplied by the solar collector. Then a fan can provide an additional heat flux to the evaporator. The difference between the serial asset for direct and indirect expansion SAHP lies in the existence of the heat exchanger, which is usually a water tank. This asset allows significative reductions in the quantity of refrigerant inside the circuit.

- Parallel asset: the two sources are disposed in distinct circuits, one excluding the other. The choice of the most profitable source is carried out according to the instantaneous boundary conditions (e.g. irradiation, air temperature) and the switch occurs by means of specific valves. This configuration allows to overcome the problems of the serial asset. Basically, the HP can work either as a SAHP or as a traditional HP exchanging with air. As far as the direct expansion SAHP is concerned (Figure 1.13b)), this solution may cause some troubles associated to the balance of the refrigerant charge at the switch from one source to the other. Indeed, the heat flux delivered at the collector/evaporator might be different to the one at the air-evaporator. So, the sudden switch carries along issues of refrigerant equilibrium at the change of the evaporator. A proper regulation of the mass flow rate is required, and it cannot be handled “manually”.

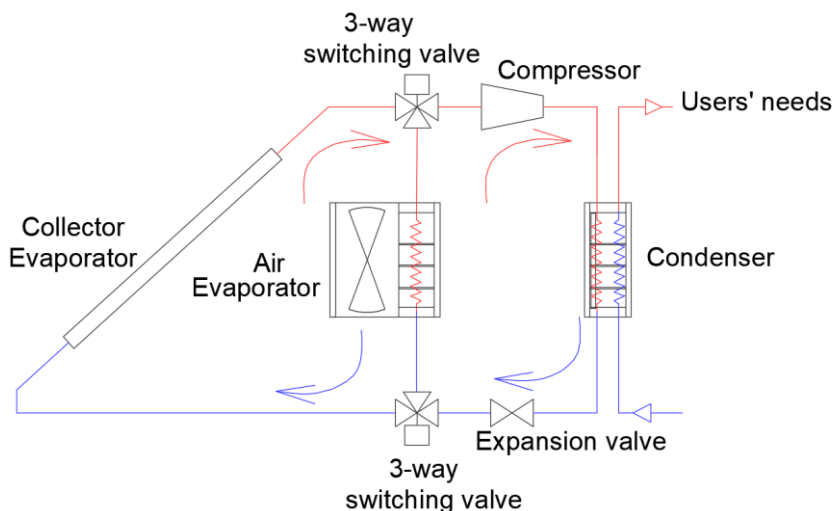
Figure 1.13d) is concerned with an indirect expansion SAHP in parallel asset with the solar and air sources. Two exchangers are necessary with respect to the direct expansion configuration (Figure 1.13b)) leading to a major plant complexity. On the other hand, a smaller quantity of refrigerant circulates in the system and the presence of an interface exchanger with the solar field allows the reduction of the problems in the balance of the refrigerant charge [40].

An automatized control system has to gradually act on the entire plant set of parameters (e.g. valves, pump speeds) up to stable conditions are reached again. In addition, this switch might occur many times during a standard day and the parameters that regulate this mechanism (e.g. irradiation, air temperature) show a highly oscillating trend. The plant has to be equipped with a DAS that automatically and almost instantaneously manages the plant asset to obtain always the optimal configuration. “Manual” intervention will be required only exceptional cases (e.g. extraordinary maintenance). Indeed, SAHPs without any control system would be bound to remain unsuccessful technologies.

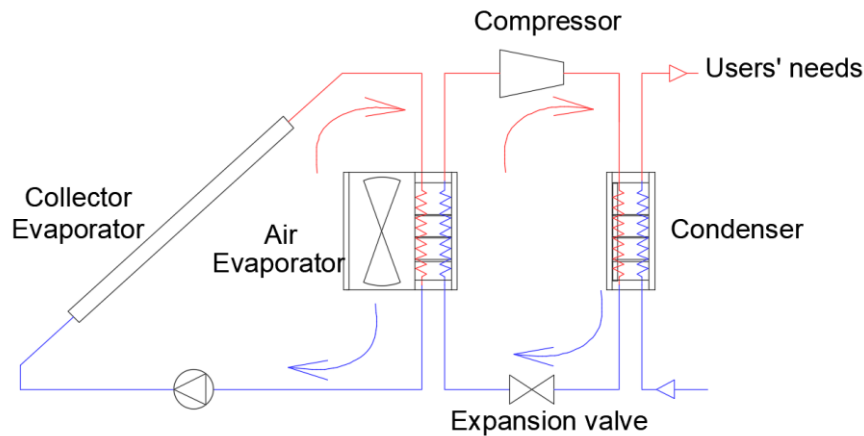
a)



b)



c)



d)

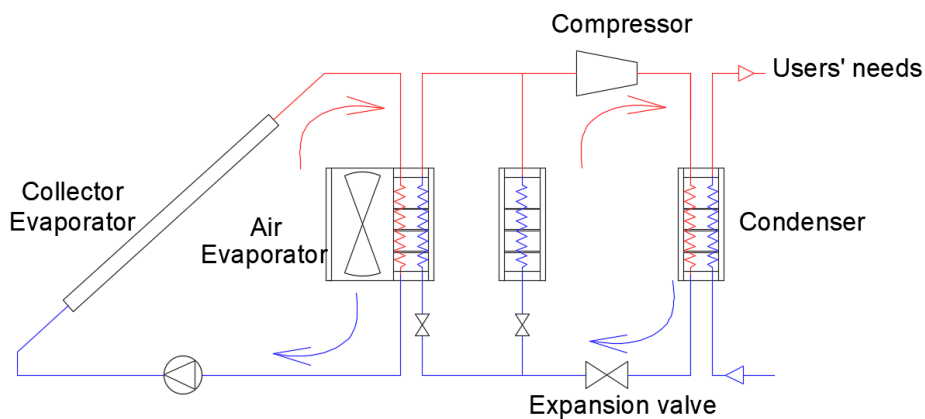


Figure 1.13. Different SAHP dual source configurations. a) Serial direct expansion SAHP, b) parallel direct expansion SAHP, c) parallel indirect expansion SAHP, d) serial indirect expansion SAHP

1.3.2. Comparison between solar thermal panels and SAHP

This paragraph is meant to give a term of comparison of these two technologies highlighting the high potential attainable with their coupling.

- The design of solar thermal panels for direct application in heating plants (Figure 1.14) is associated to an elevate working temperature. Indeed, the temperature of the panel (T_p) has to be slightly higher than the one required by the users (e.g. $T_u = 50\text{ }^{\circ}\text{C}$ for DHW needs) to account for eventual losses. This causes a higher cost of the panel, due to the insulation required to increase the panel efficiency. Furthermore, the higher T_u and the higher the losses to the environment that can even reach about 60% of the captured energy [41].

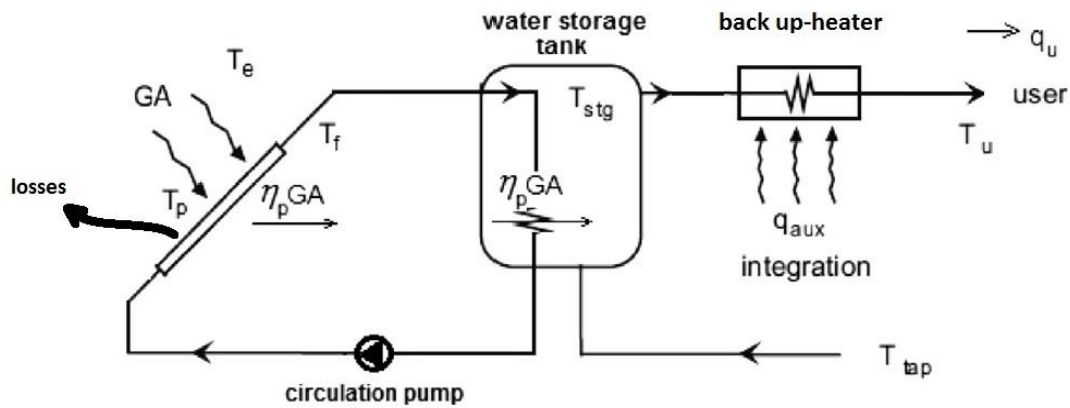


Figure 1.14. Traditional thermal solar panel concept.

Figure 1.15 better clarifies these concepts. The region on the left (light yellow) is where maximum efficiency can be reached (higher than 75%) since the gradient between collector and ambient temperature is small. Basing on the limited view of traditional design for the thermal collectors, this region can be suitable only for heating swimming pools or similar applications. Then, increasing the thermal gradient, the efficiency decreases, showing an inverse relationship with the thermal losses. This trend is unavoidable since the most common application in civil plants (DHW and SH) requires high thermal gradients and even the evacuated tube collectors suffer from a loss of about 15% of the initial efficiency. The different slope of the efficiency curves in Figure 1.15 reduces as the thermal panel is built with more advanced and expensive materials and techniques. Neglecting the former region in light yellow, Figure 1.15 clearly shows that the thermal losses are intrinsic of the working principle for this approach.

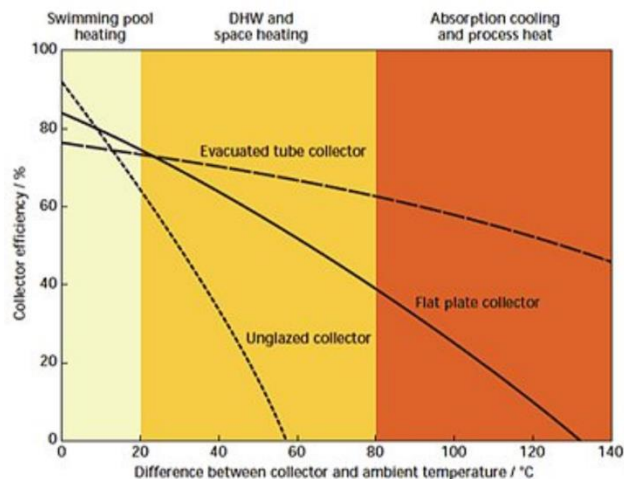


Figure 1.15. Qualitative trend of the efficiency for different kinds of solar thermal collectors as a function of the thermal gradient between the collector and the surrounding environment [42].

This leads to plants that can cover a very small percentage of the users' needs (about 15%) with very large capturing surfaces and thermal storages. Solar thermal coverage of the users' needs is not granted with continuity along the year, so an integration circuit is always required (e.g. fossil burners). In order to contain the heat losses, expensive insulated panels have to be

installed and located as close as possible to the thermal storages to shorten the hydraulic connections. From an economic point of view, a high installation cost is required (about 30€/kWh) with very long pay back periods for the investment.

- The clever design of SAHP (Figure 1.16) allows the overcome of the previous problems with multiple advantages.

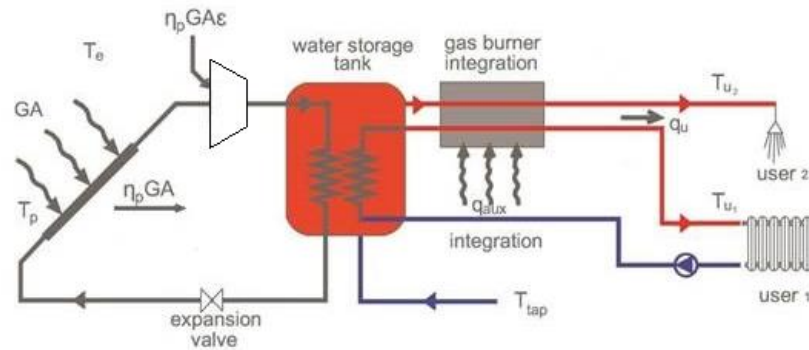


Figure 1.16. Integrated solar assisted heat pump with gas burner back-up heater.

Firstly, the connection of the solar collector to the evaporator of a HP allows a T_p that can be different from T_u . Indeed, T_p is now associated to the temperature at the evaporator, T_{evap} , which is much lower than T_u . Then, the inverse cycle of the heat pump will provide water at T_{user} by means of the condenser (T_{cond}) to meet the required needs. In this way, the panel working temperature is kept at about the ambient temperature with a very small losses to the ambient (down to 5%). With reference to Figure 1.15, this determines a shift of the panel working range from the yellow to the light-yellow region for the same SH and DHW application. The cost of solar energy decreases as well (about 10€/kWh) since bare panels cheap can be used while their efficiency increases [41]. As illustrated in the previous paragraphs (1.2.2) the COP benefits as well.

This configuration allows a greater freedom in the disposition of each component of the plant. For instance, the solar thermal field can be installed also at long distances from the HP. The water flowing inside the circuit is at about the ambient temperature, so the thermal losses are negligible and bare pipes can be adopted with very low additional cost. The collectors can work with continuity over the year and the SAHP can cover up to about 70% of the annual thermal needs.

On the other side, the additional electrical consumption of the HP is introduced and the plant scheme complication (e.g. auxiliary heat exchangers and related interface) requires a smart control to grant the correct working of the SAHP.

1.4. Palacus pilot plant

The Palacus heating plant represents a peculiar pilot plant for its relatively high-power size (up to 300 kW). It produces Domestic Hot Water (DHW) and Space Heating (SH) of the Sport Palace of the University of Genoa by means of a solar assisted heat pump integrated with hybrid panels (SAHP-PVT) interfaced with traditional gas burners (GB). This coupling has been conceived to make the plant a leading example for all other similar sport plants with similar features proposing a good

match between plant design and sustainability. The thermal need of the structure both in terms of SH and of DHW is affected by the different inflow of customers both on the short time scale (e.g. days or weeks) and on the longer time scale (e.g. year).

The installation consists in a direct expansion solar assisted heat pump integrated with hybrid panels (direct expansion SAHP-PVT). This part of the plant is coupled with two fossil burners which eventually integrate respectively the DHW and SH production.

The aim of this SAHP-PVT design is concerned with the installation of an efficient and functional plant that minimises the intervention of the auxiliary gas burners. The target of the plant is to make the sport palace self-sufficient, providing its thermal needs by means of renewable energies and sustainable plant solutions (e.g. SAHP-PVT).

Given the size of the plant and the its initial installation cost, the University of Genoa – DIME department formerly realized a small scale SAHP-PVT prototype in collaboration with Bifreezer Company. The following paragraph provides a brief description of the prototype.

1.4.1. Prototype

The experimental set-up has a smaller size if compared to the Palacus pilot plant described in the following paragraph. Besides the size, the prototype was assembled before the Palacus SAHP-PVT design took place. It consists in a direct expansion SAHP, since its compact dimensions would hardly host an indirect expansion configuration and the related exchangers. Figure 1.17 provides a global overview of the prototype.



Figure 1.17. General overview of the SAHP prototype.

This difference with respect to the Palacus pilot plant doesn't affect the validity of the results carried out from the prototypal simulation. Indeed, the target of the prototype is to establish a proper design and optimized control criteria to give the SAHP a competitive role in the renewable energies market. This issue abstracts from the type of SAHP and its COP since the concept of SAHP dates back to the '70-'80 [38], [43] of the past century and the plant performances that can be achieved

represent quite a consolidated concept in the scientific literature, especially for small refrigeration appliances [44], [30]. One aspect that hasn't been solved yet is the absence of a common approach to manage the problems of control and plant complexity [45]. Another issue is concerned with the challenge of the SAHP-PVT assembly with components available on the market instead of tailored ones, built in laboratory. This feature is the first "sine-qua-non" requirement for competitive plants and their large-scale industrial production.

Within this context, the instrumented prototype of a SAHP provides a powerful tool to characterize the best control strategies, and to measure and optimise the energy performance indexes with good reliability. In this way a preliminary analysis has been carried out as well as the outline the main control strategies for the design of the Palacus pilot plant.

1.4.2. Main outline of the plant

As shown in Figure 1.18, a standard HP has been modified and integrated with the following components:

- Solar thermal collector which acts as an evaporator. It is a very simple and low-cost element where a heating coil is installed under an aluminium blackened flat plate of about 1 m².
- Photovoltaic panels: in this prototype the benefits illustrated before for a SAHP-PVT are not completely exploited. In fact, the solar side of the plant consists in two different components, one thermal collector and two photovoltaic panels.



Figure 1.18. The SAHP-PVT prototype – main components.

Figure 1.19 provides a schematic representation of the set-up including the inner components of the HP.

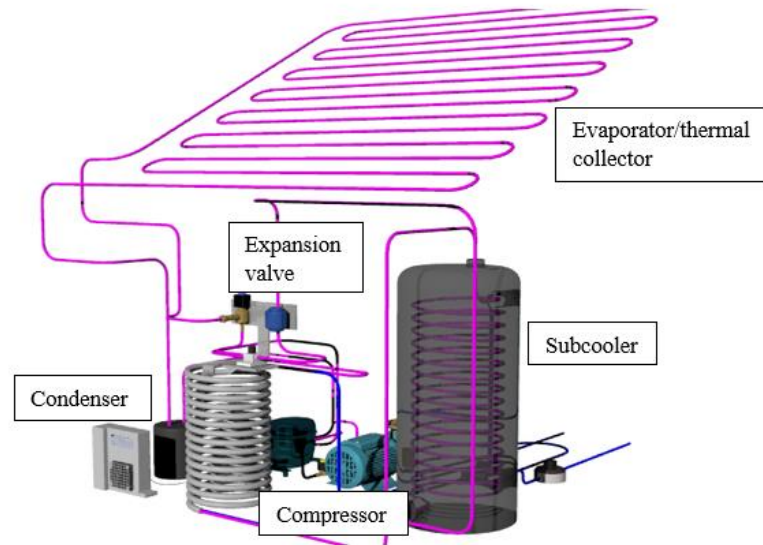


Figure 1.19. Plant scheme of the prototype and name of the main components.

The HP is equipped with a VCC (Variable Capacity Compressor) adapted to work in a higher temperature range with respect to its design working parameters due to the presence of the solar collector/evaporator.

The condenser is a coaxial pipe heat exchanger, with water circulating in the outer section loop, with an additional serial specific sub-cooler water tank.

An EEV (Electronic Expansion Valve) regulates the throttling process of the refrigerant exiting the sub-cooler, obtained from a small 20 l tank.

In parallel with the plant, an acquisition and control system has been realised. Its purposes include the refrigerant thermodynamic states calculation and automatic set-point optimization. Besides of the relatively simple scheme and small size of the plant, the onboard instrumentation consists in: 14 NTC (Negative Temperature Coefficient) temperature sensors, 2 analogical and 2 piezoelectric manometers, 1 flow meter for the water loop, 1 solar meter and 1 wattmeter for the measurement of the electrical consumption of the compressor. Ambient air humidity has been measured by means of dry-bulb and wet-bulb temperature measurements. This is the minimum data set required to have a complete oversight of the working parameters of the plant. The missing values (e.g. refrigerant mass flow rate) are deduced analytically, for instance using the global energy balance equations. Moreover, a parallel electric apparatus has been implemented to send the information to a linked “target” pc by means a standard USB data acquisition board.

These considerations provide a realistic example of the plant complexities that arise during the realisation of the relatively simple concept of SAHP. Once more the proper design of a data control and acquisition system is the only way to bypass these issues and aim to a competitive plant.

The simulation carried out under forced irradiance have led to very promising results [46]. A former estimation states that the ratio between the efficiencies of the SAHP collector and the classic thermal panel can reach a value up to 3. This means a significative reduction in costs and overall dimensions.

1.5. Palacus SAHP-PVT pilot plant – a description

This section is meant to provide a deep insight in the pilot plant, including the thermal needs of the structure and each main sub-system which belongs to the heating plant. Figure 1.20 illustrates a simplified block diagram of the plant to let the reader understand the general complexity of the problem and focus on the key components afterwards discussed.

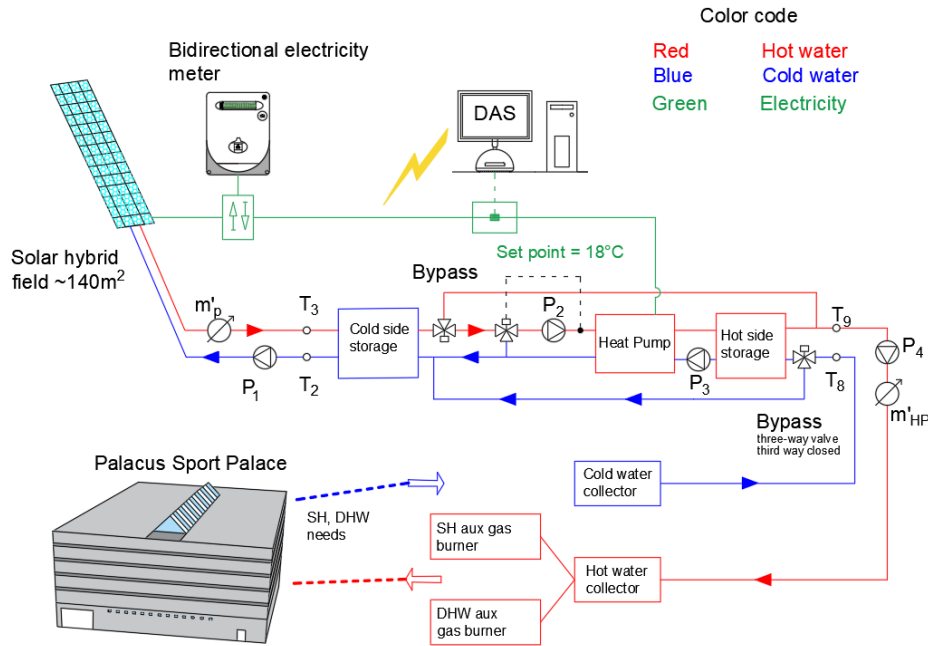
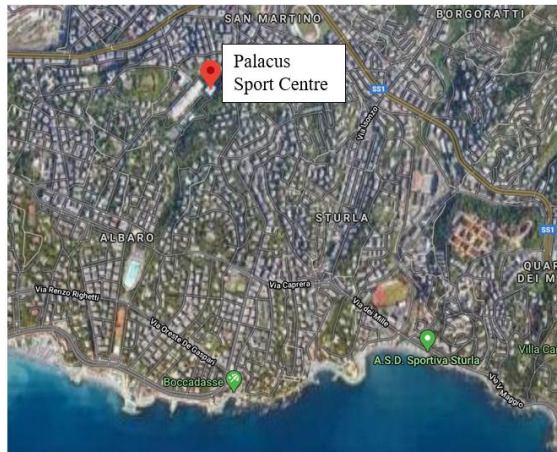


Figure 1.20. Block diagram of the pilot plant at Palacus Sport Palace, University of Genoa.

1.5.1. Palacus sport palace – the facility

Carmino Romanzi sport palace, known as Palacus, is placed in a wider green context of a sport centre run by CUS, an acronym meaning University Sport Centre. Figure 1.21 provides a global framework of the Palacus.

a)



b)

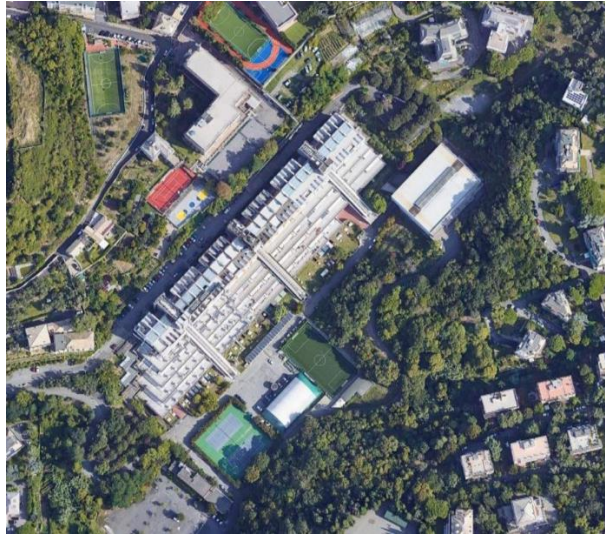


Figure 1.21. a) the position of the Palacus sport palace over the district of Albaro, Genoa and b) the multi-sportive complex with Palacus and the neighbouring sport courts [47].

The sport palace is of strategic importance for the surrounding district. It guests many different activities and classes, such as aerobics, fitness, yoga, martial arts, athletics, volleyball, basketball. A major gym Figure 1.22a) as well as smaller ones are available inside the building, Figure 1.22b) to d) together with six lockers.

a)



b)



c)



d)



Figure 1.22. Some gyms inside the Palacus building.

Around the sport palace, the multi-sportive complex is equipped with many outdoor courts as reported in Figure 1.21. In particular, six tennis courts (included the ones under the pressostatic cover) and a soccer field are accessible almost all week long from 9 to 22 on average.

The sport facility aims at multiple and diversified categories of users, from the students to senior sport classes. Individual activities as well as team sports are played even in parallel, from the amateur up to the competitive level.

This brief qualitative description is meant to give the perception of the consistent, strongly time dependant demand represented by such a wide group of users which is distributed all over the opening hours. The relevant volumes of the sport palace with all its internal environments give an idea of the energy order of magnitude spent to heat them.

According to the energy audit carried out during the design stage of the SAHP-PVT plant, the following estimations for space heating and domestic hot water demand can be provided:

- The heating system serves the lockers, the gyms and the sports hall (used for volleyball, basketball and other sport activities from classes for beginners up to competitive matches). The heated volumes are around 30.000 m³ formed by the sport hall, the bleachers, the over six lockers, the gyms, the offices and the reception. The related primary energy need is about 240 MWh/year.
- As far as the DHW consumption is concerned, the need is strongly variable and time dependant as its distribution tends not to be uniform over the day. Moreover, the lockers inside the sport palace are also used by the athletes attending to the seven external tennis courts. The related primary energy need is about 30 MWh/year.

On the stream of a very rough analysis, these primary thermal needs imply an average annual expense of 30 k€, assuming an average cost of gas equal to about 0.10 c€/kWh.

1.5.2. Solar hybrid field

A total area of 140 m^2 formed by 80 bare hybrid panels is installed 200 m far from the HP and the remaining part of the heating system (Figure 1.23).



Figure 1.23. The solar hybrid subsystem. On the background, the Palacus sport palace and the heating plant.

The related net capturing surface of about 120 m^2 allows the PVT installation to reach the peak values of 50 kW_T for the thermal power and of 20 kW_E for the electrical power. The plant is divided into 20 rows, 4 modules for each row, with a 6° tilt angle and 45° azimuth orientation (S-W), as shown in Figure 1.24. The conjoint production of electricity and heated water (photovoltaic cogeneration) has been designed to cover the electrical consumption of the elements of the circuit (e.g. valves, pumps, the compressor inside heat pump) and increase the level of temperature of the HP evaporator with consequent benefits on the coefficient of performance (COP) as illustrated in the previous sections.

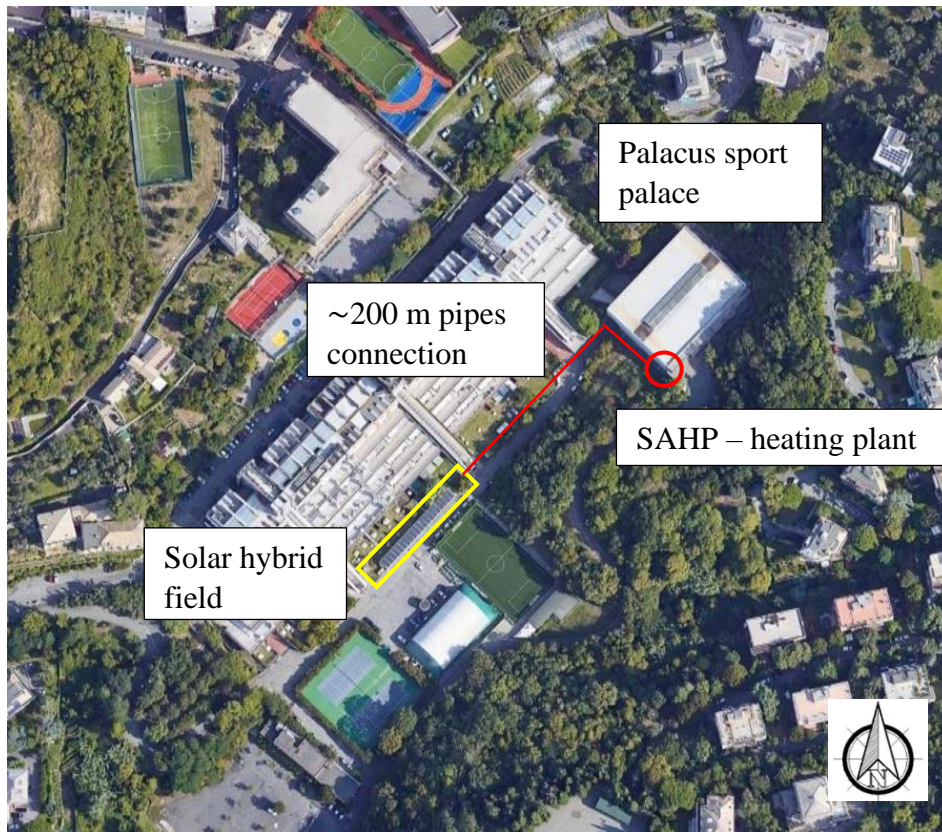


Figure 1.24. Location of the solar field with respect to the heating plant [48].

For the sake of a synthetic and clear exposition, the thermal and photovoltaic aspects will be dealt separately, with reference to the scheme reported in Figure 1.25:

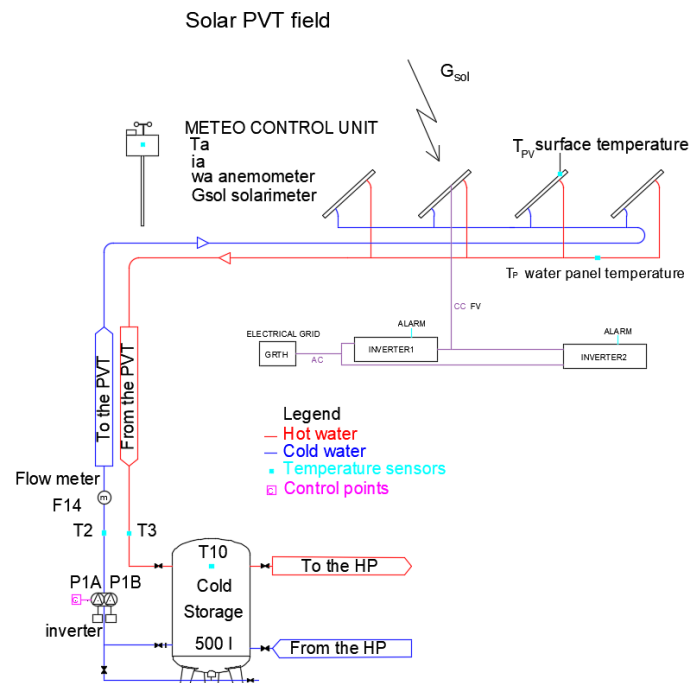


Figure 1.25. Schematic representation of the PVT solar field.

- Thermal side: a mixture of water and glycol flows inside the circuit to prevent any damage to the installation due to freezing. The water circulation is regulated by the pumping system P1. Water is heated through the panels and it is collected in a solar boiler of 500 l near the heating plant which is interfaced with the cold side of the HP. This boiler has the double function of thermal storage for the solar field and of stable temperature source for the heat pump. Neither the bare hydraulic connection 200 m long nor the missing insulation of the panels affects the solar thermal contribution to the heating plant. As outlined in the paragraph 1.3.2, the working temperature of the circuit is near to the external ambient temperature and therefore thermal losses are negligible regardless of insulation. This advantage has allowed to put the solar field in the most favorable position in terms of irradiance, regardless of the position of the heating plant and with little extra cost for the hydraulic connection. Indeed, the area of installation is not affected by relevant shading.

The interaction of the solar thermal field with the evaporator grants an almost continuous exploitation of the solar source during the year. Even during cold days, thanks to the mild climate of our region, the temperature reached inside the solar circuit is enough to heat the evaporator and grant a valuable COP.

The key measured parameters are associated to the inlet/outlet water temperatures (T_3 and T_2), the working period of the circulation system represented by the pump P_1 and the mass flow rate meter (m'_p). This pumping system is equipped with inverters, to allow a variable flow rate inside the circuit, according to the environmental boundary conditions (Figure 1.25). The solar heat rate entering the cold-water storage of the HP can be expressed (neglecting the heat capacity of the pumping and auxiliary systems) as shown in Eq. (1.9):

$$\dot{Q}_{Th,p} = m'_p c_p (T_3 - T_2) \quad (1.9)$$

And the related thermal energy (E_{Th}) computed integrating over the maximum operating time $\Delta\tau_{tot}$ (Eq. (1.10)):

$$E_{Th,sol} = \int_0^{\Delta\tau_{tot}} \dot{Q}_{Th,p} d\tau \quad (1.10)$$

- Photovoltaic side: the panels are made of polycrystalline silicon solar cells, with laminate Glass eva-Backsheet and aluminium frame. The PV hybrid field is coupled to two solar inverter groups, connected to a bi-directional counter for national grid connection. A dedicated exchange of electric power contract (feed-in-premium strategy) has been available in Italy since 1999, to use the grid connection as a virtual electric storage to use later the surplus production of electricity. The design of the solar field was meant to exploit the peak summer productions (with very low electrical consumption) to cover the peak consumptions in winter (with very low available irradiance). Indeed, the tilt angle of the panels (about 6°) gives priority to the summer production since during this season the irradiation can be considered almost perpendicular to flats surfaces. In other words, the almost horizontal disposition of the panels was designed to exploit the maximum solar energy possible (especially on the PV side) in the period of highest

availability (summer). The annual energy balance between the consumed and self-produced quantities was possible thanks to the feed-in-premium strategy up to 2015. Chapter 4 provides a detailed example on how the annual balance of the plant has been affected by this change in the law.

The correct working of the PV field is controlled by a specific signal which flags on in case of failure or malfunction. A tension signal absence means lack connection between the panels and the grid. This signal helps to know the period over which panels have been connected and worked correctly.

The electricity produced over a specified time period (e.g. from τ_1 to τ_2) can be determined by means of Eq. (1.11):

$$E_{el,PV} = \int_{\tau_1}^{\tau_2} G(\tau) \cdot A \cdot \eta_{el} d\tau = A \cdot \eta_{el} \int_{\tau_1}^{\tau_2} G(\tau) d\tau \quad (1.11)$$

Where:

$G(\tau)$ is the mean daily global solar radiation per each month [MJ/m²]

A is the net solar capture area [m²]

$\eta_{el}(\tau)$ electrical efficiency of the panels [-].

The integral in Eq. (1.12) can be simplified as a first approximation introducing the average irradiance \bar{G} :

$$\overline{E_{el,PV}} = \bar{G} \cdot A \cdot \eta_{el} \quad (1.12)$$

In conclusion a meteo control unit collects data on the external climate (temperature, relative humidity, wind velocity and irradiance).

1.5.3. Heat pump

The HP (model WRL_H 026/161 - Aermec, refrigerant R410a) represents the core of the plant and it has been designed to cover the facility needs in terms of DHW and SH with a thermal nominal power of 62 kW_T and a related peak consumption of 12 kW_E.



Figure 1.26. Heat pump of the Palacus pilot heating plant.

Both sides of the HP are equipped with Water Storage Tanks (WSTs) of 500 liters each, granting proper thermal inertia. The boilers are named cold and hot side storage depending on whether they interface with the evaporator or the condenser respectively. WSTs ensure:

- stable heat transfer rate.
- temperature regulation.
- hydraulic separation between both the solar field with respect to the HP evaporator and the condenser with respect to the DHW and SH subsystems.

The working system of the WSTs follows the stratification criterion. For instance, the colder outlet water sent into the solar field and the cold inlet water coming from the evaporator are in the lower part of the tank. On the other hand, the inlet water from the solar field and the outlet water sent into the evaporator are in the upper part. According to Figure 1.27, pumps P_2 and P_3 regulate the water flow on the cold and hot side of the heat pump, respectively.

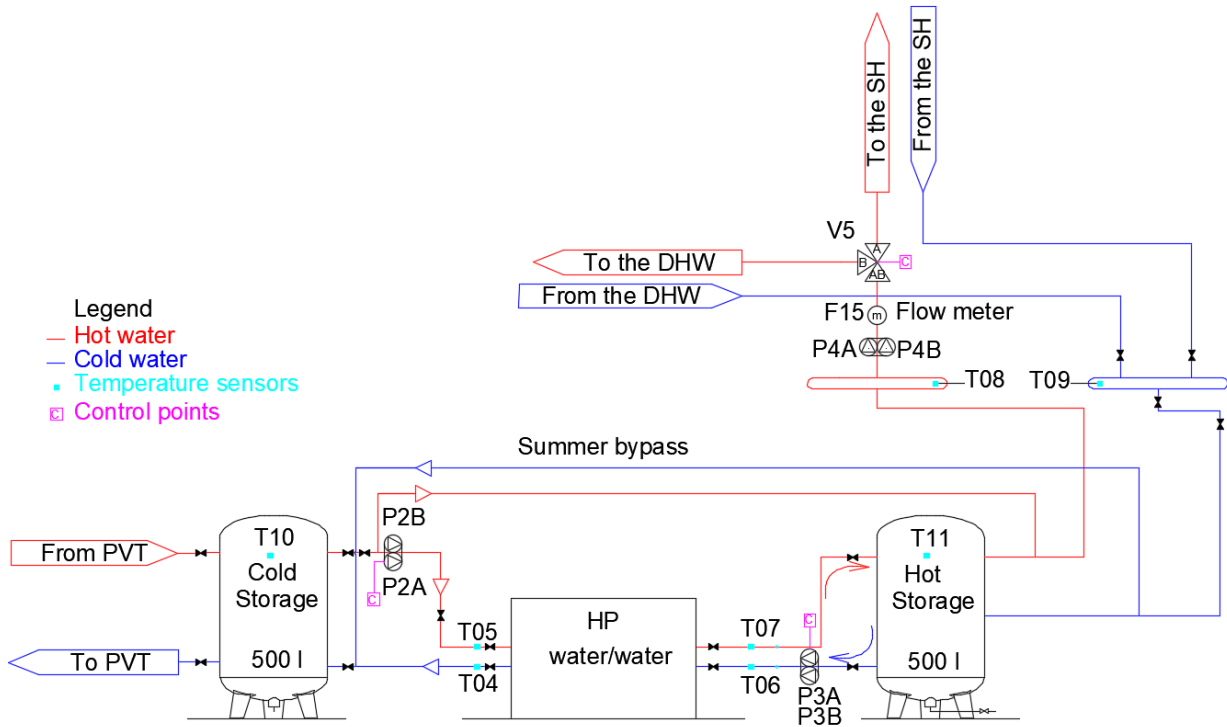


Figure 1.27. Schematic representation of the HP and the hot/cold storages.

The presence of the hot and cold storages allows an independent working of the two subsystems (correspondent temperatures T10 and T11). As far as the cold side storage is concerned, the thermal energy of the solar field can be collected even in the case the HP is off due to the absence of thermal demand. On the other hand, the HP can work also when the solar field is inactive, exploiting the thermal energy already stored inside the boiler.

Moreover, the hot storage provides a thermal inertia to the HP circuit avoiding its intervention each time a thermal need is present (e.g. single shower). In other words, if the condenser interfaced directly with the exchangers for DHW or SH production, each time a hot water draw happens (even from a sink), the HP would intervene to provide it. This in turn would cause the HP working always in transient conditions and for short time periods. Then the hot water collected inside the hot storage tank can be sent either to the DHW or the SH subsystem, according to the three-way valve V5 after pump P4.

With reference to Figure 1.27, pump P₄ allows the circulation of the water into the collector, according to the end users' needs, while a couple of temperature sensors is placed on the inlet and outlet water pipes (T₈ and T₉). A mass flow rate sensor (m'_{HP}) completes the data acquisition grid. A bypass is shown as well in Figure 1.27 which directly connects the solar field to the DHW subsystem. This particular feature will be specifically dealt later (paragraph 1.5.6). The following balances can be considered:

- *Used heat flux*: the associated heat rate exchanged on the hot-water storage side of the HP is

$$\dot{Q}_{Th,HP} = m'_{HP} c_{HP} (T_8 - T_9) \quad (1.13)$$

- *Used thermal energy*: it is related to the heat flux in Eq. (1.13) and it is computed integrating over the operating time ($\Delta\tau_{tot}$):

$$E_{Th,HP} = \int_0^{\Delta\tau_{tot}} \dot{Q}_{Th,HP} d\tau \quad (1.14)$$

Table 1.1 quantifies the benefit of the HP COP due to the interface with the solar field according to the operative outlet condenser and evaporator temperatures [°C].

COP		T _{out,cond}							
		25	30	35	40	45	50	55	60
T _{out,eva}	-8	4.46	4.26	3.9	3.41	2.82	-	-	-
	-6	4.74	4.49	4.1	3.6	3.01	2.37	-	-
	-4	5.03	4.72	4.30	3.78	3.19	2.55	-	-
	-3	5.18	4.84	4.49	3.87	3.28	2.64	-	-
	-2	5.33	4.97	4.50	3.96	3.36	2.73	2.39	-
	0	5.64	5.21	4.71	4.14	3.54	2.91	2.28	-
	2	5.97	5.47	4.92	4.32	3.71	3.08	2.46	-
	4	6.31	5.73	5.13	4.51	3.88	3.25	2.63	2.04
	5	6.48	5.87	5.24	4.60	3.96	3.33	2.72	2.13
	6	6.66	6.01	5.35	4.69	4.04	3.41	2.80	2.22
	7	6.84	6.15	5.46	4.79	4.13	3.49	2.89	2.31
	8	7.03	6.30	5.58	4.88	4.21	3.58	2.97	2.40
	10	-	6.60	5.82	5.08	4.39	3.74	3.14	2.57
	12	-	6.91	6.06	5.28	4.56	3.90	3.30	2.74
	14	-	7.23	6.32	5.49	4.74	4.07	3.46	2.91
	16	-	-	6.58	5.70	4.92	4.23	3.62	3.08
	18	-	-	-	5.92	5.10	4.40	3.78	3.24

Table 1.1. Variable COP according to the water operative outlet condenser and evaporator temperatures [°C] (water-water HP).

The operativity range of the HP is between -8 °C and 18 °C on the evaporator side and is between 25 °C and 50 °C on the condenser side. Thanks to the integration of the solar panels on the cold side, the thermal boundary conditions during the working period give rise to a variable COP, with a maximum of 6-8, as shown in Table 1.1 and in Figure 1.28.

A good performance of the HP (mean COP = 4) can be reached for temperature gradients between hot and cold sides in the range of 30 °C and 50 °C. For higher evaporator temperatures, the compressor would reach critical suction pressure and temperature levels, so that a safety valve will gradually shut down the plant. On the other hand, a decrease in the evaporator temperatures determines a progressively lower COP up to reach the HP Temperature Operation Limit (TOL). The

range of the outlet temperatures on the evaporator side are appropriate to the external conditions of the site (the design external temperature for Genoa is equal to 0 °C) while the mean efficiency (COP = 4) of the plant is granted in most operating conditions ($T_{out,cond} \in [45\text{ °C}, 50\text{ °C}]$ and $T_{out,eva} \in [0\text{ °C}, 10\text{ °C}]$).

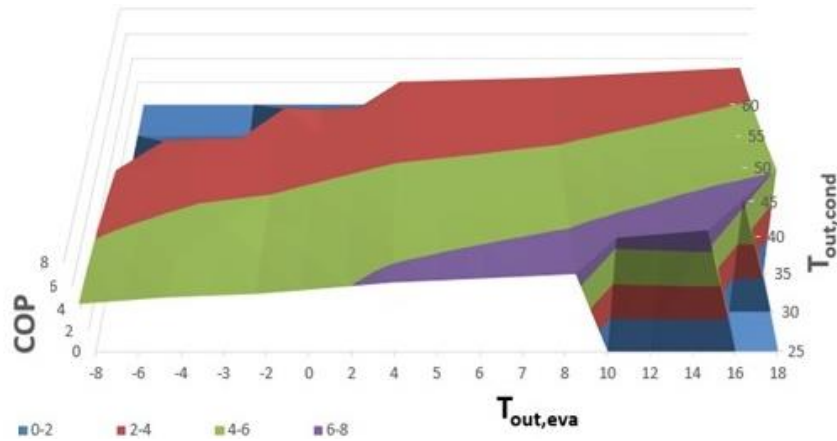


Figure 1.28. Three-dimensional graph showing the COP of the HP as a function of the outlet temperatures on the evaporator and condenser side.

1.5.4. Supplementary gas burners

The hot water produced by the SAHP-PVT is sent to a general collector by means of pump P4; here two supplementary gas burners can step in and eventually heat the water whenever its temperature lowers the imposed set points. The gas burners, respectively of 320 kW (used in winter when also SH needs are included, Figure 1.29a)) and 35 kW (used in summer when only DHW is asked Figure 1.29b)) show a mean seasonal efficiency of about 0.85.

a)



b)



Figure 1.29. Integration gas burners of the Palacus pilot plant for SH and DHW (a) and only DHW (b).

They represent the original heating plant of the structure. According to the regulation criteria, they should intervene only in strict environmental conditions, when the renewable part of the plant cannot fully meet the thermal needs of the facility on its own.

Besides the functional role of the gas burners inside the installation, the Palacus pilot plant provides a valuable example of how the existing heating plant can be integrated within the renewable one and not necessarily dismissed. In other words, a renewable-energy-based-system has been installed, supported by the non-renewable ones only in case of peak and severe environmental conditions.

1.5.5. Distribution system

This paragraph is intended to add the description of the final part of the heating plant. In particular, the subsystems for DHW and SH provision will be presented. Actually, the water heated by the HP can be sent either to the DHW or to the SH subsystem by means of the three-way valve V5. This plant configuration allows to fully exploit the contribution of SAHP sending the hot water only to the subsystem which requires it.

Domestic hot water side

A general overview is provided by means of Figure 1.30.

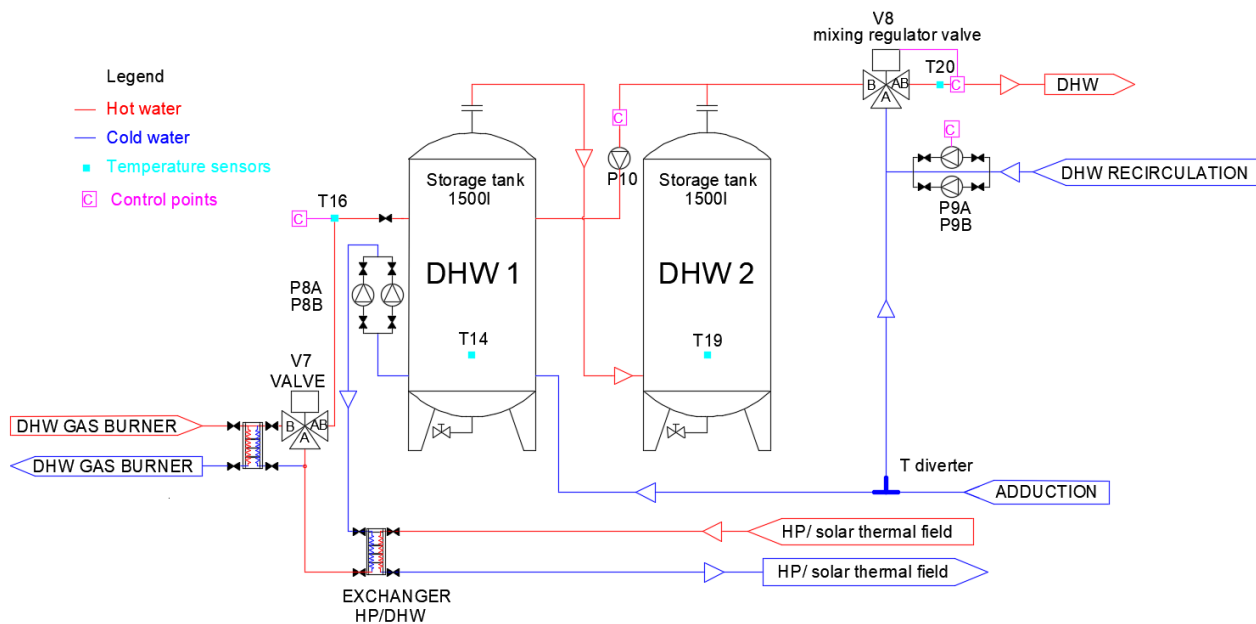


Figure 1.30. Detail of the Domestic Hot Water subsystem production at Palacus.

Two DHW tanks are named DHW1 and DHW2 in Figure 2 and they have 1500 l capacity each with 5 cm thick insulation. They store the DHW which is sent to a controlled mixing regulator valve V8 that keeps the DHW supply temperature at the set point value $T20^*$. $T20$ is the temperature measured downstream of V8 while $T14$ and $T19$ represent the temperatures in the tanks DHW1 and DHW2 respectively. The top of tank DHW1 is connected to the lower part of tank DHW2. This connection works independently from pump P10 which has been designed to create an internal recirculation between the upper part of DHW1 and top of DHW2. In this way the heating of DHW2 with the hot water from tank DHW1 is granted. The design choice of two 1500 l tanks instead of one

3000 l tank is due to problems of space inside the boiler room. Furthermore, this division allows to keep higher temperatures in DHW2 than the ones in DHW1 in which the water supply flows in. The water supply can enter DHW1 or it can be sent directly to V8 (side A) by means of a “T” diverter. The water supply before entering V8 is eventually mixed with the DHW coming from the recirculation system, granted by the twin pumps P9.

Only DHW1 is directly heated following specific priorities to maximise the renewable sources exploitation. Cold water is drawn from the lower part of DHW1 by means of the twin pumps P8 and sent to a first exchanger which interfaces with the hot technical water coming from the HP. During summer, the HP is off and a bypass directly connects the solar thermal field with the exchanger. Then if the inlet temperature T16 is lower than the required set point, valve V7 switches from A-AB to B-BA to send the water to a second exchanger interfaced with the 35 kW gas burner.

Usually the required set point temperature within both tanks is higher than 50 °C to prevent the legionnaires’ disease (actual set point value: 52 °C). The working range of the HP hot side in normal conditions is between about 45 °C and 50 °C. Neglecting the thermal losses associated to the insulated pipes and assuming an average loss of 5 °C due to the exchanger, the HP can give a significative contribution to DHW heating only when temperatures inside DHW are lower than 40 °C. In addition, any required set point higher than about 45 °C can be reached in winter only with the gas burner integration. In summer, the generally higher level of temperatures inside the solar thermal field reduces the contribution of the gas burners.

Space heating side

Two heating distribution circuits depart from the plant (Figure 1.31):

- Radiator circuit: the heaters are located mainly in the lockers. The average working temperature of the intake is at about 60 °C while the return oscillates around the value of 40 °C according to the thermal demand and the ambient temperature. The heated water coming from the collector downstream the HP hot storage reaches the SH subsystem when valve V5 is set on path AB-A. Then, it is sent to an exchanger that interfaces with the return water from the circuit of the radiators and it is sent back to the HP hot side storage. Downstream the pumping system P5, which regulates the flow rate to the radiators, a three-way mixing valve (V6) grants the intake temperature to be at T18. In fact, the return water from the radiators is heated through the exchanger with the HP circuit and then it is eventually mixed with the water heated by the gas burner to reach T18.
- ATU circuit: it provides heat flux to the heating battery of the ATU (Air Treatment Unit). The temperature levels are higher than in the previous case. For instance, the inlet temperature is set at about 70 °C and consequently the return fluid is at about 50 °C on average. The water flow inside is regulated by means of the pumping system P6. The HP operative range of the condenser, including the thermal losses along the plant, is at about 50 °C. Its eventual contribution to the ATU circuit is negligible and in fact no hydraulic connection has been planned.

Both circuits start and end in the same intake and return collectors. Consequently, valve V6 is likely to be active very often since the intake collector has to be kept at about 70 °C (inlet temperature for the ATU circuit) while the inlet temperature needed for the radiators (T18) is much lower. The configuration of V6 and the exchange with the HP circuit allow a saving in terms of exergy since the minimum amount of water heated by the gas burner is required in the mixing to reach T18.

As highlighted above, the heat pump itself cannot completely cover the SH thermal needs, especially with the kind of radiator installed. So, an integrative gas burner is required and the hierarchy in the circuit attributes the priority to the burner while the HP contribution ends up as the second place heating the return water from the radiators.

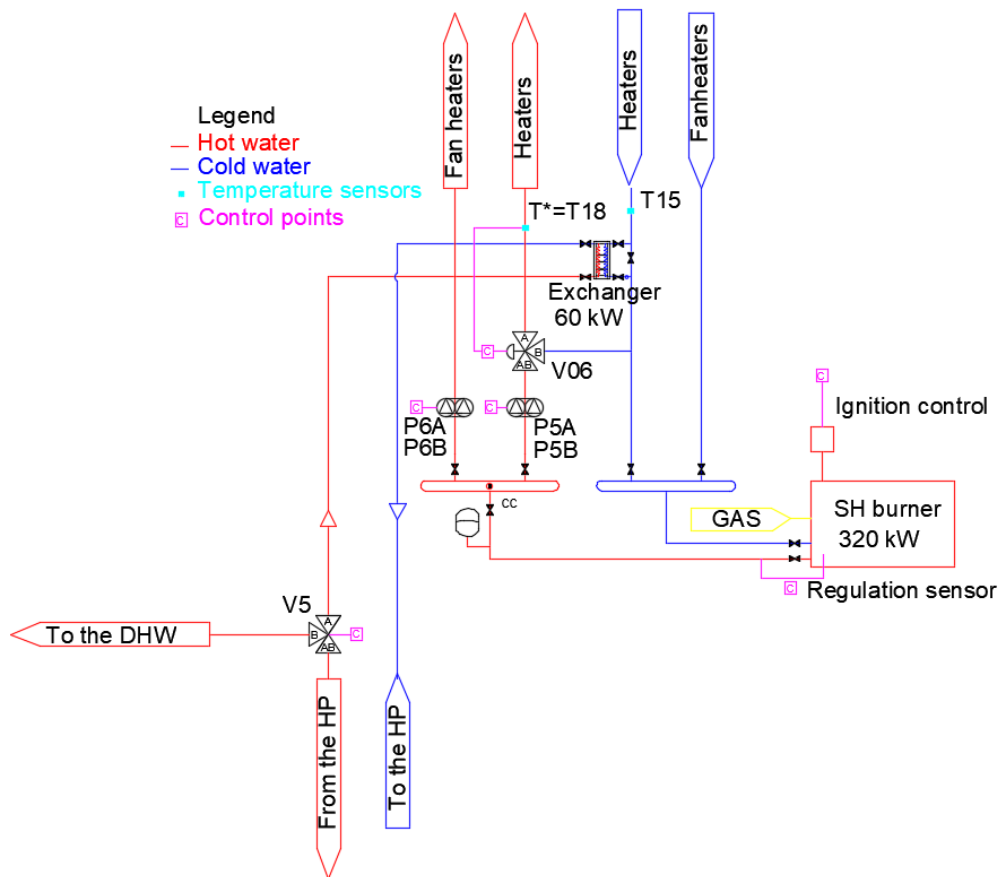


Figure 1.31. Schematic representation of the SH integration burners and the supplies.

1.5.6. Summer bypass

In the paragraph above, the standard working of each subsystem has been illustrated. Nevertheless, the SAHP-PVT has been designed as a heating plant during the cold season. If the designed working of the plant stopped here, a great amount of thermal energy would be wasted in summer. Indeed, the HP is inactive off the heating season and the thermal energy collected by means of the solar field would remain unexploited. Moreover, this condition might lead to the stagnation of the panels with a significative reduction in the electric efficiency and in the useful life of the components.

For these reasons, the summer bypass shown in Figure 1.27 has been installed. The purpose is to directly connect the solar field to the collector upstream P4 whenever the temperature T10 inside

cold side storage is higher than the one in the hot side storage ($\sim 45\text{-}50\text{ }^{\circ}\text{C}$) and can therefore provide a heat flux to the DHW1 tank (T14). This condition typically occurs in summer while it has never been exploited in other periods of the year. The bypass consists in a simplification in which the HP is bypassed and the solar thermal field works as a renewable classic installation interfaced with gas burners. The heat flux subtracted from the panels preserves high values of electrical efficiency. On the other hand, the thermal efficiency shows a significative decrease due to very high thermal losses of the bare PVT panels which are now working at $T_{\text{panel}} > T_{\text{environment}}$.

1.5.7. Monitoring and remote-control systems

The key concept at the basis of monitoring and remote system is that a proper management can be carried out only if a sufficient set of measurements is available. This aspect can be translated in the slogan “you manage what you measure”. Indeed, the acquisition of information put in the correct context is of paramount importance when approaching to an energy efficiency strategy.

The Data Acquisition and control Systems (DAS) can identify the critical and inefficient areas. Moreover, the acquisition over time allows rapid actions on the system to reduce the wastes.

Thanks to the technological progress, the data collected and the control components (e.g. valves or pump switches) can be made available on the web and even collected on a cloud platform. Once this step has been achieved, smart systems may be implemented to carry out complex calculations connecting to the cloud platform. These so called “Smart Energy Analytics” platforms are modular systems and they don’t require expensive programs to be installed by the single companies.

The DAS allows the control over:

- every energy carrier within the plant (typically gas, electricity and water).
- the related ambient parameters (e.g. temperature, relative humidity).
- the magnitudes representative of the process (e.g. status parameters, refrigerant/water flow rate, percentage of throttle opening).
- plant self-management, with particular attention to the ignition/activation of specific subsystems, automatic regulations, remote management, alarms and so on.

The common target consists in the reduction of primary energy consumption both from an environmental and an economic point of view by means of an optimal plant management. The deployment of such a wide system is representative of the awareness that a good energy management can lead to consistent savings on the medium and long-term period and to a deeper knowledge on the plant. Actually, the DAS has a wide range of action, from industrial to tertiary applications, from civil to renewable plants. For instance, some fields of application are listed below:

- Energy efficiency: reduction in the consumption, increase in production avoiding wastes by means of a greater awareness among users.
- Energy automation and industry 4.0: process automation to best exploit primary energy.
- Remote management: faster and remote control of the plant, with minor intervention costs.
- Defects control: simplified and programmed maintenance to reduce failures and grant the plant performance with continuity without sudden stops.

- Primary energy consumption control: the DAS allows a check on the energy quality and it identifies any possible failure.
- Renewable sources: this issue is concerned with performance and profitability of the investment in renewable plants.
- Environment and process measures: the parameters associated to the working of each plant component can be measured and to assess their correct working and productivity

Three essential components allow the DAS to operate:

- Physical infrastructure formed by sensors and monitoring instruments
- Network infrastructure which can be wired or wireless
- Software platform to collect and manage the measured database

As illustrated in detail for each subsystem above, the dataset is collected over a grid of 50 measurements points (e.g. temperatures, flow rates, HP performance). The plant can be managed through 16 control points (circulation pumps, mixing valves, set points, by-pass) which cannot clearly be handled by humans. Therefore, a data acquisition and control system is necessary to cope with the strongly discontinuous trends due to the dynamic working conditions of the plant and to avoid human intervention as much as possible.

A valuable DAS has to meet the following functional targets:

- Optimisation of the regulation criteria to decrease consumption of primary energy;
- Programmed maintenance instead of interventions after failures (e.g. through the measured working hours of the pumps)
- Remote failure control
- Measurement of the instantaneous consumption and data elaboration on monthly and yearly basis
- Energy efficiency evaluation as a function of the operating conditions.
- Plant management during standard conditions and choice of the most suitable asset according to the boundary conditions
- Data logging
- Remote access to the database and to the real-time parameters measured (e.g. temperature, flow rate) and eventually remote intervention.

A further improvement in the DAS equipped to the Palacus pilot plant consists in its web application, online since November 2016. An internet connected PLC (Programmable Logic Controller) has been installed to supervise and eventually operate on the plant, even remotely, according to the strongly time dependent environmental conditions and users' needs. The extended amount of data collected requires proper post-analysis and allows efficiency studies in order to build new regulation criteria and increase the plant efficiency also from the environmental point of view.

The experience given by the project presented in this article allowed to observe that, in order to couple at best old and new plants, the only reliable solution to handle the high level of complexity of the plant is the use of a remote smart control system. This is the only solution that makes the end-user able to overcome management and control difficulties.

Several operation modes have been identified, depending on the season and operation environmental conditions:

- DHW only with SAHP off: in this condition only the 35 kW gas burner is on to meet the users' DHW thermal needs, while the SAHP is inactive and the summer bypass directly connects the solar thermal field to the DHW subsystem. This operation mode is suitable especially during summer
- SH only with SAHP off: only the 320 kW gas burner is on to meet the users' SH and DHW thermal needs, while the SAHP is inactive. This operation mode is suitable especially during the heating season and represents the working condition previous to the SAHP-PVT installation. This setting can be used in emergency or extraordinary maintenance situations in which for instance the SAHP is blocked and the Palacus has thermal demands to be satisfied.
- DHW+SH with SAHP off: with this setting the summer bypass and the 320 kW burner are on, while the HP is off. This condition occurs mainly in spring or autumn. More generally this operating mode is suitable for intermediate climate conditions in which the solar thermal contribution is enough to be directly exploited.
- DHW+SH with SAHP: the HP and the 320 kW gas burner are on while the summer bypass is off. This configuration is representative of a solar thermal energy not enough to be directly sent to the DHW/SH subsystems. This situation can be associated to intermediate seasons (e.g. spring or autumn).
- DHW with SAHP on: only the HP and the 35 kW gas burner are active while the summer bypass is off. This condition occurs off the heating season when only the DHW demand is present. At the same time the thermal energy collected inside the solar circuit is too low to be used by the DHW subsystem.

The system as a whole is managed by a control unit organized in different control panels (over 11), in which each subsystem is represented with ad-hoc functional diagrams, from which all components can be controlled and all set points can be fixed. Figure 1.32 shows, as an example, the control panel related to the DHW system loop.

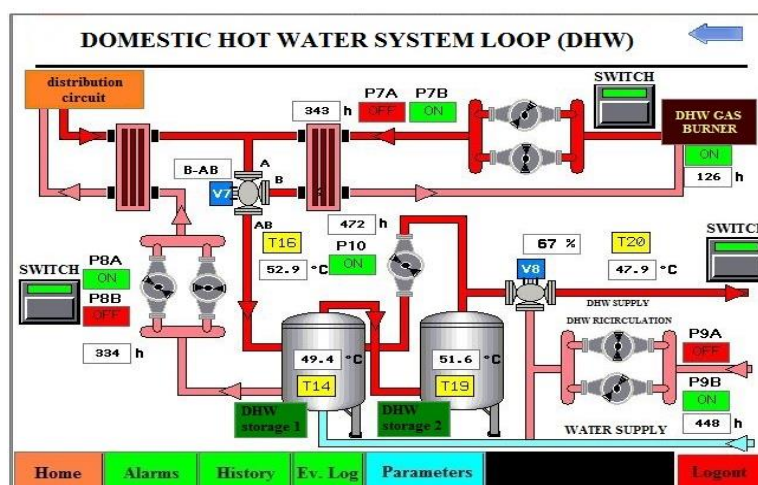


Figure 1.32. Control panels.

The five main operating modes listed before are just one of the issues allowed by the DAS. They enable/disable specific subsystems according to the users' choices. Nevertheless, inside each subsystem there is a great amount of regulation criteria which are managed by the DAS almost in real time. These criteria are about 70 in total and can be divided into two principal groups:

- *Self-maintenance criteria*: they are meant to activate independently from the users' thermal demand and their activation is led by sanitary needs or to protect the components and to keep them fully operative. For instance, the solar pumping system activates whenever the circuit is under stagnation or freezing risk, independently from the users' demand. Moreover, Legionella prevention cycles are planned as well.
- *Optimisation criteria*: they are aimed to provide rules followed by the DAS in order to always grant the plant performance with minimum integration gas burners contribution.

In conclusion, the SAHP-PVT cannot reach acceptable performances without a proper DAS. Its implementation has successfully completed the first stage in which measurement instruments that allow network connection and communication have been installed. Then, the second stage enters the final phase in which a smart monitoring and control platform is under development to provide the collected data in a coherent fashion and allow a remote and almost real-time control over the plant.

1.5.8. Palacus pilot plant - Expected performances

To conclude, a brief insight on the main magnitudes associated to the plant and their importance is presented in Table 1.2.

Annual performance of the SAHP-PVT at Palacus	
Primary SH thermal demand of the sport centre building	240 MWh/year
Primary DHW users' thermal demand	30 MWh/year
Thermal energy supplied by the SAHP-PVT to users	92,5 MWh/year
PV Electricity supplied	25 MWh _E /year
Electrical energy consumption by SAHP -PVT	14 MWh _E /year
Net yearly electricity saved (for other end-uses or for driving devices)	11 MWh _E /year
Mean heat demand energy coverage by means of solar energy	34%
Total net primary energy savings	9.4 toe/year
Total annual budget saving	6,5 k€/year
Total pilot plant construction cost	260 k€
Average annual cost facility per saved toe	27 k€/toe

Table 1.2. Main annual operating data and costs of the Palacus Sport Palace.

The input data of the primary SH and DHW thermal needs associated to the Palacus facility, the amount of thermal energy provided and the electricity consumed by the SAHP-PVT come from the energy audit carried out in the design stage. The topic of the energy needs related to the facility

are not specifically dealt in the present work, but they have been dealt in previous works and PhD thesis [49], [41].

The other parameters in Table 1.2 can be better understood and put in the correct context:

- PV Electricity supplied: the following hypothesis can be assumed

- annual average irradiance for Genoa -1430 W/m²/year
- the electrical efficiency of the PVT panels - about 15%
- net capturing area (80 panels of 1.45 m² each) - 116 m²

Following Eq. (1.12), the average annual PV production is equal to 24,88 MWh_E/year approximated to 25 MWh_E/year.

- Net yearly electricity saved: by means of a simple subtraction between the electricity consumed by the HP (14 MWh_E/year) and the one produced with the PVT field (25 MWh_E/year) about 11 MWh_E/year are produced every year and they can be employed for other electric devices within the structure.
- Mean heat demand energy coverage by means of solar energy: according to the thermal demands, a total amount of 270 MWh/year is required for the SH (240 MWh/year) and DHW (30 MWh/year) demand. On the other hand, the thermal energy supplied by the renewable plant is of 92.5 MWh/year. The ratio between 92.5 MWh/year and 270 MWh/year is equal to 34%.
- Total net primary energy savings: each year, the total primary energy saved is given by the sum of 92.5 MWh/year (from the thermal side of the plant) and 11 MWh/year (from the PV side) for a total of 103.5 MWh/year. Then remembering the relation between tep and kWh (1tep = 11.630 kWh), the energy saving of 103.5 MWh/year can be expressed as about 9.4 tep/year.
- Total annual budget saving: each tep can be valued as about 690 €. So, the total saving of 9.4 tep corresponds to about 6.5 k€/year.
- Average annual cost facility per saved toe: the total cost of the plant of 260 k€ can be expressed as function of the saved each year (9.4 tep). So, the annual cost facility per saved toe is 260/9.4 k€/tep = 27 k€/toe.
- Mean seasonal HP COP: According to the values reported in Table 1.2 the thermal energy supplied to the sport palace by the HP yearly is equal to 92.5 MWh. The related electrical consumption is of about 14 MWh each year. Basing on Eq. (1.8), the HP COP can be computed dividing the useful effect (92.5 MWh of thermal flux delivered to the structure) by the input work (14 MWh of electrical consumption at the HP compressor). This leads to a mean seasonal COP of 6.6 that might result higher than the average COP obtained by the other studies available in literature. Actually, this result is strictly related to the HP electricity consumption. In case the consumptions of the other electrical auxiliaries (e.g. the over 10 pumps of about 1 kW each, mixing valves) would be accounted, the mean seasonal COP would decrease to more suitable (and still high) values between 4 and 4.5. This aspect will be recalled in the final chapter about the revamping interventions on the pilot plant.

1.6. SAHP – another example in Liguria and the untapped potential

This section is meant to provide briefly another remarkable example of solar assisted heat pump in our region. Unfortunately, the widespread over our territory still hasn't occurred. Only about 1000 small SAHP plants have been installed all over the Northern Italy and the Palacus united with the example below are the only two “medium size” facilities available in Liguria. A little remark about the potential energy saving which might be reached is presented. The analysis has been carried out at a preliminary stage accounting for the different municipalities over the Italian Country.

1.6.1. The SAHP at the public swimming pool – Sestri Levante

Figure 1.33 provides the general layout of the 400 m² solar thermal field formed by bare panels on the roof of the swimming pool with a related peak power of 150 kW_T. The plant scheme recalls the one shown in Figure 1.19 and it can be conceived as a simplified version of the SAHP at Palacus.

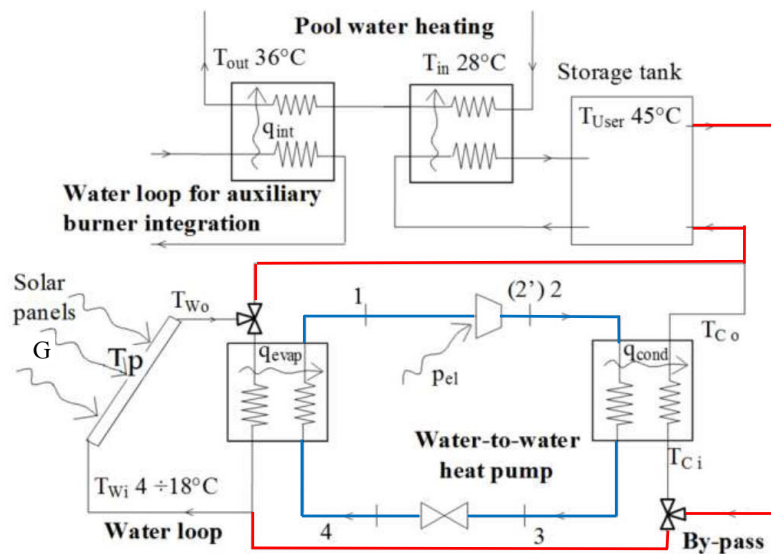


Figure 1.33. Plant scheme of the SAHP at the public swimming pool, Sestri Levante, [50]. The red circuit represents the bypass which directly connects the thermal solar field to the storage tank. The HP cycle is represented by the blue line and the numbers shown correspond to the ones used in section 1.2

The basic working concept of the plant consists in the production of hot water either from the SAHP or directly from only the solar field, when favourable boundary conditions are met (e.g. high irradiance, high external temperature). The hot water is collected inside a storage which has a set temperature of 45 °C in accordance with the working temperature range of the HP condenser and the losses within the circuit. Then water is sent from the storage tank to an exchanger that pre-heats the water in the pool. If the thermal flux delivery is not sufficient, an integrative exchanger provides an additional heat flux produced by means of gas burners.

Following the plant in detail (Figure 1.33), the water flowing inside the bare panels is heated from $T_{w,i}$ up to $T_{w,o}$. Then, a three-way valve sends the water either directly to the storage tank or to the exchanger with the HP evaporator (q_{evap} represents the heat flux transferred). Actually, when the water flowing out of the condenser is higher than 18 °C (limit working temperature for the HP evaporator), the water is left circulating inside the panels and quickly reaches temperatures of about

45 °C and the bypass is activated and the HP shut off. On the other hand, when the minimum working temperature is reached at the evaporator (about 4 °C), the HP would work with very low COP and the working of only the gas burners with the HP off is more convenient in terms of primary energy savings.

The HP cycle resembles the one illustrated in the state-of-art section for heat pumps (p_{el} is the electrical power consumed by the compressor and q_{cond} is the heat flux delivered by the condenser to the exchanger). The HP interfaces with a water loop again on the condenser side with an exchanger in which water is heated from $T_{c,i}$ to $T_{c,o}$ and then sent to the storage tank.

The SAHP facility is equipped with all the measurement and control systems needed with particular attention to the regulation parameters of the summer bypass (which works in the same way the one at Palacus does) and the auxiliary exchangers for the gas burner integration. The plant has been operating since July, 2012 and it can cover up to 60% of the winter thermal need (from November to March) and provides 100% of the thermal needs during the remaining part of the year. In addition, during summer, the bypass itself can manage the totality of the demand with negligible consumptions in the primary energy. The average annual thermal panel efficiency has reached a maximum value of about 85% that in turn can determine average HP COP up to 5.5 [51]. These performances are higher than the ones illustrated for the Palacus application. Actually, a comparison with the two operating schemes of the plant show a radical difference in the thermal demand. In the Palacus case, DHW and SH represent the thermal need to be satisfied as much as possible with the SAHP. In the swimming pool application, the contribution is concerned with the heating of water inside the pools whose temperature range [28; 36] °C is far lower than the one for DHW (set point at about 50 °C) and SH (inlet temperatures at about 60-70 °C). In addition, the user load profile can be considered constant along each day of the year with very little error.

1.6.2. The SAHP potential over the Italian territory

Actually, the positive results reported above have been both obtained from installations in Liguria, near the sea, in a very mild climate. Fortunately, the SAHP still has potential also for any other installation within every town Italy and their different weather, represents by means of the Degree Days (DD) and of the mean monthly solar radiation [50]. The key parameter used to quantify the potential savings is the Primary Energy Saving (PES) that is HP size independent and normalized with the nominal heating power of a reference gas burner. It is defined as a summation over the twelve months as follows [52]:

$$PES = \sum_{j=1}^{12} \frac{q_{boil,0}}{\eta_{boil}} - \left[(p_{hp} + p_{el,pc} + p_{el,sp}) f_{p,el} + \frac{q_{boil,0}}{\eta_{boil}} \right] \quad (1.15)$$

Where

$f_{p,el}$ is the electric-to-primary energy conversion factor, it can be computed as the inverse of the grid efficiency (η_{grid}) used in Eq. (1.4). Actually, since $\eta_{grid} = 0.49$ [53], $f_{p,el} = 2.04$. It can be conceived in other words as the kWh of consumed primary energy for each kWh of electrical energy produced. q_{boil} is the heat rate provided by the integration gas burners interfaced with the SAHP. In $q_{boil,0}$ the

heat rate is provided by a conventional gas-fired boiler without the SAHP.

η_{boil} is the corresponding gas-fired efficiency (reference value of 98% chosen in the work to fit a very efficient boiler working in the range of 50 °C and 70 °C). As far as the energy saving evaluation is concerned, the PES sensitivity to is very low, so that the variation of some percentual points in the efficiency determines no significant changes in the results obtained.

The results can be resumed in Figure 1.34.

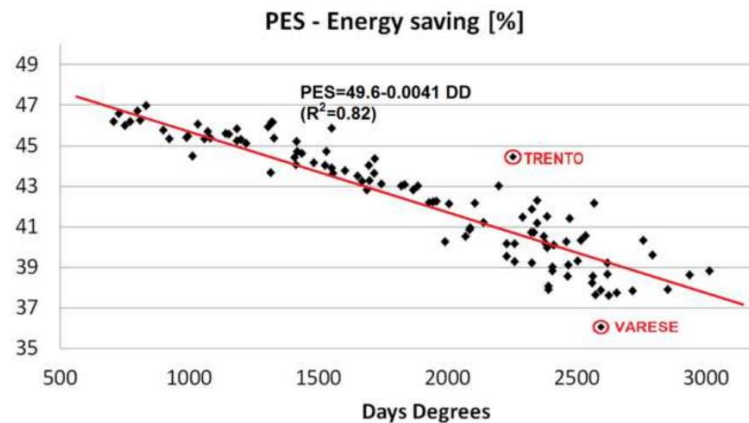


Figure 1.34. Values of the Primary Energy Saving (PES) index according to the different 110 Italian municipalities. The equation of the regression line and correlation index R are reported on the graph [50].

The correlation index reaches very high values and therefore the regression line can be applied with very good approximation. The only cities that stand clearly out from this trend are Trento and Varese. In conclusion, a saving up to 50% of the primary energy consumed can be reached for town with less than 500 DD. This occurs in very few places in Italy, well exposed and to the South (the ones belonging to the so-called climatic region A, only the two towns of Lampedusa and Porto Empedocle). For the other towns up to 3000 DD the minimum saving attainable is of 35%. Indeed, only 1048 towns out of 7989 in total (about 13%) stand out this last range and they are located mainly in the Alps. So, for about the 87% of the Italian municipalities the room for PES saving is really significative and therefore the SAHP technology reveals a potential that can be widely exploited over most of the Italian territory.

REFERENCES

- [1] ENEA, Rapporto annuale Efficienza energetica - Analisi e risultati delle policy di efficienza energetica del nostro paese, 2019.
- [2] E. Foundation, Just E-volution 2030- The socio-economic impacts of energy transition in Europe, 2019.

- [3] P. Charalambous , G. Maidment, S. Kalogirou e K. Yiakoumetti, Photovoltaic thermal (PV/T) collectors: a review, *Applied Thermal Engineering*, vol. 27, pgg. 275-286, 2007.
- [4] [Online]. Available: <https://www.itacanet.org/a-guide-to-photovoltaic-panels/photovoltaic-pv-cells/>. [Accessed 25 March 2020].
- [5] H. Wei, J. Jie e Z. Yang, «Comparative experiment study on photovoltaic and thermal solar system under natural circulation of water,» *Applied Thermal Engineering*, vol. 31, pp. 3369-3376, 2011.
- [6] isprambiente, 2019. [Online]. Available: http://www.isprambiente.gov.it/files2019/pubblicazioni/rapporti/R_303_19_gas_serra_settore_elettrico.pdf. [Consultato il giorno 6 July 2020].
- [7] [Online]. Available: <https://www.normattiva.it/uri-res/N2Ls?urn:nir:stato:legge:1999;133> . [Consultato il giorno 19 March 2020].
- [8] [Online]. Available: https://www.gse.it/documenti_site/Documenti%20GSE/Servizi%20per%20te/SCAMBIO%20SUL%20POSTO/Regole%20e%20procedure/Regole%20Tecniche%20Scambio%20sul%20Posto_2019.pdf . [Accessed 20 March 2020].
- [9] [Online]. Available: <https://luce-gas.it/guida/mercato/pun>. [Accessed 18 April 2020].
- [10] [Online]. Available: <https://www.arera.it/allegati/comunicati/CorrispettiviCUsf2018.pdf> . [Consultato il giorno 18 April 2020].
- [11] [Online]. Available: <https://www.arera.it/allegati/comunicati/CorrispettiviCUsf2018.pdf> . [Accessed 18 April 2020].
- [12] [Online]. Available: <https://lamiacasaelettrica.com/tariffa-d1-pompe-di-calore-2018/> . [Accessed 24 March 2020].
- [13] [Online]. Available: https://www.gse.it/documenti_site/Documenti%20GSE/Servizi%20per%20te/SCAMBIO%20SUL%20POSTO/Regole%20e%20procedure/Regole%20Tecniche%20Scambio%20sul%20Posto_2019.pdf . [Consultato il giorno 20 March 2020].
- [14] [Online]. Available: [https://ec.europa.eu/eurostat/statistics-explained/images/d/d9/Electricity_prices%2C_first_semester_of_2017-2019_%28EUR_per_kWh%29.png] . [Consultato il giorno 18 April 2020].
- [15] [Online]. Available: https://www.gse.it/documenti_site/Documenti%20GSE/Rapporti%20statistici/Solare%20Fo

tovoltaico%20-%20Rapporto%20Statistico%202018.pdf . [Consultato il giorno 18 April 2020].

[16] [Online]. Available: <https://www.sorgenia.it/guida-energia/mercato-libero/impianto-fotovoltaico-quanto-costa>. [Consultato il giorno 23 April 2020].

[17] [Online]. Available: https://www.gse.it/documenti_site/Documenti%20GSE/Rapporti%20statistici/Solare%20Fotovoltaico%20-%20Rapporto%20Statistico%202018.pdf . [Accessed 23 April 2020].

[18] Legge 13 maggio 1999, n. 133, "Disposizioni in materia di perequazione, razionalizzazione e federalismo fiscale", Gazzetta Ufficiale della Repubblica Italiana.

[19] Decreto Legislativo 29 dicembre 2003, n. 387, Gazzetta Ufficiale della Repubblica Italiana.

[20] Decreto Legislativo 23 gennaio 2006, n. 28, Gazzetta Ufficiale della Repubblica Italiana.

[21] Legge 23 luglio 2009, n. 99, Gazzetta Ufficiale della Repubblica Italiana.

[22] Decreto Legislativo 6 luglio 2012, n. 95, Gazzetta Ufficiale della Repubblica Italiana.

[23] Delibera 3 giugno 2008 - ARG/elt 74/08, Autorità per l'energia elettrica e il gas.

[24] Decreto Legislativo 18 dicembre 2008, Gazzetta Ufficiale della Repubblica Italiana.

[25] Delibera ARG/elt 1/09, Autorità per l'energia elettrica e il gas.

[26] Delibera 20 Dicembre 2012, Autorità per l'energia elettrica e il gas.

[27] P. Sporn e E. Ambrose , «The heat pump and solar energy,» *Proceedings of The World Symposium on Applied Solar Energy*, 1955.

[28] M. N. A. Hawlader, S. K. Chlou e M. Z. Ullah, «The performance of a solar assisted heat pump heating system,» *Applied thermal Engineering* , vol. 21, n. 10, 2001.

[29] M. Aubinet, «Longwave Sky Radiation Parameterizations,» *Solar Energy*, vol. 53, pp. 147-154, 1994.

[30] S. K. Chaturvedi , D. T. Chen e A. Kheiredinne, «Thermal performance of a variable capacity direct expansion solar assisted heat pump,» *Energy Conversion and Management*, vol. 39, pp. 181-191, 1998.

[31] X. Guoying , Z. Xiaosong e Y. Lei, «Performance of a solar-air source heat pump system for water heating on different weather conditions,» *2009 Asia-Pacific Power and Energy Engineering Conference*, 2009.

- [32] Y. H. Kuang, R. Z. Wang e L. Q. Yu, «Experimental study on solar assisted heat pump system for heat supply,» *Energy Conversion and Management*, vol. 44, n. 1089-1098, 2003.
- [33] R. Yamankaradeniz e I. Horuz, «The theoretical and experimental investigation of the characteristic of solar assisted heat pump for clear days,» *International Communications in Heat and Mass Transfer*, pp. 885-898, 1998.
- [34] A. Bridgeman e S. Harrison, «Preliminary experimental evaluations of indirect solar assisted heat pump systems,» *3rd Canadian Solar Building Conference, Fredericton*, 2008.
- [35] K. Bakirci e B. Yuksel, «Experimental thermal performance of a solar source heat-pump system for residential heating in cold climate region,» *Applied Thermal Engineering*, vol. 31, n. 8-9, pp. 1508-1518.
- [36] A. Hepbasli e Y. Kalinci, «A review of heat pump water heating systems,» *Renewable and Sustainable Energy Reviews*, vol. 13, p. 1211–1229, 2009.
- [37] O. Karaa, K. Ulgena e A. Hepbasli, «Exergetic assessment of direct-expansion solar-assisted heat pump systems: Review and modeling,» *Renewable and Sustainable Energy Reviews*, vol. 12, p. 1383–1401, 2008.
- [38] O. Ozgener e A. Hepbasli, «A review on the energy and exergy analysis of solar assisted heat pump systems,» *Renewable and Sustainable Energy Reviews*, vol. 11, p. 482–496, 2007.
- [39] S. Odeh, B. Akash e S. Nijmeh, «Performance evaluation of solar assisted double-tube evaporator heat pump system,» *International Communications in Heat and Mass Transfer*, vol. 31, pp. 191-201, 2004.
- [40] S. Li, F. Wang, L. Liu, Y. Zhao, C. Huan, Z. Wang e P. Tao, «Performance Analysis of a Combined Solar-Assisted Heat Pump Heating System in Xi'an, China,» *Energies*, vol. 12, p. 2515, 2019.
- [41] L. A. Tagliafico, A. Arteconi , A. Marchitto and C. Saio, “A pilot plant with hybrid PV/T panels; system integration of a solar assisted heat pump with existing heating devices,” in *35th UIT proceedings*, Ancona, 2017.
- [42] “Gli impianti solari termici con tubi sottovuoto,” [Online]. Available: <http://www.consulente-energia.com/av-gli-impianti-solari-termici-con-tubi-sottovuoto-come-sono-fatti-tubi-solari-termici-sottovuoto-altri-collettori-solari-sottovuoto-vantaggi-tubi-sottovuoto-per-solare-termico.html>. [Accessed 20 March 2020].
- [43] A. Cesarano, F. De' Rossi, e V. Naso , «La pompa di calore elioassistita: configurazioni d'impianto e loro caratteristiche. Una applicazione sperimentale,» *La Termotecnica*, Gennaio 1986.

- [44] J. P. Chyng, C. P. Lee e B. J. Huang, «Performance analysis of a solar-assisted heat pump water heater,» *Solar Energy*, vol. 74, pp. 33-44, 2003.
- [45] L. A. Tagliafico, F. Scarpa and . E. Carrea , “Performance analysis of integrated solar-assisted heat pumps for water heating,” in *61th ATI Congress proceedings, International session on solar heating and cooling*, Perugia, 2006.
- [46] F. Scarpa, L. A. Tagliafico, A. P. Reverberi e B. Fabiano, «An Experimental Approach for the Dynamic Investigation on Solar Assisted Direct Expansion Heat Pumps,» *Chemical Engineering Transactions*, pp. 2485-2490, 2015.
- [47] “Google Maps,” [Online]. Available: <https://www.google.it/maps/search/palacus/@44.4028147,8.9718267,392m/data=!3m1!1e3> . [Accessed 22 March 2020].
- [48] «Google Maps,» [Online]. Available: <https://www.google.it/maps/search/palacus/@44.4028147,8.9718267,392m/data=!3m1!1e3> . [Consultato il giorno 23 March 2020].
- [49] S. C., “Studio dei criteri e delle metodologie per la riqualificazione energetica e funzionale degli edifici esistenti: Integrazione architettura/impianti a energie rinnovabili verso nZEB (nearly Zero Energy Building),” 2018.
- [50] L. A. Tagliafico, F. Scarpa, G. Tagliafico e F. Valsuani, «An approach to energy saving assessment of solar assisted heat pumps for swimming pool water heating,» *Energy and Buildings*, 2012.
- [51] “Centro Galileo,” [Online]. Available: http://www.centrogalileo.it/nuovaPA/Articoli%20tecnici/Tagliafico/pompe_calore.htm . [Accessed 29 March 2020].
- [52] G. Tagliafico, F. Valsuani e L. A. Tagliafico, «Liquefied natural gas submerged combustion vaporization facilities: process integration with power conversion units,» *International Journal of Energy Research*, 2011.
- [53] «Isprambiente,» [Online]. Available: http://www.isprambiente.gov.it/files2019/pubblicazioni/rapporti/R_303_19_gas_serra_settore_elettrico.pdf. [Consultato il giorno 4 April 2020].

2. THE ISSUE OF ACCEPTANCE

2.2 Introduction

Each project has minimum standards and quality levels to be reached during both the construction stage and its management at the end of works. The economic aspect runs in parallel with the project goals in each stage (e.g. design and realisation). Furthermore, a project has to satisfy the expectations of different groups' opinion, such as developers, financiers, customers and users. Their sentiments are subjective and they can be in contrast one with the other as well [1]. Moreover, the prediction of whether a project (e.g. technology, plant) will become significant or not is a very tough task. Especially, the innovative technologies are often uneconomic and subjected to frequent failures and this leads to a general state of hesitation for investments in this field.

According to the traditional project management approach, the first and unique target was concerned with operative objectives, strictly linked to the plant performance. Still this approach is not likely to meet the investors' expectations: recent statistics show for example how in Italy about one third of projects is globally rated as unsatisfactory or inadequate [2]. The term "expectations" covers different requirements. Some of them are strictly related to the plant and its usage, such as efficiency, quality of the plant or maintenance costs. Others are more general, linked to the initial cost, strategic importance of the structure and so on. The requirements dealing with the end users' feelings about the facility are the most overlooked. This issue is named after "acceptance" in the scientific literature which includes the concept of the attitude, usage and behaviour towards the employment of a facility by members belonging to a distinct social group (e.g. organisation, community, household). In other words, the evaluation of acceptance embraces both individuals' and groups' actions contribution to acceptance.

This issue is due to the lack of a consolidated, systematic scientific approach to assess the technologies from the perspective of user acceptance.

As far as the case study of the Palacus pilot plant is concerned, the strategic importance of the installation makes an acceptance evaluation compulsory. Indeed, the complexity of the plant has a negative influence on the end users and the technicians themselves and on how the "accept" and exploit the renewable installation. For instance, they tend to bypass the SAHP-PVT plant leaving operative only the integration gas burners. Such behaviour is representative of a poor technical knowledge on advanced plants and of a general state of technicians' reluctance to get acquainted with the plant. Indeed, the particular case of a SAHP-PVT interfaced with traditional fossil burners provides too many operative modes and too many alarms. So, the system maintainers prefer to turn the SAHP-PVT off instead of understanding (and solving) the causes of the alarms.

This attitude represents a negative contribution and a barrier which can strongly affect the effective performances reached by the plant along the year. The aspect of acceptance is still neglected in the design approach. So, the way of measuring and coping with this problem are still at the beginning stage. Nevertheless, this matter cannot be overlooked to have a competitive SAHP-PVT installation.

In this chapter, a resume on the state-of-art concerning acceptance is presented. Then an overview on the main strategies to increase and to measure the level of acceptance according to the literature approaches are proposed. In addition, an innovative and quantitative approach in the evaluation of acceptance is illustrated. Thus, the subjective opinions and feelings are accounted for and their influence on the level of acceptance for the Palacus pilot plant are provided as a validation of the approach.

The topic of acceptance is very complex and still at its first stages so there is still a great deal more to do. Every high performant installation is exposed to the risk of low acceptance. Indeed, a frequent obstruction occurs and it is due to users' unwillingness to accept and use available systems. Users' shouldn't be asked to be always confident with the different workings of the plant: the correct way to remove this barrier is the implementation of a monitoring and regulation system able to limit human intervention by means of Information Technologies (IT).

2.3 The concept of acceptance

Acceptance can be conceived as a general agreement that something is satisfactory or right [3]. Many observations can be drawn from this definition: no specific field is mentioned so this concept can be easily applied to many possible areas, including technology, products or policies. As far as this work is concerned, emphasis will be payed to the acceptance linked to technologies in the civil buildings heating systems: progresses have been made both in terms of technological development and cultural background of the population, but renewable energies still are not end-users' first choice, despite of their well-known benefits. Furthermore, the term "general" points out that people or inhabitants of a specific region are involved with their opinion which can be (and usually is) different from factual measured outcomes. People express whether they are ready or feel comfortable to accept a certain facility in their neighbourhood regardless of rational judgements. This is the reason why acceptance will be here referred to as "social acceptance".

Another important remark is concerned with the distinction, not globally agreed by every Author, between acceptance and acceptability: the latter considers the judgement of experts as to whether the construction of a facility (e.g. a power plant or transmission line) is a reasonable burden under rational consideration of quantifiable criteria (e.g. health impact or noise) [4], [5].

Many Authors [6], [7] et al, have approached to social acceptance distinguishing among the socio-political, community and market aspects (Figure 2.1).



Figure 2.1. Three-point division of acceptance [4]

In the following section a resume on these three categories will be proposed; an innovative point of view concerning the technological aspects on acceptance is presented.

2.3.2. Socio-political acceptance

Only economic and environmental evaluations may not be enough to tell whether a technology will be embraced by the inhabitants, apart from technical, economic and legal aspects [8], [9], [10], [11]. The socio-political acceptance represents how political events influence people's acceptance. This wide concept affects both policies and technologies. Following Wüstenhagen's distinction [6], this kind of acceptance is focused on a wider scale, at the level of Countries. Many studies suggested that public attitudes are not stable and change over time influencing the correct integration and success of a project. A survey on the socio-political acceptance of nuclear power plants was carried out in Switzerland before the nuclear disaster in Japan. The repetition of the survey after the Fukushima disaster showed a rough decrease in the acceptance of nuclear power installations [9]. This second enquiry involved 70% of the participants to the former one. These results might result trivial to a common reader. In reality, acceptance analyses are everything but trivial and they never have to be overlooked. Indeed, a research carried out in Japan, after the Fukushima nuclear disaster in 2011, shows that nuclear power is still cheap and comparative to fossil fuels in price, even after including all possible loss compensations for the Japanese [8].

So, [4] represents a simple, but still valuable example to understand the influence that political events, even at huge distances on the opinions of each single person. On one hand gaining ground on social acceptance from a determined group of people is a very tough, delicate and complex operation result of accurate political choices. On the other, all the efforts made can be almost instantaneously deleted with very rapid and abrupt backslidings due to emblematic events.

Actually, a different trend has been recorded as far as the renewable energies are concerned. Indeed, the level of socio-political acceptance towards renewable technologies have always remained high even in Countries where very little support is provided [12], [13]. Unfortunately, this

first positive result is not necessarily reflected by the other two aspects of social acceptance (community and market). Most oppositions to new renewable installations can be traced back to a lack of acceptance in at least one of the main subsystems (socio-political, community or market acceptance). In conclusion, a high level of socio-political acceptance doesn't allow its neglect. In fact, it holds the first place in the hierarchy scale of importance since the institutional policies give force to market and community acceptance.

2.3.3. Community acceptance

It refers to the specific acceptance of siting decisions and renewable energy projects by local stakeholders and authorities or residents [6]. The so-called NIMBY (Not-In-My-Back-Yard) phenomenon belongs to the community acceptance. It is an attitude to which are usually referred to those people who might accept the new project (e.g. devices associated to renewable energies), given the place of construction is far away from their home or community. The NIMBY mood can be described as a form of local opposition to a facility siting [6], [14], [15], [16]. It interprets the strong local opposition as a selfish, irrational reaction by people living in the physical proximity of new energy developments. They acknowledge that the facilities are necessary, but not near their homes [17]. Recent research has changed the NIMBYism and outlined a different framework that changes the perspective from material aspects to the iconic nature of places: negative local attitudes toward facilities are due to prejudicial people's interpretation, for instance as a threat to place identity [18]. This kind of acceptance depends on how the inhabitants of the affected places perceive the developments as aligned with their feelings and relationships to those sites.

The comic strip reported in Figure 2.2 interprets NIMBYism and provides the perspective of satirists: each kind of traditional energy production facility (nuclear, oil, coal) has serious risks that might lead to tragic endings if not correctly managed. This is one of the main motivations which ignites the engine of research to find alternative, sustainable solutions. Nevertheless, the solutions that allow the overcome of the main risks associated to the traditional installations, such as wind power station, are likely to find a strong opposition as well.

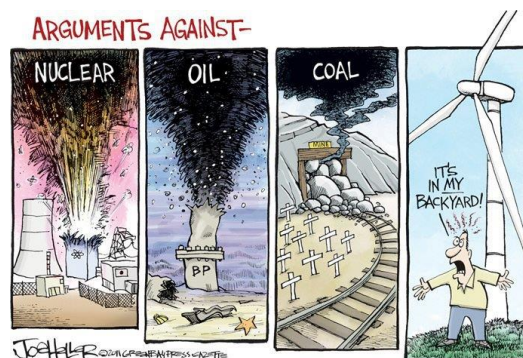


Figure 2.2. Witty and thorny comic strip showing the NIMBY attitude in an ironic way [19]

The study of community acceptance can be led with significative results when physical parameters are identified and then studied following the fashion of a classic statistical analysis. For instance, in [2] a probability distribution function has been determined about the minimum distance to obtain the inhabitants' acceptance of a technology. This approach has been reiterated for different

technologies and plotted in graphs. This is a valuable example of how an acceptance analysis can be led using common and consolidated instruments leading to more meaningful results also for people with less experience in the field. For example, two linear trends with different slopes can be identified (Figure 2.3): the former one (and the steeper one) is between 0 and 1000 m of distance from the technology. Within this range, the lower values of acceptance are reached independently from the technology considered. Naturally, the installations that are more likely to be accepted near the houses are the ones with zero pollution (e.g solar or wind), then the biomass and the natural gas power plant and to conclude the coal power plant. An interesting remark is concerned with a non-zero fractile for null distances. Assumed the reliability of the results, this means that there is a very restricted group (but still there is!) that would enjoy living next to a coal, natural gas or biomass power plant.

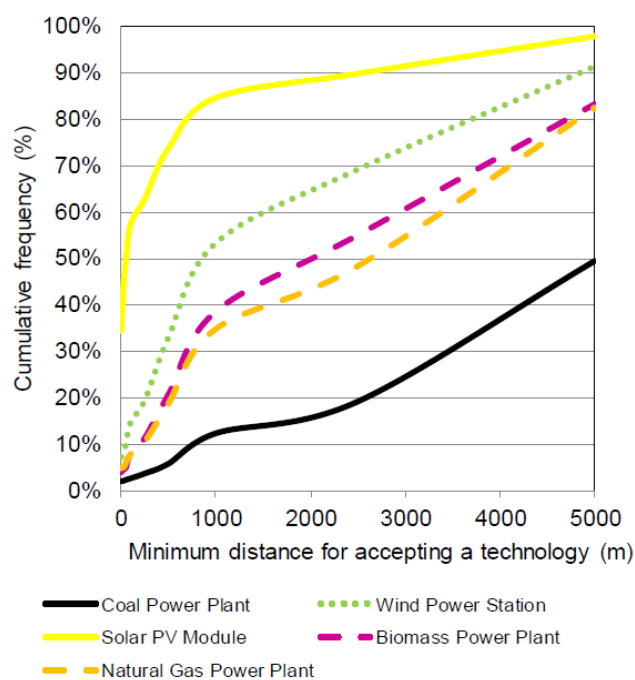


Figure 2.3. Minimum distance for accepting a technology, [2]

2.3.4. Market acceptance

Market acceptance concerns the level of economic approval of an innovation, product or facility through its adoption [4]. Namely, market acceptance is people's trust in a product and it is reflected by a widespread willingness to acquire or invest in it. This aspect allows to embrace the difference between the supply (granted by the market) and the demand (influenced by social acceptance). An important distinction between market acceptance and the NIMBYism has become necessary: the former approaches the topic only from an economical point of view while the latter concerns the social sphere. These two features might belong to the same problem. For instance, on the basis of a strictly NIMBY problem (e.g. the impact on the environment due to wind power installations), the local inhabitants might question on the use of their landscape for green energy export to other regions or countries (market acceptance of a hypothetical green energy trade). This example involves directly consumers; investors can contribute to market acceptance as well. At a small scale, the investors are the consumers themselves and their consent becomes an active acceptance,

quantified by their investments. In some cases (e.g. PV fields or wind installations) the users become an active part of the grid. The economic involvement of single consumers grouped in energy cooperatives is important as well in the field of acceptance [20], [21] and it can be put halfway between the small and large scale. Indeed, citizens can participate to project of a greater size which couldn't result affordable for a single investor/consumer.

The topic of market acceptance is probably the most under-researched and it cannot be reduced to a simple cost-benefit analysis. For sure, this issue plays a relevant role in the market acceptance, indeed the transition from fossil carbon installations has a high initial cost which affects negatively the level of market acceptance of the projects. Nevertheless, the real key motivations that drive people's decisions still have to be enquired, also depending on the different customer segments. Moreover, there are many intermediate steps which have been neglected in the chain from the production of the renewable plants up to the consumers/investors (e.g. design technicians or installers).

When larger scales are reached, the distinction between these two roles becomes necessary. In this context, market acceptance thickens, since cognitive barriers within firms step in, with regard to taking up environmental and sustainability issues [22]. Furthermore, the international companies have a different approach to the topic according to the country and most of times they own part of the grid creating real local monopolies. This last aspect confers to the energy firms the role of stakeholders as well. Indeed, they can influence the crucial decisions on the political level (e.g. concerning financial procurement systems) and at the same time on the market level they can foreclose the access to the grid for other investors in renewable energy systems [23].

2.3.5. Technological acceptance

The categories above cover the issues of social acceptance related to people's attitude and sentiment but neglect the technological aspect. The use of advanced devices is often not so straightforward or intuitive, so that the end-user prefers the use of well-known traditional systems. This diffused behavior is enough to make a potentially efficient plant unsuccessful. The fear or mistrust towards technological innovation, coupled with the instinctive belief that old devices always perform better, is a very ordinary human attitude. This common place can be partially agreed, in case of experimental devices, since the tools might be not optimized and can be subjected to unexpected failures. On the contrary, mistrust towards commercial renewable energy systems is totally irrational as their Technological Readiness Level (TRL) has reached almost its maximum value.

According to these concepts, the technological acceptance can be conceived as the users' reluctance towards the employment of new technologies due their complexity and different operating mode from the traditional ones (e.g. fossil burners). Frequently the lack of knowledge worsens this issue. Often people refuse to learn how to manage a new system and they are not compelled to. A low level of technological acceptance isn't a good reason to abandon advanced technology applications, but a motivation to adopt new automatic regulation criteria and plant monitoring.

In the field of renewable energies, a common strategy consists in the design of facilities where different renewable sources interact one another; as a consequence, technological complexity

becomes unavoidable since optimisation criteria and extended data acquisition are required. The Solar Assisted Heat Pumps (SAHPs) are a clear instance of plant complexity and how a user-friendly interface united with a working control system determines the effective plant performance. Actually, the SAHP technology has still experienced a very low diffusion. The two most remarkable examples are concerned with the Palacus pilot plant previously described and the SAHP at the public swimming pool at Sestri Levante. One of the main causes can be identified in the lack of interfaces which could bridge the technological complexity with the end users' ease of use requirement. The adopted technological means influence the final level of global social acceptance of the plant, also according to their usability, simplicity and ease of maintenance. All these topics are resumed under the concept of "technological acceptance", a field which remains almost unexplored.

Up to now the Technology Acceptance Model (TAM, Davis [24]) is available, which connects users' perceptions to technology. The model was born to predict the user acceptance of computers with good approximation. The main contribution of this model is the highlight of the need for high quality measurements and for models that might be comparable one with the other. The TAM model provides one of the first reliable approaches in which the theoretical constructs are formulated and then validated empirically. The key parameters introduced are about the attitude toward the use of technology and they can be divided into:

- *perceived usefulness*: an application is likely to be used to the extent the users perceive it will help them perform their job better (literally "perception of usefulness").
- *perceived ease of use*: given a high perceived usefulness, people might not use the application since it doesn't user-friendly. In other words, the performances attainable are outweighed by the efforts made to use the application.

The measurement of these quantities is based on the results of phone, mail, face to face interviews and questionnaires to questions such as "Overall, do I find the electronic mail system easy to use?". The weakness of the TAM approach is due to both the final global uncertainty of the results that cannot be quantified and the need of a heterogeneous sample space to validate the statistical analysis. A brief recall on the email clarifies this concept. The answer to the previous question can lead to very divergent results according to the age group enquired. So, the same email interface might result highly accepted by younger groups while the older ones might show a lower level of acceptance. Yet, the older users might hardly accept the email not for a low acceptance of the application itself, but because of their general low confidence with the computing machines. This means that the results have to be put in right context and might change according to the composition of the group under analysis for the same application. This contextualisation is compulsory not only to understand the causes of the results, but also to assess the room for improvement of the application and to quantify the contribution of other external causes (e.g. the PC is not accepted at all and consequently the applications within).

Moreover, the answers are always subjective, even if numbers are used, because the intensity of people's same feeling implies a very difficult comparison. The central problem embedded in this approach is the coupling of a number to an emotion, to make it representative for the feelings of a group of people/users.

The TAM approach works in parallel with the TRL (Technological Readiness Level) evaluation of the plant. Actually, the evaluation of technological acceptance should be integrated in the TRL approach, since a given technology is ready when both it is produced through a competitive manufacturing system and its usage and maintenance are user friendly. So, the analysis should be carried with a parameter/set of parameters able to assess the status of the facility from each perspective. As outlined in the following sections and in the case studies, this target can be achieved following the approach illustrated and defined in this work.

2.4 Means to overcome the issue of acceptance

The problem can be coped with three main strategies: i) knowledge, ii) regulation, iii) automation and domotics (known also as IoT, Internet of Things or IT Information Technology).

i) Knowledge

An appropriate confidence with the innovative technologies should be always granted. Nevertheless, renewable energies have been a relevant topic at any level (newspapers, books, papers) for about half a century and still many people are not confident with them, as shown by statistics available on the web [25]. The graph of Figure 2.4 shows that an effective increase in the renewable installations over Europe (e.g. solar) has taken place only in recent decades. This evidence reveals a general bad level of diffusion, inferring limited acceptance. This trend occurs besides of the increase of people's cultural level and of all the initiatives by Governments and various associations to promote renewable energy in the eyes of the population.

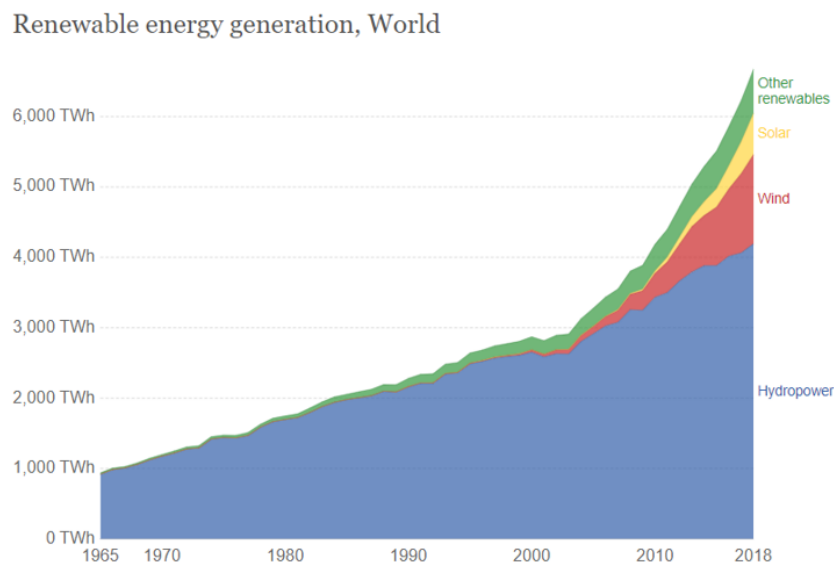


Figure 2.4. European energy sources trend during the last decades; the increase from early years 2000 is evident [26]

Furthermore, there is a great difference between having an overview over such a complex topic and being capable to manage any intervention about energy audits and renewable installations. Knowledge alone will never be sufficient to overcome the problem, but it can

represent a good initial point. This “background strategy” has to be acted on every intermediary in the decision and design chain. Technicians play an important role in the common consumers’ choice as far as the installation of new plants is concerned.

ii) *Regulation*

The explanation of the trend shown in Figure 2.4 cannot be limited to a low level of consumers’ knowledge and consequent low confidence. The economic aspect always plays an important role in the diffusion of innovative devices and it can be quantified by means of specific parameters. For instance, an evaluation of the simple pay-back time for renewable plants would reveal the need of operating periods longer than the working life of the installation itself. This is one reason why small renewable installations, not involved in academic or industrial processes, would hardly be chosen by common people. So, in Italy and in many European Countries the laws come into force within the last decades, give economic incentives in terms of tax relieves to overcome the high initial cost of innovative plants.

The financial incentive approach is usually not sufficient to grant an effective employment of renewable energy applications. Recognizing the great environmental impact linked to fossil fuels energy sources, mandatory laws oblige end-users to install renewable energy plants. For instance, in Italy, there is a body of laws asking for fixed percentages of different renewable energy installations in each new building (DM 26/06/2015 and subsequent amendments in the transposition of Directive 2010/31/UE).

A further improvement recently introduced in Italy is represented by the credit assignment. The tax relief granted to anyone who faces the costs of energy efficiency refurbishment (up to 70% of the total expenses) can be sold to a third-party society, for instance an ESCO (Energy Service COmpany), in exchange for an immediate financial contribution to the intervention. The advantage for the end-users consists in receiving immediately back part of the tax relief in the form of a discount on the total cost of the investment. The remaining part becomes a long-term additional income for the ESCO taking care of the refurbishment intervention (over a period of about 10 years). This policy is designed to involve an extended percentage of the population who either has little economic capability, either pays very little taxes and cannot deduct this relief or has a lease of life too short to be interested in this kind of investments.

Another step forward to this policy is represented by the “ren-on-bill” action launched by the EU [27]. This new approach excludes direct economic end-users’ interventions as the aforementioned ESCOs directly pay for the entire refurbishment in buildings, gaining the credit in terms of tax relief. The potential reduction of the costs in the energy bills doesn’t occur immediately to amortize the part of the investment not tax deductible. In other words, with an almost constant or lower cost of the energy bill, the end user benefits from a gain in comfort without any direct economic effort [28]. Nevertheless, long term financial analyses have drawbacks too, linked to the weak stability of the political line of the government or of the energy markets, which often lead to changes in regulations and amortization schedules.

Since the reference time period for these economic balances is ten years long, such degree of uncertainty cannot be neglected.

iii) *Control automation and information technology*

Nowadays such a large class of issues is often referred to as IoT or AAL, (Ambient Assisted Living). This last strategy gives a different perspective of the problem: a working and efficient plant is always and inherently associated to a very high level of acceptance. This happens independently from its complexity and provided that the good performance of the plant doesn't involve the end users' intervention. For instance, the radiator thermostatic valves belong to this topic. They can keep the temperature inside the rooms at a fixed level (within a very little tolerance, about 1 °C or even lower) with a regulation of the hot water flow rate inside the radiators. This working criterion starts to fail whenever a steep decrease in temperature is measured: this might be a users' response to an excessively hot environment that implies the opening of a window. In terms of needs, the heat flow rate should be stopped fast in this situation, even if a negative temperature slope has been measured, since it is due not to quick cooling of the room but represents a users' request of a better thermal condition. This "smarter" response requires an integration, with respect to the classical thermostatic valve, to measure both temperature and its derivative, introducing the need of additional regulation and monitoring criteria (in this specific case a cut-off based on the value of the time derivative of temperature). The IoT approach makes innovative plants appear more reliable for the end users, since human intervention is needed only in extreme cases, or to give simple, general rules of plant management. On the other hand, the IoT approach always lacks an economic, direct income. It is true that on the long period these improvements allow substantial money savings, but they always imply an initial significant capital investment, not always affordable for everyone.

More in general, in the recent past years a novel engineering discipline has taken place: its name is Acceptability Engineering (AE). AE aims shifts the attention from usability and convenience in mature technologies (concerned with late adopters) to the user acceptance for innovative one (concerned with early customers, visionaries) [29]. This change is not so straightforward since the two categories (early and late adopters) are separated by the so-called Moore's Chasm [30], (Figure 2.5).

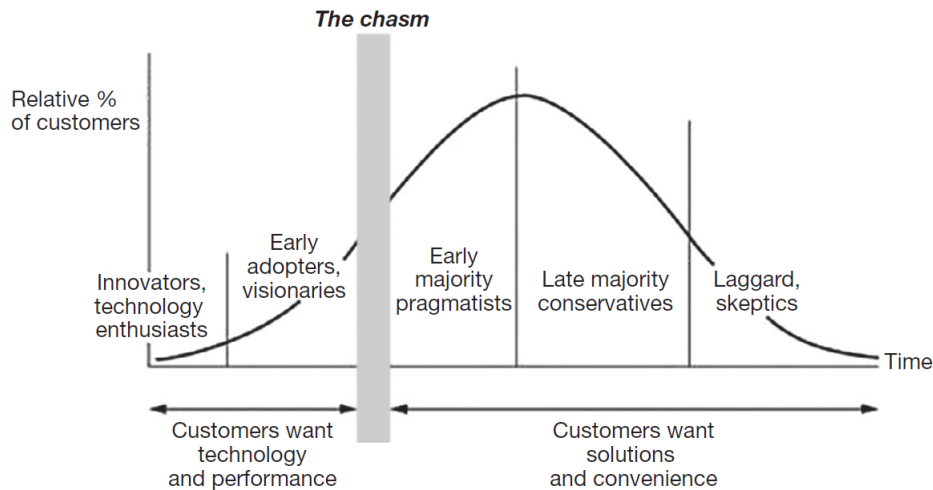


Figure 2.5. Moore's chasm in the lifecycle of a technology [29]

The chasm divides between the early and the mainstream market. According to Moore's interpretation this gap is necessarily created since the technology still doesn't present the necessary conditions to gain the trust of the majority of customers. A vicious cycle arises in which the market growth to convince the users of the merits of the products is not affordable since too few early adopters purchase the innovative products. So, the context of AE lies in the early stage before the chasm while other traditional approaches belong to the mainstream market, such as Human-Computer Interface (HCI). In other words, AE emphasises the need of an acceptance evaluation, starting from the first steps of each new technology. The innovation should even be designed according to acceptance preliminary studies and the technological advances of the product should be developed in parallel with acceptance.

AE operates at the very crucial stage of innovative technologies, where typically the performances are poor and not convenient. The early adopters' acceptance is of paramount importance both to influence others in the adoption of an innovation and to increase the diffusion rate of the technology.

In conclusion, AE is the study of the design, evaluation, and implementation of innovative computing technologies to fulfil user acceptance. Its organization as a discipline aims to the generation and validation of relevant theories, methods and phenomena providing technologies that users adopt and use, namely accept. Accordingly, the target of AE is to provide a balanced understanding of innovative technologies and user acceptance. In addition, it focuses on crossing the chasm between early and late adopters, and between early and mainstream markets.

2.5 Ways for acceptance measurement

Standard parameters to express acceptance are a very difficult task to cope with. As far as the papers and studies analyzed are concerned, two main groups can be distinguished: indicators and indices. Generally, the application of both families is not very straightforward, since a connection between subjective feeling and objective measure is a tough task. This proves how a genuine understanding of the dynamics of public acceptance remains elusive. Some further significative information on index and indicator is provided below.

2.5.1. Indicators

This term refers to a qualitative approach in which people's opinions are linked to feelings and emotions. There is a significant number of parameters that can be considered as measurable variables: some instances are anxiety, perceived adaptability, perceived enjoyment, perceived sociability, social influence, culture, perceived ease of use, system's reliability and trust [6], [31], [32], [33], [34]. Three basic indicators focused on subjectivity have been identified, among the papers, to express the fundamental physical magnitudes of the problem. An appropriate combination can express every other more sophisticated, above-mentioned indicator [6], [35], [36].

- *Perception*: meant as psychological and physical possible health implications of the technologies. The perception roots deeply in the belief, attitudes, feelings and knowledge. Very little is left to the real sense perception in this meaning. As far as feelings are concerned, each sentiment affects with different weight perception. In terms of importance, fear is at the first place, since it involves safety and survival that are primary and instinctive concepts of the human nature [6].
- *Fairness*: the outcomes from a process or a plant might result favorable for the community. The concept of favorability draws from justice principles. Outcomes that are perceived as unfair can cause protests or divide communities when this might benefit some sections of the society with respect to the expense of others. Fairness can be correctly achieved when the potential risks are defined and their management has been previously established [6], [36]. Within this context, the key word is trust, especially when investors are outsiders. The "asymmetry principle" states that "trust is fragile, as it is typically created slowly but can be destroyed rapidly" [37], so investors have to be open minded and flexible, to involve local inhabitants as much as possible to give the facility a good perception of fairness, especially at the first stages.
- *Knowledge*: it evaluates how much people feel to know and not the real cultural level. More precisely, knowledge should be referred to as "perceived knowledge". Its influence on the other parameters is evident, for instance a well-known facility might be perceived as fairer. The feeling of a having deeper awareness on the working of a plant makes people more confident improving their perception of the facility. Indeed, fear can be conquered with knowledge. The weak point consists in the evaluation of the subjective perception and not knowledge itself, so the effects of any cultural initiative (e.g. meetings, seminars) to improve the insight on the technology have different effect on people. As enquired in [7] the use of the word "knowledge" recalls the fact that the cultural background (marital status, gender, age, education and personal income) does participate to this parameter.

2.5.2. Indices

On the other hand, few papers [38] attempt to introduce indices with accurate, quantitative analyses. Some parameters which belong to this approach can be found in the following examples:

- *Inclusive Impact Index (Triple I or III)* which conjugates in a single index the ecological footprint combined to a monetary value [39], [40]. It can be expressed as Eq.(2.1):

$$III = [(EF - BC) + ER] + \gamma[HR + (C - B)] \quad (2.1)$$

Where

EF is the Ecological Footprint, environmental parameter;

BC is the Bio-Capacity;

ER is the Ecological Risk;

γ is a conversion coefficient to translate the economic quantities into environmental ones. According to the works present in literature, it is conventionally defined as EF divided by the gross domestic production;

HR denotes the Human Risk;

C and B are respectively the economic cost and benefit.

So, environmental values (EF, BC and ER) are mixed with economic ones (HR, C and B) transformed by means of the coefficient γ . Positive triple I values imply higher costs than benefits and ecological risk and footprint and it is thus associated to technologies that cannot be sustainable.

- *Emergy*, that can be defined as “the available energy of one form that is used up in transformations directly and indirectly to make a product or service” [41]. So, the emergy can be computed as the sum of each product given by the amount of energy needed to produce a unit of each product multiplied by the related total produced quantity.
- *Marginal Willingness To Pay (MWTP)*, the concept behind the coefficient draws from the definition of a utility model (made of I respondents and i attributes) and the related constitutive equations. Then assuming a given distribution for the error term (e.g. Gumbel), the maximum likelihood method applied to the probability for the I respondent to choose attribute i is used to compute the MWTP referred to that attribute.

Nowadays, no index is available in literature that expresses the three bottom lines of environment, economic and social costs by means of only one coefficient. Variation of these basic indices have been proposed, but the core problem remains unsolved. The terms inside these formulations might not result easy to estimate and their margin of error is hardly identified uniquely. In addition, the implicit dependence on economic quantities underpins the approach of indices, only adding a further degree of uncertainty linked to the market fluctuations. This approach results unbalanced since it tries to highlight explain and measure the entire issue of social acceptance only by means of the market acceptance, overshadowing the community, technological and socio-political ones.

2.6 Methodology to collect experimental data on acceptance

This issue is one of the apparently most simple problems when measuring acceptance “on-field” since people’s answers to specific questions are collected. In truth this topic reveals to be very insidious, since many aspects have to be carefully accounted for. Nowadays technology allows much more chances to involve a very wide and heterogeneous group of people, for instance phone interviews or mail, face to face interviews, field observations, web-based questionnaires.

First of all, the kind of approach is of paramount importance. A former, main classification can distinguish between direct (e.g. face to face interviews) and indirect approach (e.g. email

questionnaires). The latter is less advised due to more likely misunderstanding of the questions and the consequent wrong responses given. At the same time, the “face-to-face” approach is the more delicate since enquired people has not to be influenced by the interviewer. Especially when hot topics are dealt, either people might not feel comfortable to answer directly to the enquirers, or this embarrassment might lead to significative percentage of “misled” responses. These issues in actual “on field” studies, are almost overlooked, due to their complexity. Indeed, very seldom the influence of the interview strategy adopted on the results is at least remembered. Most of times an economic matter affects the choice: direct approaches require more time and might get many people busy. On the other hand, email or even phone interviews allow to reach a wider group of people and they speed up the entire process. From a statistical point of view, indirect approaches are more likely to provide a data-set wide enough to perform analyses on their validity. The choice of the approach might be led as well considering for instance the type of information needed, ease of data standardization, representativeness, staff requirement, time constraints and costs. A stable and good working approach could involve both the direct and the indirect interviews. The former is meant as a calibration and test on the correct comprehension of the questions, while the latter allows the systematic involvement of a very wide area [42], [43] et al.

Once the kind of approach has been chosen, the second step consists in the formulation of the question which might have either the form of a question or be in the context of a statement. Actually, in more accurate interviews, the question themselves are coupled to the require of the respondent’s personal characteristics (e.g. gender, education, age, [14], [7], [42]). Besides all, the formulation has to be as clear, brief and simple as possible. At the same time, the number of questions has to be very little, otherwise people will lose attention and will not respond to all of them. Moreover, brief must not imply general since the interview might cover both macro-topics and more specific ones, as well as too technical and professional questions will confuse interviewees and make them feel too frustrated to answer; causing very meaningless communication.

Then, the answers represent a tough task as well since they have to cover synthetically every possible reply to the question. A current of thought tries to associate the feelings to a fictitious numerical scale (e.g. Likert scale, [14], [44]) while the other just refers to feelings, such as “being aware”, “feeling comfortable”, “intention to use”, “facilitating conditions” or “cost”. This last term deserves more explanation. At first glance the concept of cost sounds like an objective quantity, but within this context it is a matter of subjective feelings. For instance, the perception of the cost is not always equal to the real cost, as the widespread fashion of “charm pricing” (namely the use of pricing ending with 9 or 99 instead of round values, e.g. 9.99 € instead of 10,00 €) can easily show. Besides of this example, the perception of the cost can be different from one person to another just due to their different feeling of the topic. Indeed, people more concerned with the environmental issue might be more likely to invest more in renewable technologies instead of the ones who feel it just as a regulatory imposition. A research carried out in Finland [45] has clearly highlighted as younger groups of people were more aware of the renewable energy topic and therefore willing to invest in them, while the really young groups (e.g. teenagers) and old ones are less likely, due to lack of knowledge on the topic.

The exclusion of any open answer is quite common, since it is very difficult to put it into context systematically. Usually only more advanced questionnaires allow this possibility, only meant as a further explanation of the choice made in the question. Indeed, these answers don't directly belong to the interviews, but they only provide an additional information that might come useful in the post-processing stage. Direct use of open questions is more time consuming and it introduces only another degree of uncertainty. In fact, the short stem has to be read and evaluated by a third person who gives a rating according to his opinion on the interviewee's opinion. The same issues can be identified as far as semi-structured interviews are concerned even, they are believed to be more appropriate for gathering information from an individual perspective, or focusing on individual experiences, beliefs, and perceptions [46].

2.7 “Carmin Romanzi” Sport Palace (Palacus)

The evaluation of acceptance should be integrated in the TRL approach, since a given technology is ready when both it is produced through a competitive manufacturing system and when its usage and maintenance are user-friendly. In many cases advanced technological installations are abandoned or overlooked because of the frequent lack of knowledge which creates a wall between the users and the plant.

A quantitative and systematic measurement of feelings has to be carried out referring to objective parameters, to allow the Acceptability Engineering (AE) discipline to take place already in the former steps of the plant.

The numerical coefficients proposed in this work have been conceived following the AE thread and they are based on objective and measurable quantities that can in turn be associated to the end users' sentiments about the facility. In conclusion, these computed parameters represent an attempt to evaluate acceptance with a quantitative and novel insight about the user acceptance.

The SAHP-PVT plant at Palacus will be presented below, before the approach itself, to apply the proposed criteria to the specific monitored data. Although each plant has its specific layout and significant parameters, the concepts applied to this case study and the considerations proposed have a general validity and they can be adapted to any installation.

2.7.1. SAHP-PVT installation recall of the significative parameters

The picture below illustrates a simplified block diagram of the plant to let the reader understand the general complexity of the problem and focus only on the key parameters afterwards discussed.

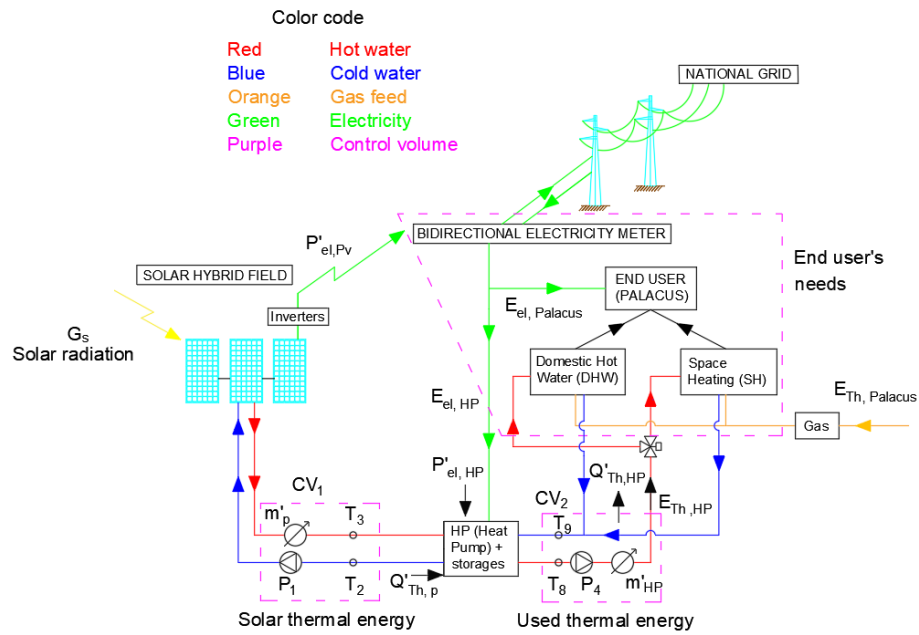


Figure 2.6. Block diagram of the SAHP-PVT pilot plant installed at Palacus

- *Solar hybrid field*: the conjoint production of electricity and heated water has been designed to cover the electrical consumption of the elements of the circuit (e.g. valves, pumps, the heat pump itself) and increase the level of temperature of the cold side of the heat pumps with consequent benefits on the HP COP. With reference to the picture above and to the Control Volume 1 (CV1), the key parameters of this subsystem are associated to the inlet/outlet water temperatures (T_3 and T_2), the working period of the circulation system represented by the pump P_1 that allows the computation of the mass flow rate (m'_p). As illustrated, a bidirectional connection through the electricity meter to the national grid is available, in order to exchange any electric overproduction to the national grid.
- *Heat pump system*: designed to cover the needs of the facility in terms of DHW and SH with a thermal nominal power of 62 kW_T and a related consumption of 12 kW_E . The connection of the cold side of the heat pump to the solar field increases the temperature at the evaporator and consequently the COP of the HP. Pumps P_2 and P_3 regulate the water flow on the cold and hot side of the heat pump, respectively.
- *Supplementary gas burners and distribution system*: the hot water produced by the SAHP stored in the hot storage tank is then sent to a collector; here two supplementary gas burners can step in and eventually heat the water whenever its temperature lowers the imposed set points. The gas burners, respectively of 320 kW (used in winter when also SH needs are included) and 35 kW (used in summer when only DHW is asked) show a mean seasonal efficiency of about 0.85 and they belong to the original heating plant of the structure. According to the regulation criteria, their intervention should be contemplated only in strict environmental conditions, when the renewable part of the plant cannot meet the thermal needs of the facility on its own.

According to the CV2 in Figure 2.6, pump P_4 allows the circulation of the water into the

collector, according to the end users' needs, while a couple of temperature sensors is placed on the inlet and outlet water pipes (T8 and T9). The mass flow rate at the HP (m'_{HP}) can be determined by means of energy balances or basing on the operativity periods of pumps P4.

- *Data Acquisition System (DAS)*: in Figure 2.6, only the parameters relevant to the goals of this paper are reported. Actually, a proper and complete regulation of the plant is carried out through a larger set of measurement and control points (respectively about 50 and 15) which cannot be entirely human-managed. So, a DAS with an internet connected PLC has been installed to supervise and eventually operate on the plant, even remotely, according to the strongly time dependent environmental conditions and users' needs. The extended amount of data collected requires proper post-analysis and allows efficiency studies in order to build new regulation criteria and increase the plant efficiency also from the environmental point of view.

2.8 Innovative approach

As formerly introduced, an exhaustive and consolidated method for the measurement of the acceptance level is still not available. Actually, two different approaches can be distinguished:

- the former and most diffused one is concerned with the representation of acceptance by means of feelings. This procedure is based on interviews, questionnaires and every other tool aimed to enquire the end users' feelings and sentiments. These sensations can be identified as the "indicators" (e.g. fairness, perception, knowledge) described formerly.
- The other approach is concerned with quantitative measurements: feelings are implicitly taken in account, but at the same time other degrees of uncertainty are unavoidably introduced. Such parameters are similar to the ones adopted in the economic field and they can be named as "indices". We can cite for instance triple I index, emergy and the Marginal Willingness To Pay (MWTP).

On the contrary, the new parameters here proposed represent a novel approach to the problem since a quantitative estimation of subjective feelings can be carried out both without the direct end users' opinion and based on objective, uniquely defined quantities. This might lead to the wrong conclusion that the end users' feelings, the core of acceptance, have been pushed into the background. In literature, the elements belonging to the sample space associated to the "end users" are always chosen according to specific criteria. Usually, the strategy adopted is a random choice of the minimum number of respondents enough to constitute a data set statistically acceptable. There are many techniques that estimate the number of individuals to be involved (e.g. Sampling method [47]). Furthermore, statistical analyses have to be carried out in order to investigate the interrelations among the data collected. Once the statistical model has been completed and validated, conclusions can be drawn. The underlying concept is that a reasonably large group is statistically homogeneous and representative of people and thus the results can be extended and generalized. In specific cases, the enquirers might be interested in a statistically heterogeneous group, formed by people meeting specific queries (e.g. working in a specific field, belonging to a specific gender or range of age) according to the topic investigated. Sometimes the researchers themselves apply some former filters to restrict the catchment area, creating fictional sampling spaces that are then assumed to have a general relevance. For example, in [7] the population of

Istanbul was the object of the surveys; the authors chose only five main districts of the city, assuming fictitiously that these would represent the entire city.

Another important aspect is concerned with the validity of the results: almost all studies don't account or try to verify whether the respondents lied or clearly understood the meaning of the questions. One of the greatest efforts taken to cope with this problem is the common advice to prefer face-to-face interviews, which prevent most of these uncertainties, but they don't completely guarantee the reliability of the results. Actually, these simplifications concerning the approach the interviews add other degrees of uncertainty which cannot be easily handled, though necessary.

So, given, but not granted, that the so-built-model statistically represents the end users under study, any explicit or implicit time dependency is neglected. In other words, the end users are assumed to have invariable opinions over time, both in short and long-term periods. Actually, three main possible kinds of time dependence can be identified:

- *People's opinion variability*: it is directly connected to the concept of fluctuation of the acceptance level. Users change their opinions on tools, technologies over time. It is true that products/technologies which have a consolidated and high level of acceptance tend to be always preferred to the newer ones. On the other hand, this reluctance towards innovations is gradually overpassed with time, even if the period needed to accept the novelty increases as people grow older.
- *Geographical mobility*: as outlined by the EU [48], the percentage of people moving within Europe is increasing. As far as the USA are concerned, statistics state that on average an American is born, grows and dies respectively in at least three States. So, the validity over time of the results might be invalidated due to consistent variation in the population sample.
- *Heterogeneity of the interviewed group of people*: this issue is affected by time as well. For instance, in the case of sport facilities there may be a daily variation in which workers attend to the gym during the lunch break. In addition, younger athletes are more likely to practice in the afternoon, when there are less classes at school. In turn this pattern might change over the week due to differences between working days and weekends. This last aspect becomes more relevant as the facility is open to wider groups of users.

In these conditions, the interview approaches would reveal useless since the results obtained could be hardly considered representative of the effective use of the facility over a sufficient time period. Moreover, the time-span spent for data elaboration might invalidate itself the reliability of the results in case of strongly time-variable fluctuations in the user's opinion.

To resume, no research carried out is provided with neither a continuous or at least discrete update over time of the results obtained. A time sensitivity analysis of the chosen samples is missing as well. Clearly an up-to-date statistical model following the literature approaches would reveal to be too expensive, unviable and almost impossible to manage, since reiterated interviews or questionnaires would be required.

To overcome most of these unsolved issues, keeping the role of end users' feelings in the core of the approach, the assumption that a highly accepted facility is a widely used one is proposed.

A Data Acquisition System (DAS) is required to monitor the plant and collect information on the level of its employment. A simple on/off control is not sufficient, in fact the DAS has to provide information both on the status of the plant (e.g. on/off of each component) and on its proper working. In case of recorded failures, specific parameters concerned with the correct usage of the facility allow the distinction between design flaws and users' dissatisfaction.

The parameters proposed in this innovative approach, follow the basic structure of the efficiency ones. Low values can be the first flag of a non-working facility but it doesn't directly and necessarily imply a low level of acceptance.

As it will be better outlined below, a proper and careful postprocessing analysis has to be carried out in order to associate the correct causes to each recorded "symptom", distinguishing among:

- design flaws: the flag of a low level of acceptance is inherent, since the plant inactivity is due to functional problems.
- absence of end users' needs: there might be some time periods during the day where the plant is not used because of the absence of the demand from the structure, despite of the availability of energy (e.g. solar irradiation).
- low level of acceptance of the plant: as highlighted in [35], [49], a plant with multiple, articulated working conditions is less likely to be used than an easier one. As far as the comparison between renewable and traditional fossil plants is concerned, the end users tend to use the fossil ones, favouring their confidence and trust towards this kind of plant, despite of the potential for pollution.

Furthermore, with the help of a DAS, the level of acceptance can be recorded over time as well, by means of operating parameters regularly updated after continuous measurements.

In this way, the users' sentiments and opinions are directly measured with numerical quantities and the margin of error and uncertainties are reduced. No statistical analysis has to be carried out on people sample because the sampling space corresponds exactly to each actual user of the facility.

In order to carry out an exhaustive and complete analysis of the level of acceptance, two main groups of parameters are proposed: "end users" and "plant efficiency" parameters. Their formulation is here concerned with the plant scheme outlined above of Palacus (Figure 2.6), but it can be adapted to any other plant. In the same way, the approach leading to the conclusions, the remarks and the results doesn't lose its general validity.

- End-users parameters: their structure is a ratio either in terms of working hours or energy, more directly associated to the end users. Several parameters of this kind can be proposed:

- $C_{1,xx}$: they express a ratio of effective working hours of a "XX" sub-system of the plant (for instance SAHP/thermal field or PV/photovoltaic field) with respect to the total possible service time (according to the users' needs) of the same subsystem, $\Delta\tau_{tot,XX}$.

As far as the photovoltaic side of the solar field is concerned, $\Delta\tau_{work,PV}$ represents all the periods of the PV working with proper electrical grid connection.

On the other hand, $\Delta\tau_{work,SAHP}$ can be computed as the time when the SAHP system is active either for SH or DHW needs (in the specific plant design only one of the two can be satisfied at a time). With reference to the plant scheme in Figure 2.6, $\Delta\tau_{work,SAHP}$ is the total time period during which P4 is on and the working temperatures recorded at the evaporator are within the heat pump operativity range.

$$C_{1,PV} = \frac{\Delta\tau_{work,PV}}{\Delta\tau_{tot,PV}} - \text{working time fraction of electrical system} \quad (2.2)$$

$$C_{1,Th} = \frac{\Delta\tau_{work,SAHP}}{\Delta\tau_{tot,SAHP}} - \text{working time fraction of thermal system} \quad (2.3)$$

○ $C_{2,XX}$: they are an energetic ratio between the net available renewable energy and the total user's energy demand; this last quantity can be evaluated for instance by means of the gas and electricity bills. Again, these parameters can be formulated both for photovoltaic (PV), Eq. (2.4) and thermal subsystems (Th), Eq. (2.5).

$$C_{2,PV} = \frac{E_{PV} - E_{el,HP}}{E_{el_consump_palacus} - E_{el,HP}} - \text{electrical solar renewable energy fraction} \quad (2.4)$$

$$C_{2,Th} = \frac{E_{Th,sol}}{E_{Th_consump_palacus}} - \text{thermal solar energy fraction} \quad (2.5)$$

Where

E_{PV} is PV electricity production;

$E_{el,HP}$ is electrical HP consumption;

$E_{Th,sol}$ is the thermal energy collected by the solar thermal field and transferred to the cold side storage of the HP;

$E_{el_consump_palacus}$ and $E_{Th_consump_palacus}$ are end user's thermal and electrical demands (including $E_{el,HP}$).

Only $C_{2,PV}$ can reach negative values, when the HP electricity consumption is not entirely provided through the solar photovoltaic field, but also a contribution from the national grid is required.

- Plant efficiency parameters: their definition is carried out under the assumption of stationary conditions. Nevertheless, the working of SAHP-PVT facilities seldom reaches stationary conditions and therefore these coefficients cannot also represent actual efficiency parameters. Their connection to the concept of efficiency and energy performance (even under the assumption of steady state) is the mean to estimate the level of acceptance.

○ *Mean seasonal solar panel efficiency*, $S\eta_P$, can be conceived as the ratio between the solar radiation collected by the thermal panels and the total one available. Their integral values are computed for each time period $\Delta\tau_i$ in which the thermal solar field is active (that is when the circulation pump P1 is on). The mean seasonal solar

panel efficiency can be computed integrating over the total time the solar panel efficiency over the i-th period, η_{pi} , Eq. (2.6):

$$\eta_{pi} = \frac{\int_0^{\Delta\tau_i} m'_p c_p (T_3 - T_2) d\tau}{A \int_0^{\Delta\tau_i} G(\tau) d\tau} \quad (2.6)$$

Where

$G(\tau)$ is solar radiation [W/m^2];

$A [m^2]$ is the solar panel active area (about $120 m^2$ in the Palacus plant);

m'_p, T_3, T_2 are respectively the mass flow rate [kg/s] and the recorded temperatures [$^{\circ}C$] of the water entering/exiting the cold side storage.

The solar panel efficiency represents the mean panel efficiency after integration over the i-th working period of the solar field.

The mean seasonal solar panel efficiency can be therefore expressed as

$$S\eta_P = \frac{\sum_{i=1}^N \eta_{pi} \int_0^{\Delta\tau_i} G(\tau) d\tau}{\sum_{i=1}^N \int_0^{\Delta\tau_i} G(\tau) d\tau} = \frac{\sum_{i=1}^N \int_0^{\Delta\tau_i} m'_p c_p (T_3 - T_2) d\tau}{A \sum_{i=1}^N \int_0^{\Delta\tau_i} G(\tau) d\tau} \quad (2.7)$$

Where

N is the number of time periods $\Delta\tau_i$ during which the circulation pump (P1) of the thermal solar subsystem is active, while the remaining quantities are the same used in η_{pi} .

The two parameters ($S\eta_P$ and η_{pi}) are expressed by means of measured quantities, collected with the DAS.

○ A further parameter, named C_3 , can be defined as a function of both the mean seasonal solar panel efficiency, $S\eta_P$ and the panel efficiency η_{pi} (Eqq.(2.6) and (2.7)). C_3 expresses the solar energy actually used (integral over the working periods $\Delta\tau_i$) with respect to the maximum attainable solar energy given the same corresponding mean seasonal solar panel efficiency (integral over the total irradiance period $\Delta\tau_{tot}$).

$$C_3 = \frac{\sum_{i=1}^N \eta_{pi} \int_0^{\Delta\tau_i} G(\tau) d\tau}{S\eta_P \int_0^{\Delta\tau_{tot}} G(\tau) d\tau} = \frac{\sum_{i=1}^N \int_0^{\Delta\tau_i} m'_p c_p (T_3 - T_2) d\tau}{S\eta_P A \int_0^{\Delta\tau_{tot}} G(\tau) d\tau} \quad (2.8)$$

It is important to highlight that C_3 is referred to the total solar radiation, irrespective of the plant operativity.

A further substitution of Eqq. (2.6) and (2.7) in Eq. (2.8) leads to a different, simple formulation of C_3 :

$$C_3 = \frac{\sum_{i=1}^N \int_0^{\Delta\tau_i} G(\tau) d\tau}{\int_0^{\Delta\tau_{tot}} G(\tau) d\tau} \quad (2.9)$$

By means of Eq. (2.9), C_3 can be more directly expressed as the irradiance exploited during the operativity periods of the plant ($\Delta\tau_i$), divided by the total irradiance over time ($\Delta\tau_{tot}$). Under these terms, $C_{1,Th}$ and C_3 can be conceived as complementary. The former provides information about the plant period satisfying the users' needs while the latter quantifies the solar thermal resource actual exploitation.

Figure 2.7 better explains the difference between the denominators appearing in the definition of $S\eta_P$ (Eq. (2.7)) and C_3 (Eq. (2.8)). Given a sample of solar radiation over the day, $S\eta_P$ is computed referring only to the periods in which P1 (the pump of the solar thermal field sub-system) is on; in other words, the area dashed in green. On the other hand, the denominator of C_3 includes the entire area swept by the total solar radiation over the day (blue line), regardless of the working periods of P1.

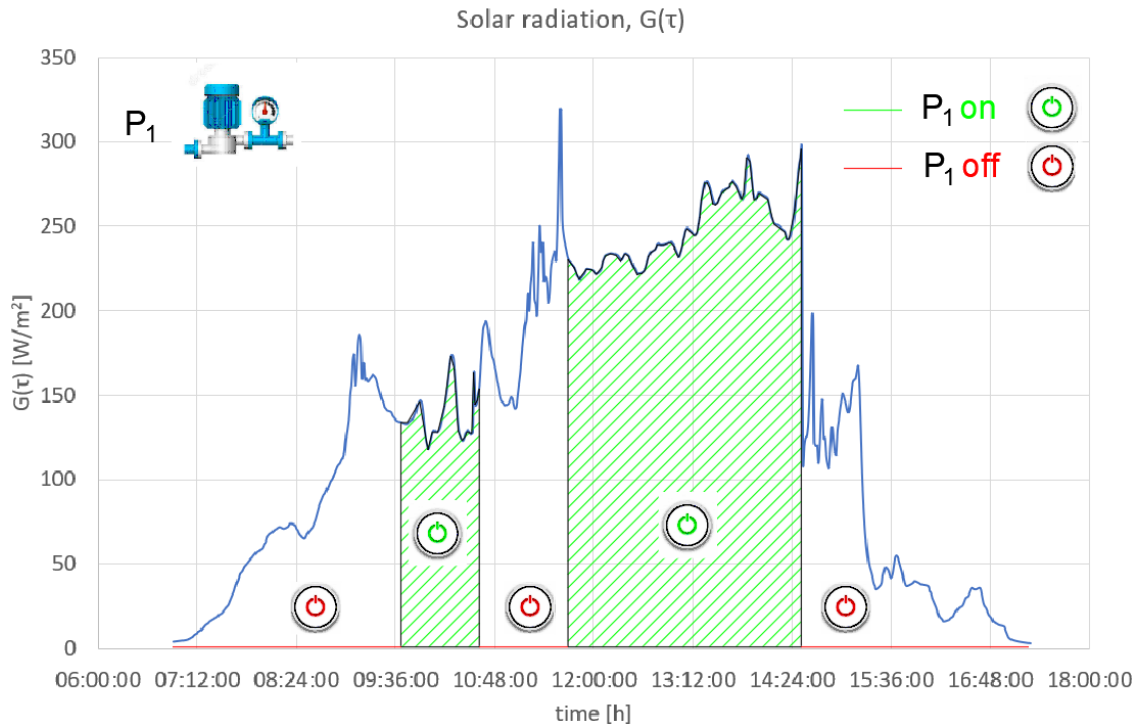


Figure 2.7. Solar radiation of a generic day: total irradiance (area swept by the blue line) used for C_3 computation and the total irradiance with the active solar thermal subsystem (dashed green areas) used for the $S\eta_P$ evaluation. The reference (monitored) signal is P_1 activation.

Keeping in mind these formulations, C_3 and $S\eta_P$ give complementary information and they allow the identification of both the total solar energy available and the actually

exploited one. This concept is not associated to plant efficiency issues or energy losses. It is meant to distinguish among the total available solar energy, the one available during the operativity periods and the irradiance effectively exploited by the solar plant.

In this framework the DAS has the double role of both post-processing tool of the parameters proposed and continuous update of the level of acceptance over time. For instance, only the data recorded through the DAS can highlight low acceptance parameters and associate the results to the proper causes, e.g. technical problems, acceptance issues or inactivity of the plant. Furthermore, the primary function of the DAS is the data collection which allows multiple applications, such as the acquisition of an appropriate knowledge of the nominal, effective working ranges of each subsystem of the plant and the fluctuations of its parameters (e.g. temperatures, pump working periods) along with different boundary conditions.

Two operating conditions of the plant have always to be defined when approaching an acceptance analysis: effective and nominal ones. The former is concerned with the real, recorded working of the plant. The latter is necessary to establish a reference benchmark, the answer to the question “What do we/they expect from the plant/facility?”. In other words, the reference/nominal conditions shouldn't be confused with the optimal performances, but they should represent the closest and most likely operating conditions, according to the usual environmental parameters and to the usage of the plant. Taking a step back, the core of the nominal condition concept allows to assess whether the project results successful or not and to understand the fields in which there is room for improvement. According to this more general definition, the optimal performances could be chosen as the nominal ones as well: this point has to be accounted carefully during the coefficients post-processing. Indeed, the evaluation of the parameters above would lead to lower values in case of reference optimal conditions instead of the effective ones. This difference is due to the not-obvious gap between nominal and optimal conditions.

This aspect seems obvious and it is often overlooked in most of literature works on acceptance evaluation. Only in some papers, numerical coefficients are expressed as a percentage and these results are implicitly compared with the unity that is assumed equal to the nominal condition.

More generally, the numerical results become meaningful when referred to a benchmark that cannot be assumed to be always equal to 100% even when speaking of parameters under percentage. For instance, η_p is expressed as a percentage; the benchmark (or nominal as named later) cannot be considered equal to 100% due to unavoidable (yet minimal) thermal losses as a matter of efficiency.

So, the nominal reference conditions have to be calibrated as a function of the facility under analysis: in this background, one of the most complete and exhaustive reply can be provided only with the help of the DAS. Furthermore, the chosen nominal condition has to be defined, just to have a benchmark to which coefficients can be referred and compared.

Basing on the concepts outlined previously, the nominal operating range of the HP is given by the sum of two main time periods. The former includes the time spans in which the SAHP is effectively active. The latter is concerned with the periods in which the gas burners have substituted and not

integrated the SAHP in the production of DHW and SH services. Indeed, the periods in which the SAHP was active but the gas burner integration was required are excluded, since they belong to the case of active SAHP. It is important to remark that the terms “operative” and “active” referred to the SAHP don’t imply the full coverage of the thermal needs by means of the only solar assisted heat pump. The plant scheme and its design account for conditions in which the SAHP contribution is not sufficient and the gas burners are compulsory. In conclusion, the nominal conditions can vary over time as well, since for instance they partially depend on the effective usage of the plant. The parameters proposed will be applied and validated with two case studies of the pilot heating plant at the Palacus Sport Palace, following the key concepts outlined in this paragraph.

2.9 Case study: the acceptance evaluation of the DHW subsystem

In the present study, the heating and domestic hot water production system is proposed as an example of a project that has not completely met the performance expectations, even after the high performances obtained with the first prototype [50] and the positive cost benefit analysis carried out during the design stage.

The innovative approach proposed has to be applied in a simpler context than the one represented by the entire SAHP-PVT installation. The main reasons are concerned with the validation of the approach and the need to run a debug analysis to assess whether the innovative process leads to realistic conclusions or not. In addition, the proper causes and remedies (e.g. mistrust toward the plant, technological problems, economic reasons) have to be associated to the results obtained. So, only the DHW production has been considered in the following two examples.

A simplified and pertinent set of coefficients have been chosen from the group above (C_3 , $S_{\eta p}$ and $C_{1,Th,solar}$). According to (2.3), $C_{1,Th,solar}$ represents the contribution of the solar thermal system to the DHW production, both directly with the summer bypass and indirectly, heating the HP evaporator. It can be formulated as:

$$C_{1,Th,solar} = \frac{\Delta\tau_{work,solar}}{\Delta\tau_{solar}} \quad (2.10)$$

With

$\Delta\tau_{work,solar}$ is defined as the times when a DHW production period has been recorded. This happens when two requirements are simultaneously met:

- Active pump P1;
- Temperature decrease in the DHW storage tanks.

$\Delta\tau_{tot}$ is the period during which the temperature of the hot storage tanks lowers (which corresponds to an end-users’ energy request).

The proposed coefficients $C_{1,Th,solar}$, C_3 , $S_{\eta p}$ have been evaluated in advance under the nominal conditions in order to constitute a “status zero” for the plant. Then the computation based on the data recorded by the DAS and representing the effective usage of the facility has been carried out.

The following approach has been followed to compute each parameter under nominal usage:

- $C_{1,Th,solar}$: reference equation Eq. (2.10). The nominal working hours are represented by the sum of the solar field effective working periods and the hours in which the gas burners substituted (not integrated) the SAHP-PVT.
- C_3 and $S\eta_p$: reference equations Eqq. (2.9) and (2.7) respectively. The nominal usage computation refers to the periods in which either P_1 was effectively operative or the gas burners supplied the DHW needs instead of the SAHP-PVT.

On the other hand, the computation of these coefficients based on the effective usage always refers to the same equations, but it employs only the data recorded during the actual working of the renewable part of the plant.

In the following sections, three case studies will be proposed:

- *Case study 1*: it is meant to introduce the reader into the innovative approach illustrated above. In these terms, a very simple case of HP sudden stops in which the cause was known is considered and a former application of the acceptance coefficient $C_{1,Th,solar}$ is provided.
- *Case study 2*: the application of a dataset concerned with the acceptance coefficients illustrated is proposed. This example is meant as a validation and as an instance of how the innovative approach has to be applied. The purpose is to show how any difference between actual and nominal coefficients cannot be immediately associated to acceptance issues, but it has to be carefully analyzed.
- *Case study 3*: the same dataset shown in the case study 2 is applied to a longer time period and the coefficients are compared to the ones obtained for case study 2. The target is to highlight the time-sensitivity of the parameters and show that their value is not constant over a given reference period (e.g. year). In turn this means that the application of the coefficients has to be referred to time periods long enough to be representative of the plant working and its usage.

2.9.1. Case 1 – sudden stops of the heat pump

The example of sudden, frequent HP blocks will be illustrated highlighting three main aspects:

- The importance of a DAS for
 - o Real time problems detection
 - o Troubleshooting, to understand the causes of each failure and identify the most appropriate actions.
- A former quantification about the influence of this issue by means of the coefficient $C_{1,Th,solar}$
- The definition of a simplified criterion to estimate the environmental conditions that cause the HP block.

Many periods of sudden HP stops have been recorded along the heating seasons 2017/2018. Their occurrence was quite uniformly distributed over the central part of the day and a general alarm was reported each time. Whenever the stop happened, the HP safety controls required a manual re-activation. The technical staff reported each intervention made to start up the HP again. After the first blocks, a general check on the plant was executed to assess any eventual failure, rupture or

clogging of the circuit that might have caused a safety block in the HP. Then, the technical manually reset the HP and made it work again. Unfortunately, after few minutes of operativity, another HP safety stop took place. The only choice left to the technicians was to bypass the HP, leaving operative only the integration burners. This problem is typically concerned with pilot plants, since the user load profile is not simulated and has to be satisfied, differently from a didactic workbench. As far as the acceptance field is concerned, this issue fits into the context of technological acceptance. The technical staff is not trained to manage innovative plants (different from the gas burners or the air-air HP installations), so every time an anomalous situation occurs, they cannot completely understand the reasons (and thus the causes). Consequently, they are compelled to switch off the innovative part of the plant to grant an operative facility.

This issue can be explained thanks to the dataset made available by means of the DAS. Assumed the correct working of the circulation twin pumps of each subsystem, the HP blocks are associated to a matter of temperature, not water flow rate. As illustrated in the introductory chapter, the HP is directly interfaced with two 500 l water storages, one on the evaporator and on the condenser side (named respectively cold and hot side tanks). This configuration is meant to grant a stable heat flux and water flow rate on both sides of the machine. So, given that the user load profile doesn't show significative variations, the problem might be concerned with the evaporator, in particular with the interface between the HP and solar subsystems.

The plot of the external temperature and irradiation over time collected by the DAS was superimposed to the periods in which the HP stopped. This analysis was carried out along the entire period of the two heating seasons. The occurrence of the HP sudden blocks was often in conjunction with stable meteorological conditions characterised by high irradiance and external temperatures between 10-15 °C.

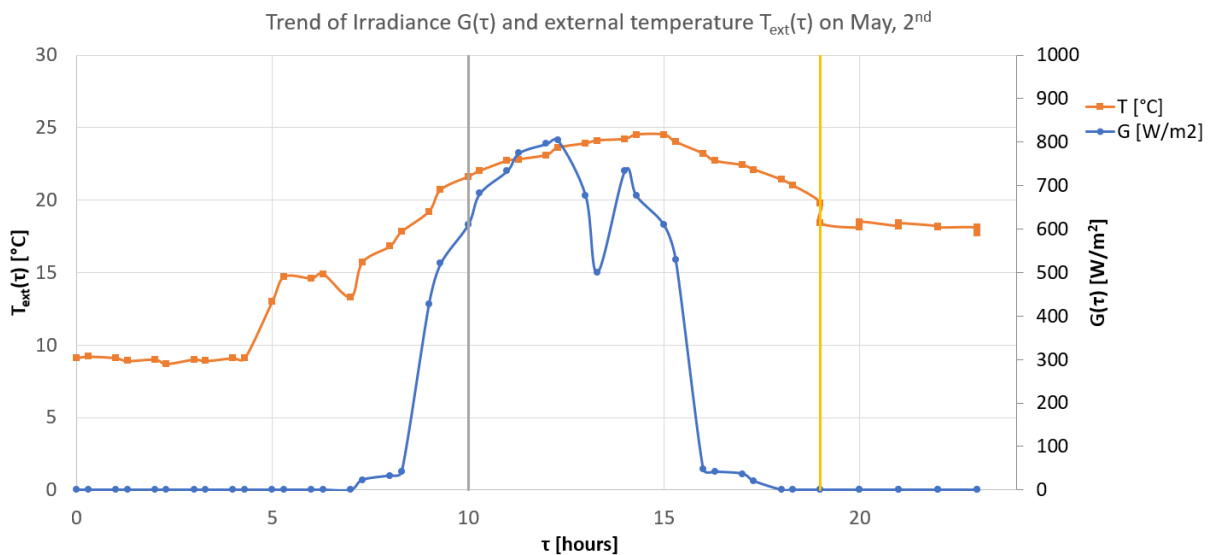


Figure 2.8. Trend of irradiance $G(\tau)$ and external temperature $T_{ext}(\tau)$ on May, 2nd. The grey and yellow vertical lines represent respectively the hour at which the HP arrested (about 10.00 a.m.) and the hour at which the plant might have worked (7.00 p.m.).

For the sake of brevity, the other recordings have been omitted and a single reference day, May 2nd has been chosen as representative of the problem. Figure 2.8 shows the recorded trend of these two parameters (temperature, orange line; irradiance, blue line) over one day reference time.

The sudden stop during this reference day occurred at about 10.00 a.m. (grey vertical line in Figure 2.8). After an interview to the technical staff, the facility resulted to be open and no manual switch from HP to fossil burners was done. Furthermore, no rupture was detected in the HP. According to the monitoring system, the integration burners for DHW and SH were operative during the period of the HP stop (between the grey and yellow line). This means that the HP stops could not be attributed to the lack of user thermal demand (e.g. DHW for showers).

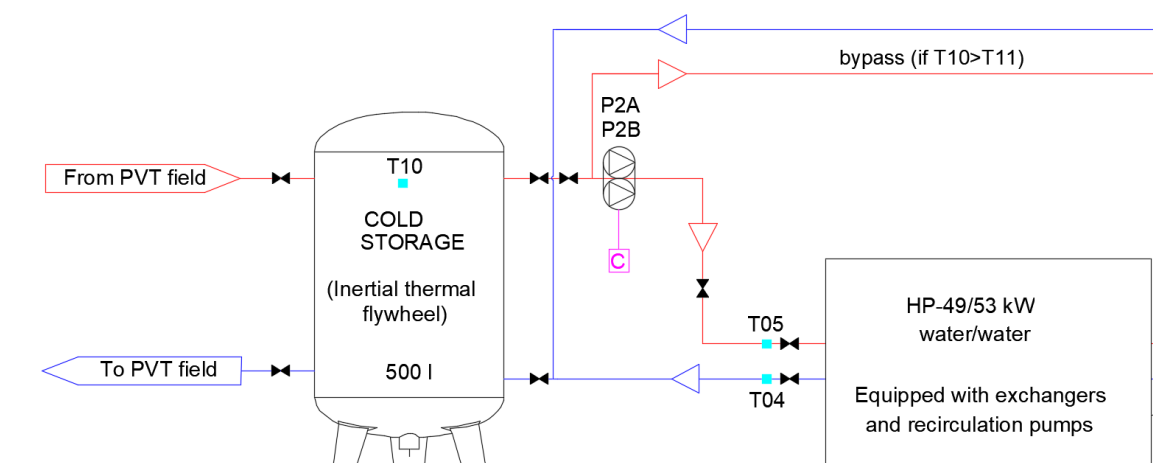
So, excluding issues associated to end users' acceptance or maintenance aspects, the problem is concerned with the operativity range in terms of temperature and pressure of the heat pump. Indeed, a temperature between 20 °C and 25 °C was recorded in the cold storage during the period analysed in Figure 2.8.

According to the handbook for the HP installed (model AERMEC WRL-H 026-161) [51], each time the temperature of the inlet water on the exchanger between the cold storage and the evaporator reaches temperatures of about 25 °C, a safety valve stops the HP to limit the suction pressure on the compressor to prevent early cracks.

In a general context, this issue can be easily avoided, with the substitution of the HP or at least with a variation of the HP components to adapt the machine to the specific working conditions. Actually, these two alternatives cannot be considered for the particular case study of the Palacus. In fact, any substitution has to be necessary and as economic as possible, since the annual budget of the sport facility is limited. On the other hand, any HP internal variation (if possible) leads to a tailored heat pump. This is in contrast with one of the potentials (and challenges) of SAHP technologies, which are obtained with the assembly of commercial components (e.g. solar panels and heat pumps).

So, a variation with respect to the original asset (Figure 1.27) of the HP subsystem was designed to overcome this limit. A short circuit between the summer bypass and pump P2 has been created. With the use of a three-way mixing valve, the cold water exiting the evaporator is mixed with the hot one entering the exchanger whenever a temperature within the critical range is measured. Figure 2.9 proposes a comparison before and after the variation inherently the HP subsystem.

a)



b)

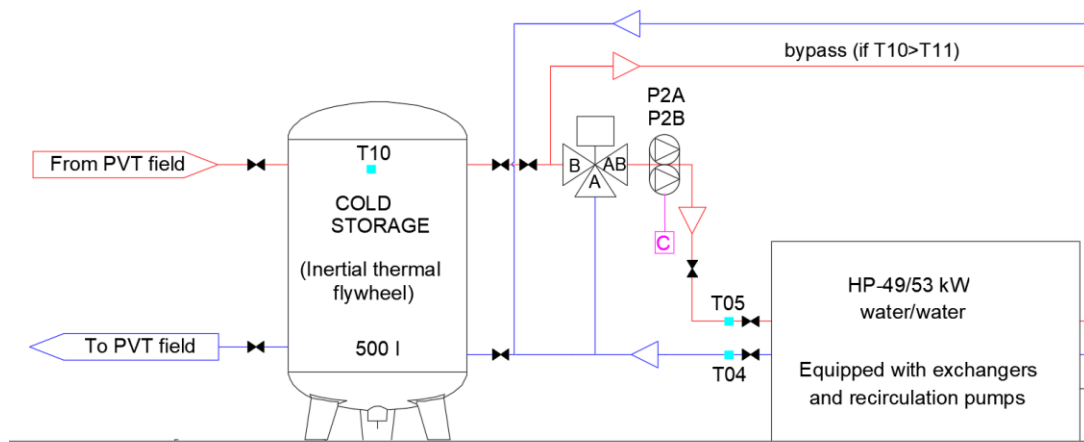


Figure 2.9. Detail of the functional scheme of the HP (shown in Figure 1.27 before a) and after b) the introduction of the three-way mixing valve.

With reference to Figure 2.9 some interesting considerations can be drawn:

- In energetical terms (area swept by the irradiance between the vertical grey and yellow lines, Figure 2.8), the heat pump has completely lost the solar thermal energy available in that period. Furthermore, the system automatically activates the gas burners to compensate the DHW and SH needs.
- Each time the HP stops suddenly, a safety control requires the manual restart of the machine. According to the maintenance contract, the technicians' intervention would occur within 48 hours after the call. This means that every-time a sudden stop occurs, 24-36 hours are completely lost to get the HP operative again. Moreover, the issue of technological acceptance described in the initial part of this section, forces the technical staff to switch the HP off, leaving active only the fossil burners. During these occasions, the HP inactivity period can extend up to about 48 h.

The greater losses in terms of operativity time are due not to the stop itself, but to the end-users' and technicians' "acceptance". Indeed, it can lead to the HP shut off for even some days without any technical effective reason. In addition, the issue of acceptance causes an increase in the maintenance cost, each time a technical extraordinary intervention is required.

- A brief estimation from the dataset collected by the monitoring system has brought to the following table in which are shown, month by month, the total amount of nominal working hours (considering only the days in which the sport facility was open) and the actual recorded working hours. Actually the different operative modes allowed by the DAS and illustrated in the introductory chapter (paragraph "Monitoring and remote-control systems", chapter 1) allow the SAHP operativity both in winter (for DHW and SH needs, coupled to the gas burners) and in spring/autumn (only for DHW needs coupled to the 35 kW gas burner). During summer, a bypass allows to directly connect the solar subsystem to the DHW distribution one, bypassing the HP which is off. For these reasons, the values reported in Table 2.1 is referred to the entire year, focusing on the solar field contribution to DHW. The quantity $\Delta\tau_{tot}$ shown in this table has been obtained from the data recorded counting the number of hours over the year in which a

DHW demand took place. As shown in the following case study, each time the temperature in the WSTs for DHW decreases, a domestic hot water draw occurs (e.g. from a sink or a shower). According to a rough analysis the 2200 working hours in Table 2.1 could represent a DHW demand of 7 hours over about 300 working days per year of the facility.

$C_{1,Th,solar,nominal}$ and $C_{1,Th,solar,actual}$ have been computed following Eq. (2.10), using as $\Delta\tau_{work,solar}$ the total nominal and actual working hours respectively.

2017-2018 - Month	Nominal working hours	Actual working hours	Variation [%]
January	87	30	65.5%
February	98	35	64.3%
March	104	34	67.3%
April	111	16	85.6%
May	115	43	62.6%
June	135	90	33.3%
July	150	107	28.7%
August	141	99	29.8%
September	127	34	73.2%
October	105	47	55.2%
November	88	41	53.4%
December	64	20	68.8%
Total	1325	596	55.0%
$\Delta\tau_{tot} = 2200 \text{ h}$	$C_{1,Th,solar,nominal}$	$C_{1,Th,solar,actual}$	
	0.602	0.271	55.0%

Table 2.1 Nominal and actual working hours of the solar field and computation of $C_{1,Th,solar}$ under nominal and actual conditions

A brief examination of Table 2.1, different, significative gaps can be identified:

- *Summer months*: an average difference of about 30% is recorded. This occurs especially in July, June and August, when the summer bypass has been active and SAHP off.
- *Spring/Autumn months*: the variation reaches its maximum during these periods. In particular, average variations of 71% and 60% are appreciated respectively in spring (March, April and May) and in autumn (September, October and November).
- *Winter months*: the average variation (65%) recorded between nominal and actual working hours lies between the ones estimated for summer and spring/autumn months.

The difference between the coefficients $C_{1,Th,solar,nominal}$ and $C_{1,Th,solar,actual}$ of about 55% give an idea about the relevance of the HP stops during year 2017-2018. The second case study proposed later shows that the variation of 55% can be mainly but not totally attributed to the HP block, due to the presence of other contributing causes.

Moreover, the main deviation between nominal and actual working hours is recorded in spring and not during winter as it might be expected. Indeed, the mild climate shifts the critical months from winter to spring (or autumn). In fact, the ambient temperature and irradiance during spring and autumn are more likely to determine the critical temperatures that cause the HP safety block.

The issue derived from the coupling between the cold side of an HP and a solar thermal circuit is due to an excessively high temperature at the evaporator (and therefore pressure at the compressor) in intermediate seasons. In fact, during spring and autumn the solar radiation and external temperature are not enough to produce directly hot water for the DHW/SH needs, but are high enough to cause the block of the HP. The “high” panel temperature (over 25 °C for the specific case) becomes even more likely in locations with mild climate, such as in Genoa. From a design point of view, the maximum panel temperature can be estimated by means of Eq. (2.11)

$$T_{max,panel} = T_{amb} + \frac{\alpha GA}{U_{panel}} \quad (2.11)$$

Where

α absorption coefficient [-]

G solar radiation [W/m²]

A area of the panel [m²]

T_{amb} ambient temperature [°C]

U_{panel} panel global thermal loss coefficient [W/m²K]

This simple evaluation relates the key thermal properties of a panel (absorption coefficient and global thermal loss coefficient) to the external ambient conditions (mainly solar radiation and external temperature). It can be obtained with a simplified application of the energy balance (I principle of thermodynamics for open systems under stationary or “lumped” conditions), neglecting the irradiation heat exchange (the hybrid panel temperature is near to the ambient one and therefore convection prevails) and the PV production. In order to estimate the maximum value reached at the panel, even the useful flux of the water flowing inside the panel is neglected. This might represent the case in which after a period of inactivity during the day, the plant activates again to integrate the DHW consumed. The relation expressed by Eq. (2.11) is indeed very approximated, but it still provides an idea about the frequency of the temperature of 25 °C being exceeded.

Table 2.2 shows the maximum temperature that can be reached by the solar panels according only to the external temperature (in green) and solar radiation (in blue) using Eq. (2.11). A value of 0.85 for the absorption and 15 W/m²K for the global thermal loss coefficient have been assumed. This last value is quite high, with respect to the thermal insulated panels, but it is still representative of the bare ones, like the hybrid panels installed at the Palacus SAHP-PVT plant.

		Solar radiation, G [W/m ²]						
		100	200	300	400	500	600	700
External temperature, T_{ext} [°C]	0	5.7	11.3	17.0	22.7	28.3	34.0	39.7
	2	7.7	13.3	19.0	24.7	30.3	36.0	41.7
	4	9.7	15.3	21.0	26.7	32.3	38.0	43.7
	6	11.7	17.3	23.0	28.7	34.3	40.0	45.7
	8	13.7	19.3	25.0	30.7	36.3	42.0	47.7
	10	15.7	21.3	27.0	32.7	38.3	44.0	49.7
	12	17.7	23.3	29.0	34.7	40.3	46.0	51.7
	14	19.7	25.3	31.0	36.7	42.3	48.0	53.7
	16	21.7	27.3	33.0	38.7	44.3	50.0	55.7
	18	23.7	29.3	35.0	40.7	46.3	52.0	57.7
	20	25.7	31.3	37.0	42.7	48.3	54.0	59.7
	22	27.7	33.3	39.0	44.7	50.3	56.0	61.7
	24	29.7	35.3	41.0	46.7	52.3	58.0	63.7

Table 2.2. Maximum panel temperature (T_{panel} , [°C]) according to external air temperature (T_{ext} , in green) and solar radiation (G, W/m², in blue). Red values represent temperatures higher than 25 °C

Values of either external temperature higher than 20 °C or solar radiation higher than 500 W/m², directly determine panel temperature over the critical limit of 25 °C (fixed limit for the present study). As far as the winter season in Genoa is concerned, the external temperature can reach a minimum of 0 °C (design temperature) up to peaks of about 20-22 °C. Table 2.3 provides the average air temperatures for each month.

Month	Average air temperature [°C]
January	10.2
February	10.3
March	10.9
April	15.1
May	18.5
June	22.2
July	24.4
August	23.4
September	22
October	18
November	13.1
December	9.8

Table 2.3. Mean air temperature for each month [52].

On the other hand, during sunny winter days, the solar radiation easily reaches 500 W/m² with peaks of 600-700 W/m². This means that the panel temperature is very likely to overpass the limit

of 25 °C even during winter as shown in this preliminary evaluation. Case 2 will highlight a significant increase in terms of $C_{1,Th,solar}$ (namely working hours of the plant) after the plant integration with the mixing valve (Figure (2.9)b) has taken place.

2.9.2. Case 2 – evaluation of the acceptance level for the DHW system

In this second example, the set of coefficients is computed always referring to the DHW subsystem. The case study 1 was a simplified example in which the problem and the related causes of the HP stop were already known just by means of the DAS. The application of only $C_{1,Th,solar}$ was meant to introduce a former application, to make the usage of the coefficients in the present case study easier.

Indeed, the main purpose is to illustrate the innovative approach with a practical example, highlighting:

- the importance of using a set of coefficients instead of only one when performing an analysis over a part of the plant (as well as the entire installation) and any eventual failure is due to unknown reasons. This is the most frequent and general case with respect to case 1 where the data set collected itself cannot directly explain the causes and a post analysis is required.
- the need of a post-processing analysis to associate the correct causes to the values computed
- the time sensitivity of the proposed coefficients and the importance to define an adequate reference time period

This section is concerned with the evaluation of the parameters $C_{1,Th,solar}$, C_3 , $S\eta_p$, referred to a period subsequent (2018/2019) to the integration of the mixing valve within the interface evaporator/cold side solar storage (case 1 Figure (2.9)b)). During this period, no significative alarms were recorded by the DAS neither complaints were received by the users or the technical staff. As usual, both nominal and effective usage conditions have been applied, following the previous definition (paragraph “Case study: the acceptance evaluation of the DHW subsystem).

Table 2.4 resumes the nominal and effective indicators for the time from November 2018, to May 2019.

Indicator	Nominal usage	Actual usage	Variation
$C_{1,Th,solar}$	0.584	0.356	39.0%
C_3	0.320	0.172	46.3%
$S\eta_p$	0.799	0.520	34.9%

Table 2.4. Indicators computed assuming nominal and effective usage of the solar thermal field for DHW production

The following observations can be drawn:

- the application of the coefficients only to the nominal usage provides a term of comparison to which the effective usage indicators can be referred to. In this way, considering for instance the seasonal efficiency, we can notice that a value near 0.8 for this specific installation shows a case in which the solar thermal plant is widely used. In fact, the nominal usage can be conceived as the value reached by means of a plant which is normally used. It is associated to (but different from) efficiency, under very strong and simplified assumptions (e.g. steady state). This link with the concept of efficiency allows the evaluation of how much the plant is used and therefore accepted. Clearly, the usage of the plant does affect its performance independently from its efficiency. This can lead to a limit case of an unused and overlooked installation (no matter its efficiency) with an acceptance level equal to zero.
- Coherently with the definition, c_3 is generally lower than $S\eta_p$ since it is referred to the total irradiance and not only the i^{th} working periods of the solar subsystem pump. Its major percentage variation (46.3%) over the nominal conditions with respect to the one about $S\eta_p$ (46%) is connected to the variable speed of pump P1. In fact, the flow rate within the solar field is modulated according to both the end users' need and the thermal gradient between the inlet/outlet water within the solar circuit.
- As far as $C_{1,Th,solar}$ is concerned, a first remark is about the nominal value: a small variation can be appreciate between Case 1 ($C_{1,Th,solar,nom} = 0.602$) and this case study ($C_{1,Th,solar,nom} = 0.584$). This difference is due to the connection of the nominal conditions as the sum of the solar field effective working periods and the hours in which the gas burners substituted (not integrated) the SAHP-PVT. As a consequence, the nominal value can vary and resize itself according to the external conditions (e.g. irradiance availability which influences the effective working periods) and the usage of the facility (which influences the hours in which the gas burners substituted). In conclusion the value of $C_{1,Th,solar,eff}$ has shown an increase from 0.271 to 0.356 (about 25% increase) after the design integration on the interface between the HP evaporator and the solar field (case 1 Figure (2.9)b)).

At first analysis, all the indicators might show that the actual usage has been about 60% of the nominal one and this might be symptom of a low level of acceptance. The influence of the high temperature alarm can be excluded since, after the installation of the new mixing (case 1 Figure (2.9)b)) any sudden HP block was no more recorded. An in-depth analysis and comparison with the data collected showed that in many cases in which the end-users needed DHW, the external irradiance was very low: as a consequence, the gas burner had to cover the needs of the facility and the solar subsystem was not operative. So, these low indicators are associated to periods in which a DHW need was present, but the solar thermal field couldn't supply heat because of the border environmental conditions (e.g. low irradiance). This situation didn't depend on the end-users' employment of the renewable plant and so it cannot stand for low levels of acceptance. Figure 2.10 provides a useful graphic example:

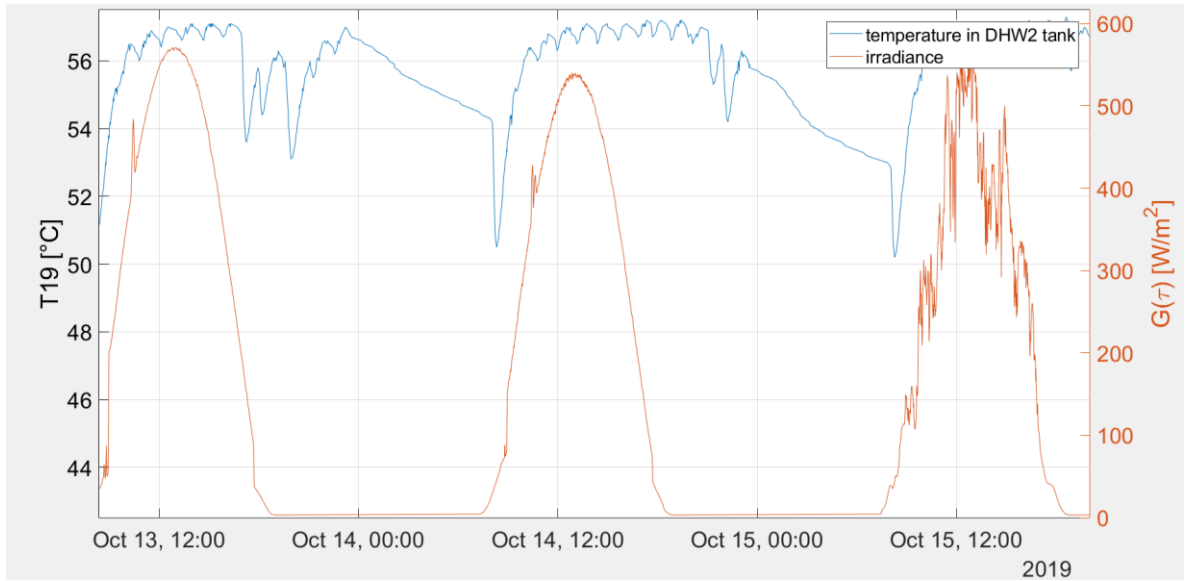


Figure 2.10. Plot (on the left y-axis) of the temperature in the DHW2 water storage tank (blue line) against (on the right y-axis) irradiance G (orange line) associated to almost sunny days.

The plot is referred to the temperature inside the DHW storage tank directly connected to the inlet water (while DHW1 is the tank concerned with the water load and the heating interface with fossil burners/HP). Indeed, the oscillations in the temperature trend are very small, but represent the end users' DHW consumption. As far as the time period used in Figure 2.10 is concerned, a consistent hot water draw can be appreciated late in the afternoon or even at night. This trend occurs quite uniformly over the year. Even assuming a sunny weather, the thermal field can at least contribute significantly only in the first part of the day while the latter is almost completely left to the fossil burners.

Figure 2.11 shows the same quantities in Figure 2.10, referred to cloudy days:

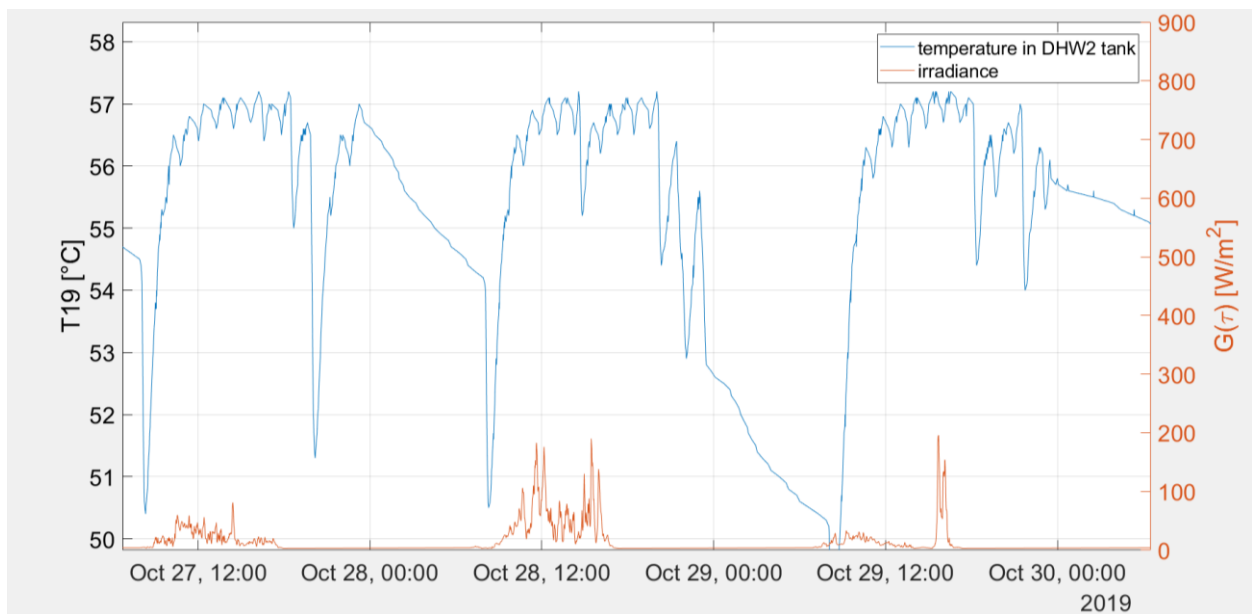


Figure 2.11. Plot (on the left y-axis) of the temperature in the DHW2 water storage tank (blue line) against (on the right y-axis) irradiance G (orange line) associated to cloudy days.

In this case, the cloudy and variable weather almost excludes the contribution of the renewable part of the plant, which has been substituted by the gas burners, negatively affecting the indexes above. However, the cause is concerned with physical limits associated to the external weather and to the period in which the DHW need occurs and it cannot be linked to acceptance issues.

Even neglecting the weather, Figure 2.10 and Figure 2.11 show that many peaks in DHW needs occurred in correspondence with minimum solar irradiance. As a consequence, the low value of end user and efficiency parameters computed in this case means only that the solar thermal energy available in the considered period is almost trivial and the gas burners have switched on, to meet the instantaneous end-users' DHW needs.

This case study provides a validation of these coefficients and a strategy to their correct application. The use of a single parameter can determine misleading conclusions and they must be used grouped, also referring both to the experimental data collected and nominal usage conditions of the plants. In this way parameters can be put into context and low acceptance/efficiency subsystems can be identified. In this example, the differences highlighted between actual and nominal coefficients cannot be representative of significative low acceptance issues, since their percentual variation was almost uniform. Nevertheless, the conclusions have to be post-analysed to put into the correct context each result obtained.

The potential of this approach consists as well in the multiple possible application at different levels, from a specific subsystem to the entire plant, with high versatility and self-adaptation of the reference, nominal coefficients employed. The key concept of this approach is linked to the definition of "status parameters" referred to the plant and not necessarily concerned only with acceptance. In this way the entire problems, faults and anomalies in the plant can be accounted for, associating to each case the proper causes and remedies (e.g. more effective regulation criteria, plant integrations). This organic approach allows to integrate acceptance analyses (usually performed apart) in a global evaluation system.

2.9.3. Case 3 - evaluation of the level of acceptance over time

In this section, the coefficients provided in Table 2.4 has been integrated, computing the parameters over a longer time period. In particular, the coefficients in case 2 were almost referred to the heating season 2018-2019 (from November 2018 to May 2019 – period A). On the other hand, in this case the coefficients have been evaluated over a second time period as well (named period B, from November 2018 to September 2019) which is concerned with both period A and the following summer. In other words, the new calculation of the parameters in period B is meant to show how the results change as an update over time is carried out (Table 2.5).

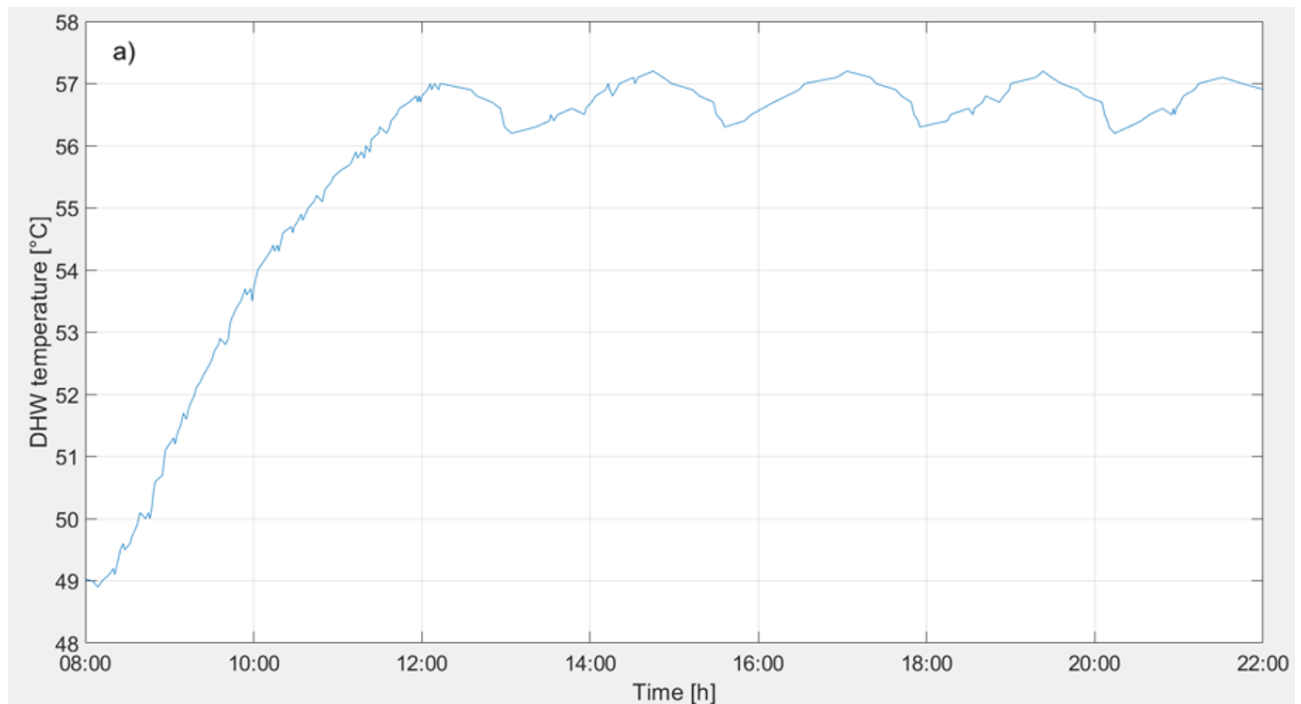
The comparison between nominal and actual usage (period A) have been already examined in the previous section. Some considerations on the values between period A and B can be drawn: as shown in Table 2.5, a general quite uniform increase can be noticed, about 5%, in particular concerning $C_{1,Th,solar}$.

Indicator	Nominal usage	Effective usage over period A (November 2018-May 2019) [49]	Effective usage updated over period B (November 2018-September 2019)	Percent variation (effective usage over period B vs period A)
$C_{1,Th,solar}$	0.584	0.356	0.376	5.6%
C_3	0.320	0.172	0.179	4.0%
$S\eta_p$	0.799	0.520	0.542	4.2%

Table 2.5. Parameters evaluation under nominal and effective usage for DHW application with the contribution of the solar field, updated over time (periods A and B).

Following the same approach illustrated in case 2, the difference with the values referred to period A (and consequently with the nominal ones), needs a post-analysis, based on the measurements collected. The plant hasn't undergone any variation during the summer period and the consumption of DHW can be considered almost unchanged. This statement can be better understood considering Figure 2.12 which shows the average temperature trend in the DHW tanks during a standard day in winter and summer, respectively. Each decrease appreciated represents a DHW usage (mainly for showers) which is then heated up by the plant in a very brief period. The comparison of case a and b of Figure 2.12 shows that the usage of DHW increases its frequency with a simultaneous reduction in the temperature gradient associated to each peak.

Physically, this change is coherent with the expectation of more common and colder showers. In turn, the energy demand over the day has remained almost unchanged from winter to summer, but with a different distribution over time (Figure 2.12).



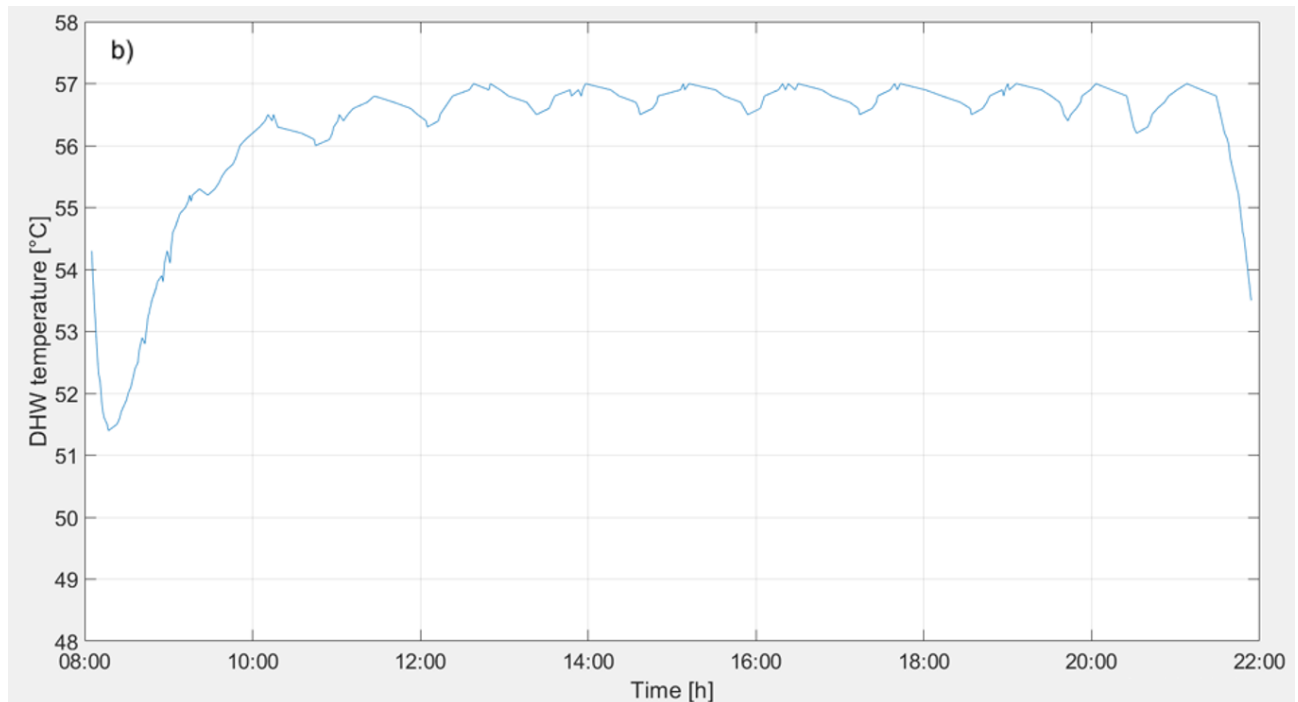


Figure 2.12. DHW usage based on DHW hot storage tank temperature profiles. Typical day trends for a) winter and b) summer.

Moreover, an increase both in the average temperature for the solar thermal circuit and in P1 operativity period have been recorded during summer, coherently with the increased solar radiation. This means that the coefficients variation recorded between period A and B (Table 2.5) cannot be associated to matters of plant improvements or end users' acceptance.

The main cause is associated to the seasonal fluctuations of the environmental conditions: during summer, the direct solar thermal contribution for DHW is more likely and significant than in winter. This in turn determines an increase of the parameters, as shown in Table 2.5, without implying any plant flaw or variation of the global end users' approval of the facility.

Some key concepts can be outlined from this example:

- *Time sensitivity*: as shown in Table 2.5, the innovative acceptance parameters show time dependence and they need to be updated. The real time DAS acquisition meets this target, but it is important to highlight that the application of the innovative approach over different time periods leads to different results. So, comparisons between different years have to be referred to the same time periods in order to be analysed. Moreover, the choice of the reference time span should base for instance on a yearly period. This time length is long enough to cover the fluctuations associated to the plant over the different seasons. Analyses on shorter time periods (especially among similar plants) might determine misleading results if not put in the proper context and comparable time period.
- *Nominal conditions*: As stated formerly, the nominal conditions represent a necessary reference point to which compare the parameters computed under the actual use. As the dataset covers more years, the parameters computed referring to previous time periods and historized can be employed in the update of the nominal conditions over time accounting for the evolutions in the plant usage. So, the nominal conditions defined formerly can

represent a good initial point whenever there is no data available or it cannot completely define the typical conditions of the plant working.

2.10 Conclusions

The correct and exhaustive evaluation of acceptance plays a central role both in the design of new plants and in the management of the existing ones. In particular, acceptance might be the swing vote between a successful or unsuccessful facility. Anyway, this issue hasn't been consolidated yet in the standard procedures for the evaluation of plant design/management, but it is often even neglected. Up to now, the traditional heating plants (e.g. gas burners) haven't emphasised this need, due to their simplicity, but the relevance of acceptance is expected to grow as complex technologies and plants (e.g. the SAHP-PVT) take place on the market. No unique sets of coefficients or consolidated methodologies have been presented or widely adopted, so far. The enquiries normally carried out often neglect that the answers collected might not really and fully be representative of the people's opinion. In other words, the degree of uncertainty of measurement linked to people's feeling is often overlooked. Moreover, the temporal validity range of these surveys is often limited or not appropriately considered. The parameters proposed and the innovative approach in which they are framed aim to bridge the gap providing a common methodology to the problem. In this way the acceptance evaluation becomes one aspect of a complete, organic assessing approach in which the general status of the plant is studied. Thanks to a DAS, the same working parameters recorded can be employed to perform for instance efficiency analysis, transient simulation and even an evaluation of the subjective feeling about the installation. The need of a post-analysis is always advisable, especially in complex installations, to understand the causes of each recorded anomaly and find the correct "remedy".

The three examples provided are meant both to outline the methodology to apply the innovative approach and to show how acceptance analyses cannot be carried out separately.

In Case 1, no direct acceptance issues were identified, since the main problem was associated to a technical flaw (high suction pressure at the compressor). Nevertheless, it caused indirectly a lack of confidence in the plant, since frequent, sudden HP blocks occurred. As the plant integration with the mixing valve on the inlet water to the evaporator occurred, a significative benefit has been recorded in the following analyses (Case 2). This is a clear demonstration of the motto "a working and user-friendly plant is an accepted one". Indeed, the integration of the mixing valve has solved the problem without requiring either the end-users' or the technicians' constant intervention.

In Case 3, time sensitivity has been enquired since the results need to be constantly updated and it cannot be ignored to perform analyses evolving with the usage of the facility.

The validity of the innovative proposed approach, even if formulated for a SAHP-PVT installation, can be generalised with ease: the key outlines and the coefficients themselves can be best adapted to the specific case. Furthermore, the criteria behind the approach can be employed in fields of acceptance not directly concerned with plants. Indeed, the versatility of the parameters allows their reformulation referring to both the total plant and its specific sub-systems. The uncertainty associated to the end users' involvement in the evaluation process has been removed with the exclusion of their direct contribution (e.g. interviews, questionnaires). The level of the end users' satisfaction and approval of the plant is directly estimated through the customers' usage of the facility. In this context, the implementation of a DAS becomes doubly necessary, to allow both the

normal plant management and the data acquisition to carry out a time varying evaluation of the level of acceptance.

As far as future developments are concerned, the application of this innovative approach proposed has to be extended to the other subsystems of the plant, analysing their variation over time. Among the plant efficiency parameters, an assessment on SCOP shall be carried out, in order to provide a parameter suitable to assess both the plant performance and the issues connected to the level of acceptance.

REFERENCES

- [1] P. M., «The Stakeholder Perspective: How management of KPIs can support value generation to increase the success rate of complex projects,» in *16th Int'l Conference on Project Management and Scheduling*.
- [2] "PMI's Pulse of the Profession, 10° Global Project Management Survey," 2018. [Online]. Available: <https://www.pmi.org/-/media/pmi/documents/public/pdf/learning/thought-leadership/pulse/pulse-of-the-profession-2018.pdf>. [Accessed 19 December 2019].
- [3] "Cambridge Dictionary," [Online]. Available: <https://dictionary.cambridge.org/it/dizionario/inglese/acceptance> . [Accessed 18 February 2019].
- [4] V. Bertsch, M. Hal, . C. Weinhardt e W. Fichtner, «Public Acceptance and Preferences Related to renewable Energy and Grid Expansion Policy: Empirical insights for Germany,» *Energy*, vol. 114, pp. 465-477, 2016.
- [5] D. Schumann, W. Kuckshinrichs e J. F. Hake , «Public Acceptance,» in *Carbon Capture, storage and use*, Springer, 2015, pp. 221-251.
- [6] R. Wüstenhagen, M. Wolsink e M. J. Bürer, «Social Acceptance of Renewable Energy Innovation: An Introduction to the Concepts,» *Energy Policy*, n. 35, p. 2683 – 2691, 2007.
- [7] A. O. Erbil , «Social Acceptance of the Clean Energy Concept: Exploring the Clean Energy Understanding of Istanbul Residents,» *Renewable and Sustainable Energy Reviews*, vol. 15, pp. 4498-4506, 2011.
- [8] T. Takashi e T. Sato, «Inclusive Environmental Impact Assessment Indices with Consideration of Public Acceptance: Application to Power Generation Technologies in Japan,» *Applied Energy*, vol. 144, pp. 64-72, 2015.
- [9] R. Sauter e J. Watson , «Strategies for the Deployment of Micro-Generation Implications for Social Acceptance,» *Energy Policy*, vol. 35, pp. 2770-2779, 2007.

- [10] H. Saizarbitoria, I. Zamanillo e I. L. Iker, «Social acceptance of ocean wave energy: A case study of an OWC shoreline plant,» *Renewable and Sustainable Energy Review*, vol. 27, pp. 515-524, 2013.
- [11] M. Maack e B. Skulason, «Implementing the hydrogen economy,» *Journal of Cleaner Production*, vol. 14, pp. 52-64.
- [12] «Energy: issues, options and technologies, science and society. A report produced by The European Opinion Research Group (EORG) for the Directorate-General for Research,» Eurobarometer, Luxembourg, 2003.
- [13] A. Simon e R. Wustenhagen, «Factors influencing the acceptance of wind energy in Switzerland,» in *Workshop "Social acceptance of renewable energy innovation"*, Tramelan (Switzerland), 2006.
- [14] F. D. Musall e O. Kuik, «Local acceptance of Renewable Energy – A Case study from Southeast Germany,» *Energy Policy*, vol. 39, pp. 3252-3260, 2011.
- [15] L. Xin-Le e L. Wei-Haur, «Public Acceptance of Marine Renewable Energy in Malaysia,» *Energy Policy*, vol. 65, pp. 16-26, 2014.
- [16] R. Bhandari, A. Trudewind e P. Zapp, «Life cycle assessment of hydrogen production via electrolysis – a review,» *Journal of Cleaner Production*, vol. 85, pp. 151-163, 2014.
- [17] D. M., « Understanding and Overcoming the Nimby Syndrome,» *Journal of the American Planning Association*, Vol. 58, pp. 288-300, 1992.
- [18] D. Wright, e Patrick, «Rethinking NIMBYism: The role of place attachment and place identity in explaining place-protective action,» *Jour. of Com. & App. Social. Psyc*, vol. 19, pp. 426-441, 2009.
- [19] [Online]. Available: <https://metal-gaia.com/2012/07/19/not-in-my-backyard/> . [Consultato il giorno 28 March 2020].
- [20] K. Langer, T. Decker, J. Roosen e K. Menrad, «Factors Influencing Citizens' Acceptance and Non-Acceptance of Wind Energy in Germany,» *Journal of Cleaner Production*, vol. 175, pp. 133-144, 2018.
- [21] P. Upham e J. García Perez, «A cognitive mapping approach to understanding public objection to energy infrastructure: the case of wind power in Galicia, Spain,» *Renewable Energy*, vol. 83, pp. 587-596, 2015.
- [22] P. Bansal e K. Roth, «Why companies go green: a model of ecological responsiveness,» *Academy of Management Journal*, vol. 43, n. 4, p. 717–736, 2017.
- [23] S. N., «The Stern review on the economics of climate change,» 2006.

- [24] F. D. Davis, «Perceived Usefulness, Perceived Ease of Use and User Acceptance of Information Technology,» *MIS Quarterly*, vol. 13, pp. 319-339, 1989.
- [25] “Eurostat,” [Online]. Available: https://ec.europa.eu/eurostat/statistics-explained/images/8/80/Figure_4-Gross_inland_consumption_of_renewables_EU-28_1990-2016.png. [Accessed 5 July 2020].
- [26] [Online]. Available: https://ourworldindata.org/exports/modern-renewable-energy-consumption_v7_850x600.svg . [Consultato il giorno 28 March 2020].
- [27] «RenOnBill,» [Online]. Available: <https://www.renonbill.eu/methodology>. [Consultato il giorno 22 April 2020].
- [28] [Online]. Available: <https://ec.europa.eu/info/funding-tenders/opportunities/portal/screen/opportunities/topic-details/lc-sc3-ee-13-2018-2019-2020>. [Consultato il giorno 28 March 2020].
- [29] H. C. Kim, «Acceptability engineering: the study of user acceptance of innovative technologies”, *Journal of Applied Research and Technology*,» vol. 13, pp. 230-237, 2015.
- [30] M. G. A., *Crossing the Chasm: Marketing and Selling Disruptive Products to Mainstream Customers*, 2014.
- [31] V. Venkatesh e H. Bala, «Technology Acceptance Model 3 and a research agenda on interventions,» *Decision sciences*, vol. 39, pp. 273-315, 2008.
- [32] P. D. Wright, «Reconsidering Public Acceptance of Renewable Energy Technologies: a Critical Review,» *Chapter for inclusion in: Jamasb T., Grubb, M., Pollitt, M. (Eds), Delivering a Low Carbon*, 2008.
- [33] R. P. Bagozzi, F. D. Davis e I. R. Warshaw, «“User Acceptance of Computer Technology: a Comparison of two Theoretical Models”, *Manag. Sci.*,» vol. 35, n. 8, pp. 903-1028, 1989.
- [34] R. Kardooni, . S. B. Yusoff e F. B. Kari, «Renewable Energy Technology Acceptance in Peninsular Malaysia,» *Energy Policy*, vol. 88, pp. 1-10, 2016.
- [35] L. Tagliafico, A. Cavalletti, C. Marafioti e A. Marchitto, «End users’ acceptance of new technologies in building heating: An experience on solar assisted heat pumps,» *TECNICA ITALIANA-Italian Journal of Engineering Science*, vol. 63, n. 2-4, pp. 198-204, 2019.
- [36] S. Owens, «Siting, sustainable development and social priorities,» *Journal of Risk Research*, n. 7, p. 101–114, 2004.
- [37] P. Slovic, «Perceived risk, trust and democracy,» *Risk Analysis*, vol. 13, p. 675–682, 1993.

- [38] T. Takahashi e T. Sato, «Inclusive environmental impact assessment indices with consideration of public acceptance: application to power generation technologies in Japan,» *Applied Energy*, vol. 144, pp. 64-72, 2015.
- [39] T. Sato e T. Omiya, «Triple I of CO2 ocean sequestration against ocean surface acidification,» *Journal of Japan Society of Naval Architects and Ocean Engineers*, vol. 8, p. 9–16, 2008.
- [40] K. Otsuka, «Inclusive impact index “Triple I”,» *Japan Society of Naval Architects and Ocean Engineers*, vol. 38, p. 15–8, 2011.
- [41] H. Odum , «Environmental accounting: energy and environmental decision making,» *John Wiley & Sons INC*, p. 370, 1996.
- [42] X. Yuan, J. Zuo e D. Husingh, «Social Acceptance of wind power: a case study of Shandong Province, China,,» *Journal of Cleaner Production*, vol. 92, pp. 168-178, 2015.
- [43] G. Simpson e J. Clifton , «Subsidies for residential solar photovoltaic energy systems in Western Australia: distributional, procedural and outcome justice,» *Renewable and Sustainable energy reviews*, vol. 65, pp. 262-273, 2016.
- [44] G. Simpson e J. Clifton , «Subsidies for residential solar photovoltaic energy systems in Western Australia: distributional, procedural and outcome justice,» *Renewable and Sustainable energy reviews*, vol. 65, pp. 262-273, 2016.
- [45] M. M. E. Moula , J. Maula, M. Hamdy, T. Fang, N. Jung e R. Lahdelma, «Researching social acceptability of renewable energy technologies in Finland,» *International journal of sustainable built environment*, vol. 2, pp. 89-98, 2013.
- [46] G. Guest , E. Namey e M. Mitchell, *Collecting qualitative data: a field manual for applied research*, Sage, 2013.
- [47] S. Tampakis, G. Arabatzis, G. Tsantopoulos e I. Rerras, «Citizens’ views on electricity use, savings and production from renewable energy sources: A case study from a Greek island,» *Renewable and Sustainable Energy Reviews*, vol. 79, pp. 39-49, 2017.
- [48] [Online]. Available: <https://ec.europa.eu/eurostat/documents/3217494/7089681/KS-04-15-567-EN-N.pdf>. [Consultato il giorno 18 12 2019].
- [49] L. A. Tagliafico, V. Bianco, A. Cavalletti, C. Marafioti e A. Marchitto, «Monitoring and control of a pilot plant made of solar assisted heat pump with hybrid panels,» *AIP Conference Proceedings*, vol. 2191, 2019.

- [50] F. Scarpa, A. Reverberi, L. A. Tagliafico e B. Fabiano, «An Experimental Approach for the Dynamic Investigation on Solar Assisted Direct Expansion Heat Pumps,» *Chemical Engineering Transactions*, vol. 43 , pp. 2485-2490, 2015.
- [51] [Online]. Available:
https://www.hjj.dk/Files/Data/ITB/Shop_HJJ/Documents/WRL%20teknisk%20information.pdf . [Consultato il giorno 31 March 2020].
- [52] *UNI 10349 part 1*- Heating and cooling of buildings - Climatic data - Part 1: Monthly means for evaluation of energy need for space heating and cooling and methods for splitting global solar irradiance into the direct and diffuse parts and for calculate the solar irradiance on tilted planes, 2016.
- [53] B. Sutterlin e M. Siegrist , «Public Acceptance of Renewable Energy Technologies from an Abstract versus Concrete Perspective and the Positive Imagery of Solar Power,» *Energy Policy*, vol. 106, pp. 356-366.

3. NUMERICAL MODELLING OF THE SAHP-PVT PLANT

In common applications, plant design is still carried out with very little help from computer programs, leaving only the most complex ones to numerical simulations. In addition, most of plants work and are conceived to work under steady state conditions which simplifies the design calculations. Indeed, the complexity in the plant scheme, joined with the multiple operating modes under transient regime and the total cost of the investment justify the effort of a detailed numerical modelling of the installation.

Typically, these configurations are equipped with an extended grid of measuring devices (e.g. temperature, flow rate) which belong to a DAS. In fact, the issue of plant complexity is normally countered by a data control and acquisition system, since it is the best way to make the plant competitive and self-managed. Indeed, the wider the dataset the better the plant status is known with direct insight on every component and every unexpected failure. The introduction of many measuring devices increases the difficulties in the information processing as well as data extrapolation.

On the economical side, each instrument represents an additional term in the cost of the plant, so in market applications the minimum number of sensors has to be installed within the plant.

Moreover, the topic of monitoring and data acquisition is quite a normal issue under industrial application with adequate budget. The assembly of the plants under study is performed with commercial models without tailored components or specifically designed on board data acquisition systems. In this context, the use of numerical modelling can determine a reduction in the installed measuring devices since the missing information can be evaluated by means of numerical simulations. This application for numerical modelling is still quite unusual especially in the context of civil plant management, but it represents a new frontier in which simulations can compensate the missing unmeasured parameters also at lower levels with smaller budgets. Moreover, the model becomes an additional, powerful tool to run simulations about different possible configurations of the plant and to define programmed maintenance plans.

The chance of a model calibrated on real data is one of the most significant differences with respect to the design stage where standard assumptions (and simplifications) are taken. Usually this aspect is not significant for mature and widespread technologies (most of which work under steady state conditions). The lack of a complete and consolidated design approach for SAHPs as well as their impossibility to work under steady state conditions leave a degree of uncertainty between the results obtainable and the real performances reached (e.g. [1]). For this reason, smaller prototypes are often built on the same site to get real experimental data on which base the plant design. Within this context, dynamic numerical simulations constitute the most correct way to model their behaviour since the boundary conditions show a strong oscillation over time and no effective steady state is reached. As a consequence, any steady state model will lead to results that can be hardly associated to the real working of the plant. In addition, each component is modelled to fit the data

collected, according to preliminary theoretical estimation. In this way the model can grant a good resemblance with reality and the correspondence with the components effectively installed according to the installation method.

The software adopted in this work to carry out the simulations shown below is TRNSYS. This program is a transient systems simulation program with a modular flexible structure that can be extended and upgraded by the users themselves starting from the source code of each component (written using FORTRAN language). The TRNSYS library includes many of the components commonly found in thermal and electrical energy systems, as well as component routines to handle input of weather data or other time-dependent (e.g. mathematical models user defined) forcing functions and output of simulation results. TRNSYS is well suited to detailed analyses of any system whose behaviour is dependent on the passage of time. The main applications allowed by the software include the solar systems (solar thermal and photovoltaic systems), as well as their integration with other components (e.g. HP and gas burners).

3.1. Numerical model of the DHW subsystem

A case study concerning only the DHW sub-system is presented below to provide a first insight of the numerical code, the approach followed in its assembly and for the validation/calibration. This example shows the application of TRNSYS to model a portion of the plant in detail only during night. Indeed, some properties of the plant (e.g. thermophysical characteristics of the single components) can be validated when the entire plant is off. For instance, the global thermal loss coefficients of the DHW boilers can be determined very easily once the cooling process is recorded. Actually, the installation is coupled to a sport palace and therefore the plant cannot be stopped, even temporarily, to collect this information. This problem has been overcome by means of the almost continuous recording of information of the DAS during night as well. This case study belongs to the wider context of Inverse Heat Transfer Problems (IHTPs). This issue refers to all those applications in which some quantities such as temperature or heat fluxes are measured while others are unknown. In other words, direct problems find the effect of a cause, while the inverse ones try to obtain the opposite. Commonly, an inverse problem determines quantities (e.g. properties of a body, boundary or initial conditions, shape of a body) from other observed physical quantities. This special and unstable link between experimental and theoretical research constitutes both the weak and the strong side of this approach. The instability of the process lies in its sensitivity to measurement uncertainties which is in turn worsened by the effort to obtain the maximum information from the recorded data. Under these terms, IHTPs are generally classified as ill-posed problems, since at least one of the following conditions is not met [2]:

- Existence of the solution
- Uniqueness of the solution
- Stability of the solution

The existence of a solution for an IHTP can be granted by physical reasoning. For instance, a change in the measured temperature for a transient problem implies a causal characteristic (e.g. a boundary heat flux) to be estimated. On the other hand, the uniqueness of the solution for inverse problems can be mathematically proved only for some special cases [3], [4].

Different classifications for IHTPs are available in literature for instance according to the heat transfer process that occurs or based on the quantities to be estimated. Following this last principle, IHTPs can be subdivided into the following categories:

1. *Boundary value determination inverse problems*: part of the boundary conditions is unknown while measurements/predictions (e.g. about temperatures or heat fluxes) are available for the internal points.
2. *Initial value determination inverse problems*: the initial distribution of a given quantity is not known (e.g. temperature).
3. *Material properties determination inverse problems*: these quantities can be both constant and variable over time, space or temperature.
4. *Source determination inverse problems*: the problem may concern the intensity of the source or its location (even with moving sources) or both.
5. *Shape determination inverse problems*: the location and the shape of the boundary domain is not known. So, the lack of a portion of data is compensated with additional and over-specified information.

Concerning the solution techniques, many approaches can be adopted, among which the finite differences [4], [5], [6], finite elements [7], [8], [9] and boundary elements [10], [11], [12], [13] can be identified. Actually, some common criteria can be proposed regardless of the approach employed to solve IHTPs [14], [4]:

- No a priori smoothing of the input data
- Temperature measurements from one or more sensors permitted
- Applicable to variable number of measures
- Extension of the method to more than one unknown
- Ease of use and computation of the code

With reference to the classification reported above, these models belong to the ITHP concerning the properties of the system and other boundary conditions (e.g. water draw forcing functions) which cannot be directly detected by means of the data acquisition system.

3.1.1. Brief description of the subsystem

This section is meant to recall the parameters used below. Further descriptions and details can be found at the section “*Palacus sport palace – the facility*”.

The DHW is stored in two boilers of 1500 l each (DHW1 and DHW2) installed in series. DHW1 is heated by the HP and then eventually integrated by a fossil burner (circuit with the twin pumps P8). Pump P10 grants the recirculation inside the two boilers while pumps P9 grant the recirculation. T14 and T19 represent the temperatures of water inside DHW1 and DHW2. The outlet temperature for DHW is measured by means of sensor T20. It is kept equal to the set point value (T20*) thanks to a three-way valve which mixes the water coming from the boiler, the adduction from the water supply and the flow rate coming from the recirculation circuit. T16 represents the temperature of the water heated with the integration fossil burner (Figure 3.1).

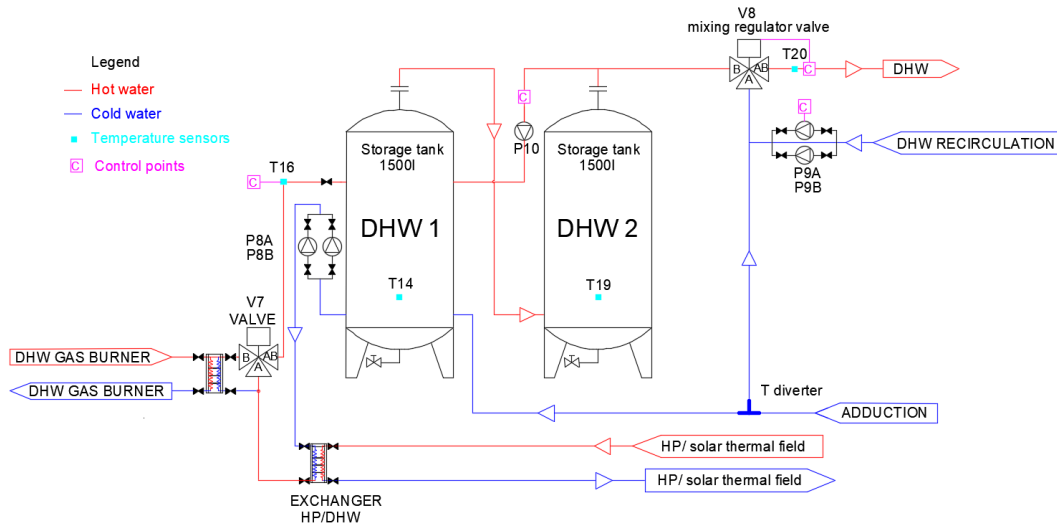


Figure 3.1 Schematic representation of the DHW subsystem and its measured parameters

Figure 3.2 shows the two DHW boilers. Their height is about 2.15 m, while the diameter is of about 90 cm. The insulation coat covers the lateral and the upper surfaces and it consists of 4 cm thick glass wool ($\lambda = 0.04 \text{ W/mK}$).



Figure 3.2. Water storage tanks DHW1 (on the left) and DHW2 (on the right). The twin pumps P8 of the fossil burner circuit can be identified near DHW1

3.1.2. The fault detected

The data collected by the DAS over the year 2019 has revealed untypical trends in the tank temperatures (T14 and T19) during about 150 nights in the months from June to August and from October to November. The differences between a normal night and the non-standard one will be analysed individually below.

- *Standard day (Figure 3.3)*

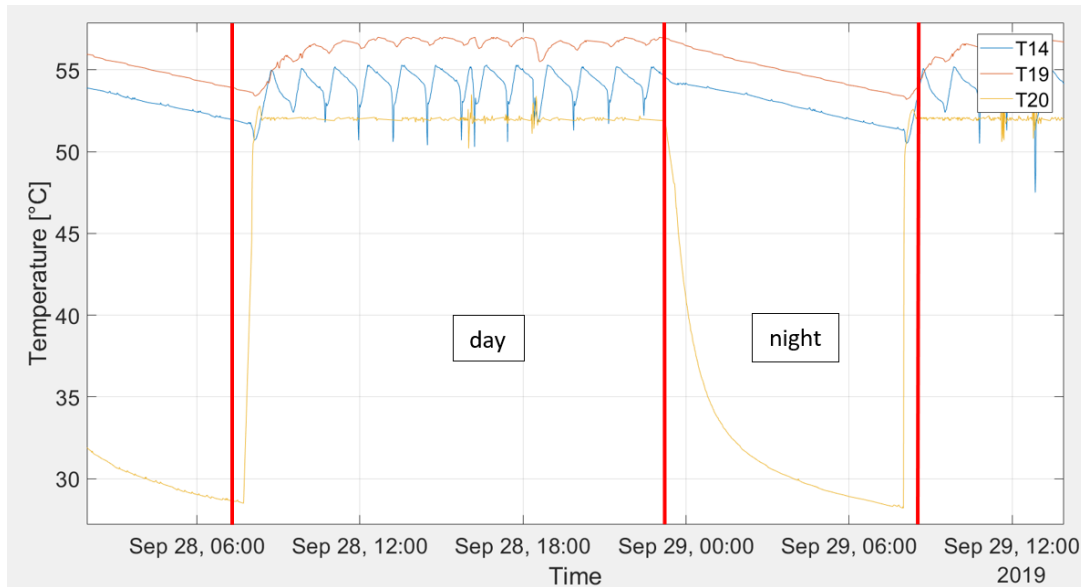


Figure 3.3. Temperatures trend of T14, T19 and T20 during September, 28th and 29th, 2019

Figure 3.3 shows the trend of the temperatures recorded in the two tanks (DHW1 – T14, blue line and DHW2 – T19, orange line) during a standard day. An initial increase in temperature is appreciated on average from 8.00 a.m. to 8.35 a.m. when the gas burners and the HP are turned on and they start heating the DHW tanks cooled in the night. Once the set point temperature has been reached in the two tanks, the initial heating phase stops. The following oscillating trend represents how the DHW subsystem supplies to the end users' needs during the day. Coherently, T19 results always greater than T14 and the sensor T14 measures a sharper decrease in temperature than T19 due to the presence of the cold water supply. In the end of the day, at about 23.00, the plant turns off and the temperatures within the two boilers follow an almost linear decrease of about 3 °C up to 8.00 a.m. of the following day. The steep and sudden decrease in temperature recorded at the end of the night-time is due to the mixing within the tanks determined by the activation of the pumps. The measured values for T20 have been overlaid in the same figure. During the day the temperature is almost constant and equal to 52 °C (the set point value) unless minimal instrumental fluctuations. When the plant is turned off, T20 cools up to a temperature of about 28-29 °C.

An interesting comparison can be drawn between T20 (immediately downstream of the valve V8) and the temperature within DHW1 and DHW2. T20 shows a clear negative exponential curve which has almost reached its asymptote early in the morning. On the other hand, T14 and T19 have a linear cooling phase. The explanation to this difference is due to the time constant associated to the two bodies: the high thermal inertia associated to the tanks determines a very large time constant (order of magnitude 40 hours) with a consequent longer time to complete the cooling process (about 200 hours). The night lasts about 8 hours and this means that the negative exponential cooling trend of the tanks can be linearly approximated with very little error. This assumption is not suitable for valve V8 (sensor T20) where the low time constant (order of magnitude 1 hour) requires a negative exponential approximation.

- *Untypical day (Figure 3.4)*

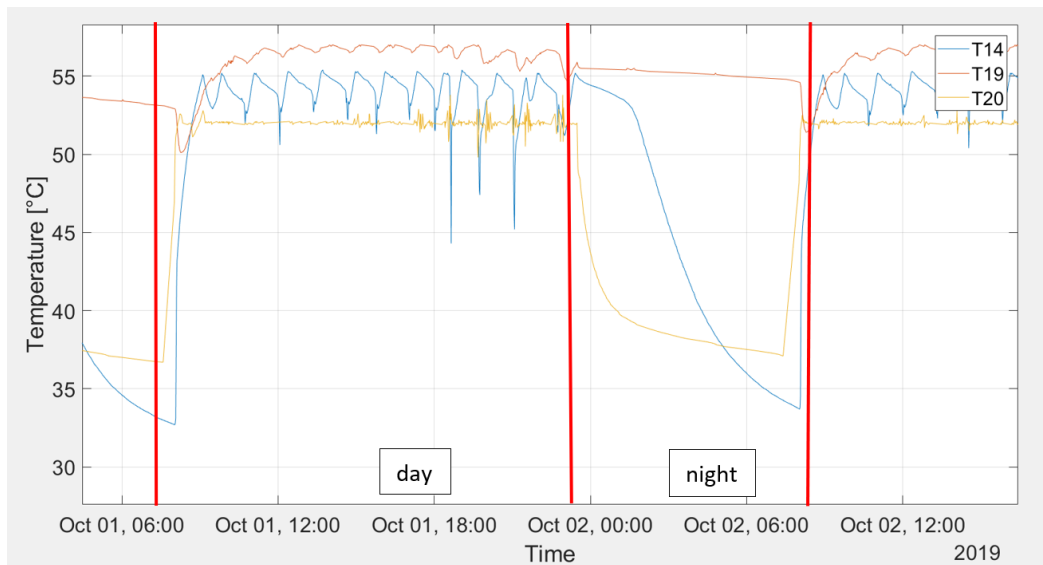


Figure 3.4. Temperatures trend of T14, T19 and T20 during October, 1st and 2nd, 2019

The trend of T14, T19 and T20 during the day is comparable with the one in Figure 3.3 and no significative variation can be identified. On the contrary, a very apparent change has been detected overnight; in particular:

- T19 (temperature in DHW2) shows a lower slope with a decrease of about 1 °C during night, while during in the previous case a decrease of 3 °C has been appreciated over the same time.
- T14 shows an almost linear initial decrease, followed by a strongly non-linear trend. Globally, about 10 °C are lost each night (Figure 3.4) with respect to the abovementioned 3 °C decrease (Figure 3.3).
- T20 has the same negative exponential trend; nevertheless, the difference in temperature representative of the overnight cooling process reduces from 25 °C (recorded over a standard night, Figure 3.3) to 15 °C (Figure 3.4).

In conclusion an increase in the thermal load has been recorded during the “untypical days” without any apparent change within the Palacus facility management. The choice of the days reported in Figure 3.3 and Figure 3.4 is not significative: the records of the “standard” days show very little fluctuations one with other, as well as very little variation has been appreciated among the “untypical” ones.

The data collected cannot provide itself a direct explanation of what happened during the so called “untypical days”. In particular, the absence of mass flow rate measures blocks any possible balance on the DHW subsystem. Furthermore, the boundary conditions are not concerned with stationarity since the transients have been clearly identified in the description of the case study. In conclusion a numerical simulation is required to carry out a likely estimation of the water flow rates which have determined the “untypical” trends in temperature.

3.2. Model assembly

Given the initial scheme reported in Figure 3.1, the period under analysis occurs during night when the plant is off. So, the following elements shall be inactive:

- Recirculation (pumps P9)
- Internal recirculation (pump P10)
- Heat exchange circuit (pumps P8)

Figure 3.5 gives the overall view of the DHW subsystem neglecting the elements above.

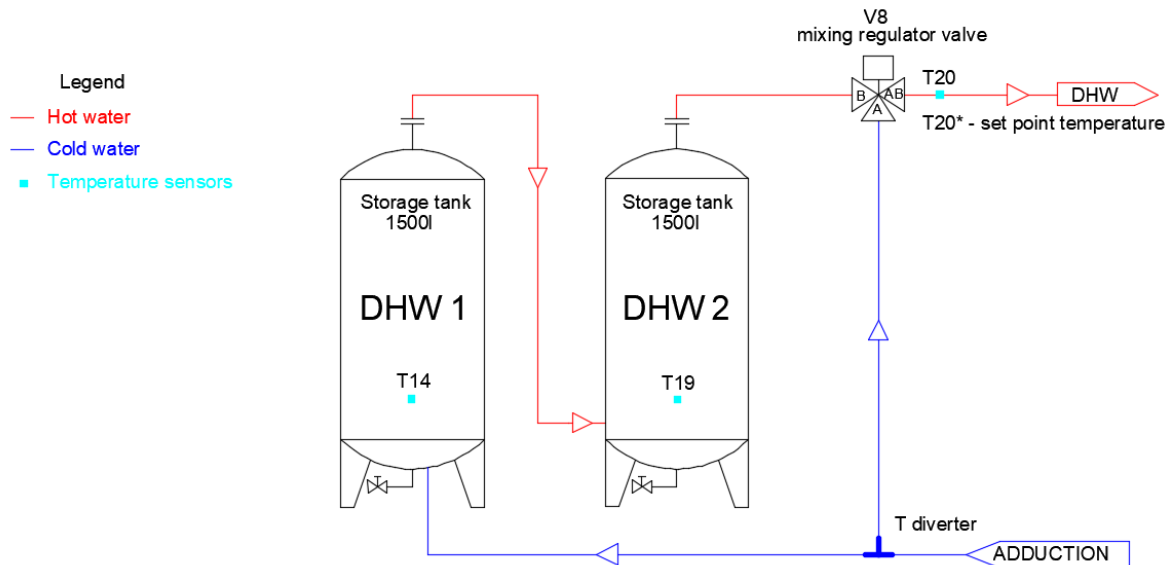


Figure 3.5. Simplified scheme of the DHW subsystem for numerical overnight modelling

The conceptual scheme of the active plant over night is really trivial, nevertheless its simplicity becomes compulsory to carry out a validation of the properties of the different components (e.g. the water storage tanks and the mixing valve). Figure 3.6 shows the main elements adopted that can be briefly resumed as follows:

- Tank of 3000 l capacity and a total height of 4.20 m equal to the double of a single boiler. Indeed, the connection between the top of DHW1 with the lower part of DHW2 makes the two tanks work as if they were stacked one on the other. A specific insight on this assumption will be presented in the section below, united with some considerations on the behavior of the TRNSYS element chosen, Type 4 [15].

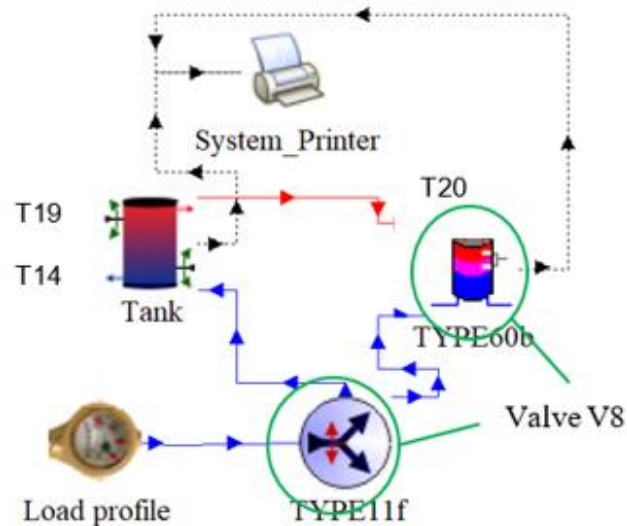


Figure 3.6. TRNSYS simplified model corresponding to the scheme in Figure 3.5

- Mixing valve V8: the modelling is performed with the attribution of regulation to the T diverter while the mixing and the inertia have been modelled with a small additional tank (TYPE60b). A “control signal” of the T diverter regulates in real time the percentage of water flowing inside the DHW tanks while the remaining part is directly sent to the valve V8. This value is fixed since during night the valves are not controlled. About 80 cm of bare pipe divide the mixing valve from the temperature sensor. The additional masses of steel and water and the short part of bare pipe have been accounted in the parameters of V8 by means of equivalent properties computed on the basis of weighted averages.
- Load profile: it represents a forcing function linked to any DHW water draw. The temperature associated to the water entering the tanks is assumed to be equal to the local average seasonal air temperature, namely 14.7 °C, since the supply line is underground.
- Printer: the element used in TRNSYS environment to print the results at each time step of the simulation of the selected outputs. In the case proposed, the temperature of V8 and the temperatures at the same height of T14 and T19 are printed.

3.2.1. Calibration of the thermophysical properties for valve V8 and the water storage tanks

- Temperature at valve V8 – T20

The equivalent volume of valve V8 and of the pipe connecting V8 to T20 has been set to 1.2 l, with a density of 7000 kg/m³ and an equivalent specific heat of 1.1 kJ/kg K. The properties derive from weighted averages between the steel and water ($c_{p,water} = 4.186$ kJ/kg K; $\rho_{water} = 1000$ kg/m³; $c_{p,steel} = 0.4$ kJ/kg K, $\rho_{steel} = 7800$ kg/m³).

The tank loss coefficient is set to 17 W/m² K which is representative of the thermal losses of a bare pipe, in accordance with the predictions of [16]. Moreover, it can be obtained from the well-known formulation reported in Eq. (3. 1) which already neglects the thermal resistance of the bare steel. So, the transmittance depends on the internal (water-pipe walls) and external (pipe walls – air) heat transfer coefficients ($h_{int} \approx 100$ W/m² K and $h_{ext} \approx 20$ W/m² K):

$$U_{V8} = \left(\frac{1}{h_{ext}} + \frac{1}{h_{int}} \right)^{-1} = 16.7 \text{ W/m}^2\text{K} \quad (3.1)$$

The ambient temperature inside the boiler room during that nights was about 17 °C and the only way to grant an asymptote for V8 of about 28-29 °C is by means of a hot water flow inside V8.

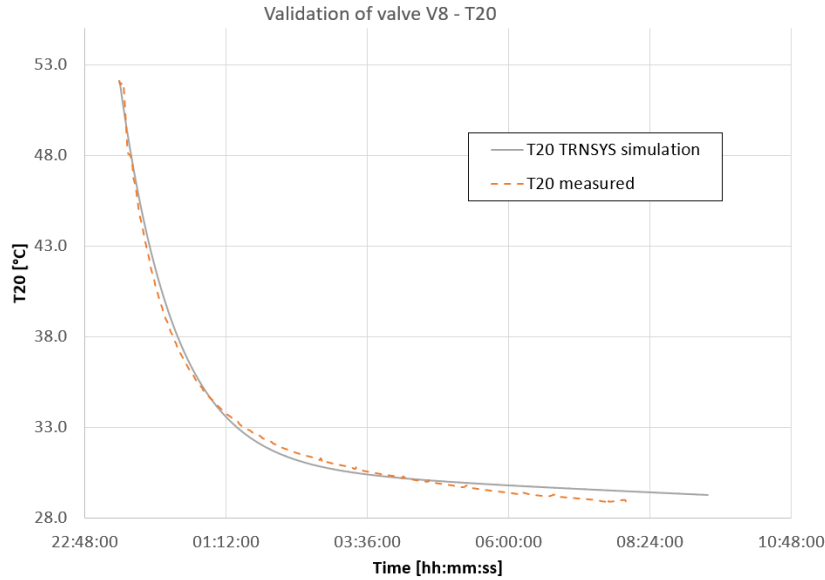


Figure 3.7. Plot of the numerical and measured time-temperature profile of T20 (assumed minimum water flow rate $\dot{m} = 7 \text{ kg/h}$ with variable temperatures in the range 57-53°C).

In other words, the process under analysis results from a mixing and a cooling process. Actually, the water flow rate inside the valve is compelled to be small, because of two different aspects:

- The cooling trend inside the tanks is linear and a significative water draw would determine non-linear trends, representative of significative mixings, especially for T14 which is in DHW1 tank, near to the cold replacement water inlet.
- The recorded negative exponential trend in Figure 3.7 requires a hot water flow rate to grant the asymptote but at the same time, the cooling process is dominant and therefore the hot water draw has to be small.

The validation of V8 is shown in Figure 3.7. A maximum difference of 1.7 °C between the measured and simulated lines can be noticed while a variation of 0.5 °C is appreciated at the asymptote of about 28-29 °C. The result is acceptable considering the precision of $\pm 0.5 \text{ °C}$ for the temperature sensors. Moreover, the interaction between cooling and mixing processes determines the wider variation (maximum of 1.7 °C), especially in the first hours of simulation, with respect to the linear cooling of the DHW tanks.

- Water storage tank (DHW1 + DHW2) – T14 and T19

The 3000 l water storage tank has a thermal loss coefficient of $2.62 \text{ W/m}^2 \text{ K}$, in accordance with the preliminary calculations shown in Table 3.1. The transmittances of each tank component have been

computed considering the lateral surface as plane, thanks to its negligible curvature. The transmittance for the lower basis of the tank considers only the steel, since no insulation is present. The global thermal loss coefficient has been determined by means of an average weighted on the different areas (Table 3.1).

Figure 3.8 shows the overlapped plot between the measured values for T14 and T19 (dotted red lines) and the TRNSYS simulated T14 (lower line) and T19 (upper line). The maximum difference between the measured and recorded data is of 0.5 °C and it can be obtained only with a very low water flow rate (e.g. a small leakage within the plant).

Additional information		
Properties	λ (W/mK)	s (m)
Steel	80	0.002
Insulation	0.028	0.04
$h_{\text{int}} = 100 \text{ W/m}^2\text{K}$ $h_{\text{est}} = 25 \text{ W/m}^2\text{K}$		

Component	U (W/m ² K)	A (m ²)
Upper base	0.68	0.93
Lower base	20.00	0.93
Lateral surface	0.68	7.35
$A_{\text{tot}} = 9.21 \text{ m}^2$, $U_{\text{glob}} = 2.62 \text{ W/m}^2 \text{ K}$		

Table 3.1. Additional information (a) and estimation of the global thermal loss coefficient for DHW tanks (b).

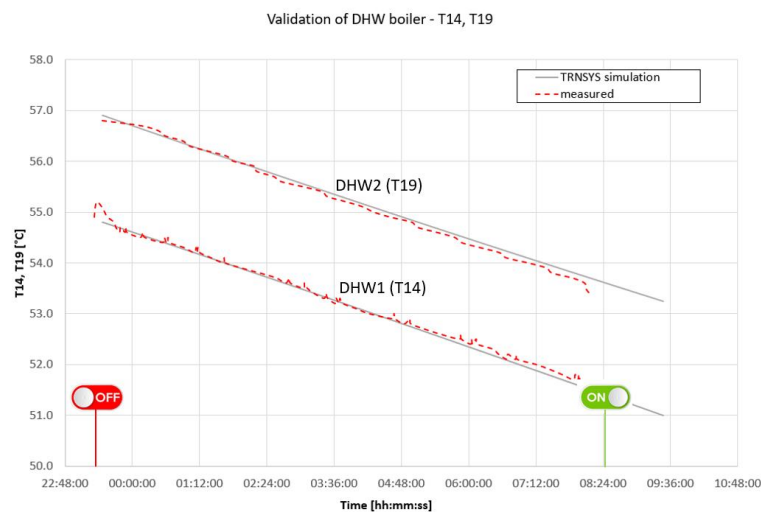


Figure 3.8. Plot of the numerical and measured overnight trends for T14 (DHW1) and T19 (DHW2) (in between the on-off status of the plant).

3.2.2. Unexpected measured data analysis and simulation

Once the validation stage has been completed, the model has been employed to simulate the unexpected data recorded over the “untypical” days. Figure 3.9 provides a global resume about the temperatures inside the two DHW tanks (T14 – DHW1 – yellow line, T19 – DHW2 – red line) and for the valve V8 (T20 – blue line). The dotted lines are concerned with the measured values while the continuous ones derive from the numerical simulation on the TRNSYS model. Differently from the validation stage, a significant water flow has been assumed, to find the best fit between the experimental and numerical data.

The results in Figure 3.9 are associated to the water draw shown in the lower part of the graph, with reference to the right axis: an initial flow rate of 50 kg/h is drawn for about 2 hours. Then, a constant value of 195 kg/h is kept for 2 hours and 20 minutes. In the last two steps the flow rate is decreased at 120 kg/h for 1 hour and 20 minutes and then at 50 kg/h for about 2 hours.

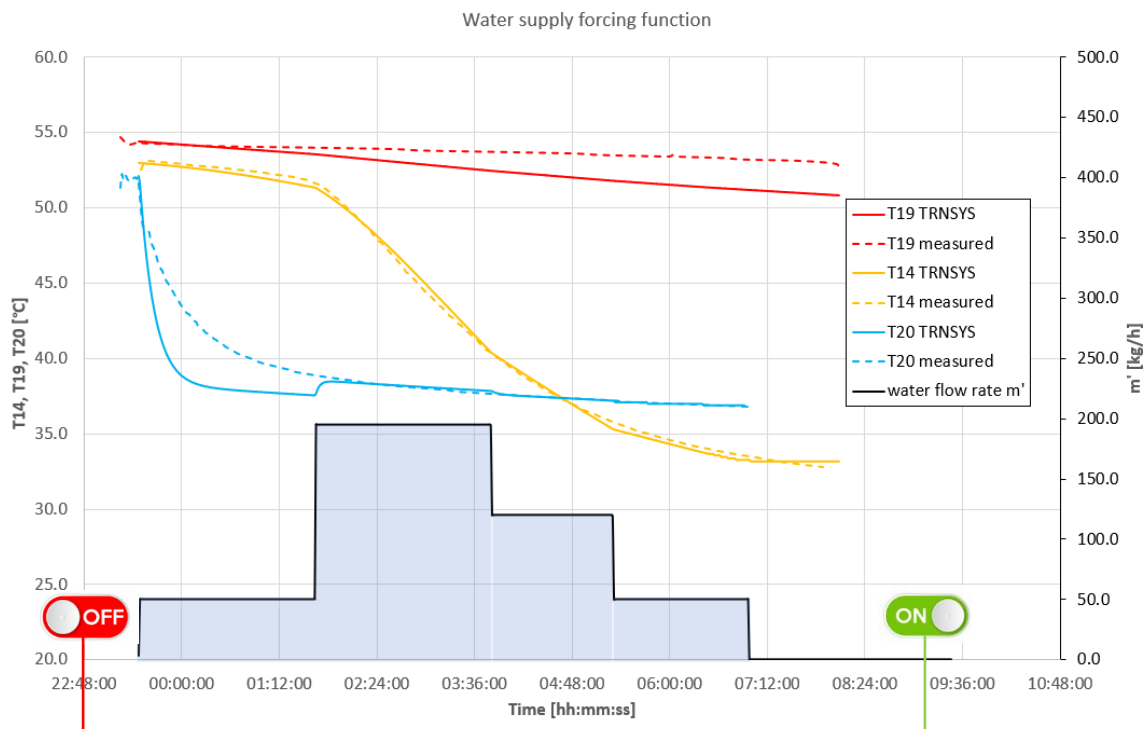


Figure 3.9. Comparison between measured data (dotted lines) and the temperatures obtained from the numerical model (continuous lines) (a). The correspondent water flow is shown in grey (ref. right axis)

The following observations and conclusions can be drawn:

- *T19 – temperature in DHW2 (red line in Figure 3.9):* the initial trend is well approximated. Then the difference between measured and simulated lines increases up to 2.4 °C at the end of the simulation. At first look, although the error is small, the trends of the two lines are different. The untypical day under analysis follows the typical one, so the boundary conditions (e.g. ambient temperature) cannot have influenced this trend. The DHW1 and DHW2 storages haven't changed, so their thermal properties have to be equal to the ones determined in the validation section. With respect to the validation stage, the decrease of the flow rate up to the

case limit of still water inside the boilers leads to a trend still different from the one measured in Figure 3.9. On the other hand, an increase of the flow rate only reduces the simulated T19 with a pronounced non-linear trend (with shapes more similar to mixing conditions, that resemble the trend for T14). In conclusion, the different behavior can be imputed to local mixing effects as the hot water coming from the head of DHW1 enters DHW2. Moreover, the connection between the two boilers is about 7 cm lower than the temperature sensor T19 and it is not on the bottom of DHW2 as in the numerical model. From a physical point of view, the water entering DHW2 from DHW1 is not so cold to destroy completely the stratification in the lower part of DHW2, but it is still low enough to rise a mixing. So, the recorded trend can be read as half-way between the two case limits of stratification and full mixing [17].

- *T14 – temperature in DHW1 (yellow line in Figure 3.9)*: the approximation obtained is very good, with a maximum difference of about 1 °C. According to the simulations carried out and to the geometry of the problem, this parameter is highly sensible to the water flow rate entering the tank. Indeed, the load profile in Figure 3.9 consists in different steps to follow the several slopes of the measured T14 with a piecewise linear approximation. Differently from T19, the behavior of T14 can be reconstructed with the numerical model, even if in both cases the inlet is near the temperature sensors (Figure 3.5). Actually, this difference is due to the lower temperature level of the inlet water in DHW1 which causes the local destruction of the thermal stratification. Indeed, the results of the numerical model have good resemblance with the recorded data because an almost complete mixing process has taken place in the lower region of DHW1.
- *T20 – temperature of valve V8*: the transient in the first two hours of the process is roughly approximated, with maximum differences of 5 °C (4 °C on average). After the transient, the difference between the two lines becomes negligible (differences lower than 0.2 °C). The leap between these two regions is due to the forced instantaneous passage from 50 kg/h to 195 kg/h at the end of the first two hours. It is therefore caused by a limit in the approximation with constant steps. The jump becomes more evident as the initial water flow rate (50 kg/h in the first two hours) is decreased. On the other side, an increase in the water supply would reduce this jump. Unfortunately, this would affect the initial trend of T14 as well, with the introduction of strong non-linearities.

In conclusion, the load profile reconstructed for the untypical days can be associated to the cleaning activities that take place after the sport palace closes. Indeed, the nearly 600 l of water consumed each night over three hours (average flow of 2.5 l/min) are comparable to the total water and time needed by the caretaker to accomplish the washing of about 2000 m² of floor (formed by the sport hall and six lockers). The average thermal loss of the boiler during a typical night is of about 3.7 °C while in the untypical nights it almost doubles. The power consumed to reach the set points doubles as well, since the plant is turned on always half an hour before the opening in the morning. Actually, keeping the plant operative all over the nights would reveal too expensive to avoid this behaviour. So, the turn on of the plant could be brought forward half an hour whenever the temperature T14 (DHW1) lowers a fixed set point (e.g. 47 °C) during night.

3.2.3. The domestic hot water storage tanks: some remarks

From a physical point of view, the working of the two tanks during the day (when the plant is active) cannot be modelled in such a simplified way. Indeed, in Figure 3.1, the top of each tank is connected with the other in order to create an internal recirculation by means of P10. During night however, the absence of significative DHW draws from the system and the inactivity of pump P10 give rise to the phenomenon of stratification inside the two tanks as the cooling process takes place. Clearly the DHW2 tank is the storage on the inlet of the mixing valve V8 and it results to be at higher temperature with respect to DHW1. Indeed, the latter has the inlet of cold water from the underground water duct and it tends to be colder. Actually, the difference between T14 and T19 late in the evening when the plant is shut off is of about 2 °C, basing on the information collected by means of the DAS. Given the assumption of null water flow rates, two tanks behave independently one from the other according to the stratification principle. The difference between the temperatures inside the two storages can be simplified and modelled as if the two tanks were one stacked on the other. However, this assumption can result quite strong and it might attract some criticism especially as the size of the tanks increases due to the natural convection. Indeed, the modelling of a unique tank with double volume and double height of one implies a 3000 l, 4.30 m height storage might be subjected to significative convection heat transfers, losing the validity of the assumption. The specific element adopted in the TRNSYS numerical simulation is the Type 4, created for the specific case of stratification inside the water storage tanks.

This section is meant to provide more details on the following topics:

- Some significative recalls on stratification in literature
- Sensitivity of the results to the number of nodes to be used inside the tank
- Sensitivity to the size of the time step adopted
- Differences between the configuration with two distinct boiler and the one with only a storage with double volume and double height.

More in general, the specific TRNSYS element for stratification inside the tanks (Type 4) is provided, concerning the different aspects above

3.3. Stratification

This section is not meant to provide a global view over thermal stratification, but to recall simple key concepts on the physics and on the basic quantities used below to assess the level of stratification at different time steps during the simulations carried out.

The density of water depends on its temperature as shown below (Figure 3.10).

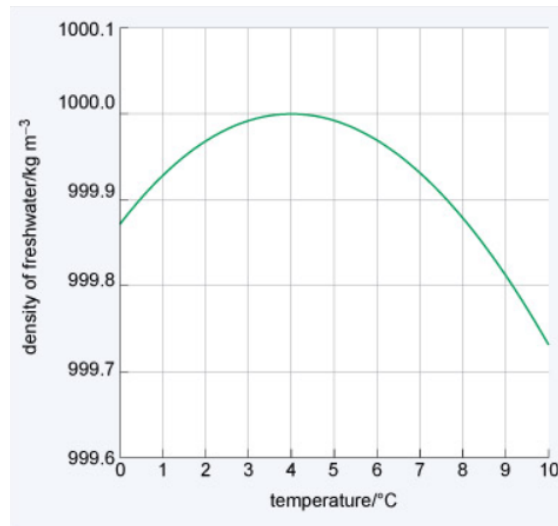


Figure 3.10. Density of water as function of temperature

In the range of temperatures higher than 4°C water becomes progressively less dense and therefore lighter. This determines a thermal layering, where warmer and lighter water is stored on top of colder water – defined as “thermal stratification”. An undisturbed water storage (e.g. no mixing, no significant thermal losses towards the environment) will be subjected to thermal stratification. So, water inside the storage can be considered as composed by different smaller volumes at different temperature and their mixing doesn’t occur. The diffusion and importance of systems based on stratification, especially in thermal solar plants is due to their simplicity as well as the advantage of collecting water at different temperatures in the same tank, without any physical separation. In the case of renewable energies, such as a solar thermal field, the colder, denser water can be withdrawn from the bottom of the tank and sent to the source side (e.g. the solar panels) to collect energy. On the other hand, the hotter water can be sent to the users’ from the top of the same tank. Clearly, the common and fundamental assumption behind this concept is that no significative mixings take place and therefore the layers of water at different temperatures remain separate. Otherwise, the quality of energy supplied at load will be decreased. In other words, in renewable applications, there is a great difference between a fully mixed tank and a perfectly stratified one (Figure 3.11). Indeed, given the average temperature in both cases were the same, the stratified tank allows to send to the solar field, colder water which increases the efficiency of the installation with the use of only one tank, without any specific physical separation between the two circuits.

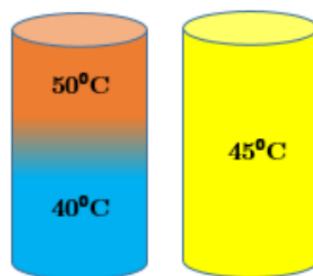


Figure 3.11 Fully stratified tank (on the left) vs fully mixed one (on the right). They both have the same average temperature

Moreover, water is non-toxic, available, with a comparatively high heat capacity and it is widely suitable for almost all applications. As far as renewable applications are concerned and more in detail solar thermal fields for DHW and SH, their performance depends on the thermal stratification in the storage tank which allows the best exploitation of the thermal energy collected during the day and used later, perhaps during night. Stratification minimises the heat losses of the storage and it ensures the lowest possible inlet temperature at the collector. Annual performances can be increased by 37% with the use of a stratified solar tank [18]. Furthermore, hotter water is at the top of the tank, which in some cases enables not to use energy supply. So, the thermal storage plays a central role when assessing the thermal efficiency of the whole system and several parameters play a role in this stratification quality. Among them, the geometrical ratio H/D (height H vs diameter D) is usually recommended to be between 3 and 4. Then a family of parameters associated to the heat exchanges which take place between the tank and the surrounding environment can be identified: for instance inputs/outputs flows, water and envelope conduction, convective exchange (water/envelope, envelope/surrounding) and radiative exchange (external envelope/walls). Indeed, thermal stratification can be destroyed by these processes and therefore other significant thermophysical parameters are concerned with the wall conductivity, the thickness of the wall, the type of insulation, the tank size, the surrounding ambient temperature and the difference in temperature between the lower and upper tank volume. These aspects can be resumed by means of non-dimensional numbers. Many Authors have proposed different numbers among which the Richardson (Ri) and MIX numbers can be remembered. The former can be conceived as a ratio between buoyancy and flow shear terms:

$$Ri = \frac{g\beta\Delta T\Delta z}{u^2} \quad (3.2)$$

Where

g is the acceleration due to gravity [m/s²]

β is the volumetric coefficient of thermal expansion [1/K]

ΔT is the temperature difference appreciated over the characteristic dimension Δz

u is the characteristic inlet fluid velocity [m/s]

This ratio can be seen as well as a division between the potential energy required for the mixing and consequent destruction of stratification and the turbulent kinetic energy available for the process. Namely, the incoming fluid can disrupt the vertical thermal gradient mixing low density and denser water together. In this way, the centre of mass moves upwards, increasing the total potential energy of the tank-system. So, a critical value for Ri can be identified, about 0.25 [19] below which the thermal stratification is broken down by the shear stresses and the water in the tank is mixed. Indeed, low Ri values have high potential for mixing and vice-versa according to the definitions provided above.

On the other hand, the MIX number expresses the level of stratification under as a ratio of quantities resembling an energetic momentum:

$$MIX = \frac{M_{st} - M}{M_{st} - M_{mix}} \quad (3.3)$$

With

M_{st} corresponds to the energetic momentum of an ideally fully stratified tank, $M_{st} = \sum_{i=1}^n y_i E_{i,st} = \sum_{i=1}^n y_i \rho_i V_i T_{i,st} c_p$

M_{mix} corresponds to the energetic momentum of an ideally fully mixed tank, $M_{mix} = \sum_{i=1}^n y_i E_{mix} = y \rho V_{tot} T_{mix} c_p$

M is the energetic momentum experimentally measured or simulated, $M = \sum_{i=1}^n y_i E_i = \sum_{i=1}^n y_i \rho_i V_i T_i c_p$

Where each formulation above assumes the tank as divided into n volumes V_i of water, each one distant y_i , with density ρ_i at temperature T_i and with specific heat c_p . Actually, the temperatures T_i of each volume assume a different meaning according to the energetic momentum under evaluation. For instance, the temperatures used in M_{st} are the ones used for the initial conditions. On the other hand, the value of T_{mix} used in the ideal case of fully mixed tank can be computed as weighted average of the temperature of each volume V_i in which the tank is divided.

In conclusion a fully mixed tank is expected to have a value near 1 while a stratified storage will have almost null values. Moreover, when measurements or numerical results are available, the MIX number can be computed almost continuously, providing a simplified and fast evaluation of the level of stratification inside the boiler. In other words, this parameter can follow and represent the intrinsic transient nature, the use of the MIX number in the design stages is frequently neglected since it cannot account for different load/unload strategies for the same geometry. Moreover, this quantity relies only on energetic analyses and it cannot represent for instance the degradation of the energy stored inside the tank due to thermal losses. This aspect enhances methods which are based on the Second Law of Thermodynamics, since the quality of stratification, its degradation etc can be analysed by means of entropy and approaches based on exergetic efficiency. As far as the simulations about stratification in this chapter are concerned, no loading/unloading phases or significative thermal losses to the environment will be analysed. So, the MIX number will be employed to assess the quality of stratification inside the whole tank during these simulations. Some considerations will be provided about the representativeness of a single number with respect to the stratification inside the boiler.

As far as the numerical modelling is concerned, three main approaches allow to model the thermal stratification:

- *Multi-layer models*: the tank is divided into layers of volume V_i , each one associated to a temperature T_i which is assumed to be homogeneous over the volume. The interaction between adjacent sections is performed by means of energy balances, solving a set of differential equations in temperature for each node over every time step considering the phenomenon one-dimensional. These models were the first to be formulated, thanks to their simplicity which

approximates the convection and conduction between two volumes by means of a single parameter, the effective thermal conductivity λ_{eff} . [20]

- *CFD models*: it allows a more complete modelling of the phenomenon, with results which are very near to reality. The lower number of assumptions, in turn, requires fewer fictitious parameters to correct the model. The comparison of a multi-layer model with a CFD one shows that the former leads to lower values of temperatures [21]. Indeed, the one-dimensional modelling of multi-layer nodes, implicitly assumes a uniform temperature layer. Actually, the isothermal zones are influenced by objects inside the tanks and inlets and therefore the CFD modelling leads to more precise results. Nevertheless, the computing time of CFD models still influences the diffusion of such simulations.
- *Temperature zonal models*: they can be conceived as an attempt to merge the need for reasonable computation times and the accuracy of the results. Briefly, the tank is not approximated as a node such as in the multi-layer models. Indeed, it is divided into layers, each divided in turn into crowns and sectors (Figure 3.12). In this way, the three-dimensional approach is preserved, without introducing an almost continuous mean such as in the case of CFD. Each i-th volume is governed by the state variables (e.g. pressure and temperature) which express for instance the mass flow rates across the boundaries and consequent mass balances.

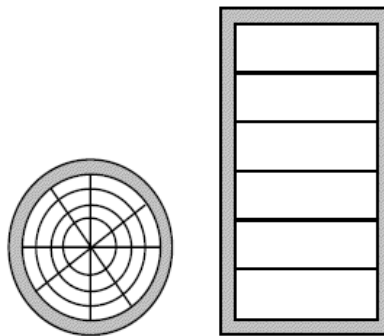


Figure 3.12. Division of the tank into layers (on the left), each one divided into crowns and sectors (on the right) according to the temperature zonal models

As far as the present simulations are concerned, the family of multi-layer models has been chosen due to different reasons:

- Specific models of single tanks or storages lose their utility when put into the context of a model of the plant as a whole. Indeed, the added information of a complete CFD model loses significance when interfaced with the other components of a plant. Namely, the approximations introduced by each component introduce a degree of uncertainty which is in contrast with the results obtained by the CFD models. Namely, the path of CFD and temperature zonal models its evolution described below provide the best approach for detailed simulation of a tank.
- The use of such precise models is justified only in presence of a large sensor grid, which can be assembled only in the context of laboratories. For instance, in the application of the SAHP pilot plant at the Palacus Sport Palace, over the 50 measurement points, only two sensors measure the temperature inside the DHW tanks.

3.3.1. Sensitivity of the results to the number of nodes

The thermal performance of a fluid-filled storage tank, subject to thermal stratification, can be modelled by means of Type 4 in TRNSYS environment. The code allows to divide the tank into N fully-mixed equal volume segments (N can reach a value up to 15) and it computes the total height of the tank as a sum of the spacing between the nodes. The higher N , the higher the degree of stratification; generally, the number of the nodes should be as small and regular as possible to fully simulate stratification. The node sizes may not be equal, according to the modelling performed and two nodes at least are always present: top and bottom nodes. In case the number of nodes N were set to 1, the top and bottom nodes would lead to the same values and a fully mixed tank with no stratification effects would be simulated. This model is provided with heaters as well which have been disabled to perform these simulations. The inlet positions are fixed and defined within the code. In particular, the element has been created with a hot and cold side flow rates. The former represents the fluid entering the eventual heater inside the boiler and therefore the inlet is set at the tank node below the first auxiliary heater (not used in these instances). The latter flow rate (the cold one) is the replacement fluid flowing into the bottom of the storage tank (at the bottom node). Due to the continuity equations, an equal amount of fluid is assumed to flow from the top of the tank to meet a load. The following simulations share the common properties resumed below:

- Ambient temperature: 18 °C
- Tank loss coefficient: the model assumes a uniform loss along the tank and therefore the value has to be considered as averaged over the area; 2.62 W/m²K, as validated before.
- Volume: 3 m³.
- Total height: 4.30 m.

As far as the initial conditions are concerned, a linear distribution in temperatures is assumed and it is based on the two measured values T14 (54.5 °C) and T19 (56.7 °C) located at their respective height. Figure 3.13 better clarifies the concept.

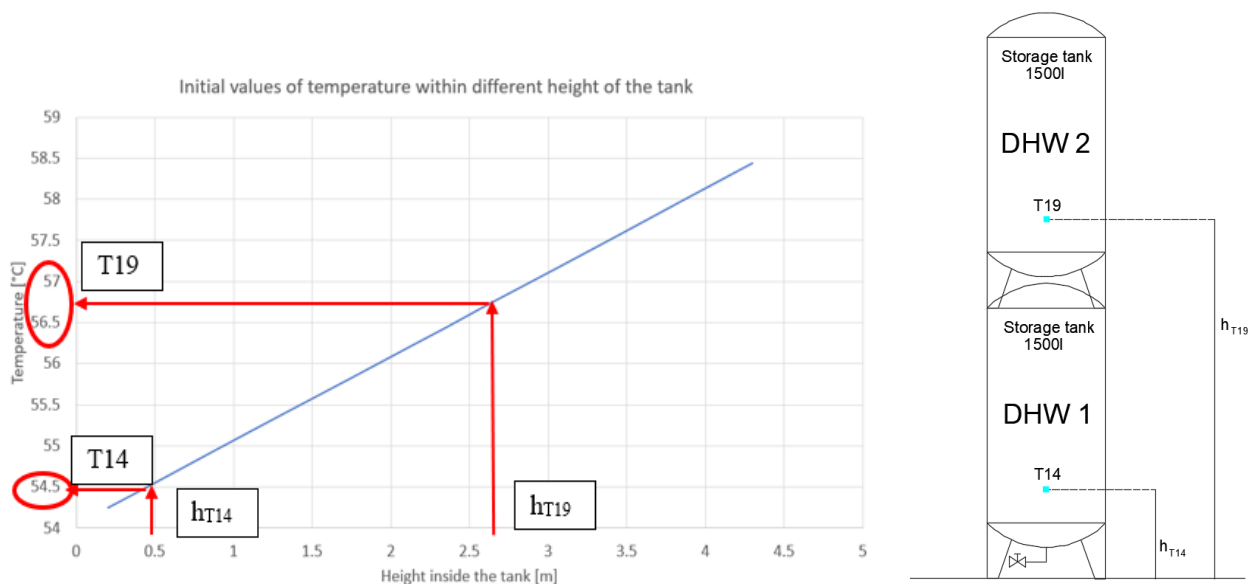


Figure 3.13. Initial values of temperature and correspondent scheme of T14/T19 used to estimate the initial conditions based on the measured values

Then, the initial values at each node are determined reading the value of temperature correspondent to the height of the node under analysis. A transient analysis will be performed for each case assuming a simulation of about 8-9 hours.

3.3.2. Case 1 – 1 node tank

In this case, no stratification can be modelled as a unique node represents the entire volume of the tank. The initial value of temperature has been determined chosen following the approach in Figure 3.12. Below, the trend during the cooling process is shown (Figure 3.13) overlaid with the measured temperatures (red dotted lines, T14 is the lower one)

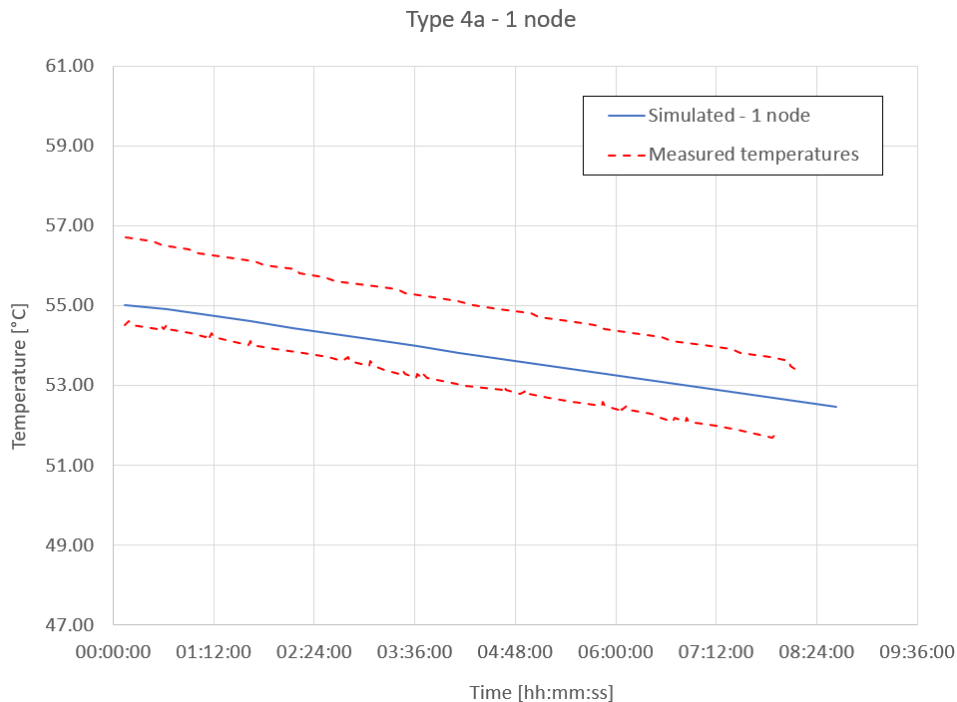


Figure 3.14. Cooling trend of the tank with 1 node

As expected from the high thermal inertia of the boiler, the cooling process reported follows a linear decreasing trend. The first non-linear part is due to the time step adopted to carry out the simulation (the issue of the sensitivity of the model to the time step adopted will be discussed later). Moreover, the slope of the simulated line seems to be different to the measured ones. Actually, this small difference in the trend is due to the chosen number of nodes and it is not due to a thermal tank loss coefficient too low. Indeed, the case with one node models a fully mixed tank and this leads to differences with respect to the measured data.

3.3.3. Case 2 – 4 nodes tank

The placement of the nodes in this instance is not regular. Their heights have been chosen to meet the following conditions:

- One node at the same height of each temperature sensor
- One node on the bottom and another at the top of the tank to which attribute the border effects due to the geometry of the boiler (the TRNSYS element allows only a global thermal loss coefficient for the tank)

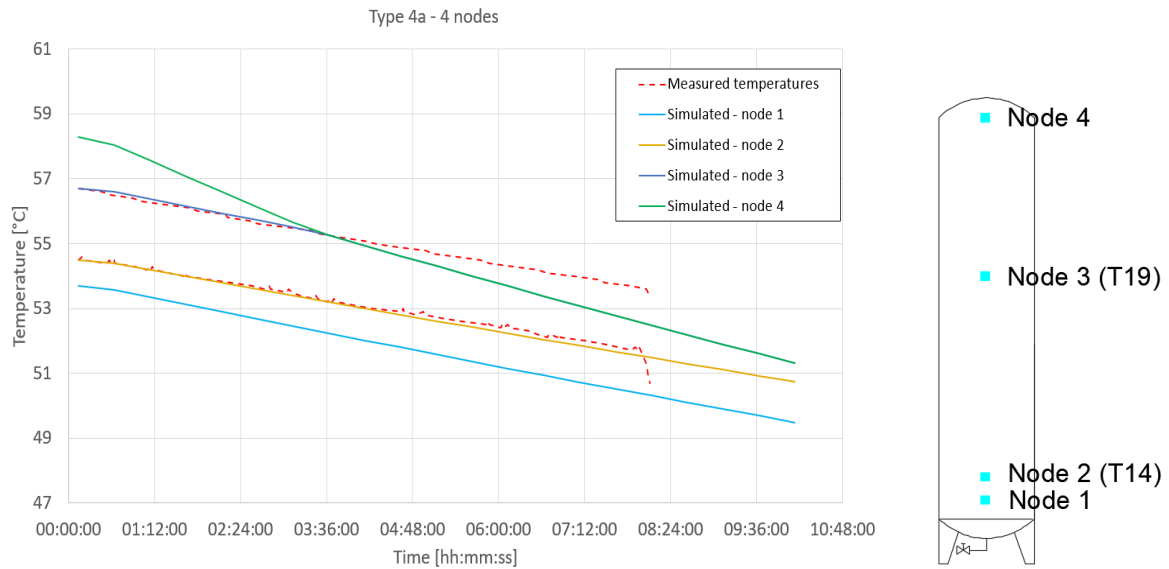


Figure 3.15. Cooling trend of the tank with 4 nodes and their positioning inside the tank

Node	Δh [m]	h [m]	T_{in} [°C]
1	0.2	0.2	53.7
2	0.25	0.45	54.0
3	2.15	2.6	56.7
4	1.7	4.3	58.8

Table 3.2. Interspacing of the nodes (Δh), height referred to the bottom of the tank (h) initial values of temperature (T_{in})

Some considerations can be drawn:

- The simulated trend of temperature at the different nodes follows a non-linear trend. In particular
 - node 1 (at the bottom of the tank) tends to lose the parallelism with node 2, due to the border effects of the cylindrical geometry of the tank
 - Node 4 (at the top of the tank) collapses on the line representing the temperature at node 3. Moreover, the trend after the intersection point between temperatures at node 3 and 4 is still linear but with a different slope. This behaviour is still linked to the border effects of the top of the tank: node 4 starts at a temperature which is higher than node 3 (according to the linear distribution formerly illustrated). Then, the major heat losses towards the environment cause a faster cooling of the volume represented by node 4, up to node 4 reaches the same temperature at node 3. After that, the border effect influences node 3 as well and this can be observed by means of the different slope of the line.
- The simulated and measured values show good accordance in the first three hours of simulation. As far as node 2 is concerned, the simulated temperature is in accordance with the values measured (T14) all the simulation long (differences lower than 0.5 °C).
- The results still show a sensitivity due to the irregular spacing of the nodes.

3.3.4. Case 3 – 6 nodes tank

The position of the nodes follows the criteria shown for the previous instance. Actually, a higher number of nodes allows a more regular interspacing between adjacent nodes. Two examples will be presented: the former in which the spacing between the nodes will be as constant as possible and the latter where the position of the nodes will be decided to better simulate the border effects due to the geometry of the tank

Case 3a – 6 nodes

The maximum distance between the nodes has been set at 0.85 m, with the position of the nodes shown in the Figure 3.16.

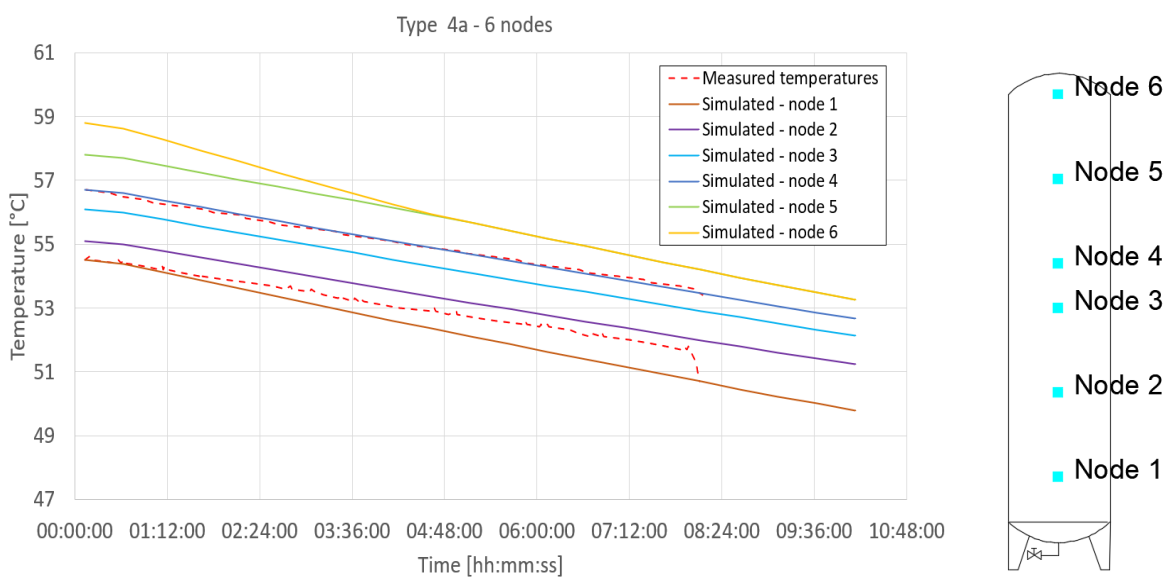


Figure 3.16. Cooling trend of the tank with 6 nodes and their positioning inside the tank

Node	Δh [m]	h [m]	T_{in} [°C]
1	0.45	0.45	54.0
2	0.85	1.30	55.1
3	0.85	2.15	56.1
4	0.45	2.60	56.7
5	0.85	3.45	57.8
6	0.85	4.30	58.8

Table 3.3. Interspacing of the nodes (Δh), height referred to the bottom of the tank (h) initial values of temperature (T_{in})

Case 3b – 6 nodes

The maximum distance between the nodes has been set at 1.08 m, with the position of the nodes shown in the Figure 3.16 and Table 3.4.

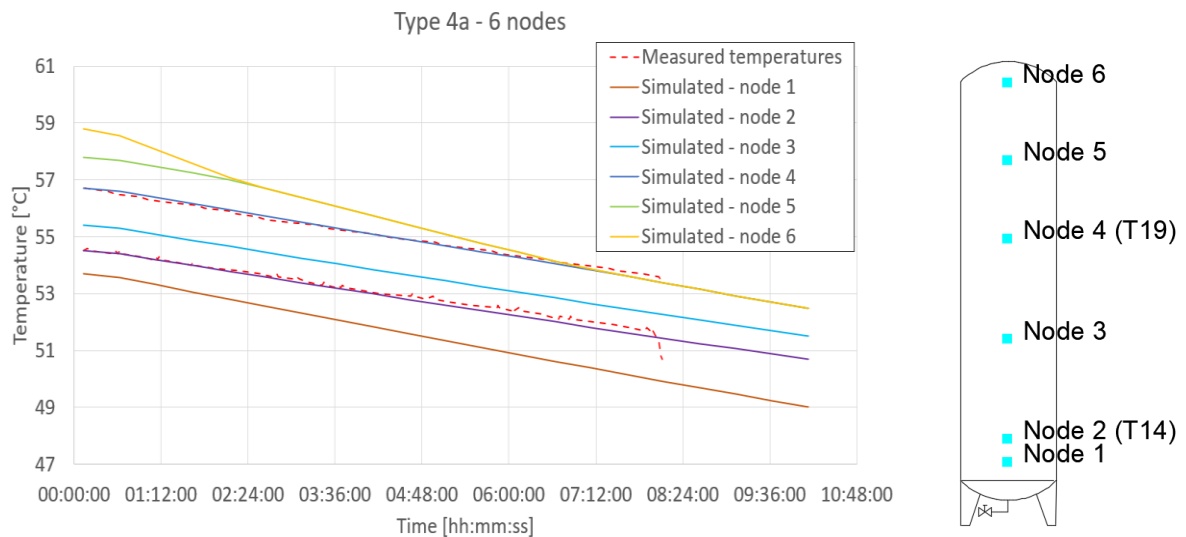


Figure 3.17. Cooling trend of the tank with 6 nodes and their positioning inside the tank

Node	Δh [m]	h [m]	T_{in} [°C]
1	0.45	0.45	53.7
2	0.85	1.30	54.0
3	0.85	2.15	55.4
4	0.45	2.60	56.7
5	0.85	3.45	57.8
6	0.85	4.30	58.8

Table 3.4. Interspacing of the nodes (Δh), height referred to the bottom of the tank (h) initial values of temperature (T_{in})

The comparison of Figure 3.15 and Figure 3.16 shows that a node is always needed on the bottom to account correctly the border effects. Indeed, in case 3a node 1 was put at the same height of sensor T14, but the simulated results initially fit the measured temperature well for small times, but then they diverged one from the other. On the other hand, case 3b leads to a very good approximation for T14 (lower red dotted line), but still some border effect can be identified in the end of the simulation (after about 7 hours).

3.3.5. Case 4 – 12 nodes tank

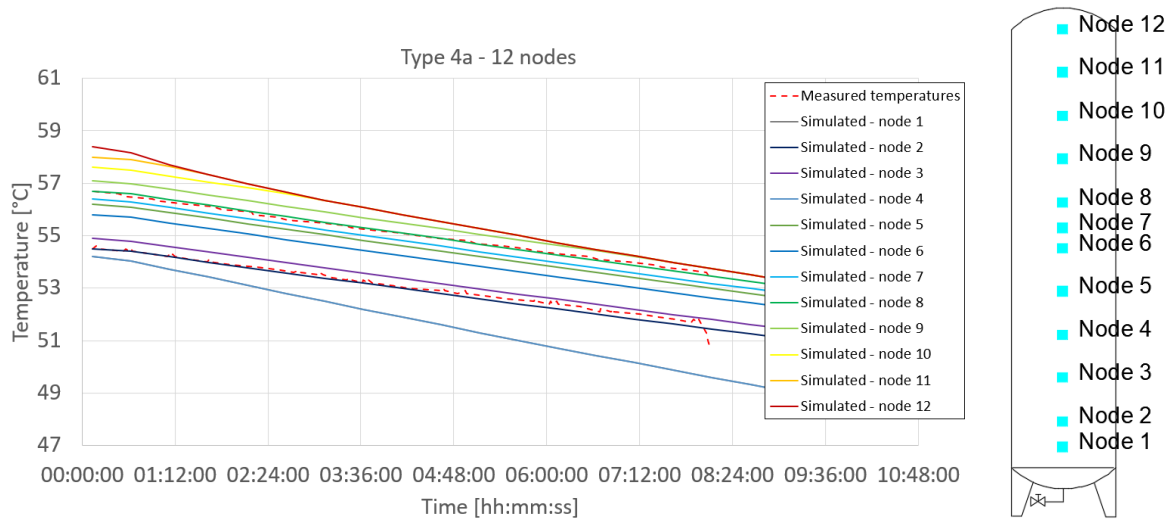


Figure 3.18. Cooling trend of the tank with 12 nodes and their positioning inside the tank

Node	Δh [m]	h [m]	T_{in} [°C]
1	0.20	0.20	54.2
2	0.25	0.45	54.5
3	0.43	0.88	54.9
4	0.43	1.30	55.4
5	0.43	1.73	55.8
6	0.43	2.15	56.2
7	0.20	2.35	56.4
8	0.25	2.60	56.7
9	0.43	3.03	57.1
10	0.43	3.45	57.6
11	0.43	3.88	58.0
12	0.43	4.30	58.4

Table 3.5. Interspacing of the nodes (Δh), height referred to the bottom of the tank (h) initial values of temperature (T_{in})

According to the results shown, the number of nodes used in this last instance allows both to limit the border effect on the bottom and to approximate with minimum error (lower than 0.2 °C) the measured values of temperature. In addition, an almost equal spacing of the nodes has been adopted, creating volumes of height equal to about one tenth of the total height. The faster cooling of the higher nodes due to the proximity to the top has been modelled and it shows that the node correspondent to T19 is not influenced within the simulation time.

3.3.6. Sensitivity to the size of the time step adopted

The simulation proposed has been carried out by means of a transient analysis performed according to the chosen elements, equations and boundary conditions. The length of the simulation and the

size of the time step to be adopted can be defined by the user. The sensitivity of the model to the time step depends on the kind of process under simulation and on the total duration of the analysis. In particular, focusing on the case study proposed of the DHW subsystem, the overnight cooling of the tanks follows an almost linear trend and therefore the time steps over a simulation 8 hours long can be assumed even equal to 30 minutes without significative variations in the precision of the results. On the other hand, cooling processes such as the one concerned with valve V8, mixing and other phenomena in which non linearities are involved, a finer time step has to be assumed (on the order of magnitude of 5 minutes with respect to a simulation 8 hours long). The convergence of the results with respect to the time step is often taken for granted, especially when the simulation is about plants which almost work under steady state regime or when the transient phase is not relevant to the research. Actually, a solar assisted heat pump depends strongly on fluctuating boundary conditions (such as irradiance, the external temperature, the users' profile of needs in terms of DHW and SH) and therefore a steady state regime is seldom reached.

The instance shown below is referred to the case of a stratified tank, with 12 nodes subjected to a constant inlet of water at 54 °C. The first simulation is carried out assuming a time step of 30 minutes with respect to two hours of simulation. The latter has been performed using the time step of 1 minute.

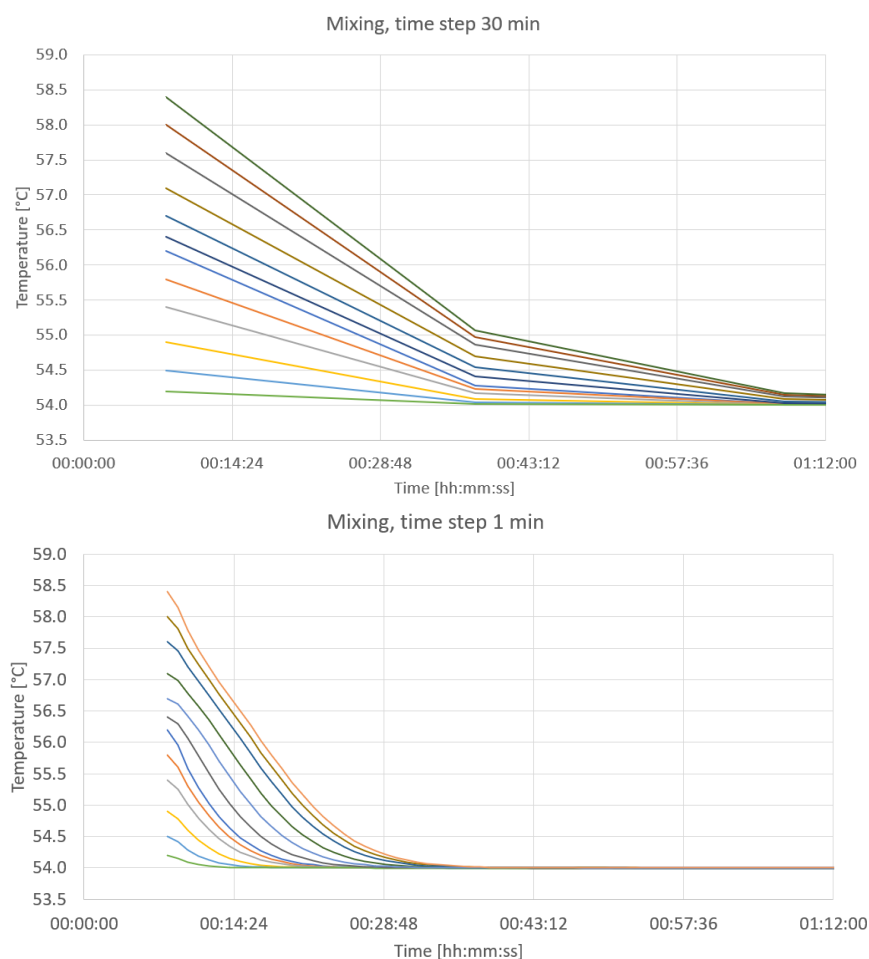


Figure 3.19. Mixing inside a 12 nodes tank performed with different time steps (30 minutes and 1 minute)

Figure 3.19 shows very significant differences; for instance, the whole tank reaches the same temperature about 1 hour with 30 minutes time step, while the finer simulation reaches the same result after almost 30 minutes.

The same comparison can be done assuming a stratified tank of 12 nodes, with no water flow rate. The results of the two analyses have been overlaid (lines in red – time step of 30 minutes; lines in blue – time step of 1 minute).

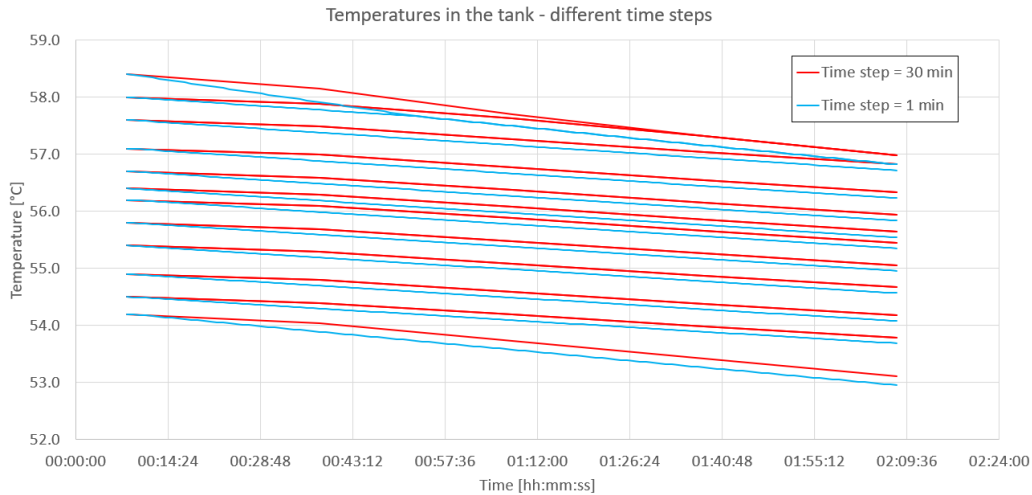


Figure 3.20. Cooling process of a 12 node tank with no water flow rate with 30 minutes time step (in red) and 1 minute time step (in blue)

These examples show how a very large time step can be adopted for simple, linear trends: indeed, the difference between the two sets of lines in Figure 3.20 is lower than 0.5 °C. The only region in which a finer time step is required is the one associated to the last two nodes on the top, where the border effect causes the intersection of the two lines. With 30 minutes time step, this occurs about 40 minutes later than in the simulation with 1-minute time step.

In addition, the choice of the time step must account the timing of the input data as well. Namely if the weather data or any other input information of the model were measured and recorded each hour, a simulation with 1-minute time step would lose significance. In fact, the finer time step would add the need of interpolation on the measured data, introducing a further degree of approximation and uncertainty on the results. In other words, too small-time steps with respect to the time scale of the problem and the length of the simulation would lose physical meaning. Usually, application to plants which work under transient regimes are performed on a yearly basis at least and in this case the scale of 1 minutes would only imply a heavier simulation.

The considerations above on the time steps refer to single components but they can be easily repeated for systems/subsystems. Clearly the time step of the simulation shall be influenced by the elements with strongly non-linear behaviours.

3.4. Differences between the configuration with two distinct boiler and the one with only a storage with double volume and double height

The aim of this section is to provide an insight on the working of Type 4 to verify whether two tanks stacked one on other lead to the same results of the case in which they were modelled separately. From a physical point of view, the question is rhetorical: the convective contribution is far more apparent in a tank with double volume (3 m^3 vs 1.5 m^3 per each tank) and double height (4.30 m vs 2.15 m). The real issue of this section is the enquiry on the working of the numerical model in order to assess how it models the real physical phenomenon. The basic working of the FORTRAN code of the element will be analysed and some simulations on the behaviour of the element will be shown.

3.4.1. Basic principles of working for Type 4

The TRNSYS element type 4 used to model thermal storages divides the given volume in N user defined nodes. Each node represents part of the total volume, while the initial conditions allow to define the initial temperatures at each node.

Figure 3.21 illustrates the basic models used to carry out the comparisons:

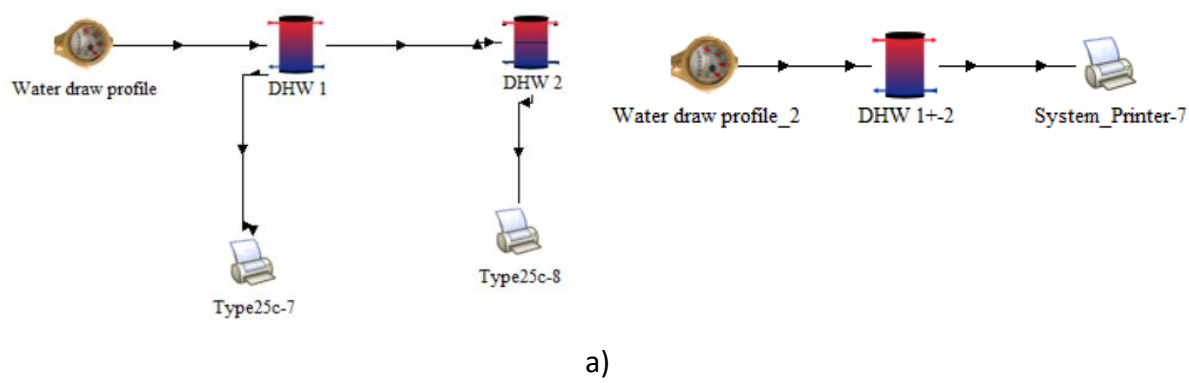


Figure 3.21. Basic TRNSYS models used to test if the simulation with the two distinct boilers (a) leads to the same results as in the case of the two tanks stacked (b)

This section is meant to provide a more specific insight on the source code used in TRNSYS environment. In particular, the temperatures of each node at different time steps is computed according to the following steps:

- *Flow rate contribution*: this term accounts for any eventual flow rate inside the tank crossing each i-th volume. The temperatures are evaluated starting with the node which has the largest entering flowstream flow rate. For each node the flows up from the node below and down from the node above are calculated.
- *Losses to the environment*: the type used in the present analyses considers uniform losses. Under this assumption, the thermal losses are quantified by means of UA (thermal loss coefficient, U, times the surface A, subjected to heat flux). The internal nodes have a UA referred to the lateral surface of the cylinder representing the i-th volume. On the other hand, the losses due to the top and bottom surfaces are added to the losses of the first and last node. This aspect has been already highlighted in the previous simulations in which the temperature trend for the

top and bottom node showed a faster cooling with respect to the nodes in between the top and bottom of the tank.

- *Capacitance of each node*: in order to solve the differential equation and estimate the temperature of each volume inside the tank at different time steps, the capacitance can be computed as the total capacitance of the tank ($\rho c_p V_{\text{tot}}$) weighted using the ratio between the height of the i-th node and the total height of the tank.

In conclusion, the code solves the linear differential equation written using the following pattern

$$\frac{dT}{d\tau} = A * T + B \quad (3.4)$$

Where

T , temperature depends on time

A , B are coefficients depending on time, capacitance, thermal losses to the environment and water flow rates entering the tank defined as follows:

$$A = - \frac{(\sum_i m'_i + UA)}{\rho V c_p} \quad (3.5)$$

$$B = \frac{(\sum_i m'_i T_i + UA T_{\text{env}} + \sum_n q_n)}{\rho V c_p} \quad (3.6)$$

With

$\sum_i m'_i$ are the water flow rates flowing inside the tank at the temperatures T_i ;

UA represents the losses to the environment (at temperature T_{env}) as described above;

$\rho V c_p$ is the capacitance of the single node (related to the correspondent volume of water into which the tank is divided);

$\sum_n q_n$ are the heat fluxes associated to the adjacent nodes.

3.4.2. Numerical simulations

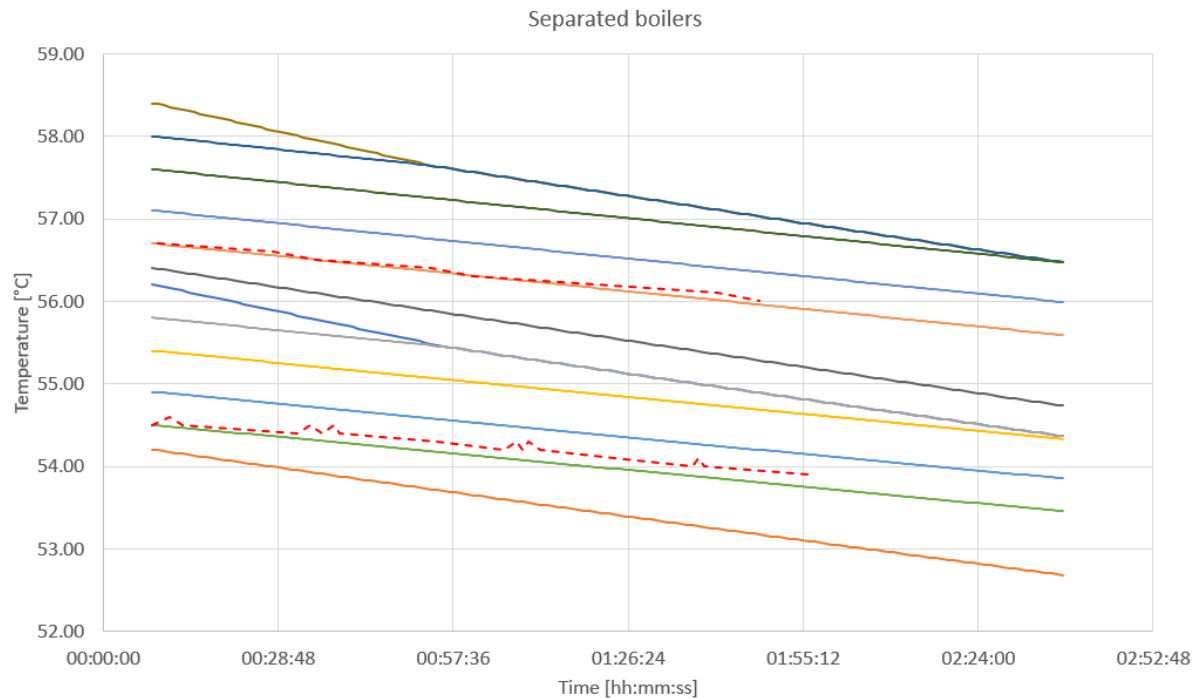
The following common features have been adopted concerning the following numerical simulations:

- *Water draw profile*: this element shall be used later in this section to simulate a water flow inlet at different temperatures. As far as the comparison with simplified case of the two boilers stacked one on the other, no water draw is assumed to flow inside the tanks.
- *Type 4*: the same element has been adopted in both cases (complete, Figure 3.21 a) and Figure 3.21 b)). The same intensive thermophysical properties have been adopted (e.g. thermal loss coefficient) while the extensive properties have been modified (e.g. height or volume). The number of the nodes and their position inside the tank follow the same principles and conclusions of the previous sections: the simplified case has 12 nodes, with the same distance as the one adopted above. The complete case has the same total number of nodes, at the same heights, except for their distribution: six nodes belong to the first tank (DHW1) and the others belong to the second one (DHW2). Their positioning is almost unchanged in order to compare the two results.

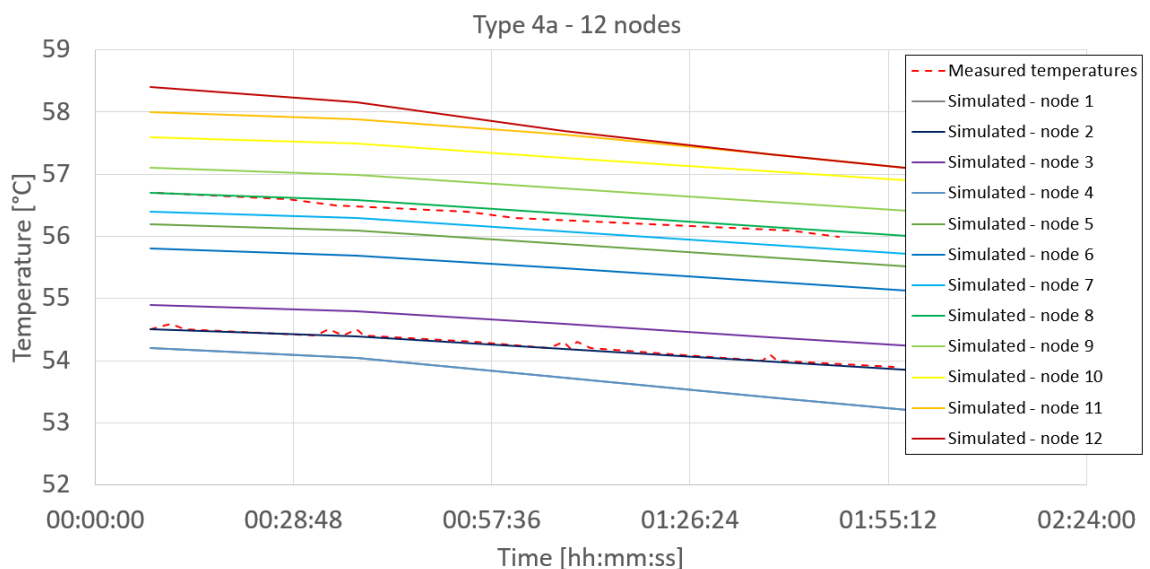
- *MIX number*: for each case presented, the evolution of the MIX number over the different time steps will be presented.

Case 1 – no water flow rates

The result with one bigger tank is reported below. Then the simulation carried out using the model in Figure 3.21 is reported.



a)



b)

Figure 3.22. Comparison between the case of distinct boilers (a) and stacked together (b). The first two hours of simulation have been considered. The red, dotted lines represent the TRNSYS simulated curves while the continuous ones are concerned with the measured trends for temperature

As far as the comparison with the experimental results is concerned, the two simulations lead to similar results with very good approximation. The real distinction between the two models is concerned with the top node of the DHW1 tank and the bottom node of DHW2 tank. Indeed, the model in Figure 3.22a) accounts for the higher thermal losses due to the top/bottom of the tank. The absence of water flow rates makes the two storages work independently and the difference in the two models is local.

In terms of MIX number, the value starts from zero at the initial time step (the ideal stratification is supposed equal to assigned the initial conditions) and within the two hours of simulation, the MIX number arises almost linearly up to the value of 0.2 (Figure 3.23).

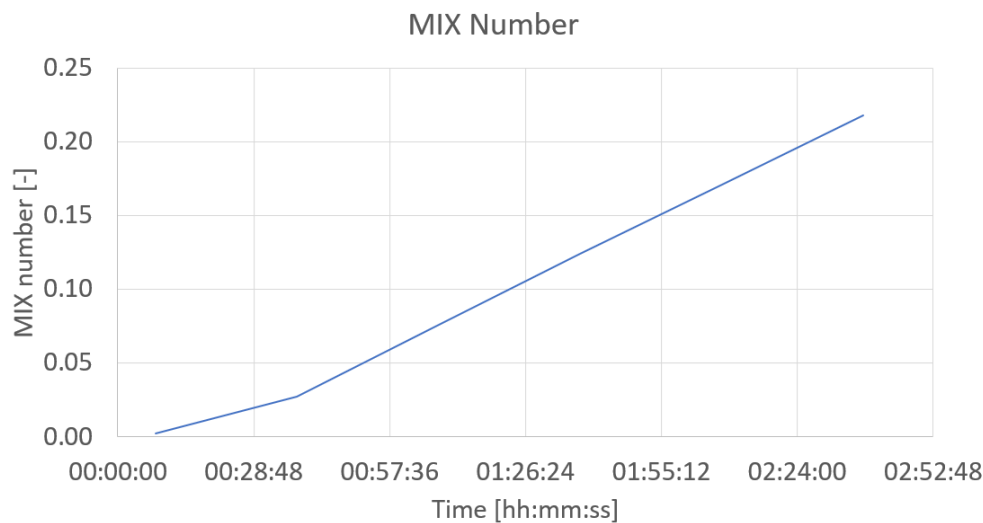
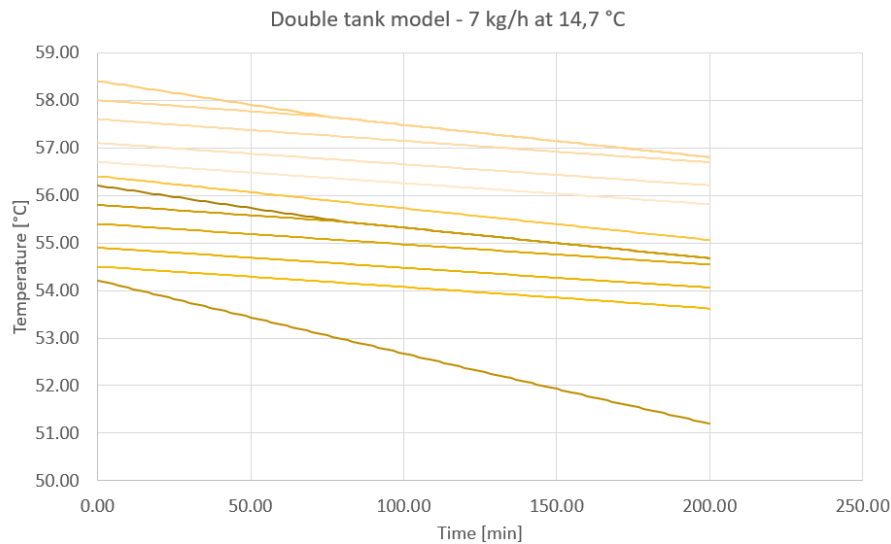


Figure 3.23. Mix number over different time steps for the case of no water flow inlet inside the storage

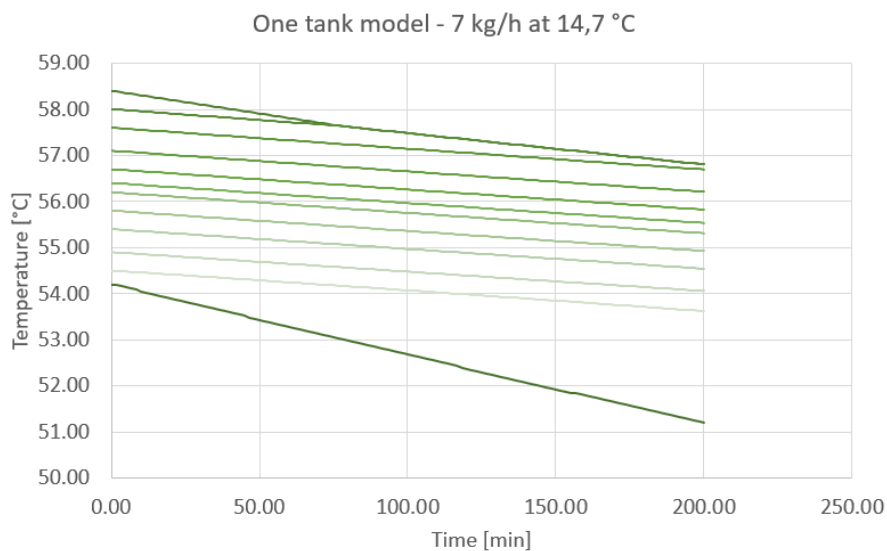
Actually, the plot clearly shows the evolution of the MIX number over time. On the other side, it completely loses the distribution of stratification over space. Figure 3.22 clearly shows that stratification at the end of the simulation has been significantly changed and lost near the top and the bottom of the tank, while the nodes in between still preserve a good level of stratification. Moreover, without the help of Figure 3.22 the regions more subjected to the lost of stratification couldn't be identified. In this case the cause was linked to the major thermal losses determined by the border conditions of top and bottom of the tank and therefore stratification was destroyed in those regions. This aspect will become more apparent as the water inlets will be added, increasing the value of the flow rate.

Case 2 – small water flow rates

In this instance, a very small water flow rate is assumed, in both cases – 7 kg/h (0.12 l/min), with an initial temperature of 14 °C, to simulate the inlet from the water, as done in the previous sections about the validation of the DHW tanks and of the mixing valve V8.



a)



b)

Figure 3.24. Temperature trend at the different nodes using the models reported in Figure 3.21.

The two models lead to a very negligible difference, concerned in particular with the nodes at the top of DHW 1 and the bottom of DHW2 respectively. A brief comparison with Figure 3.21 shows that no significant variation occurs, except for the first node on the bottom of DHW1 tank. Its temperature at the end of the simulation reaches about 51 °C in both cases. In the previous instance with no water flow rate, the final temperature was about 53 °C. Then, considering the other nodes, the effect of the inlet cold water weakens up to the top where no significant variation is appreciated. In the end the stratification inside the tank still works in most of the volume under study. So, the assumption adopted previously can be accepted.

As far as the MIX number is concerned, its trend and the maximum value reached (0.16) is comparable to the one in Figure 3.23.

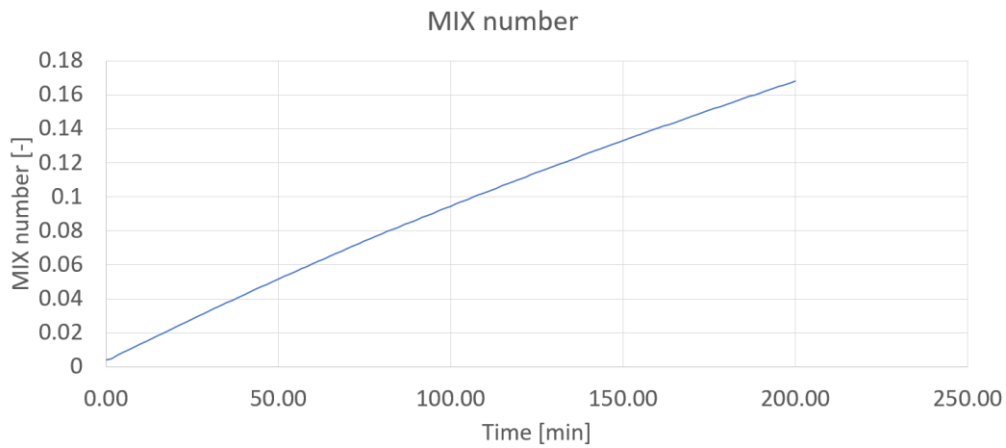
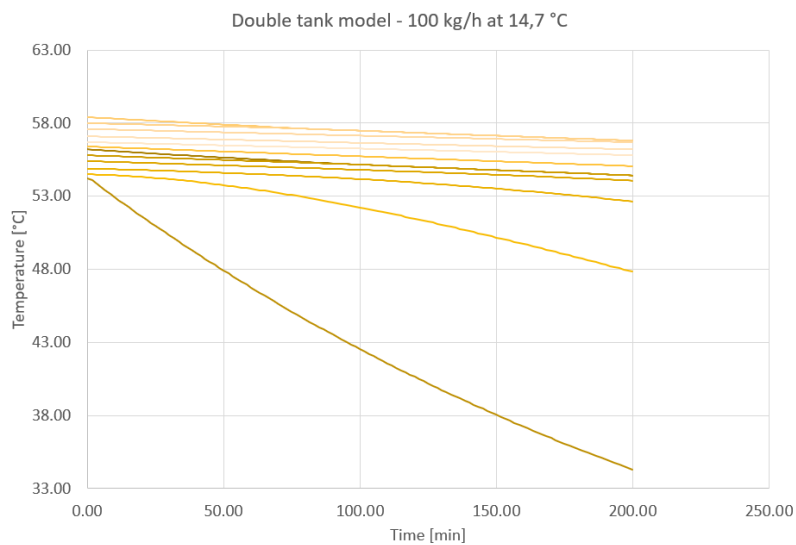


Figure 3.25. Mix number over different time steps for the case of small water flow inlet (7 kg/h at 14.7 °C) inside the storage

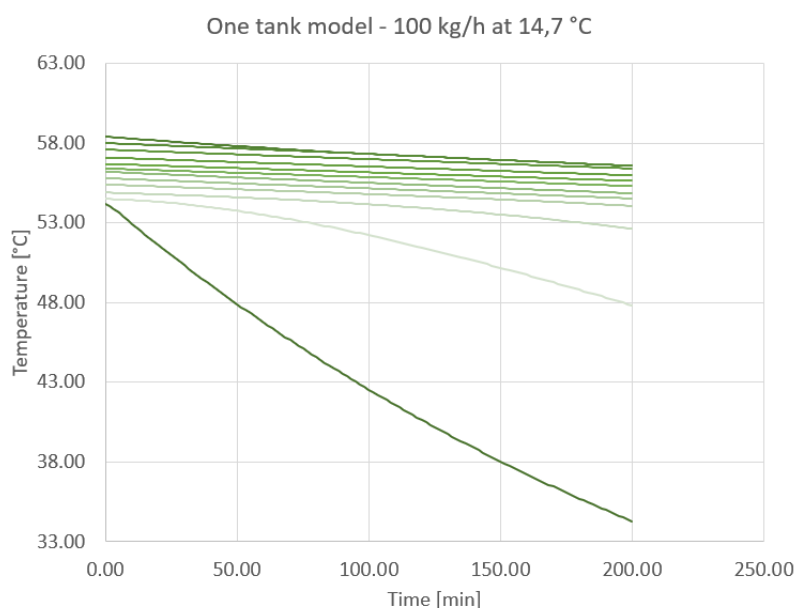
Indeed, in terms of degradation of the stratification level due to small cold water flow rates or thermal losses to the environment are comparable.

Case 3 – increasing the water flow rates

In this section higher flow rates shall be briefly presented in order to provide a clearer insight on the behaviour of the two tanks. The first instance is concerned with a constant water flow rate of 100 kg/h (about 1.67 l/min) at the constant temperature of 14.7 °C:



a)



b)

Figure 3.26. Trend in temperature for two boilers joined (a) and single boiler (b) with 100 kg/h of water flow rate at the constant temperature of 14.7 °C

The global behaviour still is similar in the two models; the two coldest nodes end up to a temperature of about 34 °C. A wider zoom on the higher temperatures (between 49 and 59 °C) shows how the increase in the water flow rate highlights the contribution of the node on the top of DHW1 as outlined in the figure below.

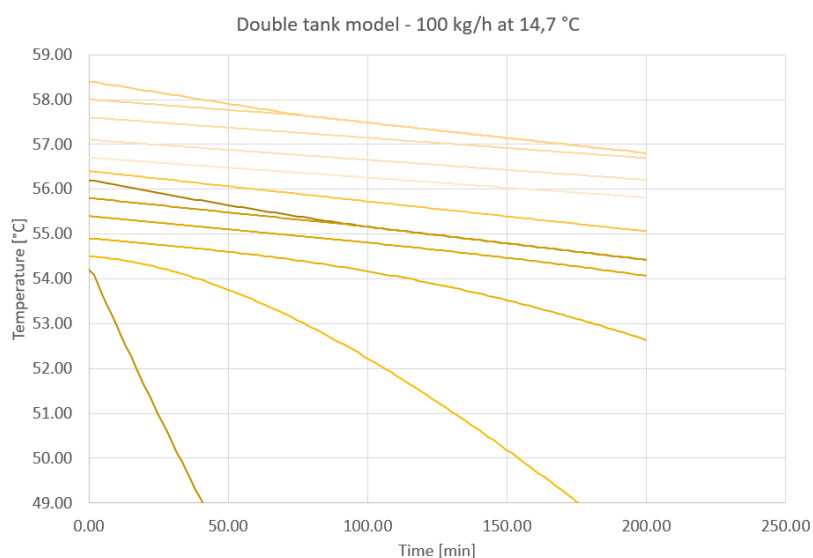


Figure 3.27. Detail of Figure 3.26a

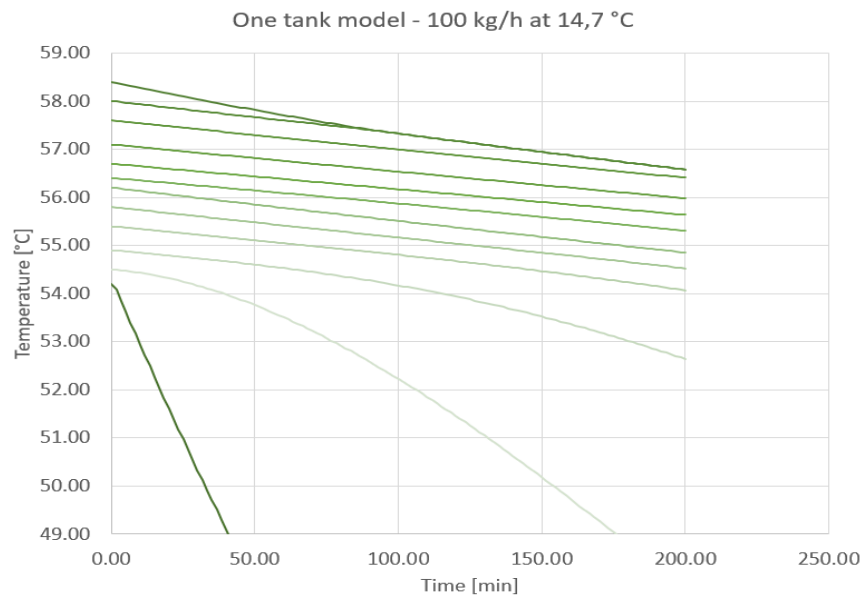


Figure 3.28. Detail of Figure 3.26 b

Indeed, as the cold water-inlet increases, the mixing has a higher influence on the behaviour of the nodes up to the case in which the border effect of the node is completely lost.

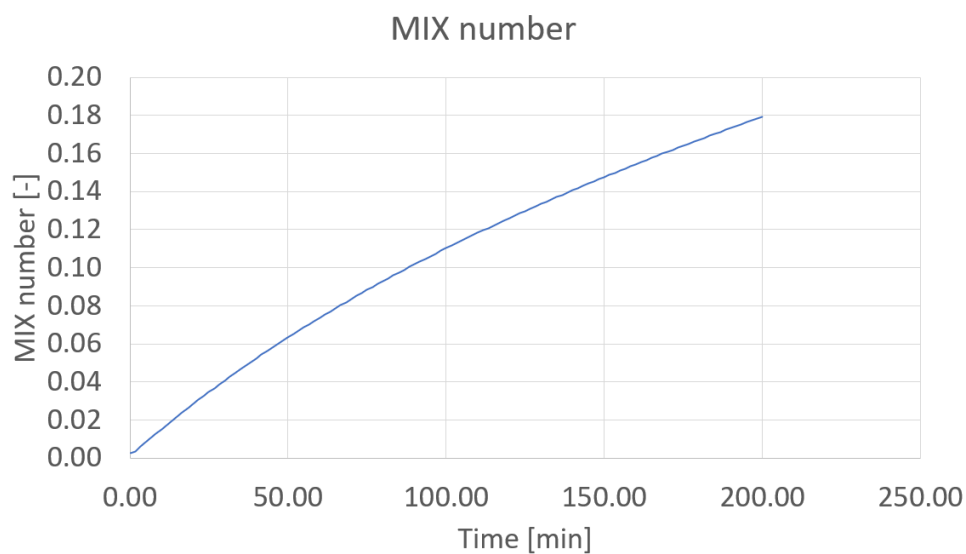
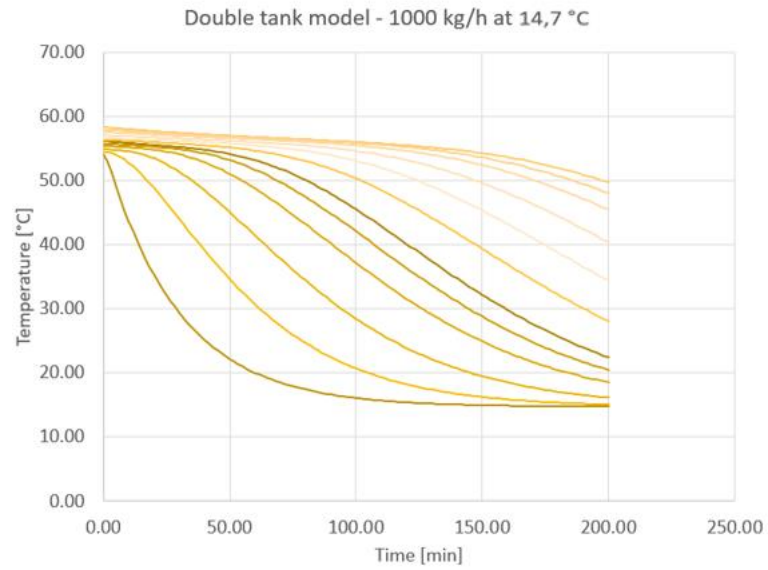


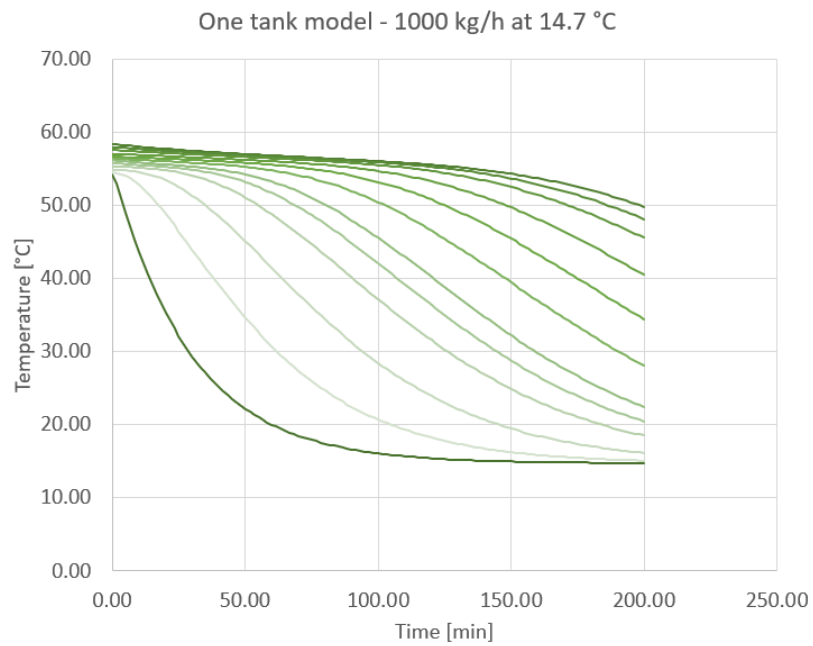
Figure 3.29. Mix number over different time steps for the case of higher water flow inlet (100 kg/h at 14.7 °C) inside the storage

The MIX number preserves the same trend shown in the previous case, reaching a greater maximum value. Indeed, the increase in the inlet water flow rate gradually destroys the stratification inside the tank.

The following instance is concerned with 1000 kg/h at 14.7 °C.



a)



b)

Figure 3.30. Trend in temperature for two boilers joined (a) and single boiler (b) with 1000 kg/h of water flow rate at the constant temperature of 14.7 °C

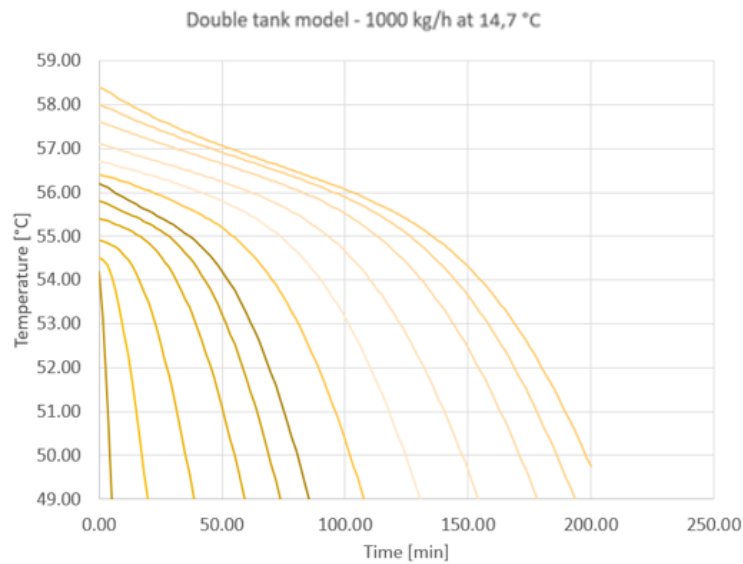


Figure 3.31. Detail of Figure 3.30a

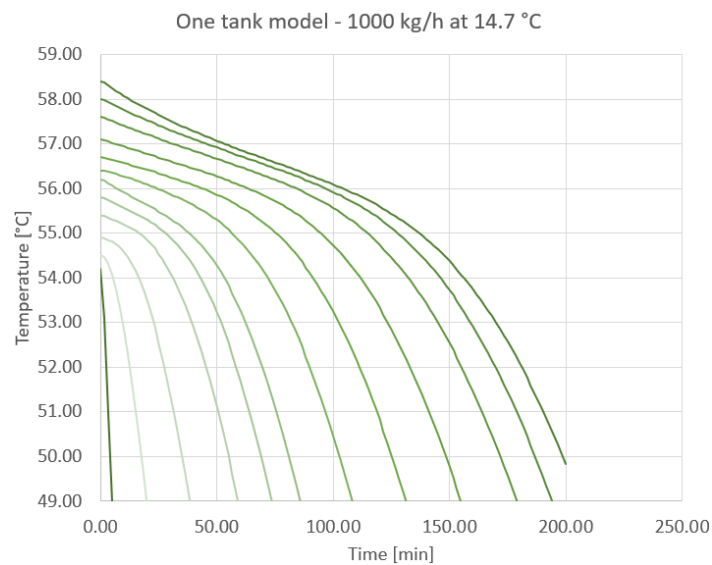


Figure 3.32. Detail of Figure 3.30b

In conclusion, no significative differences can be identified between the two models shown in Figure 3.21. The variations are concerned only with the nodes which are influenced by the borders of the geometry and their contribution becomes negligible as the water flow rate increases and the process of mixing becomes dominant with respect to the cooling one.

With respect to the previous cases, the MIX number increases, maintaining almost a linear trend as shown in Figure 3.33.

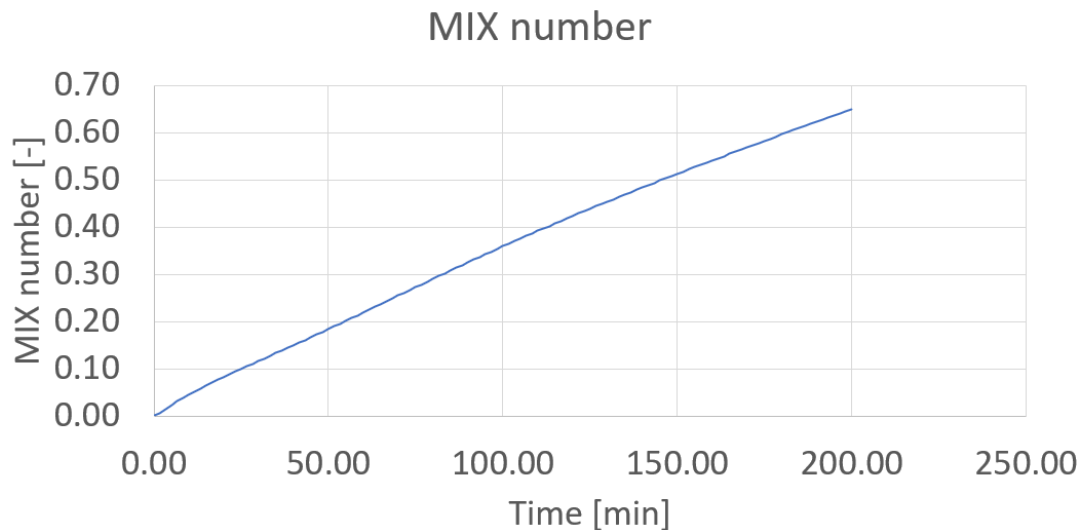


Figure 3.33. Mix number over different time steps for the case of significant water flow inlet (1000 kg/h at 14.7 °C) inside the storage

The maximum value reached (about 0.70) clearly represents the almost complete destruction of the stratification inside the storage.

3.5. Conclusions and future developments

The issue of data acquisition systems is becoming a widespread problem as technologically advanced plants take place over the market. The information collected has very different and useful applications, such as the study on the plant efficiency and of new regulation criteria to increase it. Moreover, the DAS provides real time plant status (e.g. ruptures, unusual working). Nevertheless, the cost of each sensor makes a complete DAS economically unfeasible, so numerical models can be employed to integrate the missing data. In this paper, the DAS associated to a DHW production system by means of traditional fossil burners integrated with a solar assisted heat pump has been presented. No flow rate measurement is available, only the temperature levels have been recorded over the plant (e.g. tanks). This missing information has been determined by means of a simple, but still reliable numerical model built with TRNSYS commercial code and validated with the measured data. Two particular case-studies highlighted by the DAS have been numerically simulated:

- *Typical nights:* in these periods, the trend in temperature inside the DHW tanks shows a decrease representative of the cooling within inactive plants. The results of the numerical model have highlighted the presence of a low, constant water flow rate, representative perhaps of a leakage (e.g. ruptures or partially open faucet).
- *Untypical nights:* in these periods, the trend in temperature inside the DHW tanks is very different from the previous case. This fact occurs often along the year and it is apparently unjustified, since no significative differences in the plant scheme or operative modes have been introduced. The TRNSYS numerical simulations have led to an approximate water load profile that can be compatible for duration and entity with the cleaning of the sport palace. This behaviour roughly doubles the energy and the power required in the morning to the plant to re-heat the tanks up to the set temperature. To avoid it a new regulation criterion can be

introduced to turn the plant on 1 hour before the opening (instead of 30 minutes) each time temperature in the DHW tanks lowers a set point value.

In addition, the so-built model can be integrated with all the components neglected over nights (e.g. gas burners, recirculation pumps, solar assisted heat pump) to simulate the plant during the day as well. This model shall have multiple applications, from data integration (especially on the water flow rates) to efficiency analyses under transient regime.

As far as the numerical simulation is concerned, an insight over the different available models to simulate specific components has been proposed, especially for the case of domestic hot water storage tanks. The results reported in this chapter have shown the application of the TRNSYS model for a DHW storage tank enquiring its mesh sensitivity and the dependence on the size of the time step. Moreover, the issue of stratification has been recalled and analysed by means of numerical simulation compared to the available experimental data. In particular, the quality of stratification over different time steps has been shown. In this context, the MIX number provides a useful, averaged evaluation of the level of stratification over the tank. Nevertheless, the distribution of stratification over time cannot be deduced from the MIX number; no information is provided by the mix number about the causes of the destruction of stratification. For instance, the same number could be reached both in a boiler only subjected to environmental losses and in a tank with cold water inlet flow rates. In cases where the MIX number reached values of about 0.2, the trend of temperatures inside the tank clearly showed that stratification was destroyed near the top/bottom surfaces (characterised by major thermal losses) and near the water inlets, while the remaining part of the tank still behaved following the principle of stratification. This information was lost by the MIX number which only highlighted that the conditions inside the tank decreased because of the top/bottom volumes and the ones near the water inlets.

As far as the modelling of the plant as a whole is concerned, the correct choice of the model for each component is of paramount importance. Indeed, no detailed model (e.g. CFD) can be adopted since its precision and extended computing times would not meet the targets of the numerical simulation of the plant which aims to a simple, but effective representation of the SAHP. The long-term goal of these simulations is to provide efficiency strategies which can be employed even in the design stage without necessarily referring to tailored numerical models. The availability of effective and simplified design strategies would enhance the diffusion of SAHP over the territory. In addition, a correct design would increase the efficiency of such plants, with small increase in the cost of the design and very high benefits from the point of view of the plant performance.

REFERENCES

- [1] G. Corallo, A. Franchi, A. Simonetti e L. Di Rienzo, *Messa in funzione e analisi sperimentale del prototipo di macchina elioassistita*, 2011.
- [2] J. Hadamard, *Lectures on Cauchy's Problem in Linear Differential Equations*, New Haven: Yale University Press, 1923.
- [3] O. M. Alifanov, *Inverse Heat Transfer Problems*, New York: Springer-Verlag, 1994.
- [4] J. V. Beck , B. Blackwell e C. R. St. Clair, *Inverse Heat Conduction: Ill-Posed Problems*, New York: Wiley Interscience, 1985.

- [5] J. Alencar Jr. , H. Orlande e M. Ozisik, «A Generalized Coordinates Approach for the Solution of Inverse Heat Conduction Problems,» in *11th International Heat Transfer Conference*, 7, 53-58, Kyongju, Korea, 1998.
- [6] H. A. Machado e H. Orlande, «Inverse Problem of Estimating the Heat Flux to a Non-Newtonian Fluid in a Parallel Plate Channel,» *RBCM - J. Braz. Soc. Mech. Sciences* , vol. 20, pp. 1-6, 1998.
- [7] P. S. Hore , G. W. Krutz e R. J. Schoenhals, «Application of the Finite Element Method to the Inverse Heat Conduction Problem,» in *ASME Paper n. 77*, 1977.
- [8] N. Zabaras e T. H. Ngugen, «Control of the Freezing Interface Morphology in Solidification Processes in the Presence of Natural Convection,» *International Journal for Numerical Methods in Engineering*, vol. 38, pp. 1555-1578, 1995.
- [9] N. Zabaras e G. Yang, «A Functional Optimization Formulation and Implementation of an Inverse Natural Convection Problem,» *Computer Methods in Applied Mechanics and Engineering*, vol. 144, pp. 245-274, 1997.
- [10] D. Lesnic, L. Elliot e D. B. Ingharn, «Application of the Boundary Element Method to Inverse Heat Conduction Problems,» *International Journal of Heat and Mass Transfer*, vol. 39, n. 7, pp. 1503-1517, 1996.
- [11] C. Huang e C. Tsai, «An Inverse Heat Conduction Problem of Estimating Boundary Fluxes in an Irregular Domain with Conjugate Gradient Method,» *Heat and Mass Transfer*, vol. 34, pp. 47-54, 1998.
- [12] G. S. Dulikravich e T. J. Martin, «Inverse Shape and Boundary Condition Problems and Optimization in Heat Conduction,» *Advances in Numerical Heat Transfer*, vol. 1, pp. 381-426, 1996.
- [13] T. Martin e G. Dulikravich, «Non-Iterative Inverse Determination of Temperature-Dependent Heat Conductivities,» *ASME National Heat Transfer Conference* , vol. 2, pp. 141-150, 1997.
- [14] O. M. Alifanov, *Inverse Heat Transfer Problems*, New York: Springer-Verlag, 1994.
- [15] C. J. Banister , W. Wagar e M. Collins , «Validation of a single tank, multi-mode solar-assisted heat pump TRNSYS model,» *Energy Procedia*, pp. 499-504, 2014.
- [16] *UNI EN 12831:2018, Energy performance of buildings – Method for calculation of the design heat load – Part1*, 2019.
- [17] Y. Han, R. Wang e Y. Dai, «Thermal stratification within the water tank,» *Renewable and Sustainable Energy Reviews*, vol. 13, pp. 1014-1026, 2009.
- [18] K. Hollands e M. Lightstone, «A review of low-flow, stratified-tank solar water heating systems,» *Solar Energy*, vol. 43, n. 2, pp. 97-105, 1989.
- [19] J. Turner , *Buoyancy Effects in Fluids*, Cambridge University Press, 1973.

- [20] E. Kleinbach e S. Klein, «Performance study of one-dimensional models for stratified thermal storage tanks,» *Solar energy*, vol. 50, n. 2, pp. 155-166, 1993.
- [21] K. Johannes e G. Rusaouen, «Comparison of solar water tank storage modelling solutions,» *Solar energy*, vol. 79, n. 2, pp. 216-218, 2005.
- [22] J. V. Beck e H. Wolf, «The Nonlinear Inverse Heat Conduction Problem,» in *ASME Paper No. 65-HT-40*, 1965.

4. HYPOTHESIS OF REVAMPING FOR THE SAHP-PVT INSTALLATION AT PALACUS

The experience acquired about SAHPs by means of the monitoring and control of the pilot plant at Palacus has highlighted some critical aspects which have already been partially discussed in the previous chapters. Moreover, the plant, which has been operating since 2013, has been subjected to local ruptures and a revamping is taking place. Within this context, our working group at University has contributed to the design stage of the interventions, providing the knowledge about the plant to introduce some further improvements. The chance to join the decisional process of the revamping is of paramount importance, because the concepts and the critical aspects identified in the previous chapters can be translated into operative instructions. With this intervention the plant has the possibility to improve, fix some existing bugs and reach higher performances in terms of both working and acceptance by the end users. This chapter indeed reports the key concepts over which the working group carried out simulations along the last year to support the team of engineers appointed of the design. The main topics illustrated below are concerned with some functional aspects of the plant itself as well as the data acquisition system installed. As discussed in the first chapter and then recalled in this section, the changes to the plant can be imputed to bug fixing and upgrading of the plant in term of cost effectiveness according to the current regulatory incentives. The structure of this chapter schematically presents the different issues and the correspondent suggested improvement.

4.1. Leakages in the solar field – integration of the HP configuration

After the first lockdown ended, a global check of the plant has taken place during summer 2020 to assess the conditions of the plant before the next heating season. Actually, quite a large percentage of panels (about 60%) has shown local ruptures with consequent water leakages. Unfortunately, the damage was mainly concerned with the panels themselves instead of the rubber pipes of connection. This problem was mainly due to two principal aspects:

- the solar hybrid panels are made with the roll bond technique (Figure 4.1), namely, two or more layers of metal are cold welded. This technique clearly reduces the cost of realization for each panel but at the same time makes impossible to repair them in case of rupture.



Figure 4.1 Cross section of the roll bonded thermal panel below the photovoltaic layers

- according to the preliminary evaluations carried out, it is likely that the ruptures might have taken place also because of a small percentage of glycol inside the circuit. This aspect has been then magnified by the extension of the solar circuit. For instance, about 200 m of pipe are employed just to connect the solar field to the heat pump, not to mention the volume of water inside the panels (about 140 m² of capturing area) and the 500 l storage in the boiler room. A former hypothesis is that recurring stagnation processes during summer might have taken place reducing the percentage of glycol inside the solar field. Then during the cold days in winter, the water inside the circuit froze, giving rise to the leakages.

As a first attempt, the broken panels were bypassed and a global reboot of the plant were performed. This effort didn't reveal successful, indeed it led to multiple and sudden stops of the heat pump, due to the limited water flow rate inlet to the evaporator. The Figure below (Figure 4.2) recalls the solar field and part of the heat pump already shown in the first chapter.

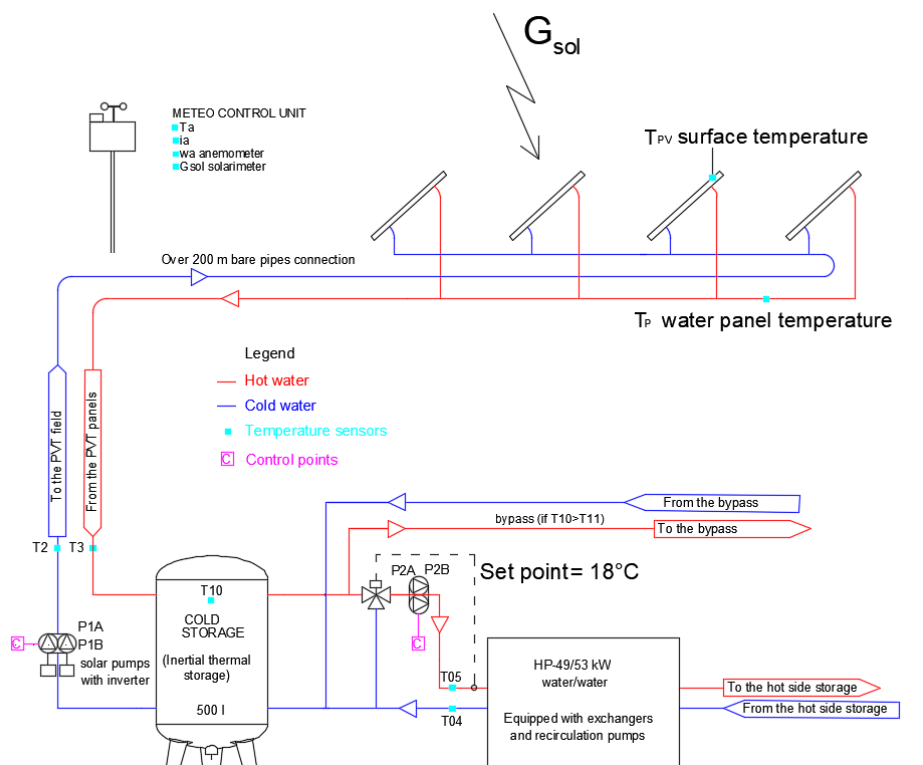


Figure 4.2. Functional scheme of the thermal side of the solar field and part of the heat pump at the Palacus pilot plant

No hydraulic separation is present between the solar field and the heat pump. This aspect is likely to have negatively influenced the concentration of glycol inside the outdoor part of the plant. Indeed, the water flowing inside the tank T10 from the outdoor solar field would eventually mix with the 500 l of the storage. Then, according to the working condition of the plant, the same technical water would be sent to the cold side of the heat pump or directly to the interface heat exchanger with the DHW subsystem.

Moreover, the partial exclusion of the broken panels has reduced the intensity of the water flow rate causing frequent blocks of the heat pump. Secondly, the reduced capturing area will determine

a reduction in the collected solar thermal energy, affecting the global performance of the plant. In conclusion at the present conditions, the plant cannot grant its operativity even reducing the solar field. Moreover, an operativity test of the heat pump itself has been performed in order to check the absence of ruptures within the machine.

To summarise, the solar field needs a deep revamping both in terms of extension (about 60% of the panels need to be replaced) and in terms of plant functionality (a hydraulic separation between the solar field and the heat pump is highly recommended). Actually, the solar field is composed by hybrid panels: this means that about 100% of the photovoltaic field is operative while the estimated 60% of damaged panels is referred to the thermal side. So, the first issue was concerned with two main aspects: the number of panels to be replaced and the kind of the new ones. The evaluated possibilities are concerned with the replacement of the damaged solar panels or part of them with:

- new hybrid panels
- new thermal panels

From the point of view of the plant performance, the substitution of the damaged panels with new ones of the same kind would lead to the same initial situation and therefore it might appear to be the best solution. Clearly, the case of replacement with new photovoltaic panels has not been analysed because the thermal field is actually not sufficient to support the heat pump and therefore it needs the principal restoration. Moreover, the actual production of electricity has been completely compromised. Indeed, no more the heat flow is removed from the panel and its photovoltaic efficiency has reduced. The implicit question behind this issue is concerned with the energy management according to the feed-in-premium strategies. As widely explained in the first chapter, when the plant was firstly assembled, the solar hybrid field had been dimensioned in order to cover with the summer production of electricity, the electrical need of the SAHP during winter.

The following figure (Figure 4.3) shows the energy consumption of the heat pump (columns in blue) against the photovoltaic production (green columns) based on averages and estimations obtained by the DAS. The grey bars represent the net monthly balance. As anticipated, the net balance is negative in the months during the heating season, while it is strongly positive during summer (the plant is almost off in summer and therefore its electrical consumption as well is negligible). Namely during summer, the needs of the facility are concerned only with the DHW production since no cooling system or air treatment is present. Within this period the availability of solar thermal energy allows to bypass the heat pump subsystem since the temperature reached inside the solar field is often almost near to the set point value leaving only the integration gas burners active in case of need.

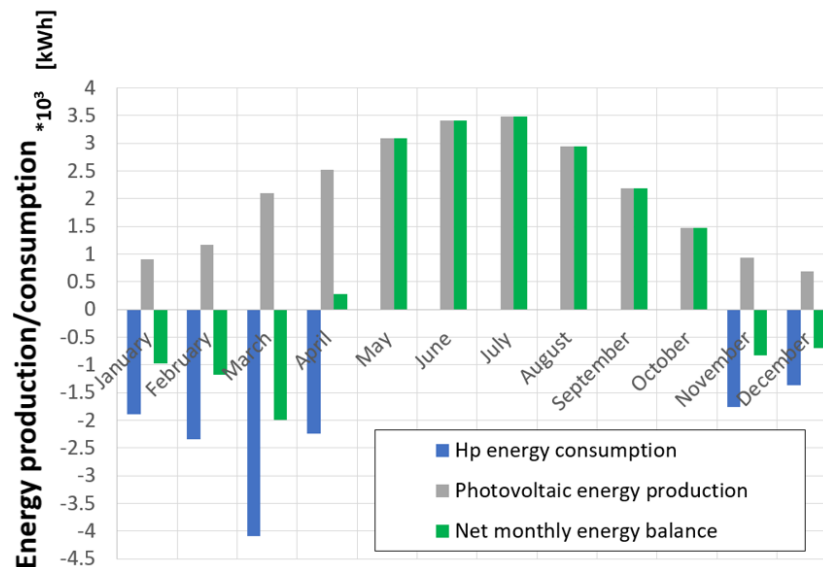


Figure 4.3. Monthly energy consumption for the HP, photovoltaic production and net monthly balance for the SAHP at Palacus

So, in case the initial feed-in-premium strategy were adopted, the energy balance between electrical consumption and production would be strongly positive (Figure 4.4, on the left, “old feed in premium”). In fact, the balance over the reference period of a year would have allowed to compensate the non-uniform availability of irradiance over the year with the consumption of the plant reaching an overproduction of about 40% with respect to the annual HP consumption. Then, basing on the same information reported in Figure 4.3, but assuming that the recent feed-in-premium were applied, the performance of the plant is over turned: applying a monthly balance, the peak summer production becomes almost lost and therefore over a year the photovoltaic field provides about 40/50% of the HP need.

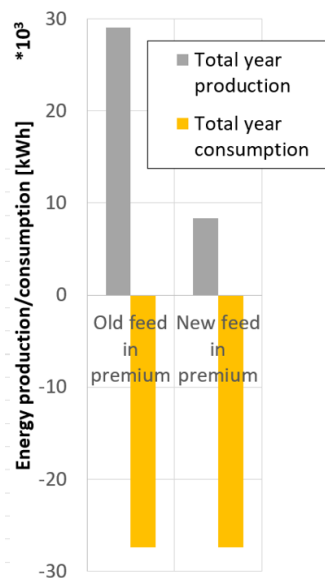


Figure 4.4. Old yearly feed in premium balance based on the values reported in Figure 4.3 **Errore. L'origine riferimento non è stata trovata.** against the new monthly feed in premium strategy

With reference to the Figure 4.3 and Figure 4.4 the graphical results can be better explained by means of the following Table 4.1 and Table 4.2.

Month	Days	$I_{\text{mean,daily}}$ (MJ m ⁻²)	$T_{\text{mean,ext}}$ (°C)	$E_{\text{El,PV}}$ (kWh)
January	31	5.86	8	899.5
February	28	8.33	9	1171.1
March	31	13.57	11	1947.3
April	30	16.82	14	2205
May	31	19.98	17	3269.6
June	30	22.73	21	3509.5
July	31	22.45	24	3684.7
August	31	19	24	2875
September	30	14.6	21	1997.7
October	31	9.48	17	1504.5
November	30	6.21	12	920.7
December	31	4.41	9	693.7
Total	365		29057.5	24678.3

Table 4.1. Measured irradiance, monthly average temperature and photovoltaic energy collected by the hybrid field over a standard year ($A = 140 \text{ m}^2$)

Table 4.1 resumes the environmental conditions (e.g. external temperature and average daily irradiance) expressed for each month against the electricity produced, which can be estimated at about 25000 kWh_E over a year, in accordance with [1], with respect to a global yearly mean irradiance of 4980 MJ/m². On the other hand, the consumed electrical power of the HP is about 12 kW_E only in nominal peak conditions, reached only in heavy duty conditions. The total energy consumed is about 13500 kWh_E. Thanks to the control system of the SAHP, the panel surface temperatures are always very close to the external one, so the only solar panels thermal losses are due to reflection (about 20%). Detailed month by month HP consumptions are shown in Table 4.2. In addition, the electrical efficiency of the panels is about 13-15% as reported in the data sheets of the hybrid panels installed.

The balance over a year is positive since the electrical energy produced is greater than the consumed one over the same reference period saving about 55% of the total electricity produced. These estimations on the records of the past two years are in accordance [1], where a prediction 14000 kWh_E of electrical consumption and 25000 kWh_E of electrical production was reported.

The electricity production, $E_{el,PV}$, during summer can double or even triple the winter production (Table 4.2), highlighting the importance of this contribution to the yearly balance. Table 4.2 shows the electrical energy consumed by the heat pump $E_{el,HP}$ during the heating season according to the thermal energy produced by the HP.

Month	COP_m	$E_{th,HP}$ (kWh)	$E_{el, HP}$ (kWh)	$E_{el,PV}$ (kWh)	ΔE (kWh) (Yearly balance)	ΔE (kWh) (Monthly balance)
January	3	5651.6	-1883.9	+908.3	-975.6	-975.6
February	3.1	7256.4	-2340.8	+1166.2	-1174.6	-1174.6
March	3.2	13087.5	-4089.8	+2103.4	-1986.5	-1986.5
April	3.5	7849.3	-2242.7	+2523	+280.3	0
May	-	0	0	+3096.9	+3096.9	0
June	-	0	0	+3409.5	+3409.5	0
July	-	0	0	+3479.8	+3479.8	0
August	-	0	0	+2945	+2945.0	0
September	-	0	0	+2190	+2190.0	0
October	-	0	0	+1469.4	+1469.4	0
November	3.3	5796	-1756.4	+931.5	-824.9	-824.9
December	3.1	4253.2	-1372	+683.5	-688.5	-688.5
Total		43894	-13685.6	+24906.45	+11220.4	-5650

Table 4.2. Summary of the electricity consumed by the HP, the photovoltaic energy collected by the hybrid field over a standard year simulation and the difference between energy consumption and collection (negative values stand for net energy consumption from the grid)

The last three columns contain, respectively, the electrical energy transformed from solar irradiation $E_{el,PV}$ and the gain/deficit computed for each month, in accordance with previous and existing laws. Negative differences show a lack of electricity compensated by the national grid, with consequent operating costs. A positive balance means a not-paid surplus in energy production injected into the grid and not payed. Under these new conditions, the solar field covers up to 60% of the average electrical need of the plant. The surplus of electricity during mild seasons is injected into the grid, but without any positive economic benefit for the prosumer, representing therefore a net economic loss for the plant financial balance.

This example clearly shows and justifies the choice to abandon the hybrid panels technology in favour of more performant thermal panels. Behind the lines, this simple instance is food for thought about how tough the design of solar fields is nowadays in Italy. Within about 7 years (the plant was tested and became operative in 2013) three main changes occurred in the feed-in-premium, each one strongly and negatively affecting the cost-effectiveness of the plant.

This was the information available half a year ago when the simulations and the main decision about the revamping of the plant were taken. After that, the very recent new laws about Superbonus 110 came into force with an even more radical review of the feed-in-premium strategy. Briefly and with no aim to provide an exhaustive insight on the topic, in case of relevant energy efficiency interventions on the structures (e.g. insulation coating, revamping of the heating plant), the cost of a new solar field becomes tax deductible to the extent of 110% of its value within five years. These incentives include the cost of batteries and other electricity storages both for new and existing solar fields but cannot apply to the specific case, since non-profit societies are not contemplated. The important remark behind the Ecobonus 110% strategy lies in the regulatory conditions: in every case each solar field must be connected to the national grid. The new concept is that the feed-in-premium strategy has just become updated and the actual “ratio legis” is to rule it definitely out in the next years. Indeed, the Ecobonus does not pay back anyhow the electricity immitted inside the national grid actually cancelling the feed-in-premium and the net-metering concepts. In other words, the concept lying at the base of these new laws is that the solar field is completely financed and therefore no payback analyses have to be performed. Within this context, the users can consume as much self-produced electricity as possible and eventually store it. In the end, all the surplus production must be freely immitted into the national grid, without any monthly/yearly compensation or valorisation of it.

In conclusion, this means that the initial approach, which justified the actual photovoltaic power installed (20 kW), is definitely abandoned. Any subsequent change in the law, up to the most recent bonuses makes the power installed useless for the sport facility under exam. Even in the case of installation of the batteries, their contribution would not allow yearly or even monthly balances without negatively affecting the cost-effectiveness of this intervention.

Basing on these reasons schematically resumed above, the hypothesis of new hybrid panels was discarded and new, more efficient, thermal ones were identified. Actually, about 40÷50% of the solar field (so most of the damaged panels) shall be replaced only by thermal ones. The option of replacement with hybrid panels would reveal due to the low likelihood to find on the market panels with thermal, photovoltaic and dimensional characteristics comparable to the existing ones. In other words, the installed peak electrical power will be halved with no negative influences on the plant since today the surplus of electricity production is worthless and the new strategy to make the photovoltaic field efficient again is to maximise the self-consumption (namely 10 kW of peak power are more adequate in terms of self-consumption for the whole sport palace even accounting for the secondary services such as lighting). This choice determines another advantage for the solar field: actually, two inverters are installed (10 kW each) and with this intervention, one can be removed with significative reduction on the costs for future maintenance/substitution in case of

thunderstorm for instance. One disadvantage that can be considered acceptable is that the absence of water flow rate inside the solar panels will have adverse effects both on their efficiency and on the useful life of the materials which will be more likely to reach high temperatures. Moreover, the contracts for the electricity supplies shall be revised according to the recent changes introduced by the recovery decree. In other words, the most adequate strategy shall be outlined to maximise the exploitation of the PV production, without accounting on the possibility of exchange with the national grid.

As far as the thermal panel is concerned, models with specific anti-stagnation license have been advised. In this way, the times of stagnation shall be reduced with a benefit in terms of the concentration of glycol within the water flowing outdoor in the solar field. Moreover, the panels are insulated and this means a higher performance. Namely, the coefficient of thermal dispersion of the thermal panels is about the half of the hybrid ones now installed. This roughly means that even halving the capturing area of solar thermal field, the increased performances of the new panels should grant the same amount of solar thermal energy collected to allow the correct working of the HP.

Moreover, a preliminary analysis has been performed about different scenarios and various surface of solar capturing surface replaced. The analysis has been carried out with balances over the plant productivity referred to a monthly basis, with an assumption of distribution for the thermal loads according to the information acquired during these years by means of the data acquisition system. Considering that the main contribution of the SAHP innovative plant is associated to the part of the heating plant equipped with radiators and the efficiency strategies adopted over the past period, the thermal load has been estimated as about 150 MWh/year. As far as the domestic hot water production is concerned, its consumption shows very little variation over the year and it can be in first approximation assumed equal to about 30 MWh/year.

According to the data recorded, the HP has a mean seasonal COP which can be approximated at about 4.1 (accounting also of the summer production of the solar thermal field directly connected to the DHW subsystem). The results briefly presented later in this chapter have been obtained the following energy valorisation:

- 0.16 €/kWh for the electrical consumptions
- photovoltaic field production value: 0.12 €/kWh assuming that the production in winter can be almost considered self-consumed, especially with the HP on, while actually the summer overproduction has not been considered, to follow an approach on the safe side. As better outlined in the section about the improvements suggested for the DAS, the extension of the automatic control of the plant to the Air Treatment Unit (ATU) as well opens a great chance to better exploit the summer production as well by means of self-consumption.
- cost for the natural gas assumed equal to 0.095 €/kWh, both in terms of consumption of the integrative gas burners and in case of estimation of the savings.

The performance of the new solar fields under the different configurations has been computed basing on the irradiance simulated by means of the online tool available on the ENEA website [2]. This tool is quite powerful and allows the estimation of the daily monthly averaged solar radiation

on a tilted surface. As far as the input information is concerned, the code needs to know the location, the extension and the tilt of the modules surface. The computation has been performed over the twelve months of the year accounting for shadings due to nearby constructions or peculiar configurations of terrain (e.g. hills). Indeed, any potential object which causes shading, can intercept the direct radiation for certain angles as the Sun follows its apparent motion in the sky. This concept is represented inside the code by means of hourly intervals during which the site is shaded from direct radiation. In addition, these parameters depend on the different seasons of the year since the inclination and apparent path of the Sun change during the year. As a consequence, the elevation of the different obstacles has been identified. The site where the solar field is installed is almost free of obstructions especially towards South. Although its plant size is about 40 m x 5 m, the shadings have been computed assuming the solar field as punctual since no significative variation in the obstacles (hills and buildings) can be appreciated at different positions over the 40 m length. In fact, the solar field is in a valley lined on the North-West with the Physics and Mathematics Faculty while on the South-East side, a hill with vegetation is present.



Figure 4.5. Satellite vie of the site [3]

The tridimensional views and the image reported below provide a better overview [3]. In particular, Figure 4.7 shows how the tensostatic coverage indeed casts no significant shadow over the solar panels, since the hill itself interferes with the solar radiation especially early in the morning when the Sun is rising.

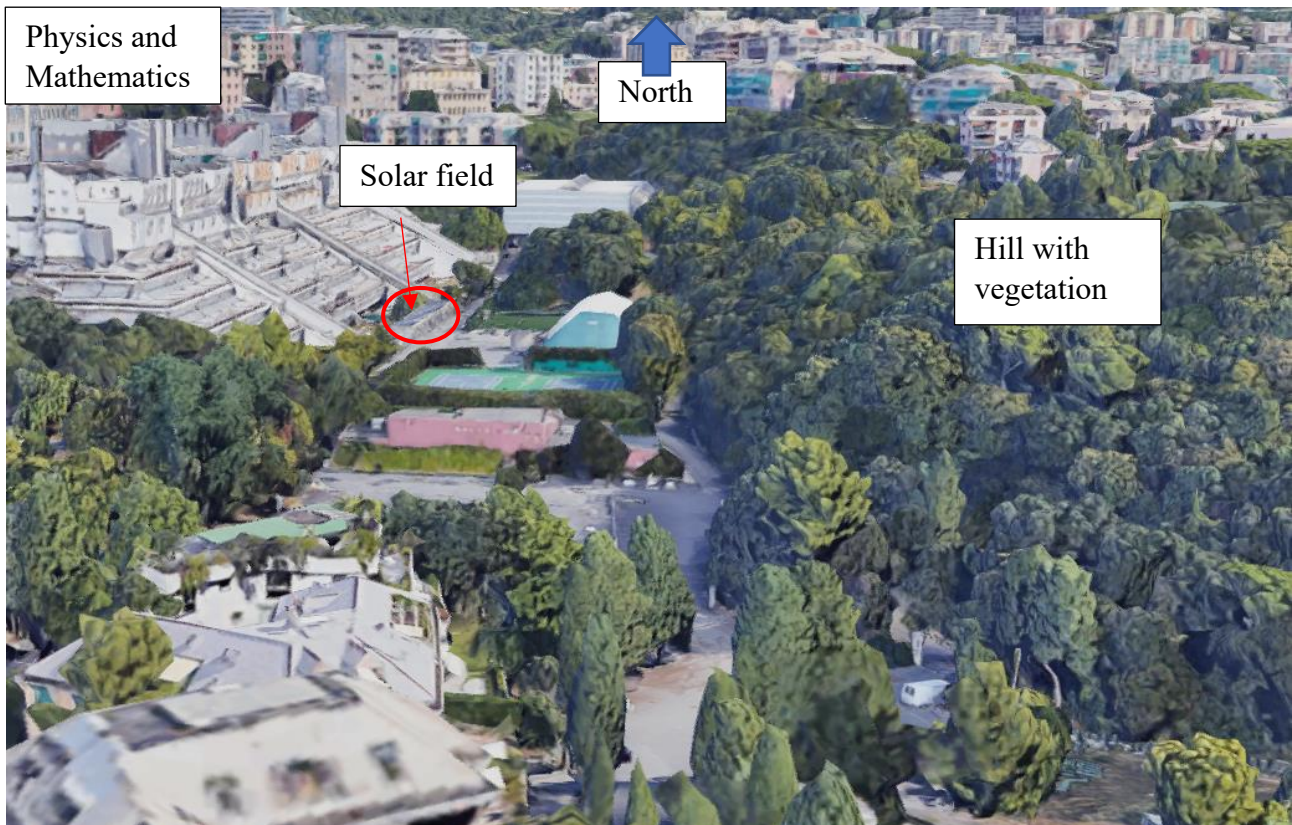


Figure 4.6. Tridimensional views of the site [4]



Figure 4.7. View of the solar field and of the hills towards East/South East

In particular, the slope of terrain has been deducted with the help of Google Earth Pro [5] along the different orientation with a spacing of 15° with respect to the horizontal plane, starting from the North and moving clockwise (see Annex A – part I for complete output of the altimetric elevation of the terrain around the solar field). In addition to this, a geometric relief has been performed on site to add the shading associated to the buildings, especially on the West/North-West side. Then, this information has been inserted in the online tool Sun-Earth-Tool [6] which allows to simulate for a specific site the hours of apparent sunrise/sunset, due to the obstacles. In the end, the solar irradiation on tilted surface of the solar panels has been simulated by means of the ENEA solar tool accounting for the shadings. The results obtained are in accordance with approach contained in [7] and are based both on the solar maps contained in [8] and on the solar maps created by ENEA. These maps have been estimated basing on the satellite images about the cloud coverage acquired by the European body EUMETSAT. Moreover, these maps have been validated over the averaged values referred to the measured values in the five-year period starting from 2011.

As far as the simulation of the HP is concerned, a first estimation of its thermal contribution/electrical consumption has been inferred basing on the information stored by DAS during the monitoring period (about 6-7 years). The following table (Table 4.3) shows the results concerning the replacement of 50% (about 70 m^2) of the damaged solar hybrid panels with only thermal ones.

	January	February	March	April	May	June	July	August	September	October	November	December	Total
Energy need covered with the HP [kWh]	9789	11654	10875	2727	2727	2727	2727	2727	2727	1754	8197	9412	68044
Natural gas integration [kWh]	28250	23466	16366	5837	0	0	0	0	0	973	15250	24541	114683
Cost of natural gas integration [€]	2684	2229	1555	554	0	0	0	0	0	92	1449	2331	10895
HP electrical consumption [kWh]	2504	2863	3167	1170	364	365	0	364	365	388	1993	2326	15870
Monthly PV production [kWh]	443	587	958	1218	1478	1532	1788	1482	1150	820	484	410	12348
Net balance between HP consumption and PV production [kWh]	-2061	-2276	-2210	47	1113	1167	1788	1117	785	432	-1509	-1916	6449
Estimation of the electrical consumption not produced by the PV field [€]	330	364	354	0	0	0	0	0	0	0	241	307	1596
Comparison with the case of only natural gas [€]	3613.7	3336.4	2588.0	814.0	259.1	259.1	259.1	0.0	259.1	259.1	2227.5	3225.5	17101

Table 4.3. Cost-benefit analysis for the replacement of 70 m² of hybrid damaged panels with thermal ones

With reference to Table 4.3, the following quantities over the different months have been shown:

- *Energy need covered with the HP*: this quantity has been inferred from the measured values of the HP performance over different years. Moreover, considering the correspondent electrical consumption as well, the average COP of the simulation reaches values at around 3.8-4, which represents a good increase with respect to the statics carried out. This increase is partially due to the accounting of the summer period in which only the solar thermal field and the DHW integration gas burners are active to grant the DHW need.
- *Natural gas integration*: given the HP thermal contribution explained above, the remaining needs of the Palacus sport centre are provided by means of the integration gas burners. This line is meant to estimate the quantity of natural gas [kWh] required.
- *Cost of natural gas integration*: it has been estimated as the quantity of the natural gas integration, referred to a cost of about 0.095 €/kWh.
- *HP electrical consumption*: this parameter has been evaluated inferring the experimental data and basing on the technical information available for the HP. Indeed, the higher consumptions occur during the months of December/January. In addition, the HP during summer is off, so the non-null consumption reported is referred to the other auxiliaries which are active during summer to grant the operativity of the plant (mainly solar thermal field + integration gas burners) to provide the plant with DHW.
- *Monthly PV production*: it has been computed accounting for the shades and the different orientation of the Sun during the reference year as widely described above. Clearly the PV production has become resized, due to the smaller PV capturing surface left. On the other hand, the overproduction in electricity over summer remains an open issue, since the cost effectiveness of the plant could depend on the quantity of self-consumed yearly production (better summer).
- *Net balance between HP consumption and PV production*: actually, a difference between the HP need and the PV produced electricity is performed. A negative value means that electricity from the national grid is used to grant the correct working of the HP while a positive net balance means available electricity, not completely exploited by the HP.
- *Estimation of the electrical consumption not produced by the PV field*: valorisation of the quantity of electricity not produced by means of the PV field and taken from the national grid.
- *Comparison with the case of only natural gas*: this valorisation refers to the case in which the whole needs of the Palacus (both space heating and domestic hot water) were provided by gas burners. This term is meant to provide a comparison in order to assess the performance of the SAHP installation with reference to traditional fossil fuel burners.

In conclusion, the SAHP under this new configuration can grant a saving over the yearly balance of about 5300 €. This value can be obtained comparing the case of need covered with only natural gas plants (17101 €) against the consumption of the SAHP (both electrical and of natural gas for the integration gas burners, 12490 €). Moreover, the summer PV overproduction can be accounted. In the present configuration, 10 kW_{el} are installed and assuming that about 75% of overproduction shall be self-consumed, about 700 € can be saved. Clearly in the limit case of solar PV over production completely lost, the minimum saving would be of about 4600 €/year. With a clever

management of the electric use of the sport facility even during summer, the saving could arrive up to 5600 €/year. In order to achieve this target, the plant management and control system must be extended and integrated in order to organically manage each energy consuming system (e.g. the already controlled heat pump, gas burners as well as the AHU or the lighting of the sport palace and of the outdoor courts).

Many configurations with different extension of replaced thermal solar panels have been analysed and here omitted for the sake of brevity. Clearly the same assumptions and approach have been adopted in order to make the results comparable and provide enough simulations to the decision-making committee. The solution here reported represents the final choice and it is the most reasonable one according to the thermal peak load required by the HP (about 50-54 kW_T according to the technical specifications).

In the same context, the hydraulic separation between the solar field and the cold side storage/interface with the HP is under design. The basic concept is to insert a heat exchanger before of the inlet for the storage T10 (storage which is in turn interfaced with the cold side of the heat pump). The figures below (Figure 4.8 and Figure 4.9) provide the comparison of the actual configuration, against the one under design.

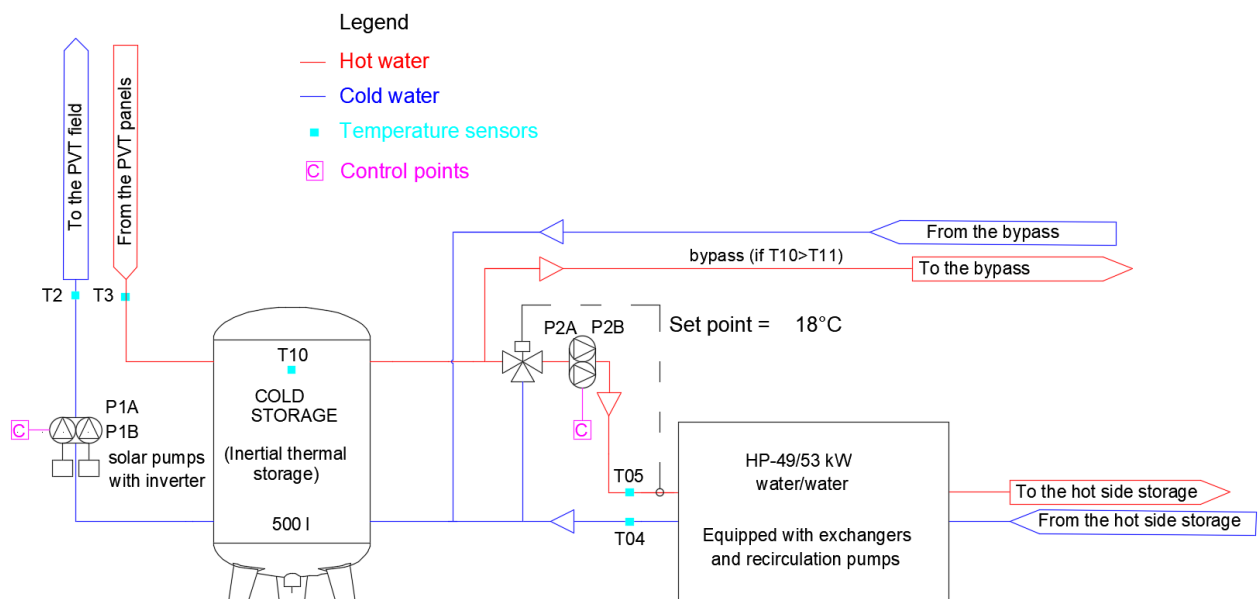


Figure 4.8. Actual configuration of the storage on the cold side of the HP and of the inlet/outlet with the solar field

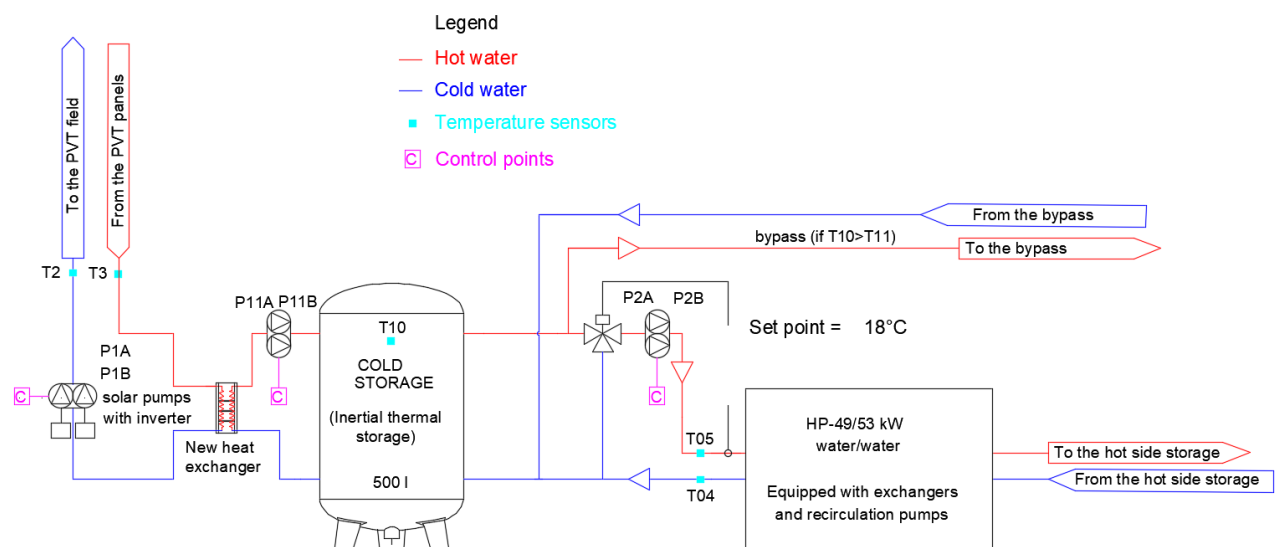


Figure 4.9. Basic design configuration of the interface exchanger between the storage on the cold side of the HP and the inlet/outlet with the solar field

The design configuration has been referred to “basic” since this solution is the one that best meets the actual needs of the decision-making committee. In particular, also in terms of economic feasibility, the revamping has to involve the minimum but necessary strategies to introduce significant improvements to the plant performance. The adoption of a heater is compulsory in order to reduce the issues described above although this means a little reduction in the plant efficiency due to the efficiency of the heater itself. In addition, it is important to remember that the size of the heat exchanger shall be exactly estimated during the design stage. Nevertheless, considering a plate heat exchanger, about 50 kW shall be required. This in turn implies relevant dimensions for the exchanger and therefore its positioning will have to be well conceived. In addition, a new pumping system will be introduced (twin pumps P11) to grant the internal circulation between the water storage on the cold side and the heat exchanger with the solar field. A potential upgrade of this condition can be represented by the integration of a heat exchanger interfaced with air, namely creating a dual source heat pump. This configuration shall be tested once completed and operative the transient model of the plant as a whole. The main advantage of this concept is to make the HP independent from the solar field. In other words, in case of interruption of the solar subsystem due to ruptures, maintenance or other causes, the HP could still operate, even if this might imply lower performances. Indeed, following the basic principles of the SAHPs presented in the first chapter, the temperature of the technical water inside the solar subsystem can be considered at a temperature which is equal or higher than the temperature of air. As a consequence, no significant improvements in the SAHP performance are expected, except for an increased operativity time which becomes independent from any eventual interruption due to the solar field. On the other side, this configuration implies the design of the control criteria to manage the switch between the two different sources according to the boundary conditions. In addition, a significant increase in the plant complexity is expected and therefore this solution requires more detailed simulation both to assess its convenience and to identify the simplest way to integrate it in the actual configuration. The integration shall take place in an existing plant and therefore any new

addition has to be minimized interferences (better if avoided); this actually represents an implicit and added degree of difficulty with reference to the case of planning from scratch.

Contextually with this intervention, the fossil gas burner for SH integration shall be replaced with a new condensing one. The decision-making committee is actually evaluating the chance of replacement of integration DHW gas burner as well, to reach a further increase in the performances of the plant. Moreover, some worn parts and components shall be replaced, e.g. a couple of pumps while the others shall be tested.

4.2. Integration of the DAS

Meanwhile, the revamping of the plant takes place, the DAS needs to be updated as well. The best strategy is to work on different levels:

- *Integration of the new sensors:* some replaced components, such as the integration gas burners, might have a larger number of sensors (e.g. thermostats, power consumption) with respect to the old ones. This added information has to be correctly inserted inside the monitoring and control system, firstly to grant always a data acquisition as wide as possible. This is the basic step over which build and perform more refined efficiency analyses. Indeed, the old gas burners date back to the period in which no SAHP was present (so more than 10-15 years ago) and therefore their level of integration with the automatic data acquisition systems was very low. Under this context the new twin pumps P11 need a specific regulation to establish the conditions in which they are operative. Following a basic and simple principle, the first regulation criterion consists in the switch on of P11 at once with the solar pumps P1. In other words, P11 shall be active when the solar field can provide significative heating to the water storage. Indeed, the aim is to preserve and increase the thermal energy stored inside the tank because this storage can act as a thermal backup either for the HP cold side or for the DHW subsystem (in case the direct bypass were active). Moreover, the three-way mixing valve inserted on the water inlet with the exchanger on the evaporator side has bypassed the problem of the HP blocks due to “high” temperatures on the evaporator side (over about 25 °C, see also the chapter on acceptance for further details). In fact, the mixing avoids critical temperatures and therefore no thermal energy is wasted or has to be dissipated to prevent sudden HP blocks. In conclusion the dimensioning of P11 (basically with an ON/OFF working) shall be performed to grant the correct working of the heat exchanger (estimated size of about 50 kW).
- *Extension of the DAS to the subsystems still under “stand-alone” management:* the Palacus sport centre still presents energy consuming plants which still are managed manually and independently from the SAHP. Actually, this fact has a double negative influence:
 - An automatic, centralised management allows to maximise the performance of the plant and to have an almost instantaneous and global feed-back on the status of the facility in each specific subsystem.
 - With reference to the concepts expressed above about the feed-in-premium/net-metering criteria, the actual target to best exploit the solar source (especially the PV side) is by means of self-consumption. This goal can be achieved with greater ease in

case of an organic control over each part of the facility which might represent a possible receiver of the electricity self-produced.

Up to now, two main subsystems are still lacking such automatization in the control system:

- *Lighting*: both referred to the sport hall and to the external courts. As far as the latter is concerned, the expense in electricity to light the outdoor courts can represent significative percentages of the monthly energy bill, especially when massive renting is practised. Within this context the indoor lighting can represent the first term to increase the self-consumption of electricity with very little expense. In fact, the indoor lighting is not necessarily performed during periods of the day in which no daylight is available. On the other hand, for the outdoor cases, the illumination is lit only when the sunlight is no longer available. This means that at the present state, no significative self-consumption for outdoor lighting can be expected. Eventually, one of the simplest solutions might conceived the adoption of storages for electricity, not necessarily batteries, to grant the availability of a given amount of PV production during the day for the next night.
- *Air Treatment over the sport palace*: two main systems can be identified, namely the air extractors inside the lockers and an ATU mainly associated to the sports hall and the bleachers. Up to now, the actual, old ATU works only in heating mode and the thermal load required to treat the external air was provided by the SAHP united with the integration gas burners. The actual management of these plants is manual and “stand-alone” with respect to the integrated, remotely controlled SAHP. The main issues faced are concerned both with thermal and hygrometric comfort inside the lockers/sports hall. The control of relative humidity plays a central role in the sports hall where consistent condensation often occurs, making the playing field slippery and unsafe for the players. In addition, the sports hall is quite wide, with about 6 m of height and 30 x 25 m in plan and therefore the volumes of air to be treated become relevant. As far as the air extractors for the lockers are concerned, their working follows the same principle of an overflow hole: in case that limit conditions of temperatures and humidity were reached inside the lockers, the extractors would activate to grant a minimum ventilation. Their working is not directly associated to the heating system (e.g. by means of radiators or fan-coils) but it strongly affects the required thermal load to keep the set point temperature inside the lockers after that ventilation has taken place.

The replacement of the ATU and the automatization of the air extractors has been decided in the same context of the revamping of the SAHP. Thanks to this chance, the DAS will be extended over this subsystem to allow a complete control over the emission system. In addition, four temperature and relative humidity sensors will be installed in the sports hall and they will be connected to the DAS to have a complete, monitored situation of the sports hall in terms of both temperature and relative humidity. Their position has been distributed both in plant and in elevation, to provide a distribution of the temperature and humidity profiles that can be hardly considered as uniform in such wide volumes (about 4000 m³). Moreover, the new ATU will be provided with pressure sensors, to check the conditions of the air filters and identify the ones which need

maintenance. All this added information needs to be integrated into the DAS as anticipated in the previous point. Clearly, the complete control over the ATU opens another branch of regulation criteria which are currently under design and they are meant to maximise the performance of the facility, according to the different boundary conditions. The first three main topics over which the regulation criteria will be defined are:

- Space heating: to grant a uniform temperature equal to the set point value. According to the first measurements of temperature inside the sports hall, this task may become tough since the concentration of people might not be uniform over space and time. For instance, two different loads might be required in case the sports hall were used for athletes' practice or in case a match were played. In fact, the audience would crowd the bleachers creating local overheated regions, while the area occupied by the play field would remain colder. In addition, in case of workouts with no audience, the temperature should be mainly maintained near the athletes while the bleachers might be put on a secondary plane of importance.
- Humidity control: as anticipated above, the condensation is a matter of paramount importance, to grant the safety of the athletes during matches, workouts, etc. This issue is clearly influenced by the quality of the water vapour inside the air inside the sports hall and the one immitted by the ATU.
- Free cooling: in case the external conditions of air in terms of both temperature and relative humidity were sufficient to meet the set point values, the AHU would activate with only the fans to provide ventilation and "free" cooling of the spaces. This issue can result particularly useful especially during the mild seasons (e.g. spring or autumn) when a primitive form of cooling can be outlined without effectively installing specific components.

Actually, all these strategies cannot be directly translated into criteria after a first glance over the problem. Firstly, the DAS needs to be implemented and a significative data set needs to be acquired, to provide the basis for the simulations and the definition of profitable and consolidated approaches.

- *Scheduled maintenance function*: actually, some breakages happened in the last semester to the plant (e.g. circulating pumps) might have been foreseen and repaired in a scheduled way with no need to significative negative influence on the plant performance. Without this function, the breakages occurred and the replacement intervention took place with a very relevant delay (partially caused by the fact that the plant was operative). In addition, some critical aspects such as the leakages in the plant might have been reduced or at least mitigated by means of a correct ordinary maintenance. In this field, the existing DAS might provide significant benefits in the correct schedule of extraordinary and ordinary maintenance. For instance, in the case of the circulating pumps, the concept of replacement in case of breaking might be substituted with an advance replacement after a given number of working hours. The check of this simple parameter could rise a flag in order to programme the substitution before

rupture. On the other hand, exceptional events, such as the stagnation of the solar panels, might require additional checks, for instance about the glycol concentration in the technical water. Under this perspective, the DAS could set to rise another flag, in case the temperature of the panels became excessively high and near the stagnation limit to require an extra check on the panels. More widely speaking, a specific panel about maintenance should be enhanced inside the PLC of the DAS, to collect the different warning signals which should allow to perform a more tailored program of the maintenance on the plant.

4.3. Conclusions

The pilot plant under exam has been subjected to leakages and failures which are being repaired by means of a global revamping of the plant. In particular, the intervention refers to the solar field and its interface with the heat pump. The experience and the information collected of the SAHP working during different years has allowed to carry out a former cost-benefit evaluation. The aim of this study is to provide the decision-making committee a sufficiently exhaustive analysis to decide which approach can be best suitable to maximise the performance of the plant. In particular, the solution involving the replacement of 50% of the total capturing area of hybrid panels with only thermal ones has been identified. Indeed, it represents the most affordable and cost-effective solution that can be integrated in the existing plant with minimum interference. The irradiation employed to perform the analysis shown in the present chapter has been carefully evaluated, starting from the obstacles responsible for shading, up to the simulation of irradiance, with the help of free, online tools, which revealed to be effective and led to results comparable to the measured quantities. The choice to employ simulated data instead of the recorded one for the solar irradiation is due to the need to provide simulated information referred to a database, statistically wide enough and therefore reliable. The recorded data has been used to perform a preliminary check in terms of orders of magnitude to validate the results obtained. As far as the interface between the HP cold storage and the solar field, a hydraulic separation represented by a heat exchanger is compulsory. This solution needs further refinement in the design stage, both for the dimensions of the exchanger (expected size of about 50 kW, the thermal peak need of the heat pump) and for its possible “upgrades”. For instance, a further configuration might conceive an exchanger that can be interfaced either with the solar field or with air. This idea requires deeper numerical simulations and it was led by the possibility of making the heat pump independent from the solar field. For instance, this possible solution would have allowed the working of the HP even with the solar thermal field broken although the performances might be negatively affected.

As far as the photovoltaic side of the solar field is concerned, the actual installed peak electrical power is by far oversized with respect to the needs of the plant. This conclusion is caused by the recent changes within the topic of net-metering/feed-in-premium strategies. Namely, the national grid can no more be considered as an economically feasible alternative to store the electricity produced for instance by means of irradiation of the Sun. This implies in turn that batteries have to be installed or self-consumption needs to be best exploited. Both cases result very challenging since the availability of solar energy changes over the year and the year itself should be the best time period to which refer the balance between production and consumption of PV produced electricity. However, no storage battery can grant such capacity as the national grid virtually did basing roughly

speaking on a give and take principle. Further insight on this topic have been widely discussed both in this chapter and in the first one.

The self-consumption can be improved and achieved basing on a working DAS, which needs to be constantly updated. In particular, the revamping over the pilot plant has provided the ideal chance to integrate the existing DAS both with new sensors and the new components used to replace the old ones (such as the integration gas burner). Moreover, the DAS will be extended to other subsystems of the sport facility which are still manually managed such as the ATU. In this way, the integrated and remotely accessible management of the plant will make a big step forward. The objective is to control and check with a unique system all the energy consuming elements inside the facility. This centralisation of the controls is the key to introduce global and effective efficiency strategies which can account for all the parameters inside the plant, starting to external ambient conditions, up to the internal ones (e.g. temperature and relative humidity in the indoor sports hall). Within this control chain, the system can control, manage and choose the best and most efficient interaction of subsystems (e.g. solar field, heat pump, air handling unit, integration gas burners) to reach the target. Last, but not least, all this added information can be almost immediately associated to specific flags which allow the definition of programmed maintenances (e.g. to replace the circulating pumps after a fixed number of working hours) or extra tests due to non-conventional ambient conditions (e.g. control of the glycol concentration within the technical water, after the panels are likely to have reached the condition of stagnation). The specific regulation criteria based on these principles shall be formulated only once the DAS will have acquired sufficiently wide datasets, to perform simulation and identify the best set point values to grant the maximum performance with the minimum expense of non-renewable sources.

REFERENCES

- [1] M. De Rosa , G. Romano , C. Rossi , F. Scarpa e L. A. Tagliafico, «Un modello teorico-sperimentale per pannelli ibridi fotovoltaici e termici,» *Termotecnica*, p. 51 – 55, 2016.
- [2] [Online]. Available: <http://www.solaritaly.enea.it/CalcComune/Calcola.php> access date . [Consultato il giorno 18 March 2020].
- [3] [Online]. Available: <https://www.google.it/maps/place/Palacus+-+Palazzetto+dello+Sport/@44.4020595,8.9717556,413m/data=!3m1!1e3!4m5!3m4!1s0x12d3430b4225019f:0xfed9c00f0fdb954a!8m2!3d44.4030913!4d8.9732216> . [Consultato il giorno 29 October 2020].
- [4] [Online]. Available: <https://www.google.it/maps/@44.3996339,8.969655,43a,35y,30.37h,79.19t/data=!3m1!1e3> . [Consultato il giorno 3 November 2020].
- [5] [Online]. Available: <https://www.google.it/intl/it/earth/>.

- [6] [Online]. Available: https://www.sunearthtools.com/dp/tools/pos_sun.php#annual .
[Consultato il giorno 18 March 2020].
- [7] *Solar energy. Calculation of energy gains for building applications. Evaluation of radiant received energy. - UNI 8477-1:1983.*
- [8] *UNI 10349-1:2016- Heating and cooling of buildings - Climatic data - Part 1: Monthly means for evaluation of energy need for space heating and cooling and methods for splitting global solar irradiance into the direct and diffuse parts.*

FINAL CONCLUSIONS

The application of the SAHPs still presents an unexpressed potential. The actual state of art of this technology is concerned with theoretical formulations joined with a small dimension prototypes in order to simulate effectively the plant on a smaller scale and test its efficiency. Up to now, both the design and management of a solar assisted heat pump relies on the results of these prototypes. This strong dependence on the experimental side is due to the climatic conditions of the site as well. In fact, the optimal set point parameters as well in the efficiency can vary according to the border conditions of the site analysis, in particular due to the extreme variability of solar radiation along the day.

Generally speaking, this technology presents a wide range of advantages: indeed, no gas consumption is directly required, with benefits about safety and the eliminated risks associated to the presence of natural gas distribution pipes. In addition, the interaction of a heat pump with the solar field (both photovoltaic and thermal ones) allows to exploit the maximum benefits coming from the HP and the solar field. In addition, solar assisted heat pumps allow a further degree of freedom, since for instance their use might concern either the interaction of different subsystems (e.g. solar and heat pump systems) or only specific ones (e.g. only solar thermal subsystem for direct DHW production during summer). The integration of a solar thermal field with the cold side of a heat pump extends the applicability of the solar technology to more places since the lower required temperatures (e.g. about 25 °C on the heat exchanger with the evaporator instead of 45-50 °C for domestic hot water applications or low temperature space heating) can be granted more easily by the solar field. On the other hand, each time a renewable source is integrated within a plant, its complexity increases. In fact, the subsystems (heat pump, solar field, integration gas burners) can interact one with the other according to different criteria, to always obtain the maximum exploitation of the renewable side of the plant. Namely, the complexity implies an advanced, automatic control system to have a full and real time control over the plant. This goal can be achieved only with an extensive data acquisition grid, connected to the sensors (mainly concerned with temperature and water flow rates) installed in the significative control sections along the plant. Actually, a prototype might require about 10-15 sensors, also according to its outline and structure. Then, increasing the size of the installation, the number of sensors to have a complete overview of the plant operativity can reach up to 50-60 sensors. The number of sensors can be a little decreased, but it cannot be neglected to perform a correct plant management according to the external and strongly time-dependant environment conditions and the thermal loads required by the sport facility. This aspect brings two negative consequences: firstly, the number of sensors does influence the cost of the installation and therefore its payback time. Their neglection in the design/realisation of a solar assisted heat pump would lead only to a plant with strong difficulties in its management. Secondly, the plant has to be as self-controlled as possible since otherwise the users might not have the knowledge to master all the information collected and choose the best operating mode/set point parameters according to the measurements of the sensors. These issues actually inhibit the effective and capillary diffusion of such plants and their development on the market, in spite of their potential performance. The next step, which can overcome these issues, is concerned with the formulation of simplified criteria to design new plants and grant the performance in the existing ones without the need of either prototypes or extended sensor grids. Following this principle, the aim of the pilot plant analysed in the present work is to acquire an extended data-set, over quite a long time period to which refer the improvements to the SAHP technology (e.g. in its configuration,

regulation criteria, set point parameters). The key advantage with respect to a prototype is concerned with the full size of the plant and its connection to a structure which has real and effective needs expressed in terms of space heating and domestic hot water.

The present work is focused on the pilot plant of a solar assisted heat pump within the context of the PALACUS sport palace. Its realisation has followed the different steps outlined above of design, prototypal simulation and installation of a full-size pilot plant.

The approach followed during the three years of PhD has developed on three different sides which converge on the common goal of an efficient working plant:

- Acceptance: in other words, the level of people's agreement towards a project, a plant. This concept is still lacking in the classic design approach in which the end users' satisfaction towards a construction, plant, facility is implicitly assumed once the performances are granted. In truth, the historized data has shown that the SAHP pilot plant was often inactive due to its complexity in the management. The low level of acceptance affects indeed the plant performance since a plant can be efficient only if it is operative. In this context, the acceptance evaluation plays a higher role since it evaluates whether a plant shall be adopted by the users or not. The problem faced in the present work is about the absence of a commonly shared, objective approach to evaluate the level of acceptance of a plant from the end users. Indeed, the measurement/evaluation stage is the first, important step to understand acceptance and identify the correct strategy to improve it. An innovative approach has been proposed to estimate the subjective quantity of acceptance by means of the parameters (temperatures, water flow rates, operating hours of pumps, heat pumps) measured by the control system. Namely the key concept behind the approach is to measure people's feelings about the facility by means of how much they use it.
- Numerical simulation of the plant: the presence of a full-size pilot plant with such a complete and remotely controlled data acquisition system gives an edge to any numerical simulation performed. Indeed, the experimental information collected allows to perform the validation of each single element (e.g. pipes, valves, pumps, water storage tanks, heat pump, solar panels) under different working conditions and weather conditions. The transient nature of the SAHPs actually cannot allow steady state considerations. For instance, the behaviour of the numerical model of the solar panels has to be performed under different sky conditions and during different period of the year. This simple instance just shows how complex and articulated the validation stage becomes for plants which are almost constantly under transient regime. In addition, the almost continuous data acquisition provides a large amount of information which needs to be correctly processed to be used as a reference in the numerical model calibration. The domestic hot water subsystem has been modelled with specific insights on the behaviour of the tank models, involving also the issue of stratification and studying the functioning of the numerical code adopted (TRNSYS environment).
- Plant revamping: the decision-making committee of the sport palace has financed a revamping of the plant, to repair the ruptures which occurred during its period of operativity (about ten years). The main problem is about the solar field in which the roll bonded panels have shown irreparable ruptures. Then some minor problems with the pumps (some of them need to be replaced) and with the plant configuration (no hydraulic separation is present between the solar thermal field and heat pump) are faced. Within this context, the experience acquired during the

three years of monitoring and plant management has played a central role to suggest and integrate the actual plant configuration to improve the SAHP and make it more efficient solving the problems above. Namely, with this opportunity the know-how has been translated into real applications as well with a significative upgrade and improvement of the plant. Within this context, the control system has been extended to other energy consuming plants (for example the air treatment unit)), moving a step forward a facility controlled with a unique, integrated and remotely controlled system.

Such diversified approach has brought the chance to follow the management and the research on this technology at different levels: from the theoretical analysis and numerical simulations validated on the experimental data collected, up to the identification and implementation of the improvements in the plant configuration. This work has been conceived as a research journal and report derived from a monitoring three years long with insights on specific problems faced during this period. The present research evolves around the pilot plant and another interesting consequence is linked to the multiple and different topics which have been enquired and the related specific obtained skills. For instance, the usage and management of the monitoring system united with the assistance to the technicians performing maintenance on the PLC has provided a deep insight on how the data acquisition system is materially made. The enquiry on the issue of acceptance has brought the research in the field of social sciences while the numerical simulation and validation of the plant has provided examples in which specific subjects (e.g. thermal stratification inside tanks, inverse heat transfer problems). In addition, the replacement of the damaged panels in the solar field has required a simplified and quick simulation, yet reliable, of the performance of the SAHP with different configurations of different panels. This task was accomplished basing on the recorded data and with the acquired experience in the plant management and a preliminary estimation of the expenses and of the payback times was carried out.

As far as the future work is concerned, the research in the different field has to be brought forward. In particular, the revamping of the plant has to be followed into its different stages, from the design to the installation. Once the intervention is completed, the data acquisition has to proceed to collect information about the new operating configuration. Within this context, new regulations could be introduced to best fit the new elements installed (e.g. the new solar thermal field or the new configuration of the interface heat exchanger between the solar field and the heat pump). Meanwhile the data acquisition system should be implemented with the estimation of the parameters for acceptance illustrated in the present work, to perform an evaluation of the global level of acceptance, detailed then for each subsystem. In this way, the system will be able to control a monitor the status parameters of the users' acceptance of the plant and it will be able to directly act on the plant and to rise flags when critical values are reached. In addition, some ruptures of the plant (especially the solar panels) might have been prevented or at least foreseen with the proper controls implemented in the data acquisition and monitoring system (e.g. glycol concentration, number of times of panel stagnation). Therefore, the PLC and the monitoring system have to be revised and implemented to account for ordinary/extraordinary maintenance as well, basing its evaluation on the recorded parameters (e.g. working hours, efficiencies). In conclusion, on the numerical simulation side, the complete model of the plant has to be carried out, coupled with specific models of each subsystem (e.g. solar field, heat pump, domestic hot water). After the validation on the recorded data, the so built model will allow the definition of simplified criteria to

manage and choose the set point parameters of the plant even without the presence of a complete and expensive grid of sensors.

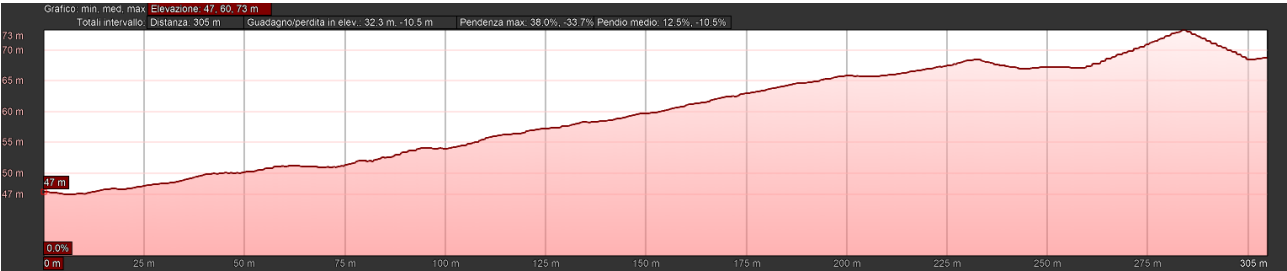
Publications

- 1) L.A. Tagliafico, A. Cavalletti, C. Marafioti, A. Marchitto *"End Users' Acceptance of New Technologies in Building Heating: An Experience on Solar Assisted Heat Pumps"*, TECNICA ITALIANA-Italian Journal of Engineering Science, vol. 63, pp. 198-204, doi: 10.18280/ti-ijes.632-412. (2019)
- 2) L. A. Tagliafico, A. Arteconi, A. Cavalletti, C. Marafioti, A. Marchitto, *"Performance Of A Solar Assisted Heat Pump For Building Heating: Control Problems And Improvements"*, Journal of Physics: Conference Series, vol. 1599, 012036 doi:10.1088/1742-6596/1599/1/012036. (2020)
- 3) L.A. Tagliafico, V. Bianco, A. Cavalletti, C. Marafioti, A. Marchitto, F. Scarpa, *"Monitoring and control of a pilot plant made of solar assisted heat pump with hybrid panels"*, AIP Conference Proceedings, Vol. 2191, 020144, doi: 10.1063/1.5138877. (2019)
- 4) L. A. Tagliafico, A. Cavalletti, C. Marafioti, A. Marchitto, *"End users' acceptance of new technology renewable plants: the pilot case of a solar assisted heat pump"* (under review)
- 5) L. A. Tagliafico, A. Cavalletti, C. Marafioti, A. Marchitto, *"Solar assisted heat pump pilot plant management and troubleshooting by means of numerical modelling: a case study"* UIT Conference Proceedings (2020)
- 6) L. A. Tagliafico, P. Cavalletti, A. Cavalletti, C. Marafioti, F. Poma, E. Sterpi, *"Numerical and experimental analysis of thermal penetration depth in bare reinforced concrete structures during fire accidents"*, E3S Web of Conferences- 75° National ATI Congress, vol. 197, No. 10009, doi:10.1051/e3sconf/202019710009 (2020)

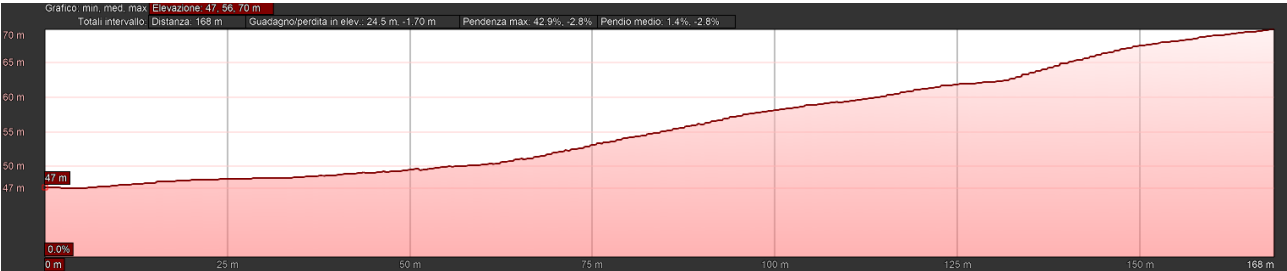
Annex A – part I

Altimetric elevation of the terrain. Each angle above the correspondent photo expresses the orientation moving clockwise with respect to the North with 15° spacing. The angles from about 270° up to 360° are occupied by buildings and the altimetric elevation of the terrain has been incremented to account for the additional shading.

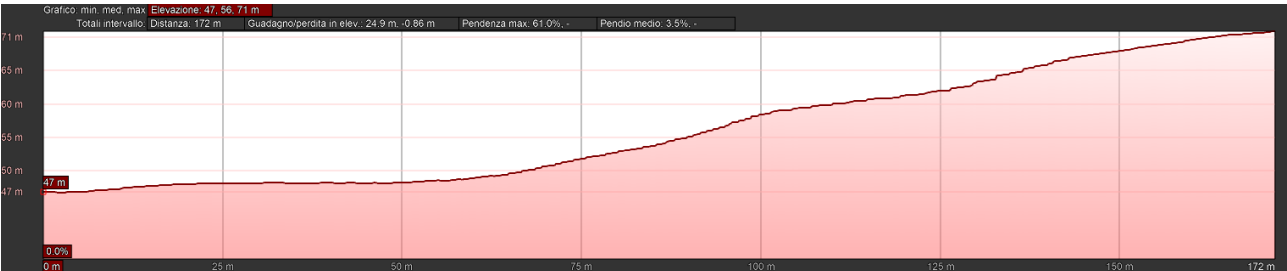
0°



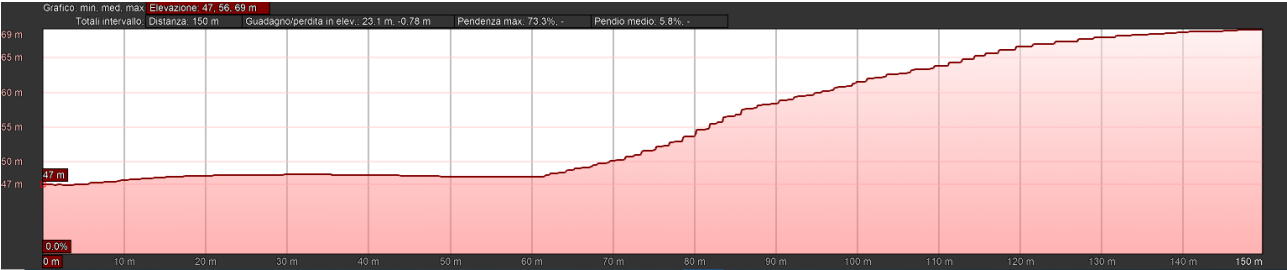
15°



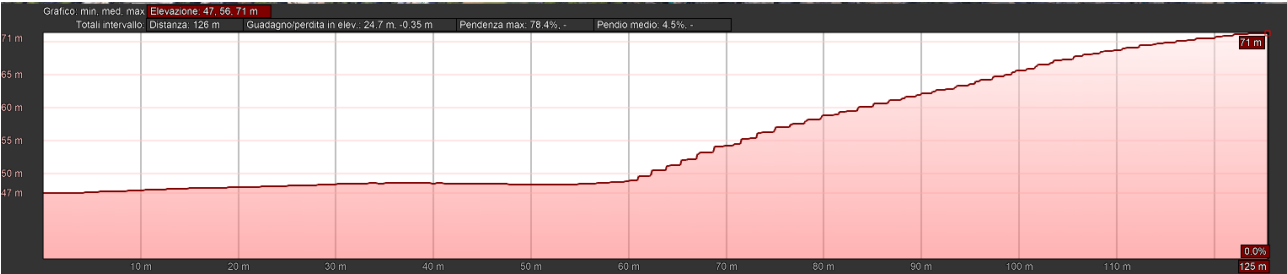
30°



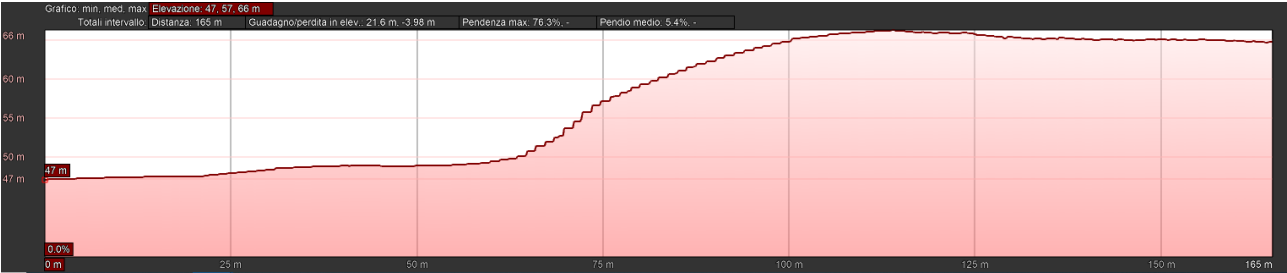
45°



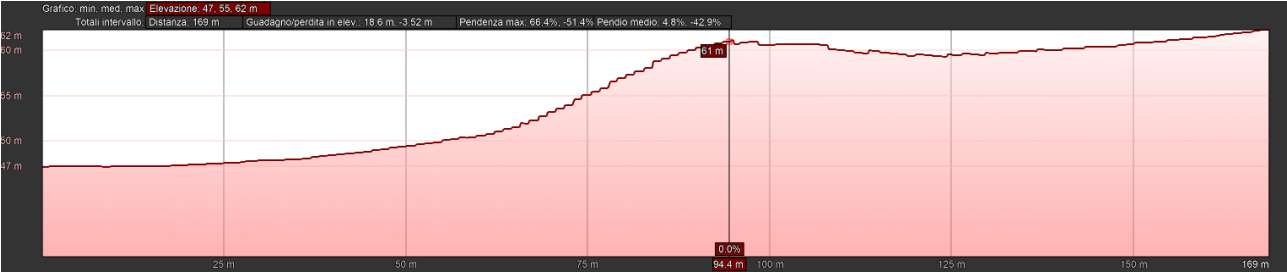
60°



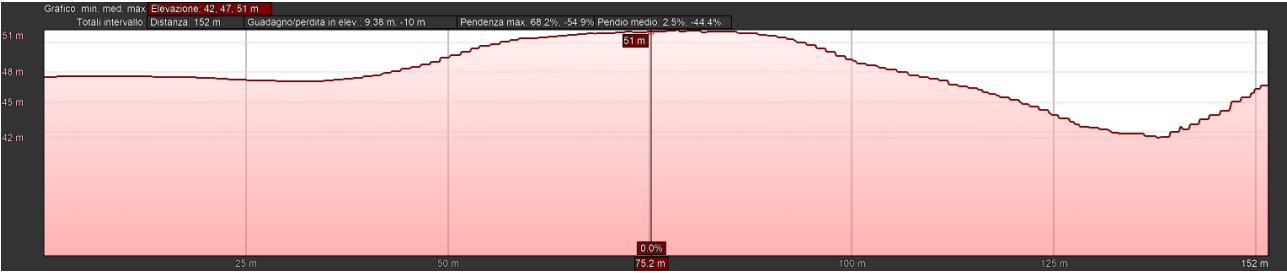
75°



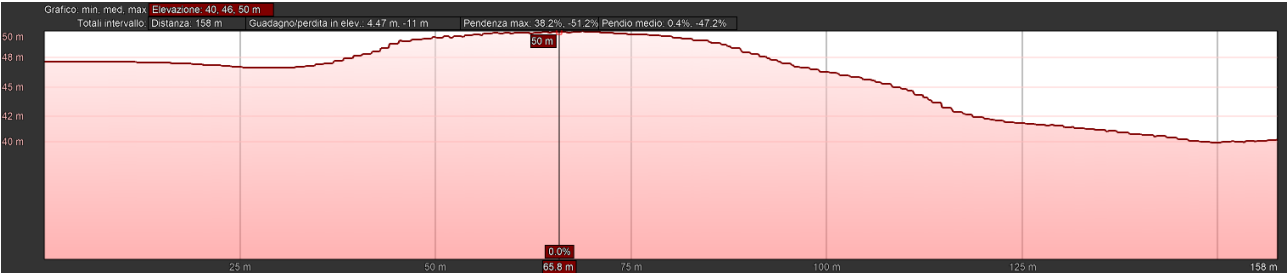
90°



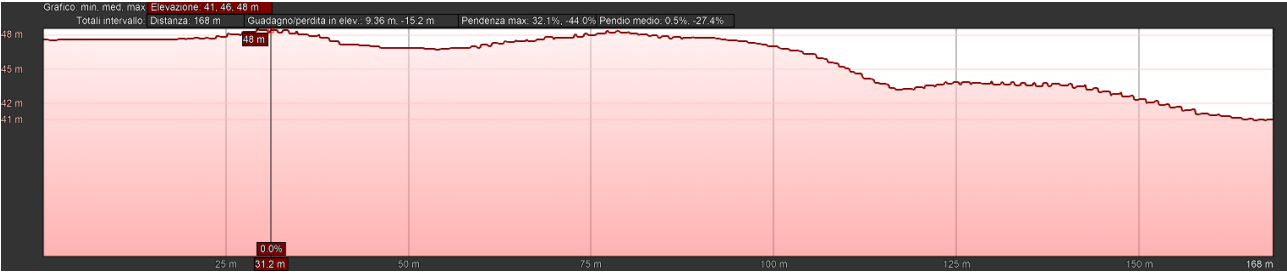
105°



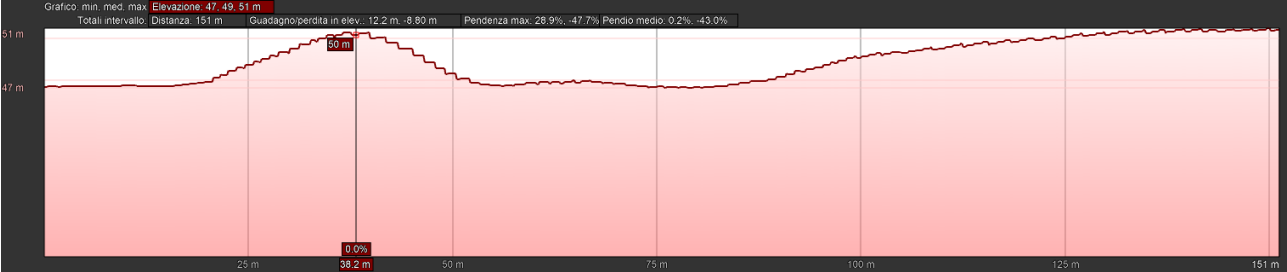
120°



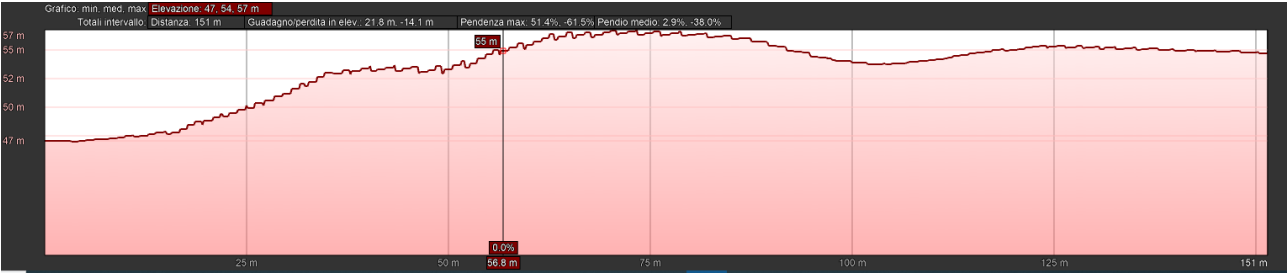
135°



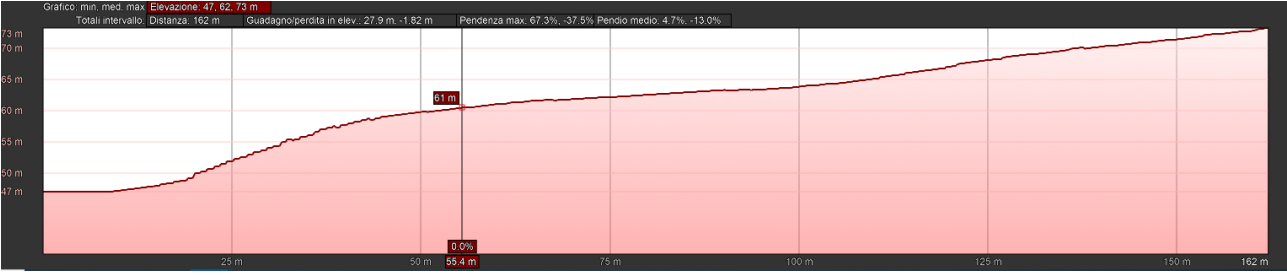
150°



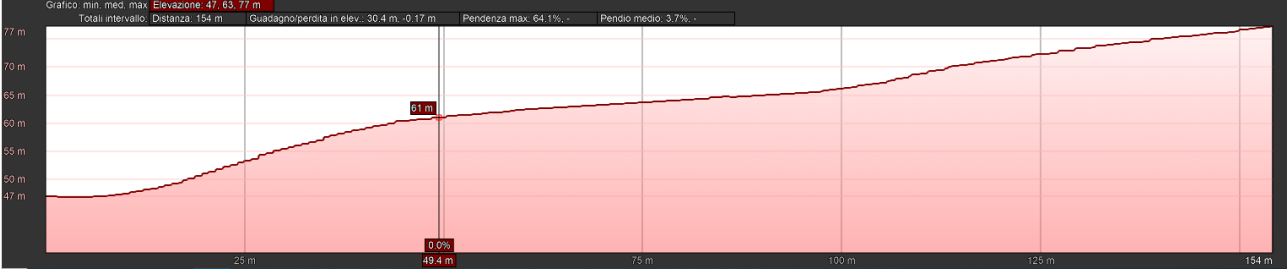
165°



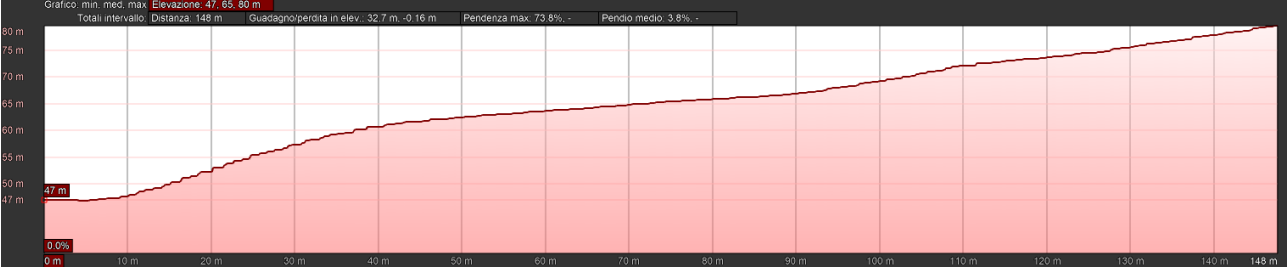
180°



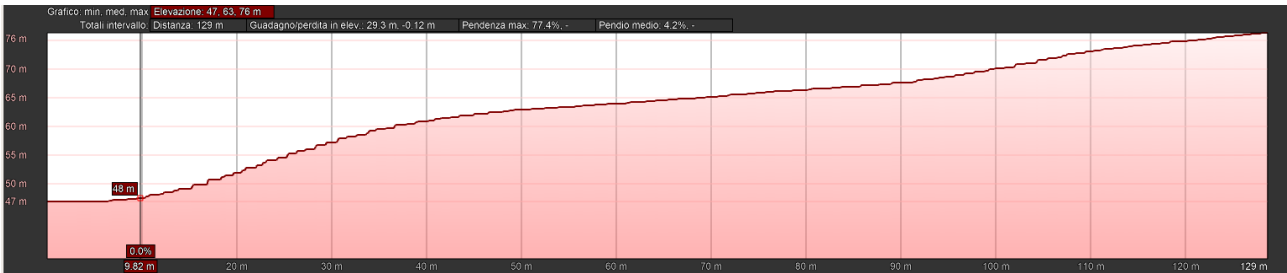
195°



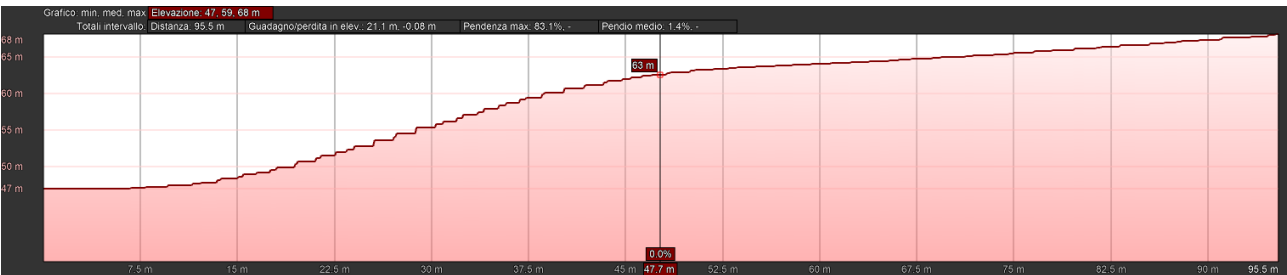
210°



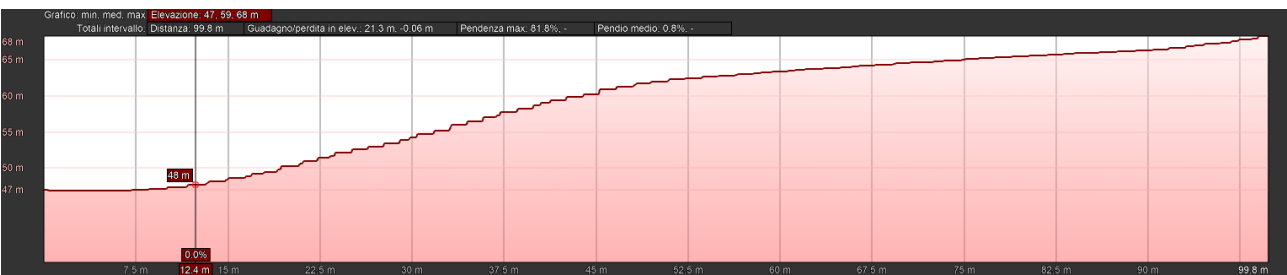
225°



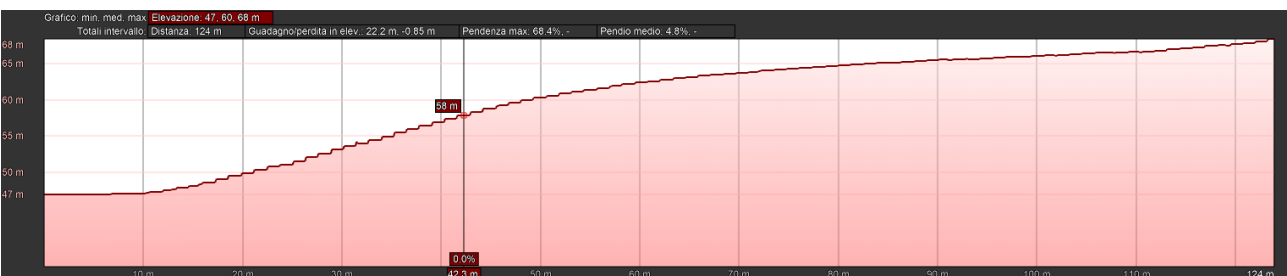
240°



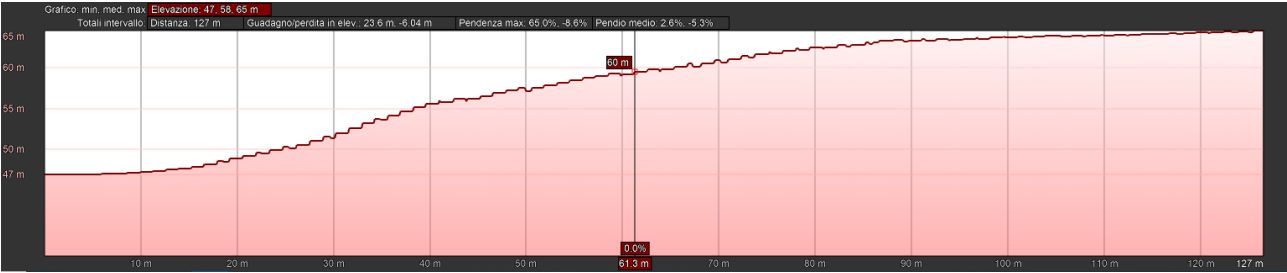
255°



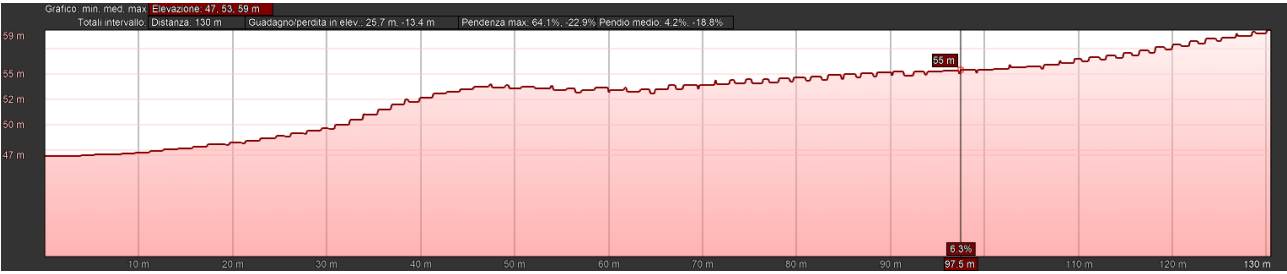
270°



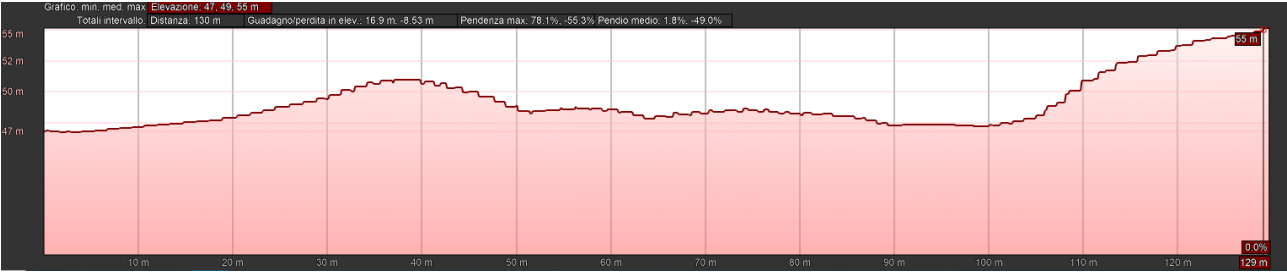
285°



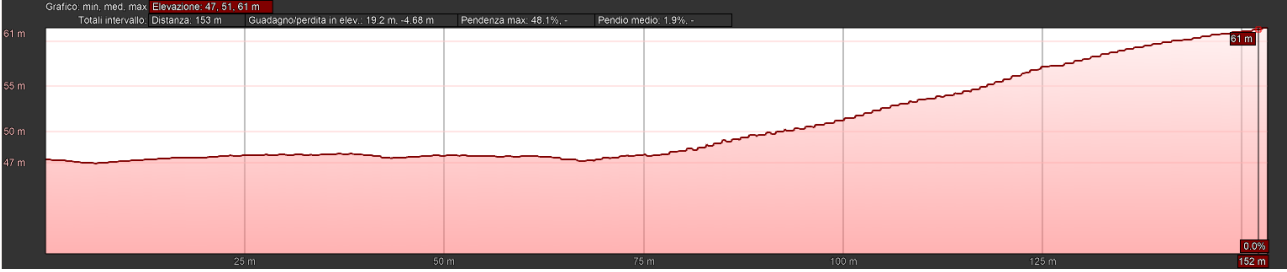
300°



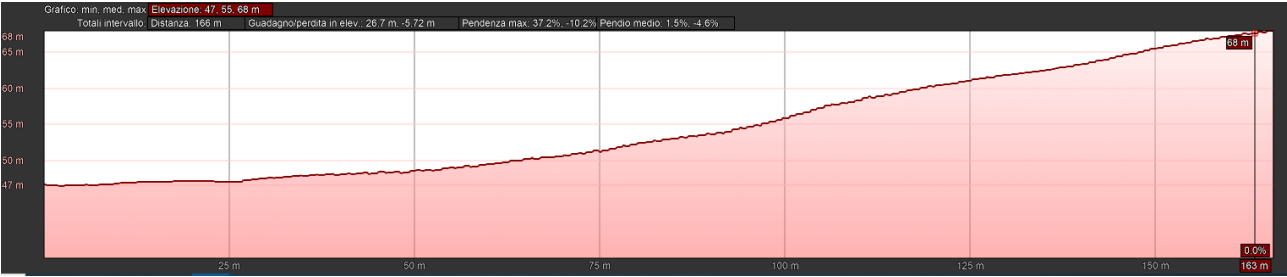
315°



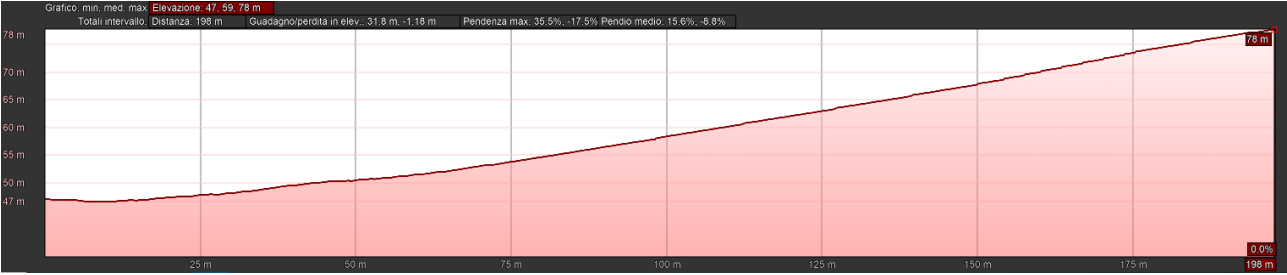
330°



345°



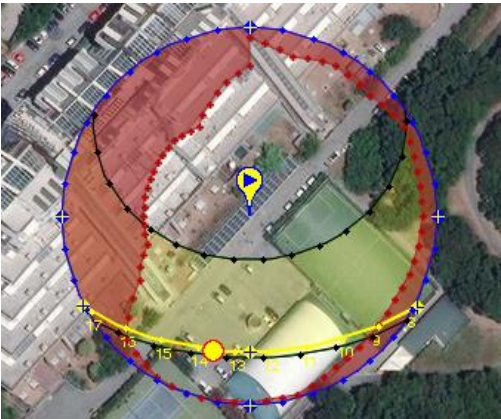
360°



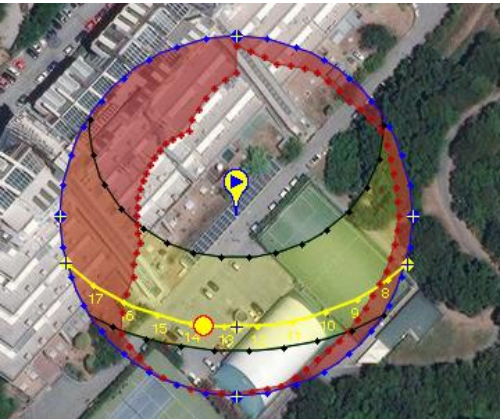
Annex A – part II

Simulation of the solar irradiation over the site for the different months according to the obstacles identified [6]. It is clear that the greatest shade is cast by the building on the North/North-West.

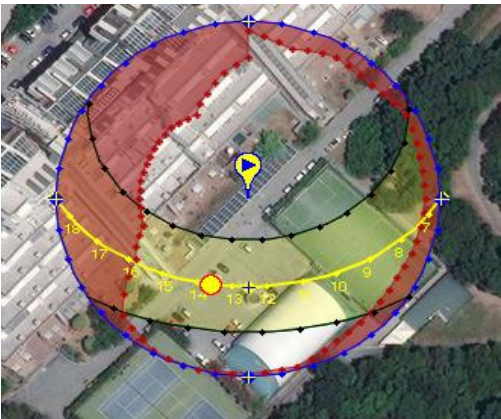
January



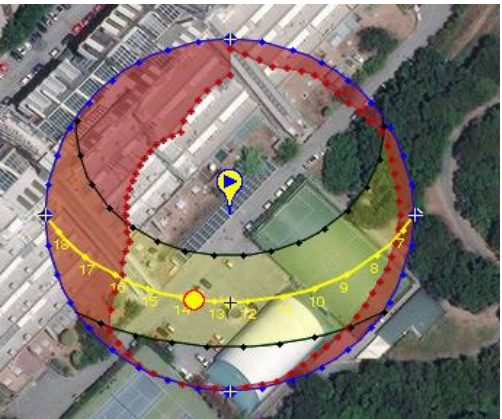
February



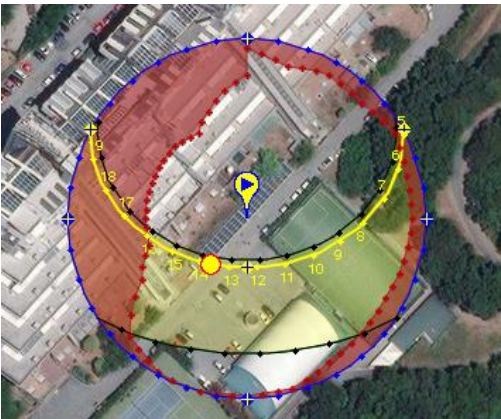
March



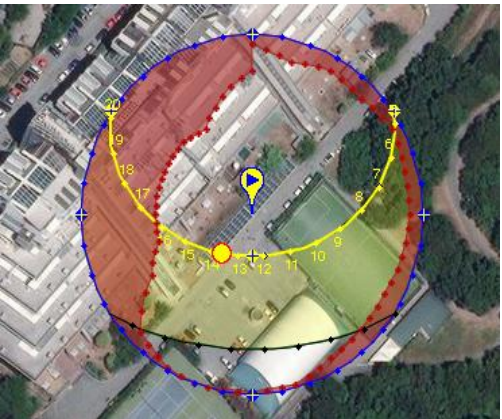
April



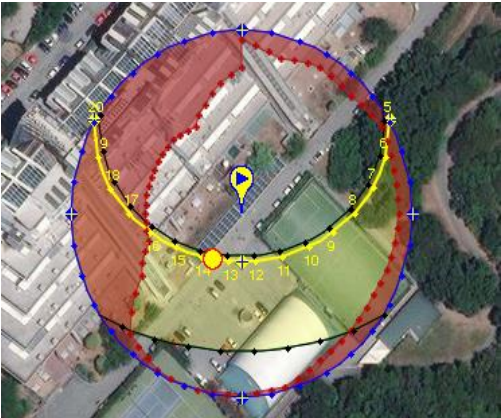
May



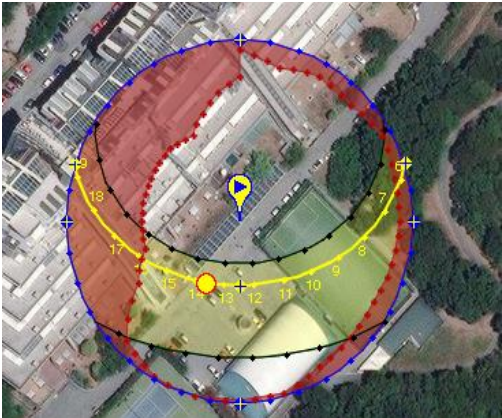
June



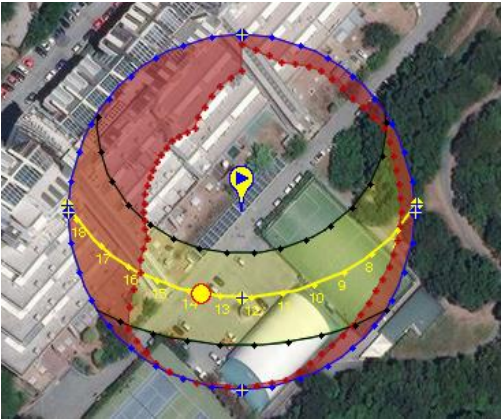
July



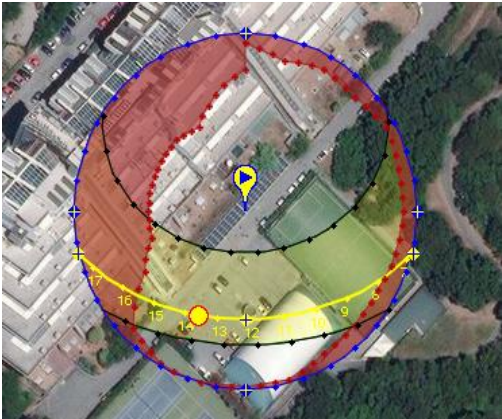
August



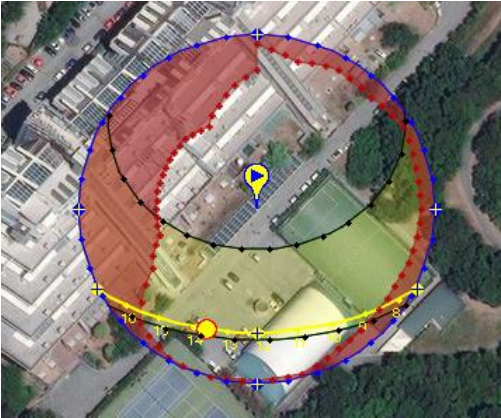
September



October



November



December

